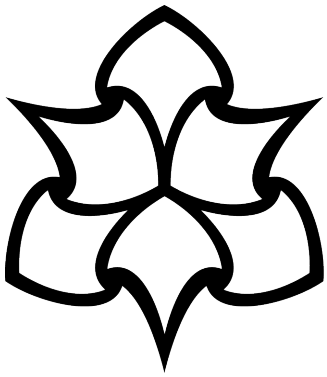

ASPECTS OF EXPANDED BED NITRIFICATION INCLUDING TREATMENT OF OIL REFINERY WASTEWATERS

IDUMA DEVINE AKHIDIME

A thesis submitted in partial fulfilment of the requirements
of the
Manchester Metropolitan University for the degree of Doctor of Philosophy.

School of Biology, Chemistry and Health Science
Manchester Metropolitan University

2009

ACKNOWLEDGEMENT

I would like to express my profound appreciation to my director of studies Dr Mike Dempsey who guided me and directed me in every step of this study. His unflinching support and can do attitude was vital to my completion of this work. My thanks also go to the staff in the microbiology research laboratory; Alan, Paul, Helen, Lindsay, Gill, Mike, for all the help with the equipment and protocols. I am grateful for the support of Kath, Lisa, Paul, Stavros, Moshood, Norman, Feeley, Lesley and David for all the help and advice in the different sections I had to cover during the study. To all the visiting students who questioned me to my bones on the methods and made me learn by heart the explanations, and for all their assistance in counting bioparticles; I am grateful - Joao, Maryam, Mikael, Damien, Marie and Stu, Maxime, William Kenza and Patrice.

I am grateful for the support of my family in Manchester; Andrew, Andrea, Tega, Sisan, Kunle, Sinmi and all of the NCC Manchester family and also for the support of my family in Nigeria for their encouragement and prayers.

I am honoured to have been a scholar of The Petroleum Technology Development Fund (PTDF) whose 16 month of funding enabled me to complete this work.

To my darling wife Angela who shared the whole experience with me and to whom I am greatly indebted to, I say thank you, for all your love and support during the long hours of work. To Danielle and David for being patient with me, thank you.

TABLE OF CONTENTS

ABSTRACT

Nitrification is an important part of the wastewater treatment process. This study involved the design and establishment of a lab-scale expanded bed biofilm reactor (EBBR) seeded with nitrifying biofilms immobilized on glassy coke support, for investigating nitrification of oil refinery wastewaters. Synthetic wastewater was used as reactor medium for the initial optimization of the nitrification process of the EBBR system using response surface methodology (RSM) which enables the design of experiments by which interactions of complex systems to be statistically analysed. This study also involved the development of methods to investigate the nitrifying biofilm with a focus of understanding the influence the biofilm thickness had on nitrification processes. The effect of pH on the EBBR nitrification process was shown to be twice that of temperature. Volumetric nitrification rates of 4.4 NH_3-N kg $m^{-3}{}_{EBBR}d^{-1}$ were achieved in the EBBR and thick biofilms which developed in the bioreactor achieved biomass concentrations of up to 50 kg m^{-3}. However, the thicker biofilms achieved lower nitrification rates. The optimum biofilm thickness for ammonia oxidation was determined to be 100 μm while that for nitrite oxidation was found to be above the 100 μm biofilm depth. Using methods developed to determine the specific nitrification rates of biofilms and image analysis of fluorescent *in situ* hybridization (FISH) stained biofilms, the presence of nitrifying bacteria at depths of about 500 μm was confirmed. There was also strong evidence that in thicker biofilms of more than 500 μm depth, there is an active layer for nitrification of about 450 μm. When the nitrifying biofilms established in the EBBR were exposed to oil refinery wastewaters, this study showed that the nitrifying biofilms survived in the oil

refinery wastewater environment and achieved volumetric nitrification rates of up to 2.0 NH_3-N kg $m^{-3}_{EBBR}d^{-1}$.

LIST OF TABLES

LIST OF FIGURES

LIST OF ABBREVIATIONS

ASTM	American Standard for Testing Materials
ATU	*N*-allylthiourea
BOD	Biological oxygen demand
BNR	Biological nutrient removal
CLSM	Confocal scanning laser microscope
COD	Chemical oxygen demand
CONCAWE	The oil companies European association for environment, health and safety in refining and distribution.
D	Dilution (d^{-1})
DAF	Dissolved air flotation
DO	Dissolved oxygen
EPS	Extra polymeric substances
EB	Expanded bed
EBBR	Expanded bed biofilm reactor
FED	Factorial experimental design
FISH	Fluorescence *in situ* Hybridization
HRT	Hydraulic retention time
HYBAS	Hybrid activated sludge process
IFAS	Integrated fixed film activated sludge process
MBBR	Moving biological bed reactor
NOB	Nitrite oxidizing bacteria
RSM	Response surface methodology
RBC	Rotating biological contactors
ORWW	Oil refinery wastewater
SB	Static bed
VVM	volume per volume per minute
VSS	Volatile suspended solids

CHAPTER 1

1.0 Introduction and literature review

1.1 Overview

The original aim of this study was to investigate the nitrification of oil refinery wastewater using the novel expanded bed technology. Nitrification is the oxidation of ammonia to nitrate by the nitrifying bacteria and is an important part of wastewater treatment processes (Gray, 1989; Nielsen *et al.*, 2009). This study involved the establishment of a lab-scale expanded bed bioreactor for the nitrification process. However, initial samples of oil refinery wastewaters obtained from the industry effluent showed low concentrations of ammonia (below 2 mg L^{-1}); much lower than the concentration reported in the literature (e.g. Xianling *et al.*, 2005 reported concentrations of 56 – 125 mg L^{-1} NH_4^+-N). Therefore, synthetic wastewater employed in nitrification processes from literature was used to establish the lab-scale expanded bed bioreactor.

Utilizing synthetic wastewater enabled the study of the bioreactor processes in controlled conditions before exposing the nitrifying community to oil refinery wastewaters. The investigations carried out to broaden the understanding of the expanded bed technology and of the nitrifying bacteria involved in the process included methods to determine the biomass concentration, the determination of the maximum and specific nitrification rates and the measurement of the biofilm thickness of the nitrifying biofilms. The ammonia and nitrite oxidizers of the

biofilms were also quantified using Fluorescent *in situ* hybridization (FISH) techniques (Nielsen *et al.,* 2009). The study therefore included different aspects of expanded bed nitrification with a focus on the influence of biofilm thickness on nitrification process and the effect of oil refinery wastewater treatment on the nitrifying biofilm.

1.2 Introduction and literature review

1.2.1 Wastewater in oil refining

Crude oil or petroleum oil is one of the most important natural resources on the Earth today and is almost invaluable in the daily operation of our society. Crude oil is found trapped in porous rocks held under pressure deep in the earth's crust and has to be extracted to the surface mainly by drilling activities. The potential of petroleum oil as a resource is immense; Gary and Handwerk (2001) reported 2347 products made by US petroleum industry which consists of about 180 facilities (EPA, 1998). Oil refining involves the separation of crude oil into its major distillation fractions and also the further processing of the fractions into finished petroleum products; the oil refining process can be generally classified into two phases; a desalting process to remove unwanted compounds and distillation into various fractions (Cheremisinoff and Haddadin, 2006).

Water is an essential part of the oil refining process from the exploration and recovery of crude oil to the refining into finished petroleum products. Reservoir rocks normally contain mainly hydrocarbons and water (called formation water) and this water is referred to as produced water when it is brought to the surface mixed with the hydrocarbons as a result of exploration and production processes (Veil *et al.,* 2004). Water is also essential to the oil refining process e.g. the desalting process of the crude oil involves mixing water with heated crude oil to remove corrosive salts, metals and suspended solids. The added water is often 3 - 10 % of the crude volume

(Cheremisinoff and Haddadin, 2006). Oily sour water is a by-product of the fractionating columns during oil distillation. Sour water contains hydrogen sulphide and ammonia and these components have to be removed (sour stripping) before the water can be used for any other process in the operations.

Crude oil is mainly made up of a mixture of hydrocarbons with some quantity of impurities, but because oil refining involves large volumes, the refining process produces a variety of gases, solid and liquid wastes (Cheremisinoff and Haddadin, 2006). For example in 2008, 148 refineries in the United States recorded operable refining capacities of 2,000 - 572,000 barrels of oil per day (Energy Information Administration, 2008) while Rajesh *et al.*, (2009) reported that India, one of the about 67 nations that produce oil, has a refining capacity of 2.6 million barrels per day. The wastes associated with oil refinery, especially the wastewaters, have to be managed to minimize environmental pollution when finally discharged to the environment. For example, the American Petroleum Institute (API) estimated that 6 barrels of produce water are generated per barrel of oil produced (EPA, 2002). Schultz (2005) also estimated that an average petroleum refinery generates about 0.6 barrels of wastewater per barrel of oil produced; this would mean wastewater volume of 1.56 million barrels per day for the entire refining capacity for the nation of India alone. Data released by the oil companies European association for environment, health and distribution (Concawe, 2004) reported that although the total aqueous effluent produced by European refineries reduced between 1969 and 2000, the total wastewater produced by the refineries was still above 2 500 million tonnes $year^{-1}$. The exact composition of an oil refinery effluent cannot be generalised because the

effluent produced depends on many factors such as crude source and which refinery processes are in operation at any specific time, moreover, because not all refineries employ the same refining processes, the effluents that are produced will have different chemical compositions depending on the type of treatment they receive (Wake, 2005; Wong and Hung, 2006).

Liquid effluent are any wastewater from a petroleum refinery, including, in particular, process water (water which come in contact with hydrocarbons or treating chemicals used in the processes of a petroleum refinery), ballast water discharged to the refinery prior to loading a vessel, once-through cooling water, storm water (the run-off that results from precipitation of any kind that falls on a petroleum refinery), cooling tower blow-down wastewater, sludges from water supply treatment facilities and other sludges or water associated with the operation of a petroleum refinery and any other equipment or reservoir used by such refinery (Veenstra *et al.,* 1998; Russell, 2006; Ahnell and O'Leary, 2008)

Oil consists of five types of components; saturated non-cyclic hydrocarbons (cycloalkanes), olefin hydrocarbons (alkenes), aromatics and non hydrocarbons e.g. sulphur compounds, nitrogen–oxygen compounds and heavy metals (Cote, 1976). Consequently, the main constituents of oil refinery wastewaters are; n-alkanes, iso-alkanes, cyclic alkanes, aromatic hydrocarbons and phenols (Gulyas and Reich, 1995). Oil refinery effluents also contain many different chemicals at different concentrations, including ammonia, sulphides and trace amounts of heavy metals

(Cote, 1976, Hayat *et al*., 2002). The composition of a typical oil refinery wastewater is shown in Table 1. 1.

Table 1.1 Composition of an oil refinery's effluent wastewaters (adapted from Xianling *et al.*, 2005)

Constituent	Concentration (mg L^{-1})
Oil	30 – 55
Volatile phenols	10.7 – 40.6
Chemical oxygen demand (COD)	250 - 613
Ammonia nitrogen (NH_4^+-N)	56 – 125
Suspended substances (SS)	108 – 159
Sulfide (S^{2-})	< 2.0
Total phosphorus (TP)	< 0.5
pH	7.80 – 8.79

1.2.2 Treatment, discharge and impact of oil refinery wastewaters

Oil refinery wastewaters are normally treated in onsite wastewater treatment facilities and then discharged to publicly owned treatment works (van Ravensway, 1998). The onsite wastewater treatment comprises primary and secondary treatment encompassed in an integrated system. The primary treatment is carried out in two stages; the first stage of the primary wastewater treatment is carried out to separate

oil, water and solids using separators e.g. API (American Petroleum Institute) separators designed to allow oil to float to the surface and be skimmed off. The second stage utilizes physical methods e.g. settling ponds, dissolved air flotation (DAF) technology and /or chemical methods e.g. ferric hydroxide or aluminium hydroxide, to also separate the emulsified oils from the wastewater (Cheremisinoff and Haddadin, 2006). The second stage may also involve some flocculation, sedimentation and filtration processes. After the primary treatment, the wastewater can be discharged to a treatment works for further treatment before being discharged directly to surface waters. The secondary treatment involves the biological treatment of the wastewater and may involve biofilters, activated sludge and aerated ponds). Some refineries have an additional advanced stage of wastewater treatment, called polishing, to remove trace metals, inorganic chemicals and any other impurities. The polishing stage uses activated carbon, anthracite coal or sand in filtration systems (van Ravensway, 1998).

Oil refinery effluent is a major source of pollution to the aquatic environment; oil refinery wastewaters final effluents are discharged into water bodies, either on site after treatment or with the final effluent from industrial and domestic wastewater treatment plants. The toxicity of oil refinery effluent is dependent on a number of factors; the effluent volume, quality, salinity and variability of the discharge, the siting of the discharge areas, the proximity of other effluents and pollutants and the biological condition of the discharge area (Concawe, 1979). Although the fate of the effluent once discharged into receiving waters depends on the conditions and hydrodynamics of the receiving water, field studies have shown that oil refinery

effluents often impact on the fauna close to the outfall (Wake, 2005). For example, using 6 constituents of oil refinery wastewaters, Hall *et al.,* (1978), reported a toxicity order for grass shrimp (*Palaemonetes pugio*); fuel oil (no.2) > sulphide > ammonia > phenol > chromium> kalinite.

The impact of oil exploration extends beyond the environment e.g. in the Niger Delta area of Nigeria, wastewater from oil exploration is a major source of pollution where, following treatment and in some cases, without treatment, wastewater is discharged into rivers and the sea making the Niger Delta one of the world's most severely petroleum-impacted ecosystems. The continuous discharge of wastewaters, including produced water, into the freshwater environment have impacted on water quality, fisheries and coastal ecosystems damaging aquatic and agricultural resources and perpetuating poverty through long-term damage to livelihoods and health in the area (Amnesty International, 2009). Also in the Shenfu irrigation area in north eastern China, where wastewater plays an important role in agricultural irrigation, the irrigated paddy soils have been highly contaminated by petroleum containing wastewaters from the nearby Fusun refinery area, and has led to changes in the soil community structure, diversity of aerobic heterotrophic bacteria and diversities in the Eubacteria population (Li *et al.,* 2005)

Ammonia in oil refinery wastewaters

Ammonia nitrogen has been identified as one of the substances associated with pollution from petroleum refining (van Ravenswaay, 1998) and the composition of

ammonia-nitrogen varies in oil refinery wastewaters. Wong and Hung (2006) reported ammonia concentrations of 4 – 206 mg L^{-1} in produce water while Xianling *et al.,* (2005) reported concentrations of 56 – 125 mg L^{-1} ammonia-nitrogen (NH_3-N) in oil refinery wastewaters (Table 1.1). Hydroheating, one of the downstream operations, is a process of removing impurities from crude oil and involves heating the oil to temperatures of 300 – 380 ^{0}C. This procedure helps to prevent damage to equipment and improve hydrocarbon quality of the final product and is the main point at which nitrogen and nitrogen oxides in crude oil are converted to ammonia in the refining process. Ammonia is also present in the sour water generated by vacuum distillation, and steam strippers or fractionators (EPA, 1995). Due to the large volume of wastewater produced in oil refineries, ammonia can lead to several environmental problems for the receiving water bodies. Ammonia concentrations of 0.2 mg L^{-1} and nitrite concentrations of 1.8 mg L^{-1} have been found to have acute toxicities to fish species e.g. Salmonids and Rainbow trout respectively (Hagopian and Riley, 1998). Ammonia in wastewaters also leads to a reduction in the oxygen demand of the water body. This is because autotrophic nitrification, which is the conversion of ammonia to nitrate, takes place normally in water bodies and reduces the oxygen demand. The presence of ammonia in wastewaters is also a precursor for eutrophication and algal bloom as the effect of both the reduction in oxygen demand and the nitrates, the final product of nitrification could set off the onset of both conditions.

1.2.3 Ammonia, nitrogen cycle and nitrification

Ammonia (NH_3) is a reduced form of nitrogen, and is an irritable, colourless gas with a pungent odour and is highly soluble at room temperature (7 kg L^{-1}, 20 ^{0}C) and is an important major element in the biosphere for the survival of life. Nitrogen is contained in many compounds essential to living systems, the most important being amino acids, peptides, proteins, nucleic acids and pigments. These compounds are complex forms of nitrogen and form the building blocks of life. Nitrogen is incorporated as a part of all living cells and is a necessary component of all enzymes and metabolites involved in the synthesis and transfer of energy. Nitrogen occurs naturally in its inert molecular form, dinitrogen (N_2) in the Earth's atmosphere as a colourless, odourless and tasteless gas where it is the largest component (78.1 %). Because the natural form of nitrogen gas is inert, plants and animals cannot utilize it directly; Molecular nitrogen is a very stable molecule because of the triple bond between the dinitrogen atoms (it takes about 930 kJ mol^{-1} to break this triple bond). Apart from dinitrogen gas, common forms of nitrogen in the environment include, NO_2 (nitrogen dioxide), N_2O (nitrous oxide), NO_2^- (nitrite ion, found as HNO_2), NO_3^- (nitrate ion, found as HNO_3), NH_3 (ammonia), NH_4^+ (ammonium ion) and complex organic forms of nitrogen (*R*-NH_2). In order to be incorporated into living cells, this nitrogen is cycled naturally from atmospheric molecular nitrogen to different complex 'fixed' forms, mainly as microbial, plant and animal proteins but eventually transformed back to atmospheric nitrogen in the nitrogen cycle.

The Nitrogen cycle

This is the cyclical transformation of nitrogen from its inert gaseous form into the biological relevant forms and back to the inert atmospheric form mainly by biogeochemical transformations. Microorganisms play a major role in the cycling of nitrogen in the environment. The method by which molecular nitrogen enters the nitrogen cycle is mainly by nitrogen fixation carried out by nitrogen fixing bacteria.

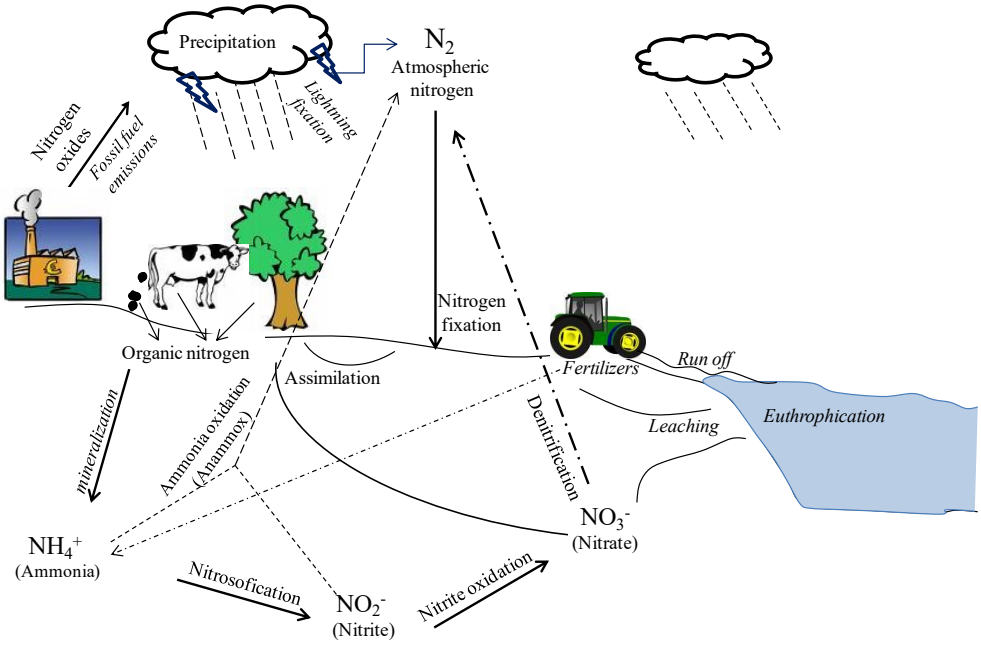

Fig. 1.1 The Nitrogen cycle (Adapted from (Rice, G. (2005). The nitrogen cycle serc.carleton.edu/.../northinlet/diaz.html).Accessed 14/04/2009)

Nitrogen fixing bacteria convert molecular nitrogen into complex organic cellular forms of nitrogen which often contain either ammonia or ammonium. In the nitrogen cycle, these complex organic forms of nitrogen are broken down or transformed into simpler forms via different biological species and pathways and ultimately back into

molecular nitrogen. Other sources of fixed nitrogen include a small amount of nitrogen fixation during the discharge of lightning; the high energy released by the electrical discharge is able to break the triple bond of molecular nitrogen. Artificially, nitrogen is fixed in the industrial production of ammonia by the Haber-Bosch process e.g. for fertilizer production and also for the production of explosives.

The transformation of nitrogen occurs mainly in five ways during the nitrogen cycle;

a. *Nitrogen fixation* – This is the reduction of atmospheric nitrogen by species of bacteria and cyanobacteria. Nitrogen fixation involves the splitting of the nitrogen molecule (N_2) and combining the N atom with hydrogen to form ammonia in the presence of a nitrogenase enzyme.

$$N_2 + 8H^+ \longrightarrow 2\,NH_3 + H_2$$

Free-living, nitrogen-fixing bacteria include *Azotobacter sp* in soils, *Klebsiella sp* and *Clostridium sp* in sediments and Cyanobacteria (e.g. *Nostoc, Anabaena*) in freshwater and marine environments. Symbiotic nitrogen fixation takes place mainly in the root nodules of legumes (e.g. *Rhizobium sp),* the roots of woody perennial plants (*Frankia sp*) and roots of maize and tropical grasses (*Azospirillium sp*), (Bitton, 2005).

b. *Nitrogen assimilation* - Nitrogen assimilation is the uptake of the fixed nitrogen by heterotrophic and autotrophic organisms and the assimilation of the fixed nitrogen into organic cell components.

c. *Nitrogen mineralization or ammonification* - is the enzyme mediated transformation of the assimilated cellular nitrogen e.g. proteins and organic nitrogenous compounds, into inorganic forms. The process is carried out by a variety of microorganisms mainly during decomposition of organic matter.

d. *Nitrification* - This is the oxidation of ammonia to nitrate via nitrite. This process is mainly carried out by nitrifying bacteria and Crenarchaea (Francis *et al.,* 2005).

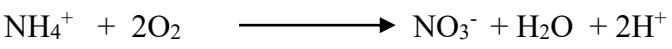

$$NH_4^+ + 2O_2 \longrightarrow NO_3^- + H_2O + 2H^+$$

e. *Denitrification* - is the reduction of nitrate or nitrite to atmospheric nitrogen. Denitrification is carried out by heterotrophic bacteria mainly in oxygen depleted soils and sediments. Denitrification is useful in wastewater treatment systems as it reduces the nitrate concentration of wastewaters before discharge into receiving waters.

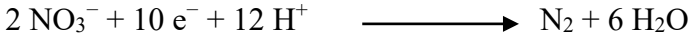

$$2\,NO_3^- + 10\,e^- + 12\,H^+ \longrightarrow N_2 + 6\,H_2O$$

The anammox (anoxic ammonium oxidizing) bacteria e.g. *Brocadia sp* also convert ammonia or nitrite directly to gaseous nitrogen. The anammox bacteria (a group of organisms within the *Planctomycetales*) are obligate anaerobes which produce N_2 from ammonia and nitrate via the intermediates hydroxylamine and hydrazine (Kuypers *et al.,* 2003; Kuenen, 2008).

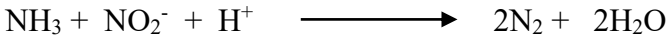

$$NH_3 + NO_2^- + H^+ \longrightarrow 2N_2 + 2H_2O$$

Also involved in the nitrogen cycle are some non biological processes, which include the release of nitrogen oxides by industrial activities (especially the release of fossil fuel emissions), the use of fertilizers which releases excess ammonium and nitrate through the soil and into surface and ground waters by leaching and runoff. The nitrogen cycle ensures that all forms of nitrogen are recycled continuously in the environment.

1.2.4 Nitrification and the Nitrifying Bacteria

Nitrification is a two-step process that involves the oxidation of ammonia to nitrite and the oxidation of nitrite to nitrate and is normally carried out by nitrifying bacteria. The nitrifying bacteria are classified according to the inorganic nitrogen compounds they oxidize (ammonia or nitrite). Nitrifying bacteria are widely distributed in water and soils and are autotrophic bacteria, due to their dependence on inorganic carbon (Carbon dioxide,(CO_2)) as their main carbon source, although some species can grow heterotrophically e.g. *Nitrobacter sp*. Kelly (1978) estimated that CO_2 fixation by the Calvin cycle consumes about 80 % of the energy budget of the nitrifying autotrophs. For each carbon fixed, nitrifying bacteria have to oxidize about 35 molecules of NH_3 or 100 molecules of NO_2 (Wood, 1986). Most nitrifying bacteria are also obligate chemolitothrophic bacteria, due to their dependence on inorganic substrates (i.e. NH_3 or NO_2), for energy production. Autotrophic nitrification therefore takes place in a two-step process by ammonia oxidizing bacteria and nitrite oxidizing bacteria (Kowalchuk and Stephen, 2001). There are no known bacteria that can catalyze the production of nitrate directly from ammonia.

Ammonia oxidizing bacteria (AOB)

Ammonia oxidizing bacteria, also called the nitrosofying bacteria, utilize ammonia as the sole energy source in a two-step reaction mediated by two distinct enzymes. Ammonia monooxygenase (AMO) first oxidizes ammonia to hydroxylamine then hydroxylamine oxidoreductase (HAO) reduces hydroxylamine to nitrite.

1. $NH_3 + O_2 + 2H^+ + 2e^- \longrightarrow NH_2OH + H_2O$

2. $NH_2OH + H_2O \longrightarrow NO_2^- + 4e^- + 5H^+$

Hydroxylamine, the intermediate formed during ammonia oxidation is a mutagen and has low free concentration. Hydroxylamine has an inhibitory effect on ammonia monooxygenase and has been shown to regulate the activity of the ammonia monooxygenase (Wood, 1986). AOB derive their energy from ammonia via the electron transport chain, with hydroxylamine oxidoreductase feeding the process with electrons.

Ammonia oxidizing bacteria include the genera *Nitrosomonas (N. europea), Nitrosococcus (N. oceanus and N. mobilis), Nitrosospira (N. briensis), N. nitrosolobus (N. multiformis) and Nitrosovibrio (N. tenuis).* Typically 1 - 2 µm in size, AOB have various shapes e.g. *Nitrosomonas sp* are ovoid rods but also form cysts, the *Nitrosovibrio sp* and *Nitrosospira*. *sp* have curved cells and *Nitrosolobus sp* have cyst-like structure with multiple flagella-like structures emanating from the cysts (Macdonald, 1986). Ammonia oxidation is the first step in the nitrification process and is also the rate limiting step of nitrification (Kowalchuck and Stephen,

2001). All AOB are obligate aerobes; therefore nitrification is reduced in environments devoid of oxygen like water logged soils.

Nitrite oxidizing bacteria (NOB)

The Nitrite oxidizing bacteria oxidize nitrite to nitrate. Nitrite oxidoreductase, a intracytoplasmic membrane bound enzyme, is responsible for oxidation of nitrite and produces no detectable intermediates.

$$NO_2^- + H_2O \longrightarrow NO_3^- + 2H^+ + 2e^-$$

The extra oxygen atom required for the reaction is supplied by H_2O and the characteristic brownish colour of nitrifying bacteria is due to the nitrite oxidizing cytochrome system in the membranes. (Bock *et al.,* 1986). Nitrite oxidizing bacteria include *Nitrobacter (N.winogradsky and N. hamburgensis), Nitrococcus (N. mobilis), Nitrospina (N. gracilis), Nitrospira (N. marina).* Only *Nitrobacter* sp have been shown to undergo both lithotrophic and heterotrophic growth, however heterotrophic growth is extremely slow and inefficient (Bock *et.al*., 1986). Although nitrification is carried out mainly by autotrophic bacteria, some heterotrophic bacteria (e.g. *Alcaligenses sp)* are involved in nitrification. Some species of the Crenarchaea e.g. *Candidatus sp* and *Nitrosopumilus maritimus* have also been recently identified to be involved in autotrophic ammonia oxidation in marine sediments (Konneke *et al*., 2005).

The nitrifying bacteria are extremely slow-growing and are recalcitrant to cultivation attempts (Wagner *et al*., 2002). Bock *et al.* (1986) reported lithoautotrophic growth

to be maximal at 28 – 30 ^{0}C at pH 7.6 - 7.8 with generation times varying between 8 hours for *Nitrosomonas,* 10 hours for *Nitrobacter sp* and 60 hours for *Nitrosospira sp.* Variation in specific growth rate of nitrifying bacteria was also reported by Prosser, (1989) who reported that specific growth rate for nitrifying bacteria are typically low; within the range of 0.014 – 0.064 h^{-1} (equivalent to a doubling time of 5 - 11 hours). Although some authors report that the rate of conversion of ammonia to nitrite is much slower than that of nitrite to nitrate (Ekema and Wentzel, 2008), Bock (1978) reported that the minimum doubling time of 7 hours for AOB and a 13 hours for NOB, while Wood (1986) reported a much higher substrate demand for NOB than AOB (almost 300 %) to fix one carbon atom. The higher substrate demand of NOBs would result in higher growth rates and growth yield of ammonia oxidizers than nitrite oxidizers. Prosser (1989), showed evidence of a higher specific growth rate for AOBs than NOBs in both batch and continuous cultures (Table 1.2). Prosser (1989), also stated the important factor in increasing ammonia oxidizing capability is the proportion rather than the amount of cell material occupied by intracytoplasmic membranes. The data provided by Prosser (1989; Table 1.5) shows that the specific growth rates of AOB range from 0.012 – 0.088 μ_{max} h^{-1}, while NOB 0.025 – 0.043 μ_{max} h^{-1} in batch culture while in continuous culture, the specific growth rate of NOB and NOB were 0.039 – 0.064 μ_{max} h^{-1} for AOB and 0.018 – 0.033 μ_{max} h^{-1}respectively. AOBs therefore have higher specific growth rates than NOB.

Table 1.2: Maximum specific growth rate (μ_{max}) values of pure cultures of nitrifying bacteria isolated from various sources (Prosser, 1989)

Nitrifying bacteria	Maximum growth rate (μ_{max} h^{-1})	
Ammonia oxidizers	Batch culture	Continuous culture
Nitrosomonas sp		
Sewage isolate	0.016 – 0.058	-
Sewage isolate	0.012 – 0.043	-
N. europaea	0.088	0.063
N. europaea	0.02 – 0.03	-
N. europaea ATCC	0.055 – 0.066	-
N. europaea FHI	0.052 – 0.054	-
N. europaea	0.036	0.064
N. europaea	0.017	0.039
N. marina	0.018	-
Nitrosocystis oceanus	0.014	-
Nitrosocystis oceanus	0.032	-
Nitrosospira AV2	0.032 – 0.035	-
Nitrospospira AV3	0.043 -0.044	-
Nitrite oxidizers		
Nitrobacter sp		
N. sp	0.058	-
N. NW	0.039	0.033
N. L	0.025	0.018
N. sp	0.043	0.035
Nitrococcus mobilis	0.033	-

Nitrification and wastewater treatment

Nitrogen appears in wastewaters as ammonia, nitrite, nitrate and organic nitrogen (Sotirakou *et al.*, 1999). Nitrification (ammonia removal) is an essential part of wastewater treatment because it converts toxic ammonia into non-toxic nitrate. While the calculated lethal concentration of nitrate to some species of fish (e.g. channel catfish) is about 6, 200 mg L^{-1}, ammonia concentrations of 0.2 mg L^{-1} and nitrite concentrations of 1.8 mg L^{-1} have been found to have acute toxicities to some other fish species (Hagopian and Riley, 1998). In drinking water, excess ammonia can cause taste and odour problems at concentrations above 1.5 mg L^{-1} (WHO, 2003a) and also illnesses. At concentrations of 0.75 mg NH_3 L^{-1} at pH 7.0, 15 ^{0}C, ammonia disturbs the hatching of fish eggs and the growth of fish (Richardson, 1997) and at higher concentrations, excess ammonia causes fish kills in water bodies. The discharge of ammonia into water bodies increases the rate of *in situ* nitrification and therefore leads to a reduction in the dissolved oxygen (DO) in the water. DO concentrations of below 2 mg L^{-1} even for short periods can result in fish kills.

Nitrate concentrations of above 5 mg L^{-1} in drinking water have been linked to the increased risk of colon cancers; in the human body, nitrate is reduced to nitrite by bacteria e.g. *Escherichia coli* which can react with amides to form a group of nitroso-compounds which are known carcinogens (De Roos *et al*., 2003). Nitrate can also cause methaemoglobinaemia (higher than normal level of methemoglobin in blood) in infants at concentrations of above 50 mg L^{-1} (WHO, 2003b) and can lead to tissue hypoxia. The WHO guideline amount for drinking water is 50 mg L^{-1} (NO_3^-) and 3

mg L^{-1} (NO_2^-) and the sum of the ratio of each to guideline values should not exceed 1.0 (WHO, 2003b). Nitrification helps to avoid environmental contamination with potentially toxic ammonia salts (Painter, 1986). In wastewater treatment, biological nitrification is the standard process of ammonia removal from wastewater and sewage.

Wastewater treatment processes and ammonia removal.

The main objectives of the wastewater treatment processes are to treat influent wastewaters, such that treated effluent meets legislative requirements for discharge. This objective ensures low risk to public health and damage to the quality of the aquatic environment. Wastewater treatment processes involve an improvement of the following; biological oxygen demand (BOD), suspended solids, concentration of ammonia and other nutrients (IWEM, 1994) although the type and amount of treatment required in a treatment plant depends on the water quality objectives for the final effluent receiving water body and the dilution available (Gray, 1989).

In conventional wastewater treatment, the composition of wastewater (sewage) is normally measured in terms of biological oxygen demand (BOD), chemical oxygen demand (COD), suspended solids, and ammonia content because its polluting strength is assessed from these determinants (Gray, 1989). The BOD and COD are a measure of the oxygen demand or consumption potential of a water body. While BOD is a measure of the demand placed by the organisms within a water body, the COD is a measure of the oxygen consumption of a water body but with chemicals

(potassium dichromate in presence of sulphuric acid), (Bitton, 2005). The BOD of wastewater is however made up of the carbonaceous BOD (cBOD) which is the oxygen consumption due to the oxidation of carbon (organic component of the wastewater) while the nitrogenous BOD (NBOD) is the demand placed by the aerobic nitrifying bacteria (Davis and Masten, 2003). The suspended solids are minute particles which remain in suspension and are differentiated from particulate matter by their size. Suspended solids are generally regarded as particles that can by retained in filters with pore size 0.45 μm (Gray, 2005).

Biological wastewater treatment involves the establishment of a population of mainly aerobic microorganisms that carry out the transformation of dissolved and suspended organic contaminants to biomass and evolved gases (CO_2, CH_4, N_2 and SO_2) which are separable from the treated waters (Horan, 1990). The treatment process is made up of several treatment units, each designed to provide a level of reduction in contamination or pollution. A major determining factor of the microbial constituent of the treatment process is that the microorganisms depend on the wastewater for their nutritional requirements; therefore those that can efficiently utilize the available nutrients will survive and flourish. No single species is capable of utilising all the assorted organic and inorganic compounds found in wastewaters. A heterogeneous microbial population which utilise a wide range of substrates is required and is therefore always present in a wastewater treatment process (essentially bacteria and protozoa).

Conventional wastewater treatment begins with a preliminary treatment carried out on influent to the treatment facility and involves mainly physical processes to remove grit, solid objects, floating objects and large debris including coarse inorganic particles contained in sewage by the use of screens and grit channels. This procedure is important to avoid the blocking or clogging of pipes and pumps in the facility and therefore reduces the rate of wear of the plant mechanical parts. The preliminary treatment is followed by a primary treatment stage which is often a sedimentation process in sedimentation tanks which removes suspended solids (< 4.5 μm) and grease.

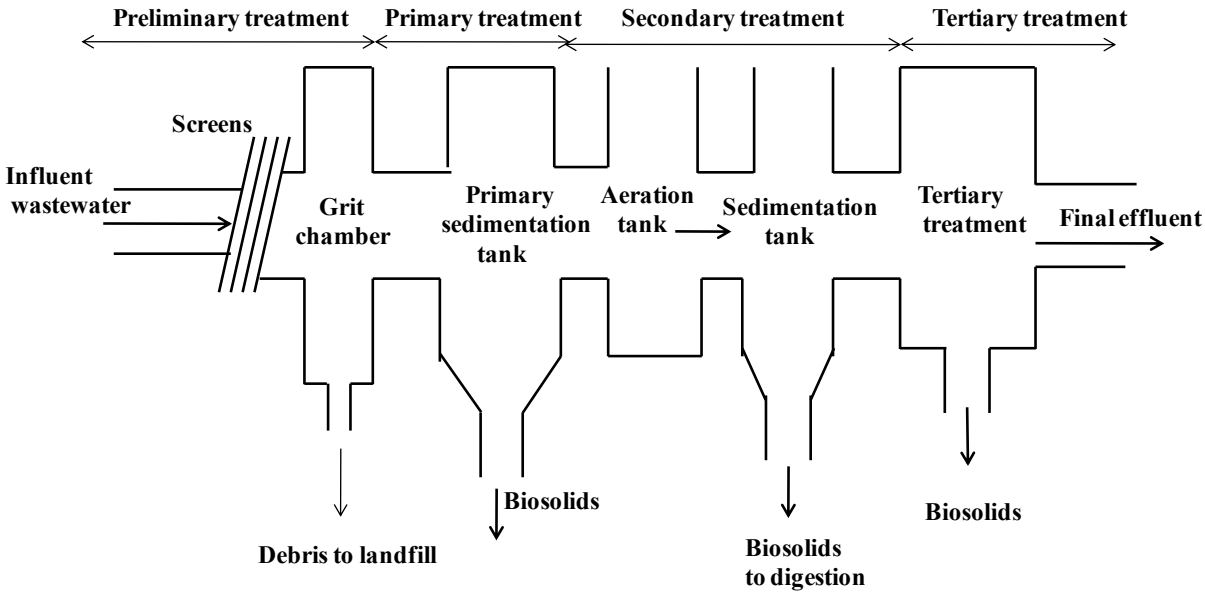

Fig. 1.2 Conventional wastewater process showing different treatment units (adapted from Bitton, 2005)

A low inflow velocity of the wastewater in the settling tanks allows for the particles to fall out of suspension forming a mass of solids called the primary sludge which is collected into sludge wells, while grease is skimmed off the surface of the wastewater. Primary treatment removes 60 - 70 % of suspended matter in sewage (Gray, 1989). The next stage is a secondary treatment and involves biological treatment processes which are basically the biological oxidation of the organic materials in the settled sewage received from the primary treatment tanks into innocuous end products. The availability of oxygen is essential for secondary treatment process and in this stage, 90 % of organic matter removal from wastewater can be achieved. The secondary treatment also involves a secondary sedimentation but the sludge produced here is mainly composed of microbial cells. Finally, a tertiary treatment stage which is a further treatment or polishing of the wastewaters to raise the quality of the final effluent before discharge to receiving environment.

Tertiary treatment is sometimes followed by advanced wastewater treatment (AWT). AWT processes are designed to achieve a high rate of removal of nutrients and suspended solids and are used either after the conventional treatment process or used to modify or replace one or more of the steps of conventional wastewater treatment. Although AWT may differ on the basis of the desired treatment goals, refractory and soluble pollutants which are not removed by conventional biological treatment are eliminated by AWT processes (Gray, 1989).

Presently, many wastewater treatment systems have been developed using a wide range of biological reactors for the treatment processes. But whatever the reactor

systems used, all the treatment processes include physical, chemical and biological processes. In biological reactors for wastewater treatment, the population of microorganisms, referred to as the biomass, comes into contact with wastewater either in dispersed or attached growth processes.

In the dispersed growth processes, which are also known as suspended growth process, the biomass grows as free living, planktonic organisms or in aggregates as flocs dispersed in the entire reactor volume without attachment to a support. Examples of the dispersed growth processes include the activated sludge process, waste stabilization ponds and aerated lagoons (Horan, 1990). The attached growth processes on the other hand are also known as the fixed-film systems. Here the biomass is immobilized or fixed on solid surfaces and as the wastewater passes over the surfaces, the microorganisms utilize the nutrients therein (EPA, 2004). Biofilm systems are mainly used in the secondary treatment of wastewaters; microorganisms are attached to the surface of solid surfaces which act as support materials for microbial growth e.g. particles or stones over which the wastewater is discharged. The biological agents of substrate transformation then grow as a biofilm on the surfaces and provide extensive surface area for reaction. Because biodegradable organic materials in wastewater are effectively removed using attached growth processes and involve low maintenance and low operational energy requirements they are ideal for small communities and even small homes (NSFC, 2004). Examples of attached growth processes include trickling filters and rotating biological contactors (RBC).

Because wastewater treatment using conventional activated sludge systems gives rise to effluent low in BOD and suspended solids but high in nutrients, biological nutrient removal processes (BNR) were developed in order to meet more stringent wastewater discharge standards e.g. the 1991 EEC Directive concerning urban wastewater treatment (Council of European Communities, 91/271/EEC, 1991). Nitrogen and phosphorus have been identified as the two most important elements controlling the growth of algae and aquatic plants in water bodies (Oldham and Rabinowitz, 2002) and therefore are targeted by biological nutrient removal processes (BNR) to meet treated effluent standards. Although nitrogen and phosphorus can be removed by physical and chemical means, biological nutrient removal is the preferred process for nitrogen removal because it produces less sludge, and the sludge produced is amenable to land application (Oldham and Rabinowitz, 2002). Phosphorus removal on the other hand is difficult and requires a combination of chemical and biological removal processes. In the removal of nitrogen, ammonia is removed by nitrification in the aerobic zones of the BNR processes while nitrate is removed by denitrification in the anoxic zones (Grady *et al.*, 1998). The discharge of nitrogen and phosphates into water bodies leads to oxygen depletion and reduction in water quality resulting in eutrophication and algal blooms. Rogalla (2009), however, stated that recent studies in nutrient management in Canada showed that phosphate inputs directly controlled algal blooms in water bodies and that algal blooms are made worse if nitrogen discharges into water bodies are reduced without decreasing phosphate inputs.

Small amounts of the greenhouse gases nitrous oxide (N_2O) and nitric oxide (NO) are produced by ammonia oxidizing bacteria in addition to nitrite, especially in low oxygen concentrations (Wood, 1986). Although nitric oxide is not an intermediate in the pathway of nitrifying bacteria, AOB in particular have been reported to produce N_2O (Kampschreur, *et al.,* 2009). The conditions whereby N_2O is produced include; low oxygen concentrations, increased nitrite concentration in both nitrification and denitrification stages of wastewater treatment and also low COD/N ratio in denitrification stage of wastewater treatment (Kampschreur, *et al.,* 2009). Reduction in oxygen supplied to aerobic wastewater treatment processes can therefore result in the emission of N_2O.

1.2.5 Biofilms in wastewater treatment and process intensification

The efficiency and robustness of a wastewater treatment plant depends mainly on the composition and activity of its microbial community (Wagner *et al*., 2002). Because wastewater treatment plants receive large volumes of dilute and contaminated influent wastewater (millions of litres per day) which would require long residence times in the reactors for complete biological conversion, intensive systems with high reaction rates and short residence times are beneficial to BNR systems. One method of achieving high reaction rates in wastewater treatment systems is by enhancing biomass retention. The retention of biomass is critical for the high reaction or conversion rates within the biological reactors because it ensures the maintenance of low hydraulic retention times and ultimately lower plant operating costs. One of the methods of biomass retention is to immobilize the microbial population in biofilms

on a support medium therefore using fixed film (biofilm) reactor ensures high biomass hold up within the reactor vessel.

Powell (1986) reported that although some workers believed that the presence of a solid phase was essential for the growth of nitrifying bacteria, and bacterial adhesion was found to be a preliminary event in nitrification in sewage treatment, the presence of solid particles was not proved to be essential for the growth of nitrifying bacteria in sewage treatment. However, because growth on soil particles was found to stimulate ammonia oxidation, Powell therefore stated that the presence of a solid/liquid interphase affects the activity of bacteria in soil. The use of support media and biofilms in wastewater nitrification systems would therefore be at the best beneficial for the treatment system as it would provide solid/liquid interfaces.

A biofilm is a complex, coherent structure of microorganisms and cells held in a matrix of extracellular material attached to a solid surface (Nicollela *et al*., 2000b). Biofilms thrive where interfaces are found, especially solid – liquid interfaces (Wuertz *et al*., 2003). The interfaces then become regions of high microbial activities which support the development of biofilms. Biofilms grow naturally as highly organized and differentiated communities with an enhanced ability to resist environmental stress (Kerksiek, 2008). An advantage of biofilm growth on surfaces is that nutrients adsorb to surfaces and therefore more nutrients may be available to microorganisms than in planktonic growth. The natural phenomenon of biofilm formation is exploited in biofilm reactors for biological wastewater treatment e.g. for nutrient removal from wastewaters or detoxification of them (Nicolella *et al.*, 2000a).

Biofilm reactors are characterised by high biomass concentrations and high reaction rates (Nicolella *et al.*, 2000a) and this makes them ideal for nutrient removal in wastewater treatment. The biofilm support material used in the reactors could either be a stationary surface or bed, or particle – supported biofilms which are "carrier particles" suspended in a reactor and supporting biofilm growth (Heijnen, 1984).

While biological treatment in the conventional activated sludge process utilizes flocs which are aggregates formed by microorganisms, especially filamentous bacteria and contain inorganic particles and exocellular polymers (Olofsson *et al.,* 1998; Bitton, 2005), some biological reactors are based on dense granules which are compact aggregates of microorganisms but with a higher settling velocity than flocs (Beun *et al.,* 2002; Fernandez, *et al.*, 2008). The basis of activated sludge floc formation is the ability of the microorganism to stick to each other and to non biological particles and this is mainly brought about by filamentous bacteria (Grady, *et al.*, 1999; Jenkins *et al.*, 2003). Microbial cells involved in wastewater treatment can adhere together to form microbial granules which resemble activated sludge flocs. Granular microbial growth have been considered as a special case of biofilm growth (Beun *et al.,* 2002) and are reported widely as synonymous with biofilm growth. Although flocs and microbial granules form biofilm-like assemblages, they are not biofilms because they are not attached to a solid surface. Particle-supported biofilms are common in biological fluidized bed systems (BFB).

Process intensification

Large scale wastewater treatment plants have certain considerations in plant construction; economies of scale, process intensification, alternative reaction system, efficiency, and cost reduction (Atkinson, 1981). Process intensification involves the use of methods that allow for a reduction in the size of individual process units while maintaining optimum plant performance (Cooper and Atkinson, 1981), and is of economic benefit in operating treatment plants. The use of biofilm reactors in biological wastewater treatment helps achieve the aim of improving overall efficiency of the treatment processes. Wastewater treatment plants based on biofilm reactors are compact, highly resistant to toxic shock loads and variations in temperature. Following the development of processes combining attached and suspended growth, the application of biofilm reactors in medium and large scale wastewater treatment plants stimulated the development of many processes (von Sperling, 2007a). The costs and availability of land, the demand of plants to meet secondary treatment standards while producing effluent of high standard, maintaining low carbon footprint and compliance with waste minimization are all factors that highlight the need for process intensification (Leikness and Ødegaard, 2006). The types of biofilm reactors developed to enhance process intensification of BNR processes include; Biological fluidized beds (BFB), Moving biological bed reactors (MBBR), Integrated fixed film activated sludge systems (IFAS), Expanded bed biofilm reactors (EBBR).

1.2.6 Expanded bed biofilm reactors (EBBR)

Expanded bed technology involves the use of biological fluidized bed reactors (BFBs). In a fluidized bed reactor (FBR) a fluid is passed through a bed of granular solid material (particles) at high enough velocity to suspend the particles and cause them to behave as if they were a fluid. When the upward drag force of the fluid exceeds the gravitational force, the particles become suspended (fluidized) in the liquid flow thereby expanding the bed. A biological fluidized bed (BFB) is a hybrid of two processes; an attached growth (fixed-film) process in which microorganisms are grown on solid support particles forming a biofilm, and a fluidized process where the particles are suspended within a reactor (Cooper and Atkinson, 1981). Thus, unlike in trickling filters, the fixed-film medium in BFBs is not stationary but moves in the mobile phase of the reactor but is not transported by it. The small support particle size provides a large surface area per unit volume available for growth (e.g. 1.0 mm particles provides 2 400 m^2 m^{-3} at 50 % bed expansion) and high biomass concentration (25 kg m^{-3} dry weight) with a high overall rate of reaction (1.7 ± 0.6 kg NH_3-N m^{-3}_{EBBR} d^{-1}), (Dempsey *et al.,* 2005). The BFBs are also referred to as particulate biofilm reactors and while the bioparticles are fluidized and initial bed expanded by the upward flowing liquid, biological growth within the expanded bed column causes further bed expansion and are therefore referred to as expanded bed biofilm reactors (EBBR).

A model of a biological fluidized bed is shown in Figure 1.2 (Atkinson, 1981). The early models were based on single columns and fluidization and oxygen supply were

supplied to the expanded bed together. This probably made the process quite difficult to control. Modern fluidized beds have improved in design and processes e.g. increase bed height due to biofilm growth and oxygen supply can be controlled with little disturbance to the reactor set up.

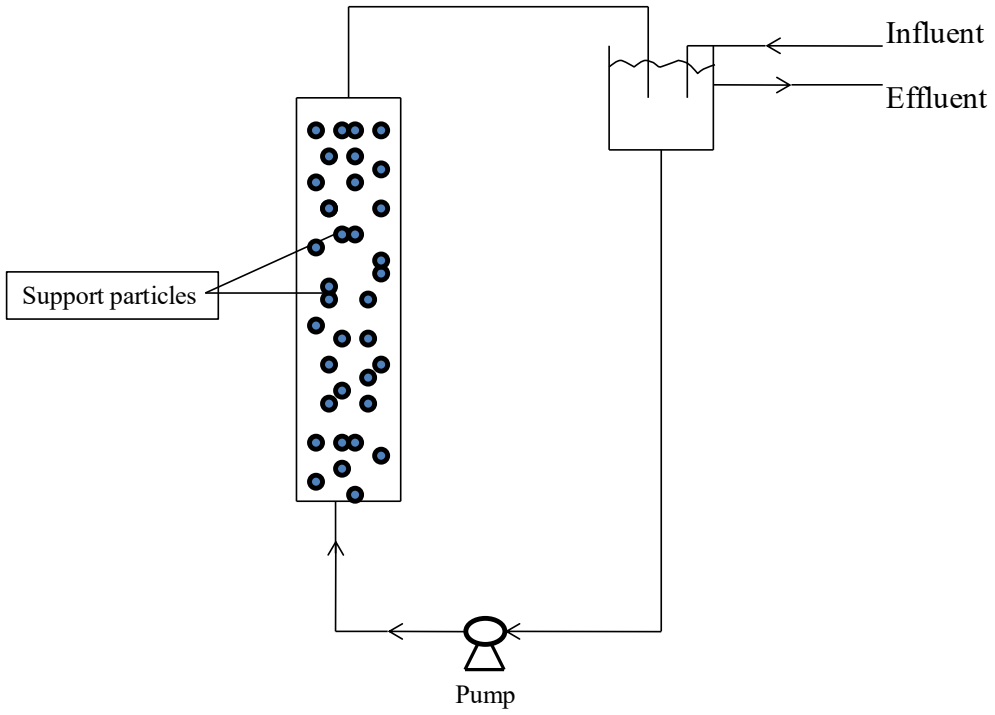

Fig. 1.3 A completely mixed biological fluidised bed (Atkinson, 1981)

Advantages of the EBBR systems when utilized in nutrient removal systems in advanced wastewater treatment include;

- The microbial cells are immobilized as biofilms and are separated from the bulk fluid and therefore retained in the reactor, thus removing the necessity for recovery of biomass from effluent or clarification of effluent before discharge.

- Process intensification; they provide a high support surface area per unit reactor volume, which gives EBBRs high reaction rates, thus reactors are smaller and the requirement for large land space for wastewater treatment processes is reduced.
- The systems have a greater stability against shock loading and do not require backwashing because clogging is not a problem (Noguerira *et al.,* 1998; Rodgers *et al.*, 2005; McQuarrie *et al.,* 2007).
- High biomass concentrations (25 – 40 kg m^{-3}) are achieved in EBBRs and therefore high substrate conversion efficiency resulting in low hydraulic retention times in the reactors (Nicolella *et al.,* 2000b; Dempsey *et al.,* 2005).
- The fixed biofilms used in EBBR separates the active microbial community from the bulk liquid phase and removes problems of sludge bulking and sludge foaming (foam formation) by the biomass (Wagner *et al*., 2002)
- A steady operational particle biomass hold up and a minimization of sludge production, (Dempsey *et al.,* 2005)
- Dempsey *et al*., (2006) reported that an EBBR developed for tertiary nitrification of activated sludge final effluent, achieved a high degree of nitrification and achieving up to 99 % ammonia removal alongside suspended solids removal (up to 56 % SS removal), reduction in BOD, *Escherichia coli* and other coliforms.

Other types of particulate biofilm reactors include;

a. Upflow sludge blanket (USB) and its variant expanded granular sludge blanket (EGSB). In these sludge digestion systems, particles are kept in an up-flowing influent wastewater and microorganisms form sludge granules within the biological bed.
b. Biological aerated filter (BAF) and Biofilm airlift suspension (BAS) where an airlift suspension is obtained by pumping air into a system. In BAFs, the active biomass is grown inside a vessel like a deep filter bed. Coarse rounded particles are used as filter media and the biofilms form on the surface of the filter media. Because the biofilm grows in the interstitial spaces and the low flow rate, the biofilms are involved in both filtration and biological treatment of the wastewater. The main disadvantage of the BAF system is that it requires backwashing due to the clogging of the media bed.
c. Internal circulator reactors (IC). The IC reactors consists of 2 reactor compartments; the first contains an expanded granular sludge bed with an internal circulation flow and the effluent produced is post treated in the second low loaded compartment.
d. Recent developments in nutrient removal systems have combined fixed biofilm reactors with the traditional activated sludge systems e.g. hybrd biofilm activated sludge system (HYBAS) systems which combine biological activated sludge with MBBR technology in the same or separate reactor tanks where the nitrate produced by nitrification is

utilized by the heterotrophs in the decomposition of organic components of the wastewaters.

e. Other systems include partial nitrification or nitritation by anaerobic ammonia oxidizing (anammox) bacteria. Ammonia oxidation is followed by nitrite denitrification processes, which can reduce plant oxygen requirements by 25 - 60 % (Guo *et al*., 2009; Wang *et al.,* 2009) and also the carbon source requirement for a standalone denitrification stage by 40 % (Guo *et al*., 2009).

$$NH_4^+ + NO_2^- \longrightarrow N_2 + 2H_2O$$

1.2.7 Dynamics of biofilm formation and growth

Biofilm formation is the result of the colonization of a solid substrate by microorganisms. Upon the attachment of pioneer organisms on a surface, microbial growth and interactions develop forming a complex community of microorganisms which are normally held together and embedded by a matrix of biological origin called extracellular polymeric substances (EPS) (Kerksiek, 2008). Although defined as communities of microorganisms attached to a surface, biofilms may be formed by single or multiple microbial species and can be established on a wide range of biotic and abiotic surfaces (O'Toole *et al.,* 2000). Most often, the ability to attach to and colonise surfaces provides the bacteria with certain advantages, for example, access to nutrients (Fletcher, 1996).

The formation of a biofilm begins with bacterial adhesion to a surface; this often starts as a long ranged, non-specific interactions, and ends with the bacteria establishing short ranged irreversible reactions that help the bacteria to adhere to the surface (Fletcher, 1996). The basic scheme of biofilm formation irrespective of environment involves this attachment by pioneer planktonic cells to the surface. Extracellular polymer substances are often secreted to cement the bacteria to the surface as the final stage of an irreversible adhesion of bacterial cells to an environmental surface (Fig. 1.4). Microcolonies, which are the basic units of a biofilm, are then formed by the recruitment of free floating cells, aggregation of cells and cell division. The microcolonies typically assume a mushroom or pillar shape and are separated from one another by water channels, through which nutrients and oxygen can be transported and wastes removed (Kerksiek, 2008*).*

Fig. 1.4 The attachment, colonization and development of a biofilm on a surface (adapted from Brading *et al*., 1995)

In wastewater treatment processes, slow growing bacteria which have a high washout rate in suspended biomass in conventional activated sludge systems would are developed as biofilm systems. In biofilm reactors, the biofilm consists of EPS and bacteria formed around a support material and entraps particulate materials such as clay, organic materials, dead cells and precipitated minerals, adding to the bulk and diversity of the biofilm habitat. This growing biofilm serves as the focus for the attachment and growth of other organisms, increasing the biological diversity of the community. A complex community of bacteria, fungi, protozoa and mesofauna are often associated with biofilms. Biofilms in wastewater treatment processes also have a wide diversity of macro-invertebrates, such as enchytraeids and lumbricid worms and a host of other groups which all actively graze the biofilm surface (Gray, 1989).

The EPS plays an important role in cell aggregation, cell adhesion and biofilm formation, and protects bacterial cells from hostile environments (Dogsa *et al.,* 2005) and sometimes make up to 85 % of a mature biofilm (Kerksiek, 2008). EPS is composed of a wide variety of organic material; including polysaccharides, proteins, nucleic acids, phospholipids, uronic and humic substances (Zhang and Fang, 2001) and is mainly responsible for the structural and functional integrity of biofilms (Raszka *et al.*, 2006). Most of the EPS of biofilms are polymers containing sugars such as glucose, galactose, mannose, fructose, rhamnose, N-acetylglucosamine and others. The composition may actually be a combined result of active secretion, shedding of cell surface material, cell lysis and adsorption from the environment (Zhang and Fang, 2001). The EPS is a highly charged polymer that interacts with water in similar ways as gels – they swell but do not dissolve in aqueous

environments. A great many interactions occur in biofilms, between the biofilm and surface, between different microbial populations in the biofilm and also between the biofilm communities.

The internal structures of wastewater biofilms are complex and are determined by factors such as water quality, substrates, type of microbial population, and type of support material. The development and growth of biofilms can also be described as a balance of the interaction between two major processes; “positive” processes like cell attachment, cell division, and polymer production, which causes biofilm volume expansion, and “negative processes, like cell detachment and cell death, which contribute to biofilm shrinking (Picioreanu, *et al.,* 1999). In EBBRs, because nutrients and substrate essential to particulate biofilms are dissolved in the bulk fluid that bathes the bioparticles, biofilm growth is driven by the fluid flow in the reactor. This is because the fluid flow in the reactor regulates the concentration of substrates and products at the biofilm - liquid interface (Picioreanu, *et al.,* 1999; Wuertz, 2003).

Biofilm structure

Traditionally, development of a biofilm was seen as the formation of a layered structure growing from substratum upward in a continuous, smooth biofilm matrix – the one dimensional model where all the properties e.g. substrate concentration, vary only in one direction; from the bulk liquid to the carrier surface (homogenous, planar biofilm structure; Picioreanu *et al.,* 1999). Microscopic tools e.g. scanning electron microscope (SEM), transmission electron microscope (TEM), atomic force

microscope (AFM), and especially the confocal laser scanning microscope (CLSM) (which allows for the examination of successive focal planes within an intact hydrated biofilm), used in the study of biofilm communities have been vital in identifying biofilms communities as microcolonies of organisms enclosed in a matrix that is interspersed with highly permeable water channels (Costerton *et al.,* 1994; Noguera *et.al.*, 2004). While in a mono species biofilm, each individual bacterial cell clearly occupies a unique spatial niche that is within a microcolony of sister cells of the same strain, studies have shown that multi species biofilms e.g. wastewater biofilms, do not necessarily grow in a confluent film over a surface, but microorganisms attach to the surfaces and form small microcolonies rising from the surfaces (Costerton *et al.,* 1994; Walker *et al.,* 1995). Because at the surface of the biofilm, fluid flow determines biofilm growth by regulating the concentration of substrates and products at the liquid-solid interface, while the flow itself shears the biofilm surface, eroding protuberances and cells, the biofilm is regarded as a dynamic structure evolving in non steady-state conditions described as a heterogeneous biofilm (Picioreanu *et al.,* 1999). The heterogeneous mosaic models describes biofilms as microcolonies consisting of stacks of bacteria held together by EPS, and appear as columns surrounding by a liquid phase (Fig. 1.5).

Within biofilms there is significant spatial variability in microbial activity, biofilm density and even shape of the biofilm e.g. Wimpenny and Colosanti (1997) and van Loosdrecht *et al.* (1997) reported that the shape of a biofilm is determined by the environmental conditions, like availability of substrates and hydrodynamics, while Eberl *et al*. (2000) noted that mass transfer conversions in biofilms are strongly

affected by surface roughness and hydrodynamic conditions. Therefore, upon microbial attachment to a substratum, a biofilm may develop with non uniform physical properties. The biofilm can then mature as clustered, columnar or mushroom growth (Wuertz, 2003). The mushroom model where the biofilm consists of mushroom shaped cell aggregates with stalks narrower than the upper surface parts, and the whole biofilm penetrated by channels through which a liquid phase is free to move with the prevailing flow (Wimpenny *et al*., 2000). The channels and pores carry substrates, e.g. oxygen, around and between the mushroom stacks (Fig. 1.5).

Microscopic examinations show that biofilms grow in many forms, including dense mats, mushroom shape (Fig. 1.5) and finger shape (Bishop, 2003). Two schools of thought exists for the development of biofilms on a substratum; Tanaka and Dunn (1982) and Wantanabe *et al*., (1985) proposed that the distribution of different populations within a biofilm was arbitrary, but Kessel *et al*., (1985) and Wanner 1985 and Gujer, 1986 reported that microorganisms grow inside the biofilm and displace other components; therefore there is a localized biomass displacement velocity perpendicular to the substratum and this displacement velocity is proportional to the growth rate at each depth within a biofilm.

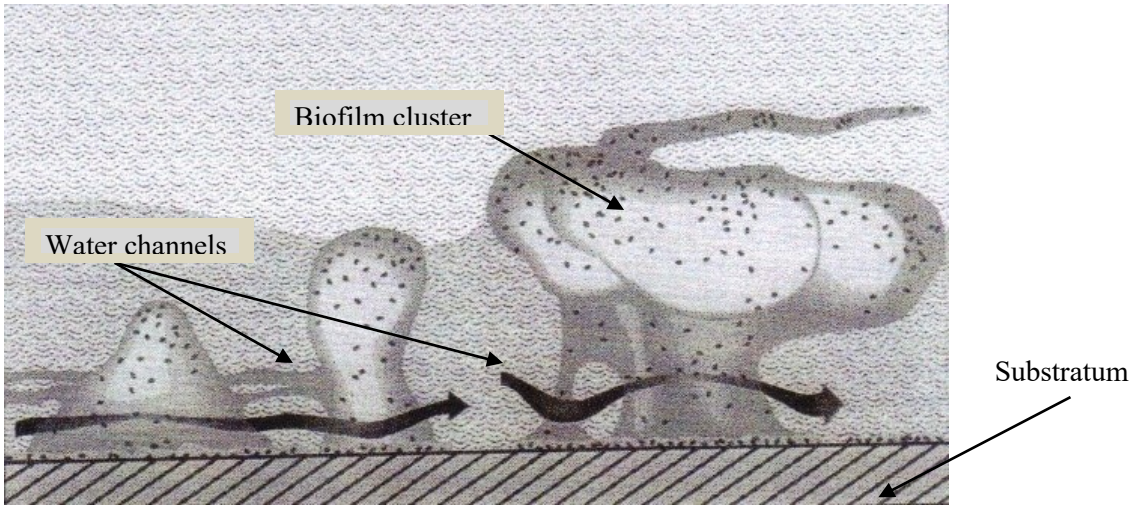

Fig. 1.5 Diagrammatic representation of the structure of bacterial biofilm drawn from confocal scanning laser microscopy of a mixed species biofilm (Costerton *et al.,* 1994)

The study of the intact fully hydrated biofilm has been greatly aided by the advent of the confocal laser scanning microscope. The CLSM, unlike other methods like SEM and TEM, does not require the dehydration and fixation of the biofilm, and therefore avoids the problems of the shrinking or destruction of the biofilm during preparation for viewing or the production of artefacts during the specimen preparation. The CLSM uses high intensity lasers to scan through sequential planes of a sample. When combined with fluorescent microscopy, CLSM becomes a powerful tool in the study of the structure of biofilms as the excitation of florescent dyed biofilms causes the detection of only the emitted light from the focal point of interest as the CLSM is fitted with special lenses which allows for the appropriate wavelength to be selected the thereby reducing noise and distortion of image. The movable stage of the CLSM allows it to capture 3-dimensional (3D) images of biofilms by scanning sections of a

sample on the same x and y- axis plane and while moving along a depth (z-axis). The images can then be compiled or stacked (z-stack) to give a complete 3D image with the use of specialized software (Merod *et al.*, 2007).

1.2.8 Coke support and bioparticle formation.

The high reaction rate per unit volume of the expanded biological bioreactor is based on the natural immobilization of microorganisms to small support particles (Dempsey *et al.,* 2006). Atkinson (1981) reported that mixed microbial cultures associated with wastewater treatment have excellent adhesion characteristics and readily form continuous layers of immobilised biomass on materials and the biomass particles for biological fluidized beds can be prepared in any required shape. The type of support used in the biofilm reactors is of great importance to obtain a stable biofilm and high reactor efficiency (Oliviera *et al.,* 2003) and the surface area provided by the support material is affected by surface texture and particle shape; rough porous media provide a greater surface area than smooth surface media of the same size (Gray, 1989). Sand, carbon, anthracite, glass, of 0.2 – 0.3 mm size range have been used as support materials in fluidized bed bioreactors and although particles of any size, shape and density can be produced, spherical particles have been found to fluidise easily (Atkinson *et al.*, 1981). Dempsey (2003) found glassy coke to be an excellent support for biofilm formation in EBBRs. Glassy coke (coke) is a grey, hard, carbon-based material derived from the destructive distillation of coal. When coal is heated to temperatures of 1000 ^{0}C in a confined space, the volatile portions are driven off and fixed carbon (90 %) and residual ash (10 %) are fused

together to form coke as one of the by products. (Schobert, 1978). Coke has a bulk density of approximately 0.8, is highly porous, hard and inert. Coke has an ignition temperature of 700 ^{0}C and a specific gravity of 1.1.

As the glassy coke is porous, it allows for the natural colonization and immobilization of the microbial species within the interconnecting coke pores (Fig. 1.6), away from the biofilm detachment force of the up flowing bulk liquid. The bioparticles are formed by the microorganisms growing out of the pores and embedding the coke particles, thereby forming a biofilm around the particles (Dempsey, *et al.* 2005). The term particulate biofilm was used by Nicolella, *et al.,* (2000a), and indicates the fact that every particle develops its own biofilm. In expanded bed bioreactors, as biological growth occurs in the particulate biofilms, their volume increases while their overall density decreases. This results in further expansion of the expanded bed.

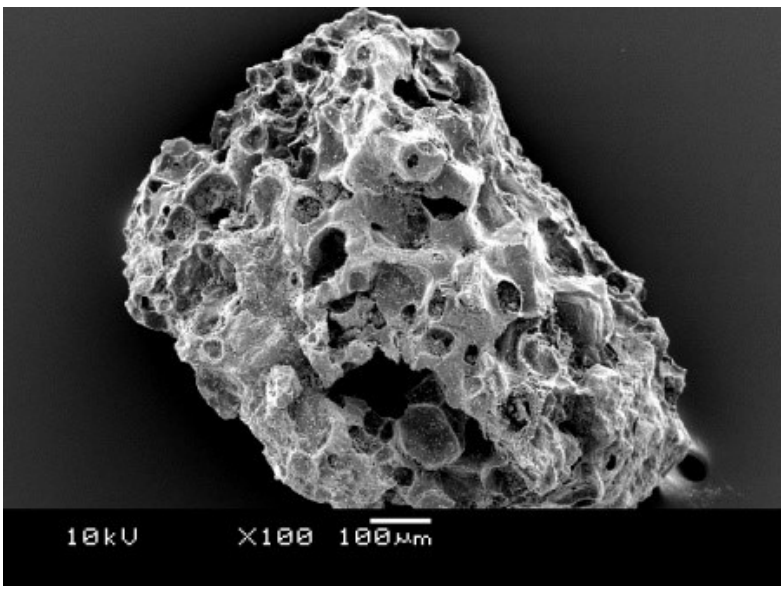

Fig. 1.6 SEM micrograph of a coke particle showing the interconnecting coke pores.

1.2.9 Mass transport in biofilms and the effect of biofilm thickness

Particle based biofilm reactors which are either three phase (gas – liquid – solid) where gas and liquid are both passed through the expanded bed column (Nicolella *et al.,*2000a) or two phase, as was used in this study; (liquid - solid), where the fluidized bioparticle constitutes the solid phase within the bulk liquid phase. The overall transformation of substrate in both biofilm reactors is diffusion dependent (Gulevich *et al.*, 1968). In two phase biofilm reactors, substrates diffuse directly from the liquid phase into the biofilm, which means that the biofilm itself acts as a "static reactor", because the nutrients are transformed by microorganisms as they penetrate into the biofilm. In aquatic heterogeneous biofilms, as water moves within the space occupied by the biofilm, because the biofilm is porous and the microcolonies of bacteria are separated by voids, the voids and the microcolonies consequently would have different mass transfer rates within them (Lewandowski and Beyenal, 2003). Flemming and Wingender (2003), reported that the performance of biofilm reactors is highly dependent upon the diffusion processes, which can be rate limiting. Mass transfer through the biofilm therefore constitutes a major factor influencing the activity of the particulate biofilm and this has to be considered in the design of the biofilm reactor.

Compared to planktonic cells, therefore, the activity of cells in biofilms is restricted by diffusional limitations because of reduced fluid flow within the biofilm and the diffusional distance from the bulk liquid to the point of use of the nutrients (Stewart, 2003). In addition, because substrates have to cross an interface (boundary layer) and

be transported through the biofilm to reach microbial cells, the penetration depth depends on the substrate concentration in bulk fluid, mass transfer at the biofilm – liquid interface and reaction rate within the biofilm (Nicollela, *et al.*, 2000b). Significant differences in biofilm thickness would therefore affect the penetration depth of substrates in the biofilm. This variation in substrate supply indicates that the rate of reaction within the biofilm would be influenced by the biofilm thickness and that the variation of substrate distribution would also affect the distribution of the microbial population across the biofilm. Notwithstanding the microcolony or cell cluster formation of biofilms with water channels, there is evidence that the 3-dimensional structure of the biofilm is determined by the flow velocity in which they develop (Beyenal and Lewandowski, 2002).

Continued growth of a biofilm microbial population, which leads to increase in the biofilm thickness, would therefore result in a change in mass transfer rate, reaction rate and hydrodynamic characteristics of the bed (Nicolella *et al.,* 2000b). The water channels in the biofilms do not guarantee access of substrates to the interior of cell clusters. This is because the water may flow through channels but not percolate the cell clusters themselves (Stewart, 2003). Thick biofilms may therefore not reach the activity potential supposed for their high biomass concentrations, and thus act as inefficient “static reactors”. Because growth rate in a biofilm is a function of nutrient concentration that diminishes in deeper parts of the biofilm and also because each microbial population competes for space in the biofilm (Hermanowicz, 2003), the microbial distribution in the biofilm may therefore be stratified or occur in layers perpendicular to the substratum (Fig. 1.7).

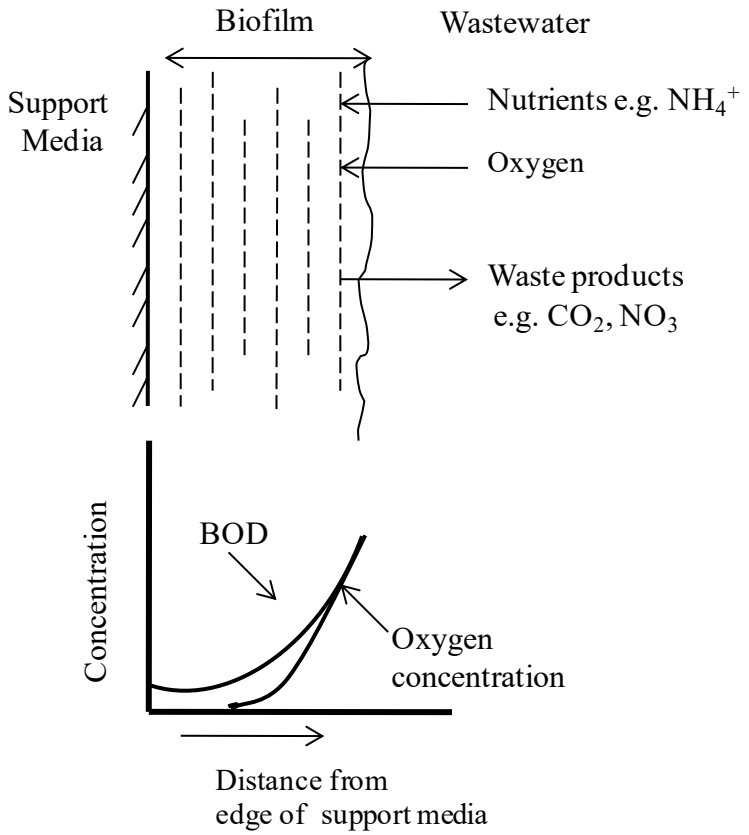

Fig. 1.7. Oxygen and substrate concentration gradient across a biofilm (adapted from Horan, 1990)

1.2.10 Oxygen requirement for wastewater treatment systems

In wastewater treatment processes, bacteria are primarily responsible for the oxidation of organic matter; while fungi, algae, protozoa and some higher organisms have secondary roles in the transformation of soluble and colloidal organic matter into biomass. Both aerobic and anaerobic organisms are present in wastewater treatment process, however, aerobic bacteria are predominant, both in biological wastewater treatment processes and natural watercourses, and utilise oxygen as the

terminal electron acceptor during respiration. The autotrophic aerobic bacteria present in wastewater treatment systems do not utilize organic carbon as their carbon source. Instead, they oxidize inorganic compounds for their energy source while they obtain carbon from dissolved carbon-dioxide. Heterotrophic bacteria therefore, are the main organic matter oxidizing bacteria in wastewater treatment systems (Gray, 1989) e.g. nitrifying bacteria have $1/5^{th}$ of the biomass growth coefficients (biomass produced per unit substrate used) of heterotrophic bacteria in wastewater treatment (Ekema and Wentzel, 2008).

Oxygen is slightly soluble in water (8.5 mg L^{-1}, 25 ^{0}C) and dissolving oxygen in water involves the oxygen molecules being transferred across the gas film of an air bubble to the bulk liquid film. Because the rate of heterotrophic cell metabolism is limited by BOD, the rate of microbial metabolism will determine the rate of oxygen demand. If the oxygen demand exceeds the rate at which oxygen diffuses through the liquid film, oxygen will become limiting (Horan, 1990). In conventional activated sludge processes, the oxygen transfer yields range from 0.6 to 4.2 kg O_2/ kWh, according to the method of aeration (Horan, 1990).

Oxygen demand of ammonia oxidizers

Classical nitrification by nitrifying bacteria is an aerobic process and nitrifying bacteria use dissolved oxygen (DO) as the terminal electron acceptor. The DO concentration in biological reactors is generally between 2 to 3 mg L^{-1} (WEF, 1998). Nitrification is inhibited at low DO concentrations; although Gray (1989) stated that

nitrification does not occur below 0.2 – 0.5 mg L^{-1} in the activated sludge system, while Dempsey *et al.,* (2005) found the limiting DO concentration to be 1.0 mg L^{-1} for EBBR processes. Using an expanded bed bioreactor, Dempsey *et al.* (2005) described the relationship between DO concentration and ammonia concentration in expanded bed nitrification and reported that, the nitrification process became oxygen limited above NH_3-N concentration 1 mg m^{-3} and below this concentration, the process was ammonia limited (Fig 1.8). The oxygen requirements for nitrification are more demanding than for BOD removal; 1.5 kg of oxygen is required to oxidize 1 kg of BOD while about 4.57 kg of oxygen is required to convert 1 kg of ammonia to nitrate (EPA, 2002; Ekema and Wentzel, 2008).

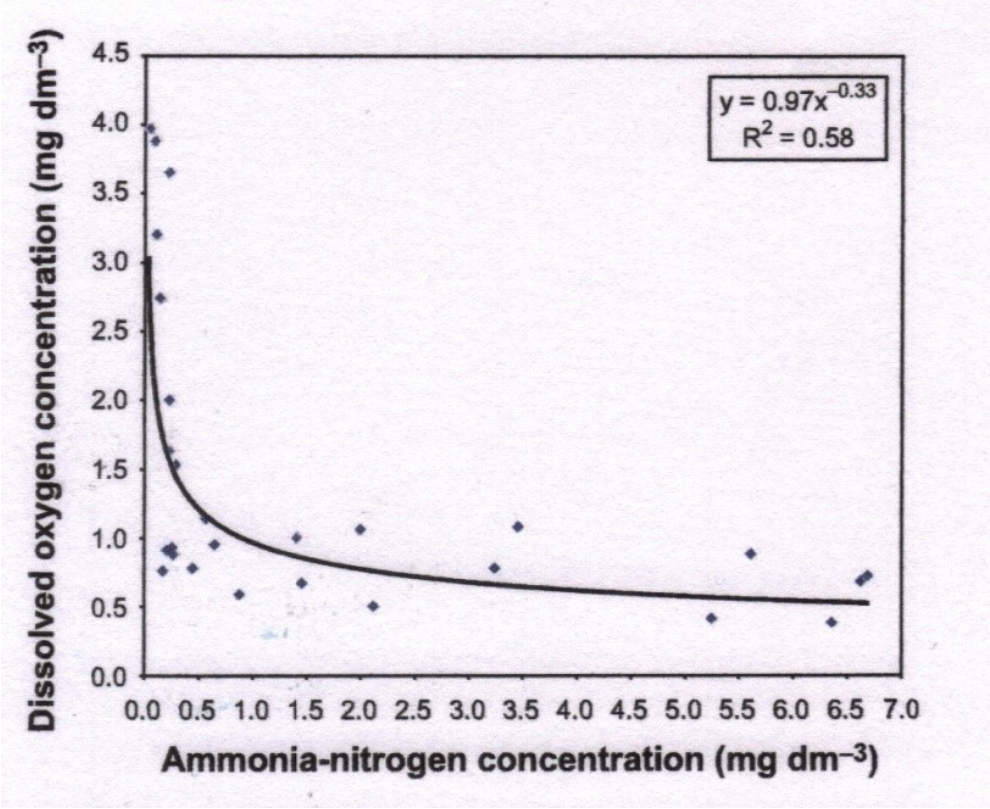

Fig 1.8 The effect of the ammonia limiting concentration on oxygen uptake (Dempsey *et al*., 2005)

Oxygen transfer mechanisms

In aerobic wastewater treatment systems, where air is bubbled through the reactor system, the oxygen is initially transferred across the gas film to the liquid film layer of the gas bubble and then by diffusion into the bulk liquid. From the liquid film, the oxygen then diffuses across the microbial cell wall into the cells, following Fick's law which states that gases move spontaneously from regions of high to low concentrations (diffusion) (Horan, 1990). Because oxygen diffuses from the bulk fluid into the microbial cells, in particulate biofilm systems, oxygen would also diffuse from the bulk liquid through biofilm to reach the individual cells. Increase in biofilm thickness therefore creates an oxygen gradient across the biofilm (Fig. 1.7), and because oxygen is consumed as it diffuses into the "static reactor", oxygen becomes a major reaction-limiting factor for the biofilm processes like nitrification. The thickness of biofilm on a support particle therefore develops an ever increasing gradient with bacterial growth and therefore is a major influence on the substrate conversion rates within the biofilm.

1.2.11 Quantification of biofilm nitrifying population using Fluorescent *in situ* hybridization (FISH)

Fluorescent *in situ* hybridization (FISH) involves the use of fluorescently labelled oligonucleotide probes for the detection of 16S rRNA sequences within prokaryotic cells. FISH is a method for the detection and localization of specific DNA sequences on chromosomes. In FISH, preformed nucleic acid sequences tagged with a

fluorescent dye (gene probes) are used to target and bind DNA sequences that have a high degree of similarity and the hybrids or complexes can then be viewed upon excitation with fluorescent light. The phylogeny, morphology, localization, abundance and activity of microorganisms are investigated using FISH (Daims *et al.,* 2005).

Hybridization of the probe with the target gene sequence enables the detection of the specifically targeted organisms by techniques such as epifluoresence microscopy, which use optical filters to block out light except the specific excitation and emission wavelengths of the fluorescent compound. An advantage of FISH techniques is that the relative abundance of different species of bacteria in complex communities like biofilms can be determined (Daims *et al.,* 2005); FISH has been used to provide information about cell activity in environmental samples (Bitton, 2005), and has been useful in the study of biofilm organisms because it enables the use of multi-FISH probes to identify different groups of microorganisms. The combination of FISH and CLSM enables both the determination of abundance and the observation of the localization and spatial distribution of biofilm microorganisms which gives an indication of interactions and metabolic networks within the biofilm community (Koops and Prommerening-Roser, 2001; Diams *et al.,* 2005).

Objectives of study

The objectives of this study were to investigate the potential of expanded bed biofilm reactor technology for oil refinery wastewaters treatment by:

a. Developing a lab-scale expanded bed bioreactor (EBBR) with nitrifying particulate biofilms for nitrification. (The impracticality to obtain constant supply of oil refinery wastewaters to maintain the continuous culture system of the bioreactor required the use synthetic wastewaters mimicking the ammonia concentration of oil refinery wastewaters).
b. Optimising the nitrification process using response surface methodology (RSM) to determine the optimum pH and temperature for that nitrification rates. (Due to the inability to get a constant supply of oil refinery wastewaters, synthetic wastewater modelled after the concentration of oil refinery wastewater found in the literature (Xianling *et al.,* 2005), was used to operate the lab-scale expanded bed bioreactor on a continuous culture basis).
c. Investigating the influence of biofilm thickness on the nitrification rate of the biofilm nitrifying population.
d. Investigating the spatial distribution and quantify the ammonia and nitrite oxidizing population of the particulate biofilm using FISH.
e. Investigating the influence of the oil refinery wastewaters on the biofilm nitrifying population.

CHAPTER TWO

2.0 The optimization of the nitrification process.

2.1 Introduction

The specific growth rate of nitrifying bacteria is influenced by environmental factors such as pH, temperature, dissolved oxygen concentration, inhibitory substances and limiting substrate concentration (von Sperling, 2007b). In activated sludge wastewater treatment plants, the maximum growth rate (μ_{max}) of the nitrifying bacteria is of utmost importance because it determines the minimum mean cell residence time below which washout of nitrifying bacteria would occur (Antoniou, *et al.,* 1990). Although washout of these bacteria is not a problem in biofilm reactors like the EBBR, the effect of environmental factors on the maximum growth rate will be evident in the nitrification rate within the bioreactor.

The factors influencing the nitrification process in wastewater treatment include:

a. Dissolved oxygen - (DO) is a rate limiting factor for the aerobic nitrification process and although high (up to 33 mg O_2L^{-1}) oxygen concentrations do not appear to affect nitrification rates significantly, low (< 0.3 mg L^{-1}) DO concentration reduces nitrification rates (Ekema and Wentzel, 2008). Dempsey *et al*., (2005) showed that DO concentrations of 1.0 mg L^{-1} is rate limiting in EBBRs (Fig. 1.8).

b. pH - Different authors have reported different optimum pH ranges for nitrifying bacteria (7.5 – 8.0, Prosser, 1989; 7.0 – 8.2, Antoniou *et al.,* 1990) but mostly

between a pH range of 6.5 to 8.5. However, Prosser (1989) noted that nitrifying bacteria, like most bacteria, have pH optima and grow in the range of with a pH range of approximately 2 pH units. Using pure cultures of *N. europaea* and *Nitrobacter sp,* Prosser (1989), found out that the maximum specific growth rate of *N. europaea w*as 0.0048 h^{-1} at 7.5 and at pH 6.0 the maximum growth rate reduced by 59 % and no growth was observed at pH 5.5, while *Nitrobacter sp* had a maximum growth at pH 8.0, which fell by 54 % by 7.0 and no growth was observed at pH 6.5.

The effect of pH on nitrifying biofilm activity is brought about by three ways. The first is the ability of H^+ and OH^- ions (at low and high pH respectively) to bind to weak basic-acid groups of enzymes and thereby blocking the active sites. Secondly, the availability of carbon mainly from CO_2 depends on pH because at low pH, CO_2 will be eliminated by stripping and at high pH CO_2 will be transformed to insoluble carbonate. Thirdly, free ammonia and nitrite concentrations are affected by pH; free ammonia concentration increases with increase in pH while nitrous acid concentrations rise at low pH (Villaverde *et al.,* 1997). Suzuki *et al.,* (1974) reported that ammonia rather than ammonium ion is the actual substrate for oxidation in bacterial cells but the exact concentration of ammonia in water depends on the pH because free ammonia in equilibrium with ammonium ion is affected by these parameters (Wuertz, 2003). The pH therefore plays an important role in the nitrification rate within the biofilm as the excess ammonia in the wastewater available to diffuse into a biofilm is dependent on the pH of the medium in the bioreactor.

$$\text{low pH} \quad NH_4^+ + OH^- - \quad \rightarrow \quad NH_3 + H_2O \text{ high pH,}$$

.....*2.1*

Furthermore, because ammonium oxidation is the rate limiting step of nitrification, the influence of pH on the ammonium ion -ammonia balance affects the rate of nitrification and is considered to be the most important effect of pH on nitrification rates (Villaverde *et al.*, 1997).

c. Temperature - Increase in temperature causes an increase in the rate of growth of both ammonium and nitrite oxidizers, however, nitrifying bacteria and take much longer to respond to changing conditions of operations at lower temperatures than at 20 ^{0}C (Painter, 1986). The maximum growth rate of nitrifying organisms is also significantly affected by temperature. Ekema and Wentzel (2008), reported that in nitrifying bacteria, for every 6 ^{0}C reduction of temperature, the specific growth rate of nitrifying bacteria (at 20 ^{0}C) reduces by half, however, nitrification has been observed between 5 to 50 ^{0}C (von Sperling, 2007b). Microbial nitrification rate increases with increase in temperature, at high temperatures however, the nitrification rate can be reduced due to the increase of free ammonia at higher temperatures (Kim *et al.,* 2006). In wastewater treatment, increase in temperature can affect the species composition of the bacterial population (Painter, 1986).

Investigating the optimum pH and temperature of the lab scale EBBR was important because the EBBR is a novel type of bioreactor and understanding the optimum conditions for EBBR nitrification is vital for establishing full scale reactors. Also, the

EBBR process involves a multispecies biofilm whereas most investigations on the optimum pH and temperature of nitrifying bacteria have been carried out with pure cultures of nitrifying bacteria. Although the optimum pH and temperature of the bioreactor may still be in the normal range for nitrification, the optimum conditions for nitrification would be influenced by the balance of the different species present in the biofilm.

d. Several compounds have been reported to inhibit nitrification e.g. N- allylthiourea (ATU), nitrapyrin (2-chloro-6-(trichlorormethyl) pyridine, potassium ethyl xanthane, salicyaldixime, MAST (2- amino -4- methyl -6- trichloromethy l -1, 3,- triazine) (Matsuba, *et al*., 2002) have chelating properties which inhibits the enzyme ammonia monooxygenase and therefore the nitrification process (Powell, 1986).

Major advancements in developing efficient wastewater treatment facilities involve the development of engineering designs for the process and the optimization of the biological process. A bridge between these two disciplines requires modelling of the performance of the bioreactor coupled with the use of computer software, e.g. where the biological parameters can be imputed and data generated.

Response surface methodology (RSM) is a powerful optimization tool in statistical design and analysis of experiments that accelerates process optimization. The objective of process optimization is to determine the necessary process input values to obtain an optimum desired output and involves the substitution of an output value for the response variable and solving for the associated predictor variable values

(Anderson and Whitcomb, 2007a). RSM is used to design experiments where more than one process variable ("factor") is altered at a time. This allows interactions between factors to be examined, which is not possible with conventional "one-at-a-time" designs. Therefore, complex systems can be investigated with one set of experimental runs. RSM is also used to estimate interactions and responses, therefore giving an idea of the (local) shape of the response surface being investigated and is meant to lead to the peak of process performance; it can also predict possible performance outcomes of a combination of the factors being considered (Anderson and Whitcomb, 2005).

The work covered in this chapter includes;

- The construction of the lab-scale expanded bed biofilm reactor.
- Seeding the bioreactor with bioparticles and maintaining the bioreactor in continuous culture using synthetic wastewater and investigations into the optimum conditions of continuous culture operation of the bioreactor e.g. investigation of the effect of bed expansion on nitrification rates.
- Investigating the surface of the biofilm using scanning electron microscopy.
- The optimization of the nitrification process was with a focus on the pH and temperature using response surface methodology (RSM).

2.2 Materials and methods

2.2.1 Expanded bed biofilm reactor

The design of a biological fluidized bed should aim at minimum hardware complexity, easy operation, the ability to remove and add particles without disturbing attached biomass, a steady biomass hold up within the reactor and a high particle support per unit area within the reactor (Atkinson, 1981). The lab-scale EBBR (Fig. 2.1) was constructed from borosilicate glass components (QVF Corning Process Systems, UK). It comprised two connected vertical columns; an expanded bed column (58 x 4 cm) and an aeration column (45 x 2 cm) that also served as a wastewater recycle column (Fig. 2.1).

The columns were connected with silicone tubing and the influent and effluent sampling points were fixed. The expanded bed was seeded with nitrifying bioparticles grown on glassy coke support particles of 0.7 - 1.0 mm diameter obtained from a pilot-plant for tertiary nitrification of activated sludge settled effluent (Dempsey *et al*., 2005). The bioreactor was fed with synthetic wastewater using a peristaltic pump (Watson Marlow 502S, UK), while the expanded bed was maintained at 50 % bed expansion by the upward flowing synthetic wastewater, flowing at a velocity of 1 cm sec^{-1}, supplied by another peristaltic pump (fluidizing pump) (Watson Marlow 505S, UK) (Fig. 2.1).

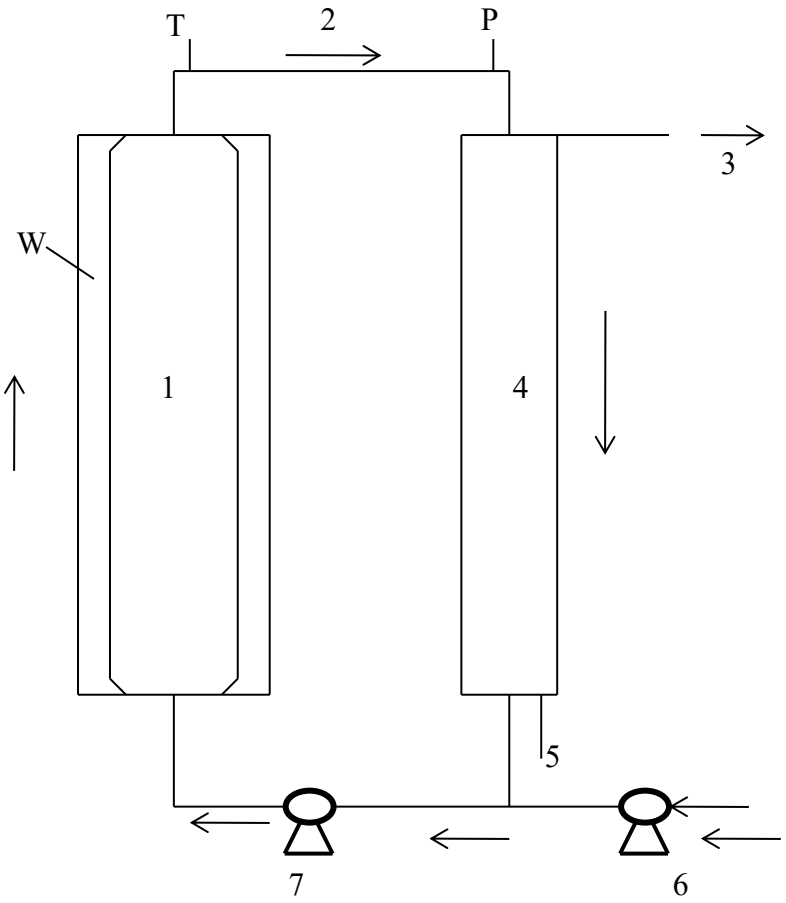

Fig. 2.1 Schematic diagram of the lab-scale expanded bed bioreactor

1 – Expanded bed column, 2 - Recycle, 3 - Outlet, 4 - Aeration column, 5 - Air inlet, 6 - Feed pump, 7 - Fluidizing pump. T – Temperature sensor, P – pH sensor, W – Water jacket for temperature control

The bioreactor had a total volume of about 700 cm^3 and was maintained in continuous culture operation with synthetic wastewater. Rodgers *et al.* (2005) reported that the microbial population of the biofilm is dictated by the type of wastewater and the environmental conditions, therefore in order to maintain the population of autotrophic nitrifying bacteria seeded into the expanded bed, synthetic

wastewater without a source of organic carbon (NH_4HCO_3 0.7 g L^{-1}; K_2HPO_4 0.4 g L^{-1}; KH_2PO_4 0.3 g L^{-1}; $MgSO_4.7H_2O$ 0.4 g L^{-1}, van Neil *et al.*, 1993) was used as bioreactor influent. The ammonia –nitrogen (NH_4^+-N) concentration was increased to achieve the desired concentration of 125 ± 10 mg L^{-1}, to simulate the ammonia concentration of oil refinery wastewaters (Xianling *et al*., 2005).

The main aim of wastewater treatment systems is to remove all polluting matter in wastewater. Biologically, this is achieved by oxidizing all the polluting substrates or reducing the concentration of the oxidizable substrates in the effluent. In activated sludge systems, a method used to achieve this target is the recycling of the microorganisms (by recycling sludge back into the aeration tank) to maintain a high cell - substrate contact. In the lab-scale EBBR, however, the wastewater or effluent leaving the expanded bed column (without bioparticles) was recycled via an aeration column. Recycling of the wastewater increased the bioparticle – wastewater contact time and also served to aerate the system as compressed air was injected at the base of the aeration column through which the liquid phase was re-circulated (counter current to the liquid flow, Fig. 2.1). The compressed air flow was measured by a GAP airflow meter, UK and set at 700 L cm^3 (1.0 VVM). The oxygenated wastewater from the aeration column combined and diluted influent wastewater from the feed pump and ensured that oxygenated influent wastewater always flowed into the expanded bed column. A constant reactor volume was maintained by the outlet point at the top of the aeration column that balanced the outflow from the reactor with the inflow into the reactor. The temperature of the expanded bed column was controlled using a thermo-circulator (Thermo Haake K10, USA), via a water jacket

which enclosed the column. The thermometer and pH sensors were placed in the connecting tubing between the expanded bed column and the recycle column and measured the temperature and pH of the wastewater flowing out of the expanded bed column; they therefore measured the temperature and pH of the wastewater after contact with the bioparticles. The pH of the bioreactor was controlled using NaOH (10 g L^{-1}) which was supplied by a pH controller (Electrolab 260, UK). Because nitrification results in the lowering of the pH of the immediate environment due to the production of H^+ ions; the oxidation of 1 mg N uses up about 7 mg of alkalinity (Painter, 1986). Nitrification activity within the bioreactor therefore reduces the pH of the system. As a result, only alkali, (NaOH), was used to control the pH of the EBBR. The point of NaOH entry into the bioreactor system was positioned after the entry point of feed to ensure adequate alkali dilution before it reached the immobilized biomass. The inlet feed flow rate was calibrated to give a hydraulic retention time of about 0.05 d^{-1}.

To determine the degree of bed expansion, the expanded bed height (EB) was determined by the height of the bioparticle bed when the bed was expanded and operating undisturbed. The static bed height (SB) was determined after the fluidizing pump was switched off and the particles were allowed to settle. The difference in bed height was used to calculate the percentage expansion of the bed and the increase in static bed height over time was calculated as the biofilm growth rate of the bed as it is a more reliable indication of biofilm growth than the expanded bed height, which can be influenced by the gas fraction in the aeration column and the process temperature (Dempsey *et al.,* 2005).

Bed sampling

The influent and effluent wastewaters of the bioreactor were sampled by using a syringe to collect influent and effluent wastewater from fixed points in the bioreactor system. The temperature and pH of the bioreactor were recorded manually as indicated by the respective controllers. Bioparticle samples were obtained from the top of the bed by inserting a silicon rubber tube into the bed to the desired bed height and the bioparticles collected into the tube by suction.

2.2.2 Investigation of bioparticle structure

The biofilm structure was investigated using a phase contrast light microscope (Prior B3000, Cambridge, UK), and also with a scanning electron microscope (SEM), (JEOL 5600 LV, Japan). The preparation of the bioparticles for SEM observation involved fixing the samples of bioparticles in 2 % glutaraldehyde and dehydrating in a 90 % ethanol with a stepwise reduction of glutaraldehyde fraction (from 100: 0 ethanol to 0: 100 ethanol % v: v) in 6 hours. The bioparticles were then air dried shortly to allow for ethanol evaporation and sputter coated with a layer of gold for observation in a SEM microscope.

2.2.3 Determination of bioreactor volumetric nitrification rates

Nitrifying activity is commonly determined by measuring ammonia oxidation, production of nitrite and oxygen uptake (Hagopian and Riley, 1998). Because the oxidation of ammonia by AOB is the rate limiting step of this nitrification process

(Nicol and Schleper, 2006; Ekema and Wentzel, 2008), and the intermediate, nitrite, is rarely found to accumulate in the environment and in wastewater treatment reactors (Kowalchuk and Stephen, 2001; Ekema and Wentzel, 2008), the oxidation of ammonia is an important indication of the nitrification potential of any biological nitrification system, the rate of ammonia oxidation was taken as the nitrification rate in all the calculations in this work.

The nitrification rate is a function of the activity of the nitrifying organisms present in the aerated zone of a reactor. Although nitrification is the rate at which ammonia is converted to nitrite, a two-step reaction, most calculations are done assuming that nitrification is a single reaction and not a two-step reaction (Von Sperling, 2007b). The nitrification rate is therefore expressed as;

ΔTotal Nitrogen/Δt =

unitary concentration rate x concentration of bacteria

$$\frac{\Delta \text{Total N}}{\Delta t} = \frac{\mu_N}{Y_N} \times \mathbf{X}_N$$

Where;

ΔTotalN/Δt = nitrification rate (oxidized g Total N m^{-3} d^{-1})

μ_N = specific growth rate of the nitrifying bacteria, based on μ_{max} and the environmental conditions (d^{-1}).

Y_N = yield coefficient of the nitrifying bacteria (g X_N/g Total N)

$\mathbf{X}_N$ = concentration of the nitrifying bacteria in the aerated zone of the reactor (g m^{-3})

The change in total nitrogen (ΔTotal N) corresponds to the product of the flow rate multiplied by the difference in the influent and effluent Total nitrogen, and the concentration of the nitrifying bacteria is expressed in terms of the volatile suspended solids (VSS) in the reactor (von Sperling, 2007b).

In the expanded bed bioreactor, the volumetric nitrification rate was calculated and expressed as kg NH_3-N m^{-3}_{EBBR} d^{-1}. The volumetric nitrification rate was based on the ammonia removal in the total reaction volume (expanded bed) available for nitrification in the expanded bed column (Fig. 2.1) at the time of sampling which is an indication of the volumetric conversion (nitrification) capacity of the bioreactor. The total reaction volume is calculated based on the bioparticle bed height upon expansion by the fluidizing pump in the expanded column and is expressed as V (m^3). The dilution rate D (d^{-1}) of the system is then calculated as

$$D = \frac{F}{V}$$

Where F = influent flow rate (m^3 d^{-1})

The dilution rate is then multiplied by the concentration of ammonia consumed by the nitrifying biomass (kg m^{-3} $_{EBBR}$). Thus, the reactor volumetric nitrification rate =

Conc. of NH_3-N consumed by the nitrifying biomass (kg m^{-3} $_{EBBR}$) x D (d^{-1})

While NH_3 or NH_4^+ represents the concentration of ammonia and ammonium ions in solution respectively, NH_3-N or NH_4^+-N represents the concentration of nitrogen in the form of ammonia or the ammonium ion. All the calculations in this work are based on the concentration of nitrogen in the form of the ammonium ion, which represents the available nitrogen to the nitrifying biomass (NH_4^+-N).

2.2.4 Chemical analysis

The ammonia concentration was determined using a manual spectrophotometric method (ISO 7150-1:1984). This method involves the absorbance measurements at 655 nm of the blue compound formed from the reaction of ammonium with salicylate and hypochlorite ions in the presence of sodium nitroprusside. The concentration of the nitrogen associated with ammonium (NH_4^+ -N) is determined and taken as the ammonium concentration. The nitrite concentration was determined using the molecular absorption spectrophotometric method (ISO 6777-1984). The method involves the reaction of nitrite with *4*-aminobenzene sulphonamide (colour regent) in the presence of orthophosphoric acid to form a diazonium salt. The diazonium salt foms a pink coloured dye with with N-(1-naphtyl)-1, 2-diamoethane dihydrochloride and the absorbance measurement is made at 540 nm. The nitrate concentration was measured using the American Public Health Association standard method for examination of water and wastewater (APHA 4500-NO_3^-). The method is based on the measurement of the UV absorbance of nitrate at 220 nm. HCl (1M) is added to acidify the sample and reduce interference from hydroxide and carbonate. Measurements are also taken at 275 nm to correct the reading obtained because

organic matter also absorb at 220 nm. The absorbance of NO_3^- is derived by a calculation (abs $_{NO3^-}$ = abs 220 nm – (2 x abs 275 nm).

2.2.5 Optimization of nitrification process.

A major concern of wastewater treatment is to optimize microbial activity and retain an active biomass for efficient transformation within the wastewater reactors (Gray, 1989). The nitrification process in the expanded bed bioreactor was optimized using (DESIGN-EXPERT® STAT-EASE Inc., USA) software to produce a 2-factor central composite RSM design. The two factors were pH and temperature and the chosen ranges were pH 7.0 to 8.5, and 15 ^{0}C to 30 ^{0}C. The design was a 13-run experiment, and the responses measured were nitrification rate, effluent concentrations of ammonia (NH_3-out), nitrite (NO_2^--out) and nitrate (NO_3^--out) from the expanded bed.

The experimental procedure involved sampling of bioreactor influent and effluent at 30 minutes intervals, to ascertain when the system was operating at a steady state (the steady state operation of the expanded system was determined by a constant effluent NH_3-N concentration between 2 to 3 sampling periods). Upon the determination of steady state operation of the expanded bed, the pH and temperature variables were changed simultaneously to the conditions for the next run. The influent and effluent were then periodically sampled until steady state operating conditions was attained again. This process was repeated for the entire 13 runs and the change in effluent concentrations of NH_3, NO_2^- and NO_3^- were the output responses as a result of each change in process variables. The difference in ammonia

concentration (ammonia consumed) was used to determine the nitrification rate of the expanded bed using the method described above.

While the flow rate of the influent wastewater was kept constant, the expanded bed height was altered by the changing the fluidizing pump flow rate (Fig. 2.1). The expanded bed height could therefore be altered without disturbing the influent flow rate into the bioreactor system.

2.3 RESULTS

2.3.1 The structure of the Biofilm

The nitrifying biofilm immobilized on glassy coke particles had a characteristic orange-brown color when examined visually (Fig. 2.2). The coke support is embedded in the biofilm - a gel-like structure resulting in bioparticles with smooth, even and sometimes rounded appearance despite the irregular shape of the embedded coke support (Fig. 2.2)

Fig. 2.2 Images of uncolonized glassy coke, developing bioparticles and fully developed bioparticle showing the biofilm completely enveloping the coke support.

When the bed was expanded, the bioparticles are fluidized and separate one from another in the upward flow and are thus suspended in the wastewater (Fig. 2.3). Although the expanded bioreactor received clean synthetic wastewater, light

microscope investigation of the surface of the biofilm revealed a close relationship with surface feeding protozoa and mesofauna e.g. *Rotifer* sp (Fig 2.4). These higher microorganisms grazed the surface of the biofilm as secondary feeders and helped to reduce the amount of sludge (due to cell death and disintegration) produced by the bioreactor. The source of the microorganisms most probably were the bioparticle samples seeded into the bioparticles (they were present from pilot plant source) or from the air and wastewater used in operating the bioreactor as no attempt was made to use aseptic techniques.

Fig. 2.3 Expanded bed column showing bioparticles in the expanded state, fully separated one from another in the upflowing wastewater.

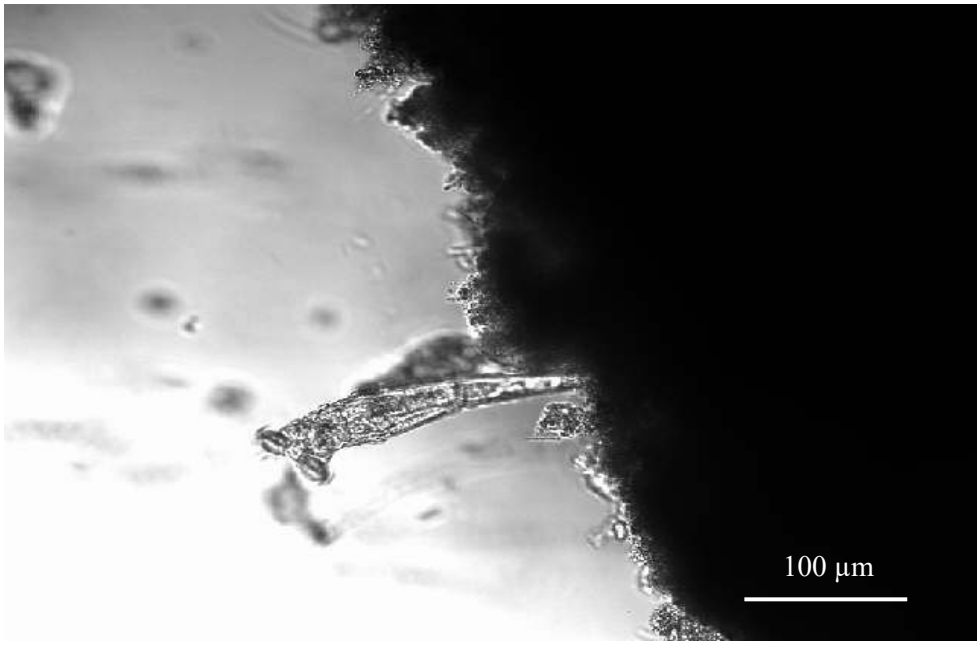

Fig. 2.4. Light microscope image of the surface if the biofilm showing association with *Rotifer sp*

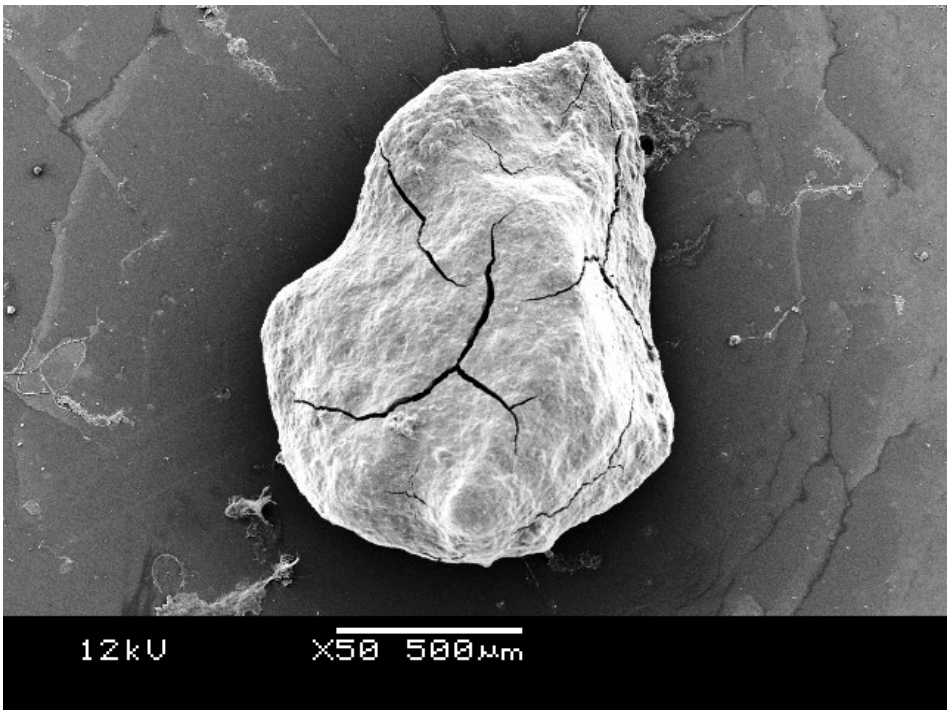

Fig. 2.5 SEM micrograph of a bioparticle.

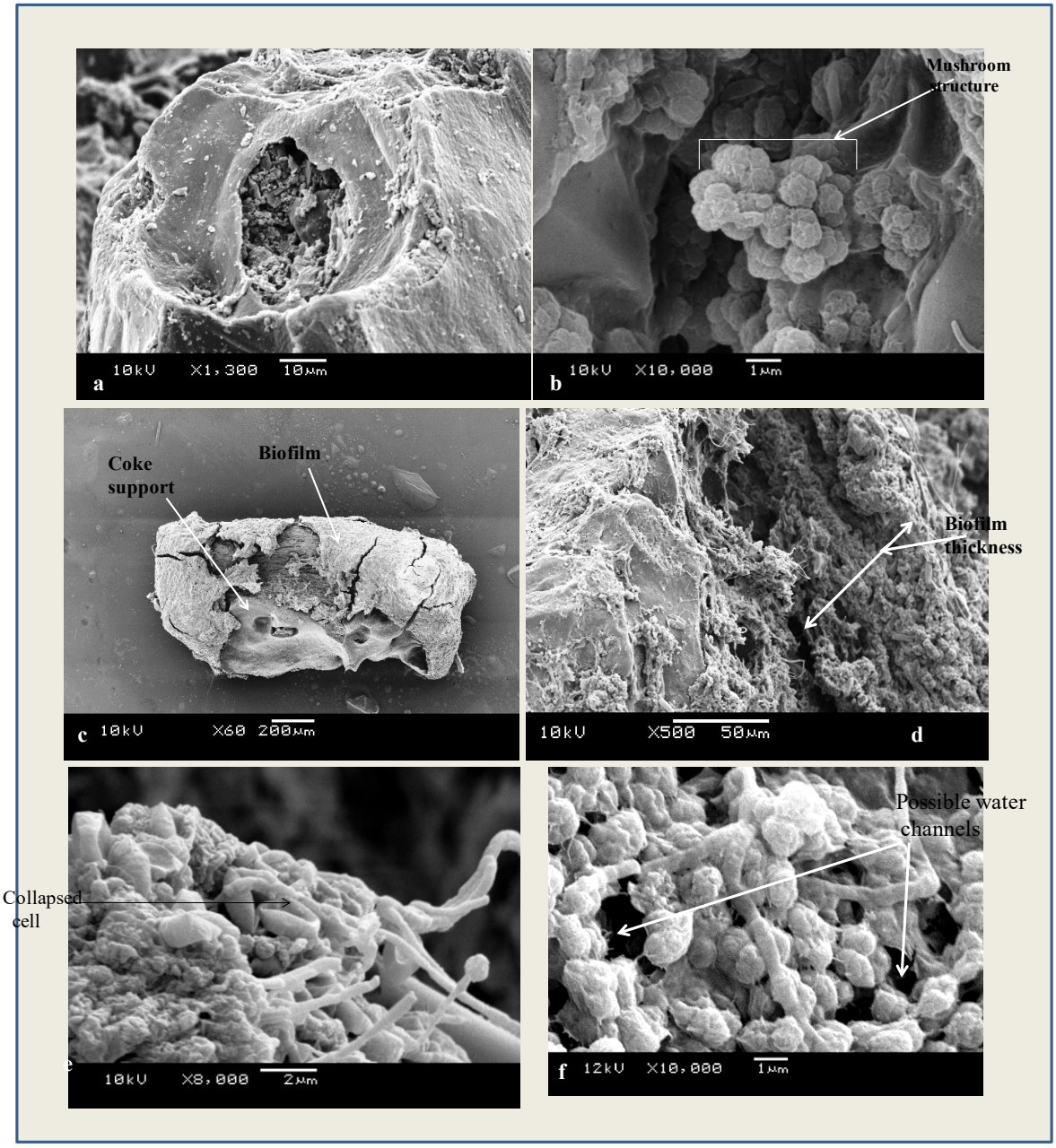

Fig. 2.6 SEM images of the bioparticles from the lab-scale EBBR; **a.** Bacteria colonization of the coke support. **b**. Bacterial growth on the coke surface showing a mushroom microcolony structure attached to the coke particle **c.** Bioparticle with disrupted biofilm, showing colonized pores of coke support and bacterial attachment to the surface of the coke (the biofilm was intentionally disrupted to aid viewing). **d.** Image of edge of the biofilm showing the dehydrated biofilm thickness of about 100 µm dried biofilm thickness. **e** Different bacterial cells on the biofilm surface **f.** Image of the surface of the biofilm showing a dense and diverse bacterial population with possible water channels.

2.3.2 The optimization of expanded bed process

Investigation into the effect of bed expansion on the nitrification rate revealed the optimum nitrification rate occurred between 40 – 50 % bed expansion (Fig. 2.7).

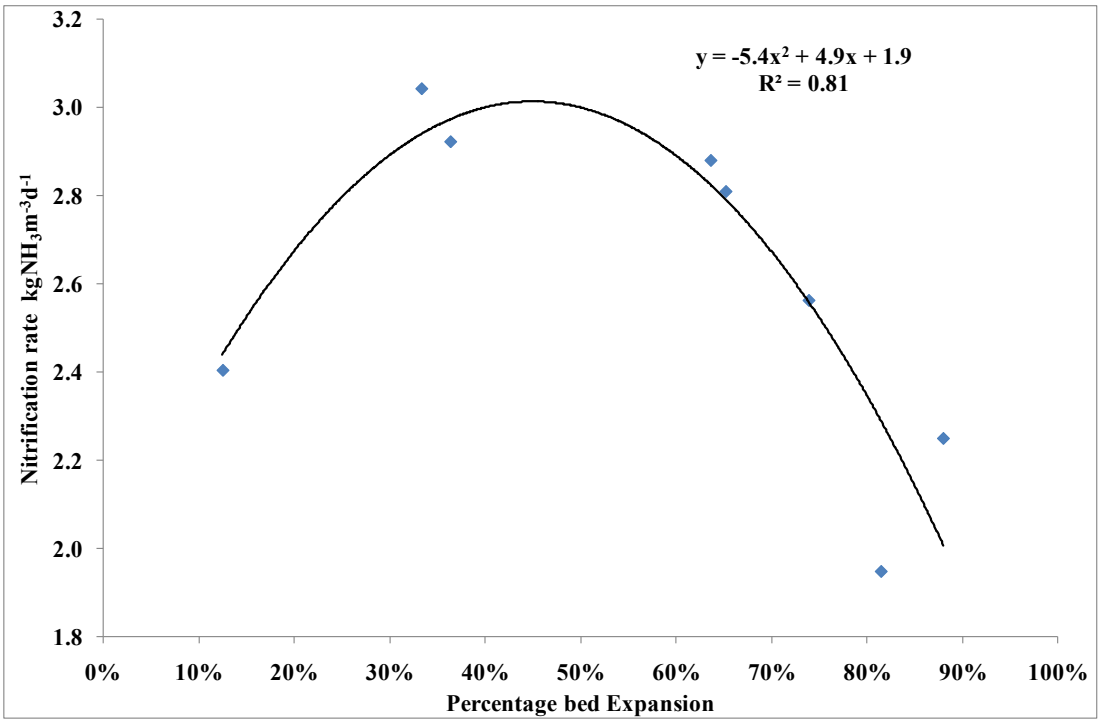

Fig. 2.7 The effect of bed expansion on nitrification rate

The different percentage bed expansions were achieved by altering the fluidizing pump flow rate which caused an expansion or reduction in bed height.

Upon establishing continuous culture, the expanded bed achieved nitrification rates of up to 3.0 kg NH_3 $m^{-3}d^{-1}$ (Fig. 2.15). The expanded bed was quite a robust system in its ability to recover quickly when mishaps occurred e.g. loss of compressed air supply, fluidizing pump breakdown and sometimes reactor connection tubing damage. Because nitrification rate of the bioreactor was determined by the product

of the difference in ammonia concentration in the influent and effluent, and the dilution. The dilution (D = Flow rate /Volume) however, was based on the volume of the expanded bed and not the total volume of the reactor. The influent flow rate, pH, air flow rate and temperature where kept constant and the ammonia consumed and expanded bed height obtained for the calculation.

Optimization process

The 13-run RSM experiment to optimize the pH and temperature of the expanded bed bioreactor involved 4 mid-point runs of pH 7.8, 22.5 ^{0}C, lowest and highest temperatures of 12 ^{0}C and 30 ^{0}C, and lowest and highest pH of 6.7 and 8.8 respectively (Table 2.1). The experiments were performed in the run order shown in Table 2.1 and the responses were recorded in the same order.

During the optimization experiment, the bioreactor reached stable operating conditions on average 3 hours after each change in operating conditions; this was the case when a change was from a low to a high temperature or *vice versa* (Fig. 2.8). The lowest and highest nitrification rates achieved were 2.5 and 4.4 kg NH_3-N m^{-3}_{EBBR} d^{-1} (Table 2.1). The bioreactor was able to achieve 97 % ammonia removal at pH 8.8, 22.5 ^{0}C with an effluent (NH_3-Nout) concentration of 3.3 mg L^{-1} (run 5; Table 2.1). The mid-point runs (pH 7.8, 22.5 ^{0}C; runs 3, 4, 6, 7, and 13) all had nitrification rates of 4.2 ± 1 kg NH_3-N $_{EBBR}$ m^{-3} d^{-1} except for run 13 which was 3.7 kg NH_3-N $_{EBBR}$ m^{-3} d^{-1}.

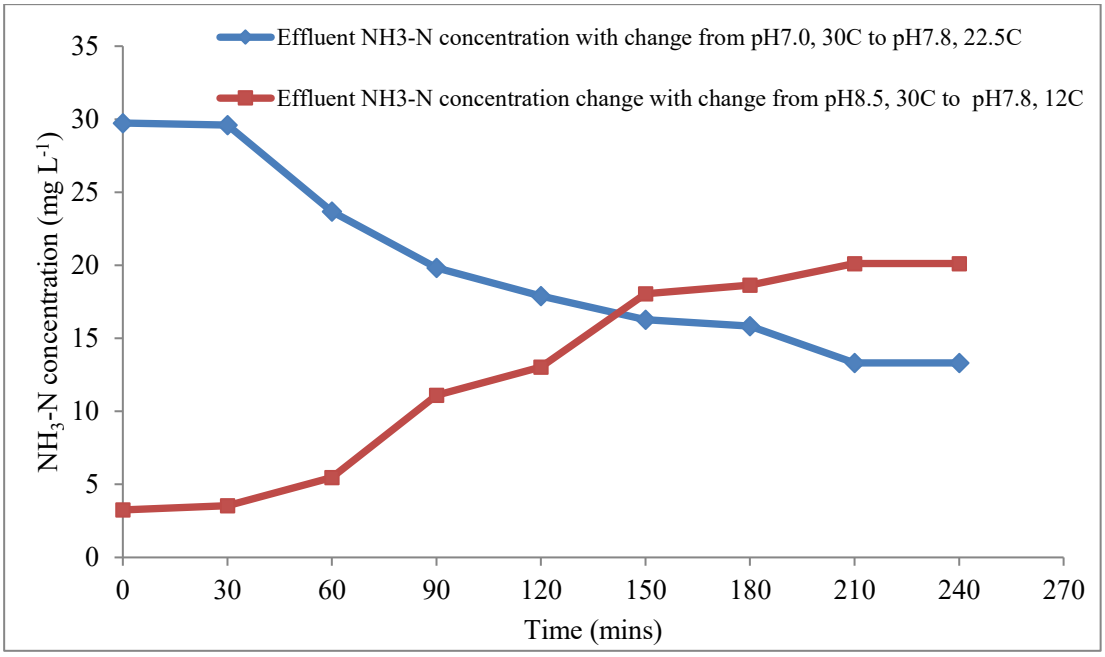

Fig. 2.8 The change in the NH_3-N effluent concentration response in lab-scale expanded bed upon changing pH and temperature during RSM experiment.

Showing the point at which the change occurs (30 mins) until bioreactor stable conditions is attained.

Using the DESIGN-EXPERT software, 3D response surface graphs were obtained for the relationships RSM showing the effect of pH and temperature on effluent ammonia, nitrite and nitrate concentrations, and nitrification rate (Figures 2.9 - 2.14). The normal plot of residuals were also obtained by the DESIGN-EXPERT software and showed a normal distribution of the responses obtained during the experiments (Fig. 2.8 – 2.13)

Table 2.1 Results of RSM experiment showing the process variables and reactor effluent response measured (NH_3, NO_2^- and NO_3^- concentrations)

Run	Factor 1 pH	Factor 2 Temp (^0C)	Response 1 NH_3-N out (mgL^{-1})	Response 2 NO_2^- out (mgL^{-1})	Response 3 NO_3^- out (mgL^{-1})	Response 4 Nitr.rate ($kgm^{-3}d^{-1}$)	Response 5 Total Nout (mgL^{-1})
1	7.0	15.0	48.7	0.5	79.3	2.5	128.4
2	7.0	30.0	32.3	8.6	91.8	3.7	132.7
3	7.8	22.5	13.3	36.5	60.5	4.1	110.3
4	7.8	22.5	8.1	38.3	34.2	4.2	80.7
5	8.8	22.5	3.3	37.2	52.1	4.4	92.5
6	7.8	22.5	8.1	37.0	62.2	4.2	107.3
7	7.8	22.5	4.6	37.7	75.1	4.3	117.4
8	8.5	30.0	4.0	37.2	53.8	4.3	95.0
9	7.8	12.0	20.4	33.1	74.3	3.4	97.9
10	6.7	22.5	36.3	26.9	84.3	3.2	147.5
11	7.8	33.0	6.4	35.3	45.1	4.2	86.8
12	8.5	15.0	3.3	35.9	68.0	3.9	107.2
13	7.8	22.5	28.9	33.6	43.8	3.7	106.3

The effluent concentrations of ammonia and nitrate reduced with increase in pH, while there was no change in their effluent concentrations with change in

temperature (Fig. 2.9 and Fig. 2.11). The effluent nitrite concentrations meanwhile showed a linear increase in effluent NO_2^- concentration with increase in pH but only a marginal increase in NO_2^- effluent concentration with increase in temperature (Fig. 2.10). Because nitrite is the end product of ammonia oxidation, conditions for high ammonia oxidation and therefore low (NH_3-N) concentrations in effluent would correspond to that for high effluent NO_2^--N concentrations and this occurred at high pH of about 8.0 (Fig. 2.9. A reduction in NO_2^--N concentration would mean an increase in effluent NO_3^--N concentrations as nitrite oxidation would produce high NO_3^--N concentrations in the effluent and this at about pH 7.0 (Fig. 2.11).

The nitrification rate increased with increase in both temperature and pH (Fig. 2.12) and the optimum nitrification rate was achieved at about pH 8.5, 28 ^{0}C. Although the DESIGN-EXPERT software suggested a linear relationship for the analysis of the ammonia effluent concentration, it suggested a quadratic relationship for the nitrification rate analysis which is based on the ammonia effluent concentration (Fig. 2.9 and Fig. 2.12). High nitrification rates are therefore achieved at higher pH and temperatures. The derived equations for the relationships were;

$pH = -0.21B^2 + 0.17B + 4.34$

$Temperature = -0.18A^2 + 0.27A + 4.21$

where A = pH unit and B = Temperature unit.

Solving of the equations by substituting unit values for pH and temperature, revealed that a unit change in pH causes the nitrification rate to change by 0.46 kg NH_3 m^{-3}_{EBBR} d^{-1} while a unit change in temperature causes the nitrification rate to change by 0.27 kg NH_3 m^{-3}_{EBBR} d^{-1}. The pH therefore had twice the effect temperature had on the nitrification rates of the EBBR.

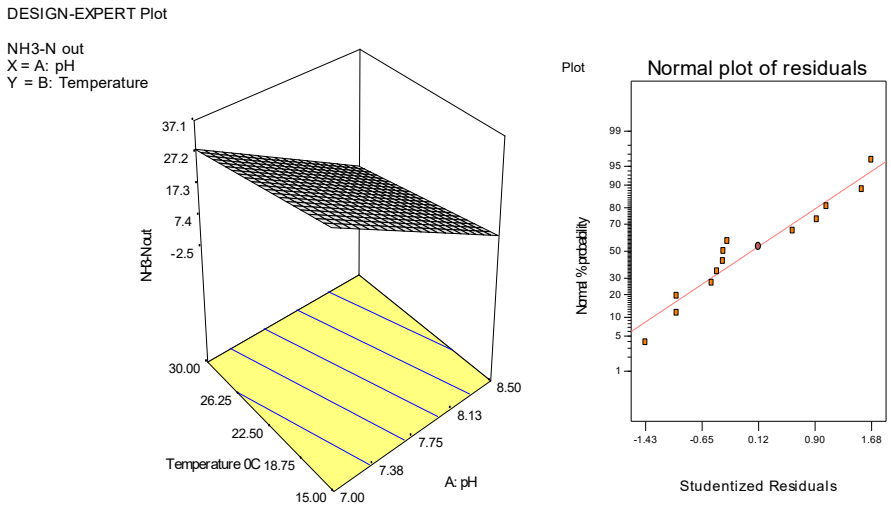

Fig. 2.9 The RSM graphs showing the interaction between temperature, pH and effluent ammonia concentration and the normal plot of residuals for the interaction

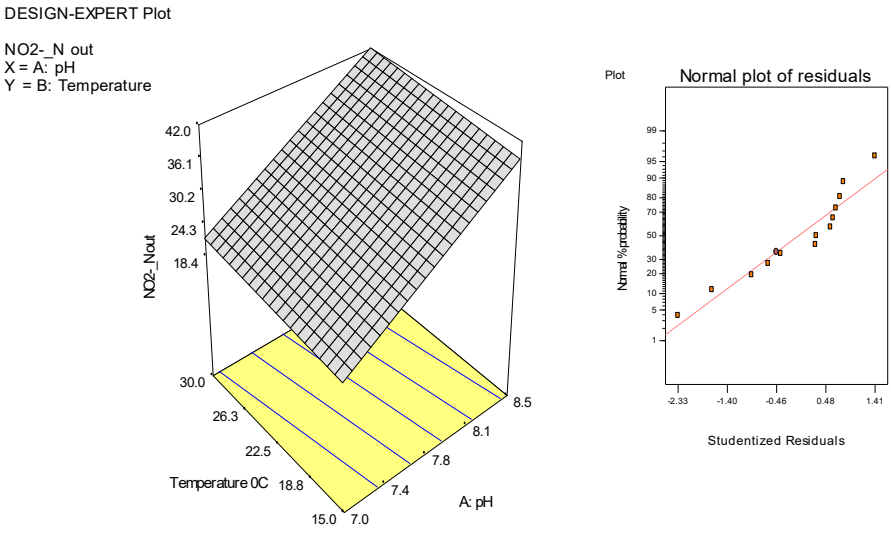

Fig. 2.10 The RSM graphs showing the interaction between temperature, pH and effluent nitrite concentration and the normal plot of residuals for the interaction

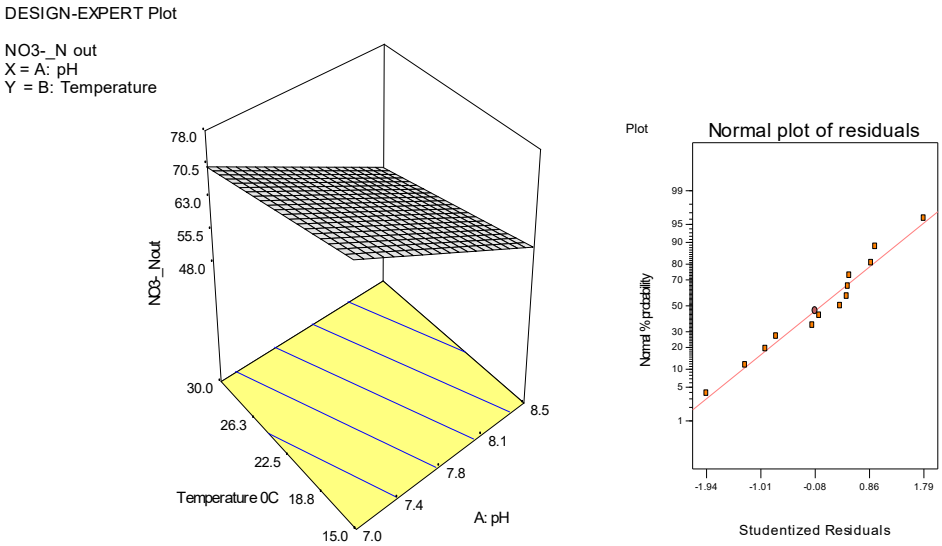

Fig. 2.11 The RSM graphs showing the interaction between temperature, pH and effluent nitrate concentration and the normal plot of residuals for the interaction

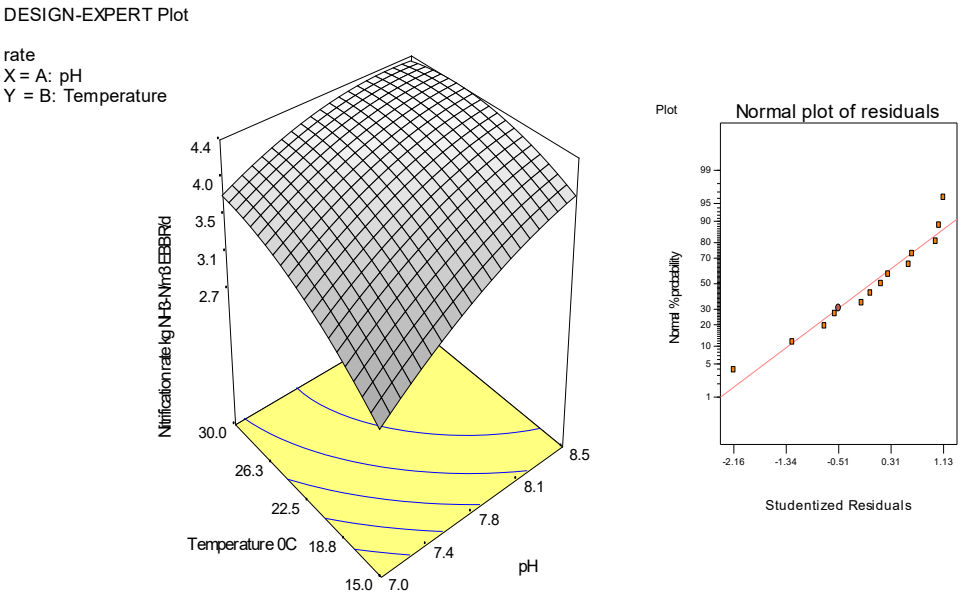

Fig. 2.12 The RSM graphs showing the interaction between temperature, pH and nitrification rate and the normal plot of residuals for the interaction. The plateau shows the optimum response brought about by the interacting factors.

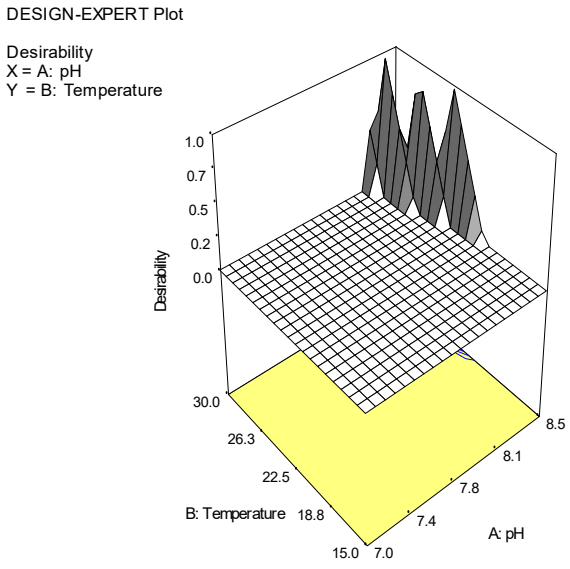

Fig 2.13 The RSM derived graph of the predicted region of pH and temperature interaction for the production of effluent of 1 mg L^{-1} of NH_3-N.

Because RSM is able to predict the optimum conditions for a process, the data derived from the RSM experiment were used to predict the expanded bed bioreactor operating conditions for an NH_3-N effluent concentration of 1 mg L^{-1}. Nine possible combinations of pH and temperature were identified within reactor operating limits of pH 7.0 – 8.5, 15 - 30 ^{0}C (Table 2.2) and effluent (NH_3-N out) concentrations of 1.0 mg L^{-1} (Table 2.12). One point out of these nine combinations (pH 8.46 and 25.67 ^{0}C) was selected to achieve the target NH_3-N effluent concentration of 1.0 mg L^{-1} NH_3-N (Table 2.2; Fig 2.13).

Table 2.2 Prediction values for an ammonia –nitrogen effluent concentration of 1.0 mg L^{-1} from the lab scale expanded bed.

No.	pH	Temperature	NH_3-Nout	Desirability	
1	8.46	25.57	1.0	1.0	Selected
2	8.38	28.33	1.0	1.0	
3	8.47	25.30	1.0	1.0	
4	8.42	26.85	1.0	1.0	
5	8.47	25.15	1.0	1.0	
6	8.49	24.33	1.0	1.0	
7	8.43	26.41	1.0	1.0	
8	8.38	28.11	1.0	1.0	
9	8.48	24.87	1.0	1.0	

The effluent nitrite concentrations of the lab-scale bioreactor were unusually high (maximum 38.3 mg L^{-1} which was about 1/3rd of the inlet NH_3 concentration, Table 2.1). Nitrite is toxic but is readily converted to nitrate by NOB, therefore, the production of nitrite in the bioreactor was investigated between pH 6.9 – 7.6 to determine the ideal pH for the lowest nitrite production in the expanded bed when the bioreactor was maintained at 22.5 ^{0}C, the midpoint experimental temperature. The outlet NO_2^--N concentrations were measured at the pH values in the range every 24 hours after the pH was changed. The results are shown in Figure 2.13.

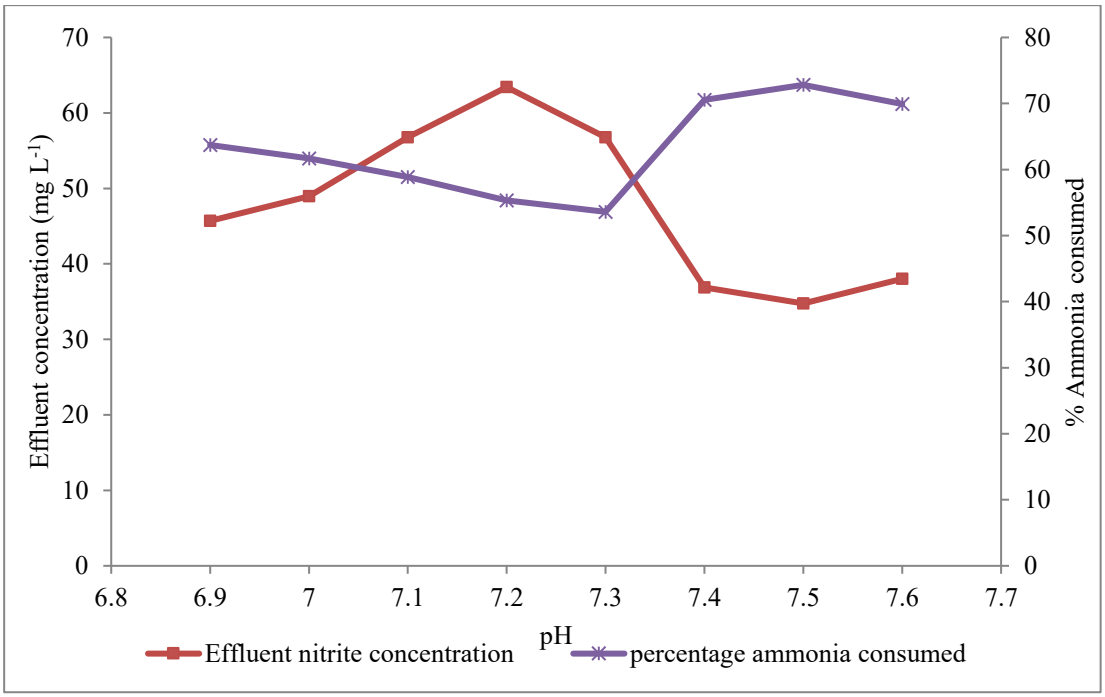

Fig. 2.14 The comparison of the percentage ammonia consumed and the effluent NO_2^--N concentration produced in the EBBR at different pH when the bioreactor was operated in continuous culture at 22 ^{0}C. The bioreactor was left to stabilize overnight at a set pH before sampling.

The lowest effluent NO_2^--N concentration was achieved at pH 7.4 – 7.5 while the highest concentration was at pH 7.2 (Fig. 2.14), which was in contrast to the lowest pH of 7.0 for NO_2^--N production in achieved during the RSM experiments. The difference was probably because the temperature of the bioreactor was maintained at 22.5 ^{0}C in the latter experiment.

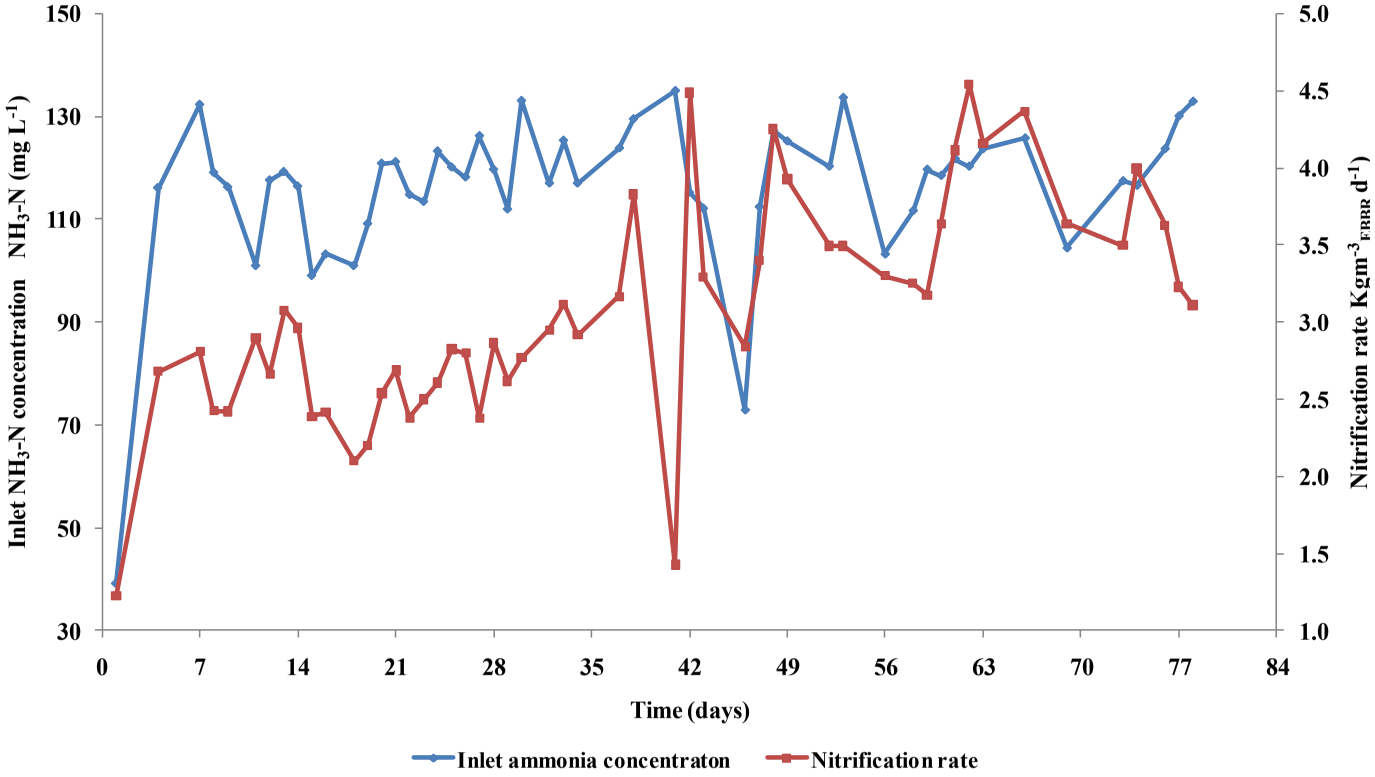

Fig. 2.15The ammonia concentration of the inlet feed and the nitrification rate of the EBBR.

2.4 Discussion

The preparation of bioparticles for SEM observation involved dehydrating the biofilm, nevertheless, different arrangements of the bacteria were visible on both the surface of the biofilm and in the inner regions of the biofilm including on the surface of the coke particles (Fig 2.6a - f). Although internal bacterial configuration cannot be identified in the SEM as it only shows the surface topography, the size of individual cells could be determined (about 1 μm) although some appeared to have collapsed (Fig. 2.6e and f) probably due to the dehydration process. The bacterial colonization of the coke pores, which is the initial stage of biofilm formation on coke and the subsequent embedding of the coke support, could be identified. The mushroom shape of the biofilm growth could be identified from the SEM micrograph of attached cells in a coke pore (Fig.2.6b) and the dried bioparticles achieved a biofilm thickness of about 100 μm, which was far less than the observed hydrated biofilm thickness (Fig. 2.2; Fig. 2.3). Information on the spatial configuration of the microcolonies was not deducable from the SEM images, neither was the identification of the different species present in the biofilm possible.

The high nitrification rates achieved by using the EBBR (maximum rate 4.4 kg m^{-3}_{EBBR} d^{-1}, Table 2.1) is an indication of the potential of the EBBR. Previous studies using a pilot plant for the nitrification of activated sludge final effluent, where the inlet NH_3-N concentration was on average 12.6 g m^{-3} (low strength NH_3-N concentration) achieved a nitrification rate of 1.7 ± 0.6 kg NH_3-N m^{-3}_{EBBR} d^{-1} (Dempsey *et al.*, 2005). The bioparticles used in this study were obtained from the

pilot plant EBBR used by Dempsey *et al.* (2005) and although the lab-scale EBBR received clean synthetic wastewater, the high nitrification rates of above 4.0 kg NH_3-N m^{-3}_{EBBR} d^{-1} were an indication of the ability of the nitrifying biofilms to use higher strength ammonia feed (125 mg L^{-1}) in the lab scale EBBR as well as low strength feed (12 Mg L^{-1}) in the pilot plant EBBR. The nitrifying biofilm was able to adjust to a 10-fold increase in influent ammonia concentration.

While individual effluent NH_3-N, NO_2^--N and NO_3^--N concentrations showed little or no response to changes in temperature, effluent concentrations of both NH_3-N and NO_3-N reduced with increase in pH (Fig. 2.9 – Fig. 2.12). The nitrification rate however, increased with increase in both temperature and pH (Fig. 2.9). Using the derived equations for the response for pH and temperature ($pH = - 0.21B^2 + 0.17 B + 4.34$; $Temperature = -0.18A^2 + 0.27A + 4.21$). The pH was found to have twice the effect temperature had on the nitrification rate. This sensitivity of the nitrifying community to pH makes the regulation of reactor pH a critical factor in the design and operation for efficient expanded bed expanded bed nitrification in addition to the supply of oxygen which is vital for nitrification process.

Painter (1986), reported that ammonium had been oxidized in high strength ammonium wastes in earlier work carried out by Hutton and LaRocca (1975) using 700 mg N L^{-1} and de Wilde (1977) using 1 400 mg N L^{-1}. In these studies, the pH of the medium largely determined the final nitrogen species in the effluent, (nitrate at pH 7.1 for the 1 400 mg N L^{-1} and nitrite at pH 8.0 to 8.4 for the waste of 700 mg N L^{-1} waste). An excess of nitrite in the effluent is a strong indication of the incomplete

nitrification process which may be due to the inactivity of the NOB. Using NH_3-N concentrations of 125 ± 10 mg L^{-1} in the lab scale EBBR, the effluent NO_2^--N concentrations were predominantly lower than the effluent NO_3^--N concentrations in even at pH 6.7 (Table 2.1).

When the effluent concentrations of NH_3-N, NO_2^--N and NO_3^--N were considered separately, the lowest reactor effluent NH_3-N concentrations were observed at pH 8.5 (maximum ammonia oxidizing bacteria activity, Fig. 2.9) and coincided with the highest NO_2-N effluent concentration, but the lowest effluent NO_2^--N concentration (maximum nitrite oxidizing bacteria activity) was achieved at pH 7.0 (Fig. 2.10). The optimum pH therefore differed for ammonia and nitrite oxidation.

Optimum operation conditions of the EBBR process should aim at low NH_3-N and NO_2^--N concentrations and high NO_3^--N effluent concentration because in the EBBR, nitrification takes place in the biofilm, as NH_3-N diffuses into the biofilms and not in the bulk liquid. The products of ammonia and nitrite oxidation (NO_2^--N and NO_3^--N) which are produced within the biofilm also diffuse out of the biofilm and together with excess NH_3-N are present in the effluent. The effluent NO_2^--N and NO_3^--N are therefore products of the complete ammonia and nitrite oxidation processes while the effluent NH_3-N concentration is the concentration of the unoxidized NH_3-N.

Complete nitrification of ammonia to nitrate would mean low NH_3-N concentrations and high NO_3^--N concentrations in the effluent. Because the EBBR was fed with only NH_3-N as influent nitrogen source and the effluent NO_3^--N concentration

depended on the NO_2^--N concentration produced by the ammonia oxidizers; high effluent NO_2^--N was an indication of high AOB activity and low NOB activity. High NO_2^--N could also indicate either unsuitable environmental conditions for NOB activity (and growth) or an indication of either a smaller population of NOB when compared to the AOB in the biofilm. Although several workers have reported end point inhibition of ammonia oxidation on the activity of NOB and also excess NH_3-N inhibiting the activity of AOB activity (Wood, 1986; Kim *et al.,* 2006), the effect is not taken into consideration in this study because there is evidence of 97 % NH_3-N removal (run 5, Table 2.1), without any adverse effect on the NOB activity as the effluent NO_2^--N concentration was not unusually high (37.2 mg L^{-1}) compared to that obtained at other experimental run settings e.g. (26.9 mg L^{-1} at pH 6.7, 22.5 ^{0}C, run 10, Table 2.1). The maximum effluent NO_2^--N concentration of 38.3 mg L^{-1} from the bioreactor was unusually high as nitrite and would not be acceptable in a large scale EBBR as NO_2^--N is known to cause death in channel catfish (*Ictalurus punctatus*) at concentrations of 10 mg L^{-1}(Tomasso *et al.,* 1980) and is usually found in concentrations of < 0.005 mg L^{-1} in fresh waters (Lewis and Morris, 1986).

The highest NOB activity occurred at pH 7.0 (Fig. 2.9), therefore the optimum pH for NOB activity would be beyond this point, as the effluent NO_2^--N concentration increased with increase in bioreactor pH and while temperature had only a marginal effect on effluent NO_2^--N concentrations. The complex multispecies composition of the biofilm must be taken into consideration when setting operating conditions of the EBBR as the nitrifying community did not allow for the complete total conversion of the NH_3-N to NO_3^--N at any set conditions of pH and temperature as reported in the

literature. The concentration of NO_2^--N was therefore an indication of the relative activities of the both species of nitrifying bacteria as NO_2^--N could build up in the EBBR.

The investigation into the ideal pH for operating the lab scale EBBR revealed that the highest ammonia removal (71 %) in the bioreactor also coincided with the pH 7.4 – 7.5 range for the lowest effluent NO_2^- concentration (32 mg L^{-1}), (Fig 2.14). In order to maximize ammonia removal and therefore nitrification rates, and also low bioreactor nitrite concentrations, which indicates adequate nitrite oxidizing bacteria activity, the expanded bed was maintained in continuous culture at 22.5 ^{0}C, pH 7.5.

In the determination of the effect of bed expansion on nitrification rate, the highest nitrification rate was achieved between 40 – 50 % bed expansion (Fig. 2.7). The bed expansion was increased by increasing the flow rate of the fluidizing pump; this resulted in the increased flow in the recycle column and therefore reduced the oxygenation contact time in the recycle column. The effect of increasing the pump flow rate could have been caused a lower dissolved oxygen concentration in the wastewater arriving at the bottom expanded bed column. Due to lack of an adequate dissolved oxygen probe, the dissolved oxygen was not measured to confirm this assumption. This effect therefore may have been an artefact of the lab scale system. Another factor was that increasing the flow rate of the fluidizing pump reduced the contact time between the wastewater and the biofilm surface. The lab-scale EBBR was therefore, maintained at 50 % bed expansion.

Operating the EBBR in continuous culture under the conditions stated above resulted in EBBR nitrification rates ranging from 2.5 – 4.4 kg $m^{-3}_{EBBR}d^{-1}$ (Fig. 2.15). The nitrifying bacteria proved to be quite resilient to shocks and disturbances as the they recovered quickly from bioreactor mishaps e.g. the nitrifying population was able to withstand a pH of less than 5.0 overnight when the fluidizing pump broke down on day 38 (Fig. 2.15), without the complete destruction of the nitrifying community and regained normal nitrification rate in 24 hours.

2.5 Conclusion

- The lab scale bioreactor was established and achieved nitrification rates of 2.7 – 4.4 kg $m^{-3}_{EBBR}d^{-1}$ and achieved up to 97 % ammonia removal.
- The AOB and NOB in the nitrifying biofilms have different pH for optimum activity and this should be considered in EBBR set up and operating conditions.
- The nitrification process was more sensitive to changes in pH than changes in temperature (pH had twice the effect temperature had on the nitrification rates). Thus pH is a more important process variable than temperature for EBBR operations.
- The temperature had little effect on the nitrification rate and expanded bed operation in the 15 – 30 ^{0}C range. Therefore, this means that expanded bed technology can probably be applied in both temperate and tropical climates without temperature control.
- RSM easily identifies optimum conditions of activity within biological systems when more than one process variables are considered.
- The DESIGN-EXPERT software is a useful tool in RSM analysis for the optimization of complex environments. Maximum nitrification rate for the lab scale EBBR operations for the range of pH and temperature used was about 4.4 kg $m^{-3}_{EBBR}d^{-1}$ at pH 8.5, 30 ^{0}C.
- The DESIGN-EXPERT software was also able to predict desired responses like the conditions for expanded bed operation, to meet standards can be changed by new legislation. Although the lowest outlet NH_3-N concentration

in this investigation was 3.3 mg L^{-1}, the software was able to predict the optimum ammonia oxidation rate and optimum conditions for a concentration as low as 1.0 mg L^{-1} (i.e. pH 8.6, 25.6 ^{0}C).

CHAPTER THREE

3.0 The influence of biofilm thickness on nitrification rate

3.1 Biomass hold up, biofilm thickness, and nitrification rates in EBBRs.

Nitrification is an essential part of nutrient removal in wastewater treatment processes. Nitrifying bacteria grow slowly and, when other bacteria are present in wastewater treatment systems, autotrophic nitrifying bacteria are always at risk of being out grown by the faster growing heterotrophic organisms e.g. nitrification rates by autotrophic bacteria in conventional wastewater systems are 3 to 4 times slower than heterotrophic oxidation rates of organic matter (Gray, 1989). De Beer *et al*., (1993) reported that the application of nitrifying bacteria in continuous – flow wastewater processes requires the efficient retention of biomass with good settling properties. In the EBBR however, the immobilization of nitrifying bacteria in particulate biofilms essentially retains the nitrifying population in the reactor and negates the need for secondary settling.

The EBBR process can be a useful part of biological wastewater treatment because, although the volume of influent wastewater like oil refinery effluent in municipal and industrial plants is very high e.g. up to 570, 000 m^3 d^{-1}, the concentration of ammonia is low e.g. 5 – 30 mg L^{-1} (Pocernich and Litke, 1995). Also, the nitrification process is associated with low – rate loading because increased loading rates leads to a loss of the degree of nitrification (Gray, 1989). The intensified EBBR process, where high biomass concentrations of nitrifying bacteria can be achieved, therefore enables

the limitation due to slow growth to be overcome and the achievement of high nitrification rates leading to high reactor loading rates.

3.1.1 Biofilm growth and biomass hold up

The amount of biomass associated with an individual particle (biomass concentration) in an expanded bed bioreactor (EBBR) depends on several factors, such as the organism being immobilized, the fluidization mechanics within the reactor, the biofilm characteristics and the carrier media characteristics (Fabah and Dahab, 2004; Webb, 1986). Although some biofilms can take up to 10 days to reach full maturity (Stoodley *et al*., 2002), nitrifying bacteria biofilms grow more slowly. Upon starting up a pilot scale expanded bed bioreactor for tertiary nitrification of activated sludge final effluent Dempsey *et al.,* (2005) could measure biofilm growth only after 7 weeks of expanded bed operation (determined by increase in static bed height). In EBBRs, increase in biofilm thickness is dependent on the balance between microbial growth rate and the attrition acting upon the bioparticle by the flowing liquid. While microbial growth is dependent on substrate concentrations within the reactor, the upward flow velocity of liquid influences attrition. Bioparticle growth or expansion, indicated by increase in biofilm thickness, only occurs by microbial growth within the biofilm and the production of EPS (Picioreanu *et al.,* 1999) but this has to overcome the rate of biofilm attrition due to shearing by fluid flow.

Dempsey *et al*., (2005) also estimated biomass hold-up of up to 43 kg m^{-3} for 1 mm support particles upon 100 % bed expansion and showed that smaller particles can achieve higher biomass concentrations than larger particles (Fig. 3.1). In the expanded bed bioreactor used in the study, an increase in the static bed height indicated biofilm growth and, consequently, increase in biofilm thickness, bioparticle size, and biomass holdup (biomass concentration).

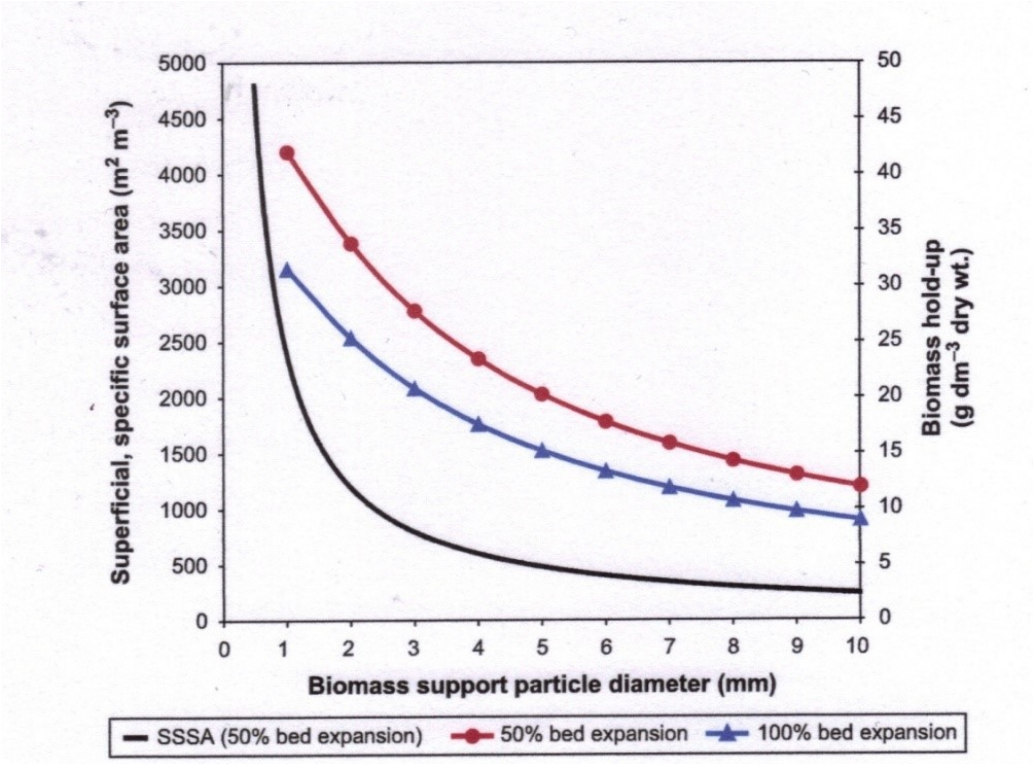

Fig. 3.1 Superficial specific surface area (SSSA) and biomass hold-up for particulate support material (Dempsey *et al*., 2005).

Because continued biofilm growth results in increased bioparticle size, the bed continues to expand unless the biofilm thickness is controlled. Dempsey *et al.,* (2006) controlled the increase in expanded bed height and thus maintained the

bioparticle bed height in their pilot plant EBBR by inserting a bioparticle recycle column into the EBBR design (Fig. 3.2).The bioparticle were prevented from entering the effluent collection channel (q) and the wastewater recycling and aeration column (Q –q) by the bioparticle recycle channel which was fixed at a lower point than effluent recycle and aeration column in the expanded bed column. As the bioparticles were pumped back up the expanded bed column, the biofilm was stripped off the coke and biofilm re-growth began at the bottom of the bed (Fig. 3.2). The stripped biofilm was mineralized in the expanded bed column by the invertebrates and surface feeding protozoa present in the expanded bed and did not increase the sludge output from the EBBR (Dempsey *et al.,* 2006)

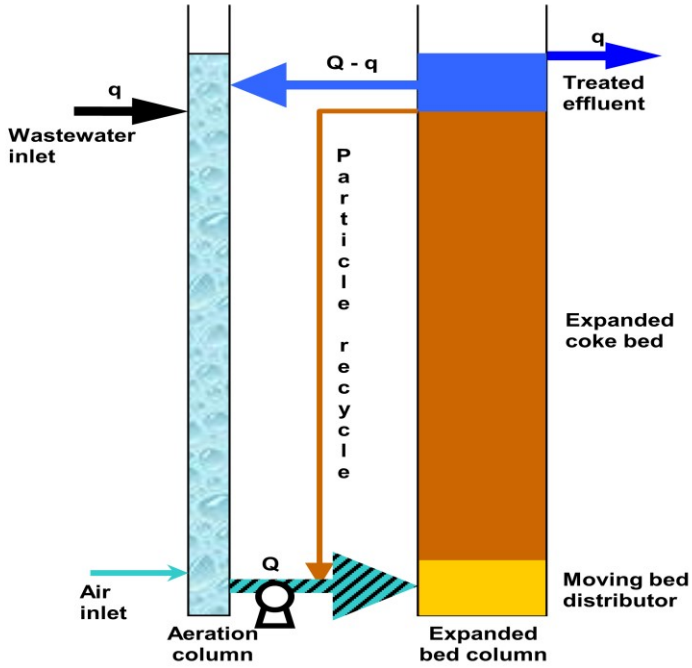

Fig. 3.2 An expanded bed biofilm reactor fitted with a bioparticle recycle channel for the control of the expanded bed height (Dempsey *et al.*, 2006). (q- wastewater flow, Q-recycle flow)

In the lab-scale EBBR, control of bed expansion was achieved by removing bioparticles from the top of the bed, where they were thickest, agitating them in a closed vessel to remove excess biofilm and returning the partially-cleaned support material to the bed. Because the biofilm stripped coke particles were denser than the bioparticles, they sank to the bottom of the expanded column and biofilm re-growth occurred on them. This biofilm control procedure resulted in the production of two distinct populations of bioparticles; thinner biofilms (smaller bioparticles) at the bottom of the bed and thicker biofilms (larger bioparticles) at the top. Di Felice (1995) reported that bed stratification or differentiation was due to a difference in drag and buoyancy which affects particle terminal settling velocity. Nicollela, *et al.,* (2000b) also stated that biofilms have a tendency to change in density, thickness and shape, in mass transfer rates and hydrodynamic changes in a particulate biofilm bed over time. Biofilm composition and biofilm specific activities e.g. specific bioparticle nitrification rates would therefore change across the bed.

The investigation in this chapter therefore focused on;

1. Development of methods to accurately determine the biomass concentration of coke based particulate biofilms, the maximum and the specific volumetric nitrification rates of bioparticles from the lab scale expanded bed.
2. The relationship between biofilm thickness and biomass concentration for the bioparticles in the EBBR
3. The influence of biofilm thickness on maximum and specific volumetric nitrification rates of bioparticles in the expanded bed.

In view of the fact that the external biofilm is the active portion of the bioparticle, the activity of the biofilm was calculated by determining the specific volumetric nitrification rates of biofilms in the intact state (while still attached to the support particle) and the maximum volumetric nitrification rates when the biofilm was disrupted and the biofilm cell contents distributed throughout the reactor vessel.

3.2 Materials and methods

3.2.1 Determination of biomass concentration

Harvesting the biofilm

The external biofilm was detached from bioparticle by the vigorously shaking samples of the bioparticles in a closed conical flask. This harvested biofilm or detached biomass was then decanted and centrifuged at low speed (2 000 rpm, 8 minutes) using a laboratory centrifuge **(**Sigma, Osterode am Harz, Germany). The liquid supernatant discarded and the partially dewatered biomass residue used for the experiment. The dry weight of bioparticles sterilized coke particles and harvested biomass samples were determined by placing samples in pre weighed porcelain crucibles and heating to 105 ^{0}C in a hot air oven overnight. The samples were cooled in a dessicator and reweighed to obtain the dry weight (ASTM E1756-01).

The determination of the biomass concentration of the biofilm associated with coke support was investigated by measuring the ash content of the bioparticle when the organic matter was volatilised by heating to a high temperature. Two methods were used in the investigation; thermogravimetric analysis (TGA) and a combination of the determination of total solids in biomass (ASTM E1756-01) and total ash in biomass (ASTM E1755-01). The 575 ^{0}C heating temperature of biomass to ash reported in the (ASTM E1755-01) method was used as the target heating temperature.

The thermal stability of materials can be determined using TGA analysis. This technique is used to monitor the change in mass of a specimen as it is heated. TGA analysis is normally carried out in air and the mass lost by the sample is recorded as a function of increasing temperature. TGA was used to determine the mass lost from the biomass attached to the coke when bioparticle samples were heated, which can be used to calculate the percentage biomass in the bioparticles. The TGA analysis was carried out on oven dried (105 ^{0}C) samples of bioparticles, clean (uncolonized) coke particles and harvested biomass. Samples were heated to 575 ^{0}C in air at a rate of 5 ^{0}C min^{-1} using a thermogravimetric analyzer (NETZCH TG 209, Germany). Upon attaining 575 ^{0}C, the samples were held at this temperature for 3 hours.

The biomass concentration of bioparticles was also determined by adapting the American Standard for Testing Materials (ASTM) method for determination of total solids in biomass (ASTM E1756-01) and ash in biomass (ASTM E1755-01). The method for the determination of total solids in biomass involves drying bioparticles overnight in a hot air oven (105 ^{0}C) to determine the biomass dry weight. The method for the determination of ash in biomass involves the incineration of the biomass portion of the bioparticle to ash in a muffle furnace, to determine the ash free dry weight from which the percentage biomass of the sample is calculated as;

$$\% \text{ biomass} = \frac{\text{Dry weight of sample (g)} - \text{ashed weight of sample (g)} \times 100}{\text{Dry weight of sample (g)}} \quad \text{..... } 4.1$$

3.2.2 Measurement of biofilm thickness

The biofilm thickness was measured using a phase contrast light microscope (Prior B3000, Cambridge, UK) with a graticule mounted in the eye piece. Care was taken during measurements to ensure that the bioparticles did not lose moisture, by mounting in a drop of water on a microscope cavity slide. Due to the fragile nature of the particulate biofilm once removed from the bed, handling of individual bioparticles to measure biofilm thickness was challenging. Various methods of measuring bioparticle and biofilm thickness are available; however, the above method was chosen because it enabled two or more experiments to be carried out on a sample of bioparticles. The use of SEM images was not satisfactory, owing to the necessity for specimen dehydration. Confocal scanning laser microscopy (CLSM) though better for the measurement of biofilm thickness as hydrated specimens can be used, was not ideal as the technique is difficult and time consuming. Although the effect of gravity on the particulate biofilm outside its fluidized state is not fully understood, the measurement of biofilm thickness with the light microscope while maintaining the wet state of the entire particulate biofilm was chosen as the preferred method. Due to the irregular shapes of the coke support material, the longest and shortest biofilm thickness of each bioparticle was measured and the calculated average was taken as the biofilm thickness. The average biofilm thickness of 100 individual bioparticles was used as the biofilm thickness of a sample.

3.2.3 Determination of specific nitrification rate of bioparticles

The specific volumetric nitrification rate of bioparticles was determined by transferring intact samples of bioparticles from the lab scale expanded bed bioreactor to a miniature expanded bed bioreactor of 25 cm^3 total volume constructed from a 1 cm^3 disposable plastic pipette tip as the bioreactor and using a syringe barrel containing aerated synthetic medium (BS EN ISO 9509:2006) as the feed reservoir, (Fig. 3.3). The full medium synthetic wastewater for this standard method contained $(NH_4)_2\ SO_4$ (5.04 g L^{-1}) and $NaHCO_3$ (2.65 g L^{-1}) to give a NH_4^+-N concentration of 56 mg L^{-1}. The buffering effect of the full medium maintained the bioreactors at a pH of 7.6 for the duration of the experiment. The miniature expanded bed was maintained at 100 % expansion by a multi-channel peristaltic pump (Watson Marlow 505LA, Falmouth, UK) and series of individual bioreactors were run simultaneously as batch culture systems for 4 hours (Fig. 3.3). Similar to the main EBBR, the miniature expanded bed reactors were set to run at an upward fluid velocity of 1 cm s^{-1}. To aerate the system, compressed air was bubbled through the synthetic wastewater in the syringe barrel. The experimental set up for the determination of specific nitrification rate is shown in Fig. 3.3 and Table 3.1. One of the miniature bioreactors was used as a control; Allylthiourea (ATU) was added to inhibit nitrification. The specific volumetric nitrification rate of bioparticles represented the nitrification rate of a selected sample of bioparticles in the intact state when expanded 100 % in the miniature EBBR run for 4 hours.

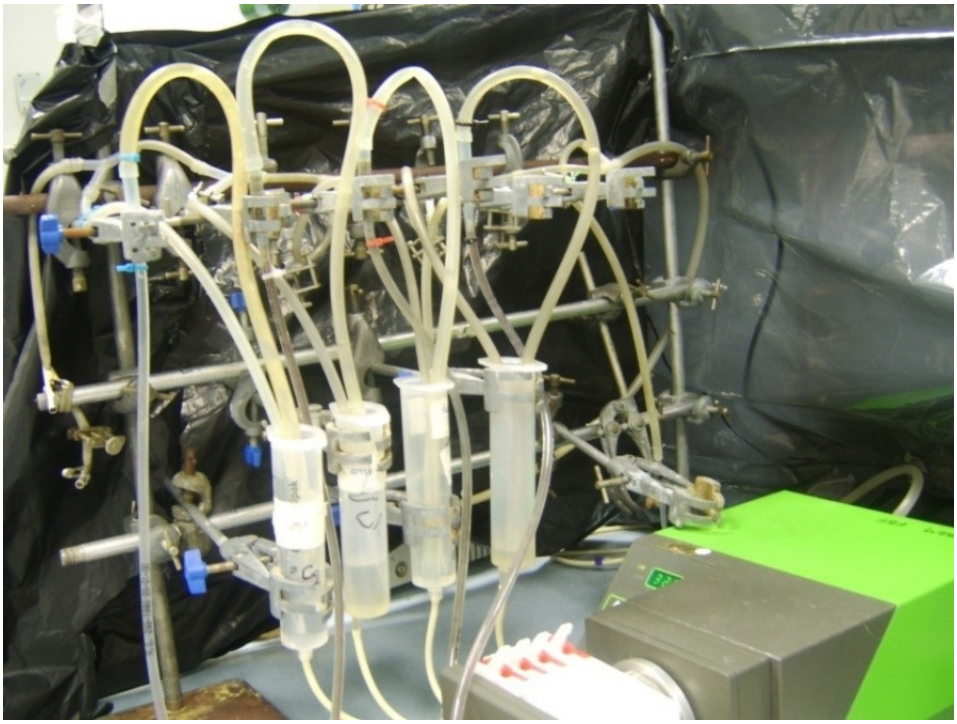

Fig. 3.3 The miniature expanded bed bioreactor system for the determination of the specific nitrification rate of bioparticles.

Table 3.1: Experimental set up for maximum nitrification rate experiment.

	Full medium (cm^3)	Water (cm^3)	Inhibitor (ATU) (cm^3)	Bioparticles (cm^3)	Total volume (cm^3)
Control	25	225	-	-	250
Bioparticles sample	25	220	-	5	250
Bioparticles control	25	217.5	2.5	5	250

3.2.4 Determination of maximum nitrification rates of bioparticles

The maximum volumetric nitrification rate represents the maximum nitrification achieved by biofilms when they are liberated from their support media and their contents distributed in the entire reactor volume. The maximum volumetric nitrification rate of biofilms from bioparticles was determined by transferring samples of bioparticles into Dreschel bottles (MF 48/13/250, Quickfit, Stone, England). With a total reactor volume of 250 cm^3, the Dreschel bottles were fitted with sintered glass spargers (B24/29), through which compressed air was passed to aerate the reactors. The Dreschel reactor vessels containing synthetic medium (BS EN ISO 9509:2006), were placed on magnetic stirrers (IKA lab disc) and the bioparticles were kept in constant suspension by a rotating 2 cm magnetic flea. The vigorous aeration and continuous stirring caused the detachment of the biofilm from the coke support and also disrupted and kept the detached biofilm in suspension (Fig. 3.4). The biomass was incubated for 4 hours and the ammonia concentration was measured at intervals using spectrophotometric analysis (ISO 7150-1:1984). The experimental set up is shown in Fig. 3.4, Table 3.2. A control reactor was also set up with ATU added to inhibit nitrification.

In the experiments with intact biofilms (specific nitrification rate) or disrupted biofilm (maximum nitrification rate), the nitrification rates were calculated after 4 hours of incubation. A 1: 50 ratio of bioparticle to reactor volume was maintained in both maximum and specific nitrification rate experiments. Two methods of sampling

were used to determine the influence of biofilm thickness of the developed bioparticle on nitrification rate and biomass concentration.

Random sampling: A preliminary investigation was made using 2 cm^3 samples of thin biofilms (from the bottom of the bed) and thick biofilms (from the top of the bed). The volumetric nitrification rates, the biofilm thickness and biomass concentration of the samples were determined.

Selected sampling: A further investigation involved sorting out bioparticle samples into sets of 100 similar sized bioparticles (estimated visually) and their biofilm thickness, volumetric nitrification rates and biomass concentrations determined.

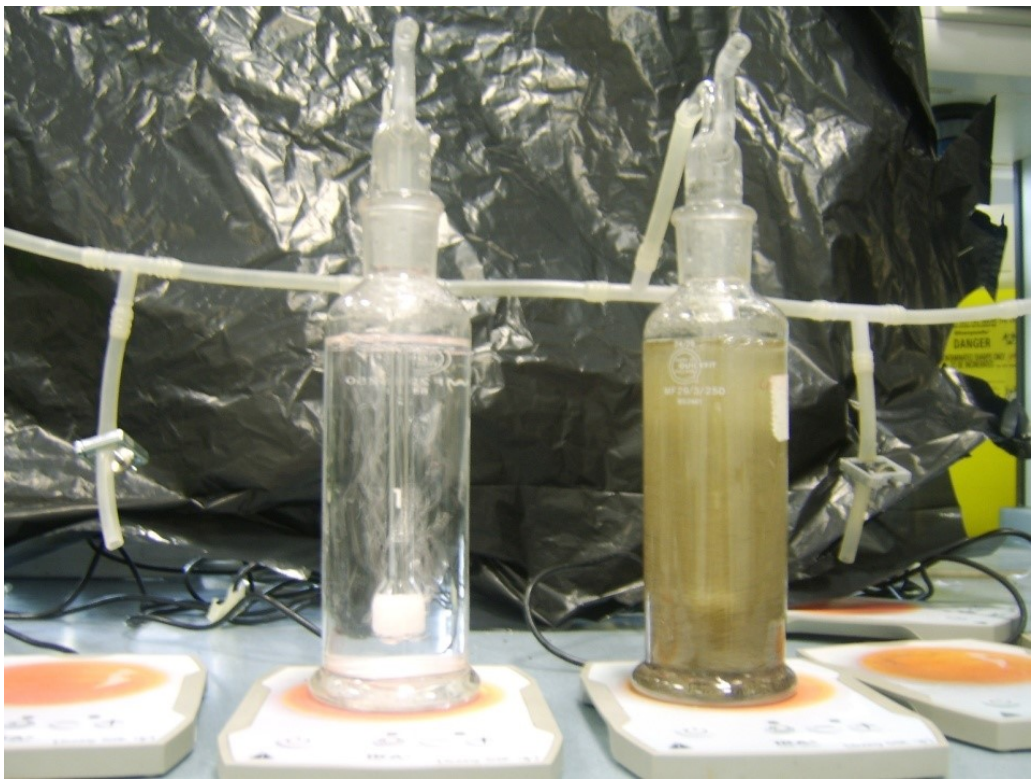

Fig. 3.4 Dreschel bottle reactors used for the determination of bioparticle nitrifying biomass activity , control reactor (left) and biomass containing reactor (right).

Table 3.2. Experimental set up for specific nitrification rate experiment

	Full Medium (cm^3)	Water (cm^3)	Inhibitor ATU (cm^3)	Bioparticles (cm^3)	Total volume (cm^3)
Control	2.5	22.5	-	-	25
Bioparticles sample	2.5	22	-	0.5	25
Bioparticles control	2.5	21	1	0.5	25

The specific surface area to volume ratio of the bioparticles was calculated by measuring the volume of the 100 bioparticles used in the experiment and calculating the average surface area of the bioparticles using the mean bioparticle radius measured by the light microscope method described above.

The ability of biofilm stripped coke particles to carry out nitrification was also investigated. Samples comprising of 50 bioparticles of 200 and 500 μm average biofilm thickness were selected and the external biofilms were manually carefully detached, using a pair of forceps. The stripped coke particles were placed in the miniature expanded bed bioreactor alongside 50 uncolonized coke particles and the ammonia lost from the reactor was calculated using the same method for the determination of the specific nitrification rate of bioparticles. A control reactor was also included which contained no particles in order to determine the ammonia lost as a result of air stripping.

3.3 Results

Operating the expanded bed bioreactor at pH 7.5, 22.5 ^{0}C and 50 % bed expansion, the expanded bed grew at about 1 cm week^{-1} (based on the static bed height measurements), (Fig. 3.5). Because the expanded bed was sampled regularly, the used bioparticles if intact after the experiment or stripped coke materials were replaced into the bed after use. But when the bioparticles could not be replaced, fresh coke particle estimates of the amount removed were periodically added to the bed to maintain an averagely constant bioparticle volume. During periods of constant harvesting of the bioparticles e.g. days 5, 15, and 21 to 24 (Fig. 3.5), the static bed height either reduced or showed no detectable increase. In spite of the harvesting of biofilms from the EBBR, the system

The need for several measurements to be obtained for an average biofilm thickness could be obtained due to the uneven nature of the coke support is shown in the images of the biofilm (SEM of biofilm completely embedding the coke (Fig. 3.6) and a light microscope illumination of a wet mount of the biofilm (Fig. 3.7)

3.3.1 Biomass concentration

Methods to determine the external biofilm of the bioparticle (Fig. 3.6 and Fig. 3.7) were developed using a TGA analyser (TG 209, NETZSCH, Germany) (Fig. 3.8a-c). 3.10) and heating the bioparticles in the uncolonized coke particles, bioparticles and harvested biofilm in a muffle furnace (Fig. 3.9). The uncolonized coke had been placed in water and sterilized by autoclaving.

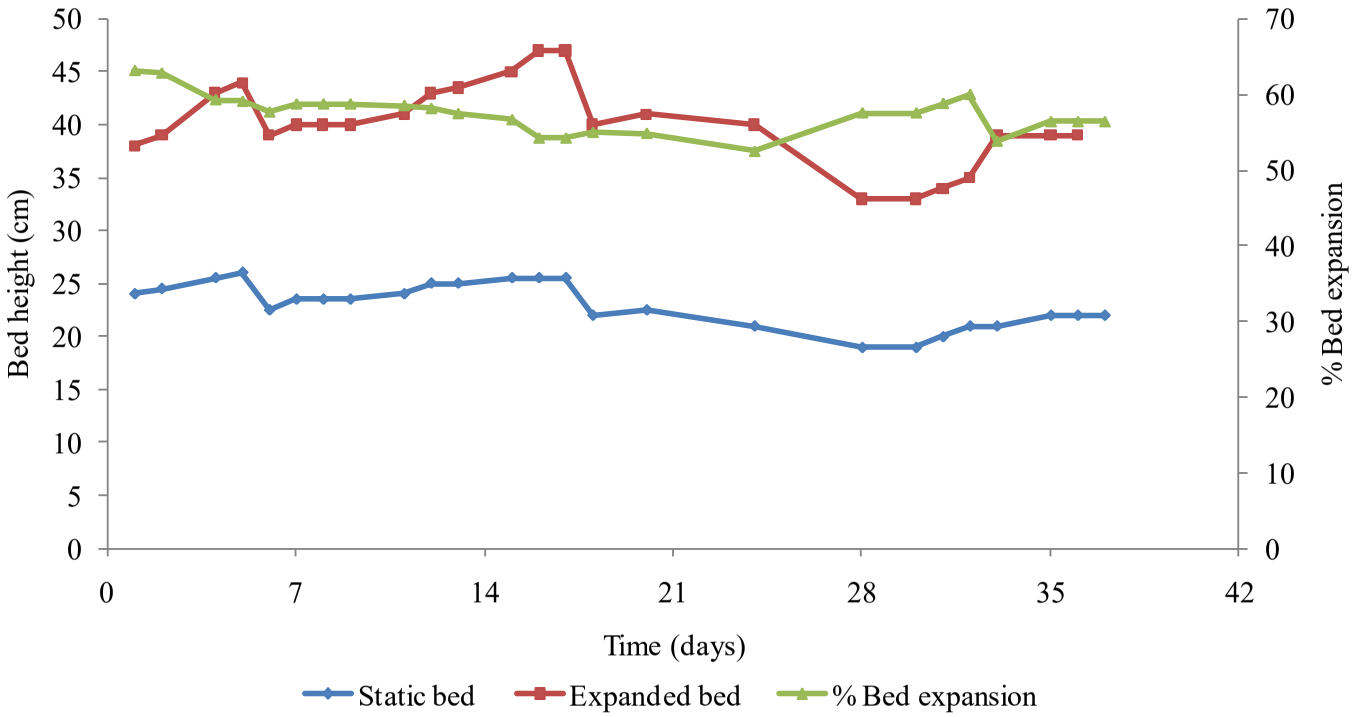

Fig. 3.5 The growth pattern of the EBBR during continuous culture

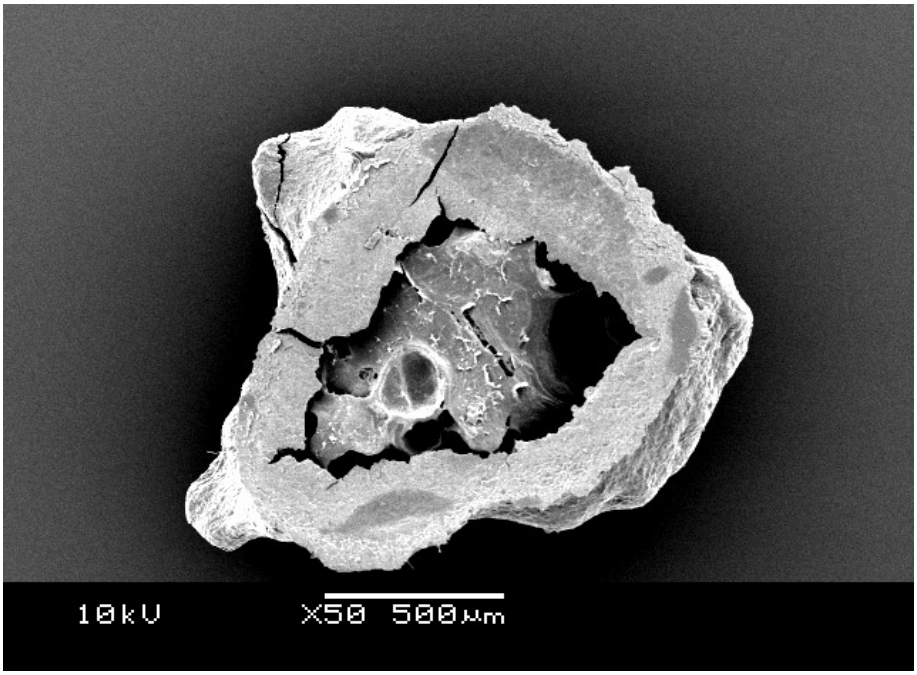

Fig. 3.6 SEM micrograph showing cross section of particulate biofilm; the coke support is seen embedded in a thick biofilm.

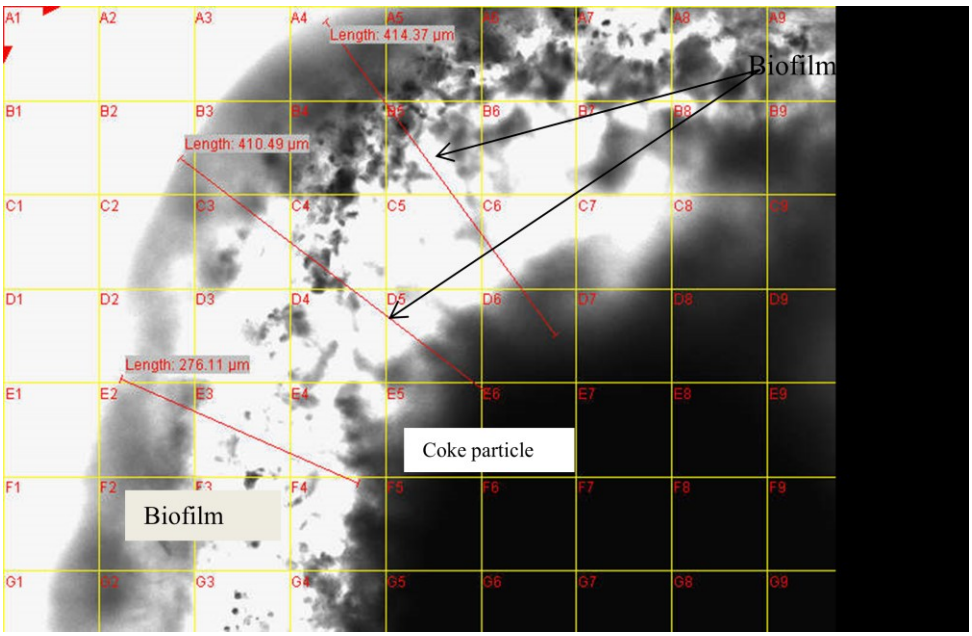

Fig. 3.7 Image of a wet, fully hydrated biofilm associated with the coke particle using the light phase of an epifluoresence microscope showing the biofilm, coke, and possible biofilm thickness measurements.

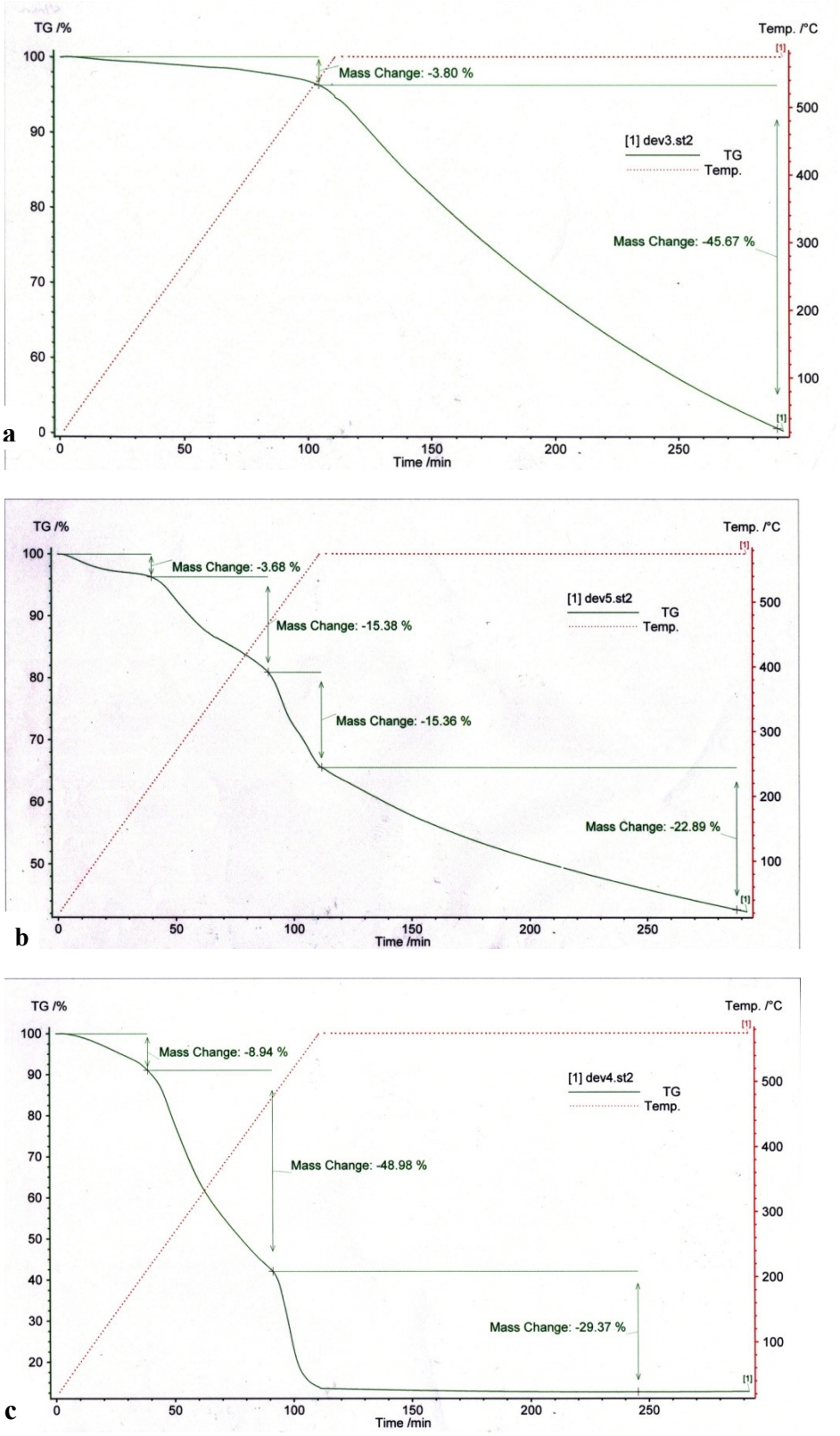

Fig. 3.8(a-c) TGA analysis chart of coke particles (a) bioparticles (b) and harvested biofilm (c) when heated to 575 ^{0}C at 5 ^{0}C min^{-1} and held for 3 hours.

In the TGA analysis, the oven dried samples were all heated at a rate of 5 ^{0}C min^{-1} and it took about 110 minutes (46 % of the total heating time) to reach 575 ^{0}C at which the temperature was held for 3 hours (Fig. 3.8 a-c). The three samples all showed different patterns of change in mass during each stage of heating.

Upon heating, the coke particles showed a 2-phase pattern (Fig. 3.8a). Coke samples lost about 4 % of total mass by 535 ^{0}C. Above 535 ^{0}C however, there was a rapid loss in the mass of coke (≈ 0.27 % min^{-1}) and, when held at 575 ^{0}C for 3 hours, the coke lost a total of about 50 % of its mass (Fig. 3.8a). The rapid loss of mass above 535 ^{0}C indicates that the coke particles will burn rapidly at temperatures below 575 ^{0}C.

The bioparticle samples showed a 4-phase pattern when heated (Fig. 3.8b). The bioparticle samples lost about 4 % of mass below 230 ^{0}C, 15 % between 230 ^{0}C and 490 ^{0}C, and 15 % between 490 and 575 ^{0}C. By 575 ^{0}C, bioparticles samples lost about 34 % of total mass. However, when held at 575 ^{0}C for 3 hours, there was a rapid loss in mass of about 0.17 % min^{-1}. The bioparticle samples lost a total of 57 % of mass by the end of the process (Fig. 3.8b).

The harvested biofilm showed a 3-phase pattern (Fig. 3.8c). The biofilm samples showed an initial 9 % loss in mass by 200 ^{0}C. Between 200 - 500 ^{0}C, 49 % of the biofilm was burnt off and between 500 - 575 ^{0}C, 29 % of the biofilm was burnt off. By 575 ^{0}C, 87 % of the biofilm was burnt off and there was no further loss of mass when held at 575 ^{0}C for 3 hours. The lack of reduction in mass of biofilm by 575 ^{0}C

indicates that all the biomass in the biofilm sample had been volatilized and the ash residue did not change in mass (Fig. 3.8c). The dry biofilm therefore contained 87 % biomass and 13 % ash. Although coke particles burn rapidly at 575 ^{0}C with this technique, it was not possible to determine the difference between the biofilm and coke when heating the bioparticle sample. However, it can be concluded that when biofilm is heated using this method, the biomass associated with the biofilms is completely volatilized to ash by 575 ^{0}C.

The percentage biomass of the samples of coke, harvested biofilm and the mass lost from the bioparticles and when heated for 3 hours over a range of temperatures (400 – 600 ^{0}C) in a muffle furnace is shown in Fig. 3.9 (data shown in table 3.3). When samples of harvested biofilm were heated in the muffle furnace for 3 hours, the harvested biofilm showed an almost constant 87 % reduction in mass between 420 ^{0}C and 600 ^{0}C. This indicates that the biomass is completely incinerated to ash by 420 ^{0}C. The coke samples however, began to burn at temperatures as low as 400 ^{0}C with less than 5 % of the mass lost. Above 420 ^{0}C, there was a rapid loss in mass with increase in heating temperature (Fig. 3.9). The bioparticle samples lost 26 % of their mass at 400 ^{0}C but also showed a rapid loss in mass similar to the coke samples when heated above 420 ^{0}C.

When heated to 575 ^{0}C for 3 hours, the bioparticle lost 63 % of its mass while the coke particle lost 48 % of its mass (Fig. 3.9). This indicates that although the biomass associated with the bioparticle is incinerated to ash at the ASTM recommended 575 ^{0}C, a large portion of the coke support will also be burnt off. This

high loss of coke material in the bioparticles when heated to 575 ^{0}C indicates that 575 ^{0}C cannot be used to measure the biomass associated with bioparticles. Another major effect of heating bioparticles above 420 ^{0}C is that between 420 – 575 ^{0}C, the rate of change in percentage of mass burnt off per degree rise in temperature was 400 % higher than that between 400 – 420 ^{0}C for coke, and 260 % for bioparticles; (y = 0.3211 *vs* y = 0.0811, and 0.1876 *vs* 0.0699 respectively). This rapid loss of mass above 420 ^{0}C was not observed when the harvested biofilm samples were heated implying that the loss of mass above 420 ^{0}C when the bioparticle was heated was not due to loss of biomass. The biomass content of the harvested biofilm when heated to 400 ^{0}C was 76 % but at 420 ^{0}C it was 89 %. Between 420 ^{0}C and 600 ^{0}C the ash weight content of the harvested biofilm was constant (about 90 %) indicating that by 420 ^{0}C, all the biomass is burnt to ash (Fig. 3.9). Therefore, heating the biofilm beyond 420 ^{0}C would not be necessary to obtain the ash weight.

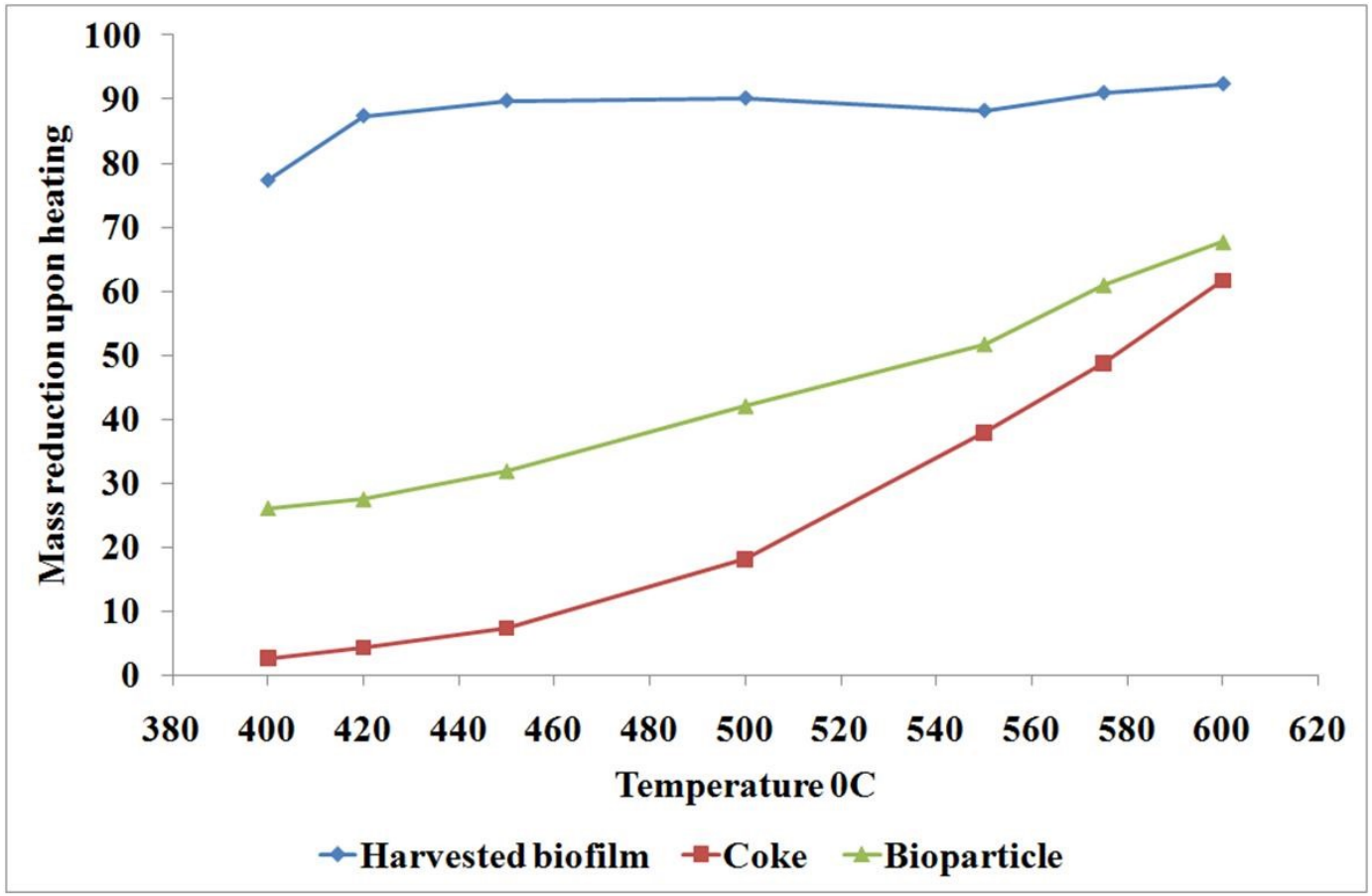

Fig 3.9. Determination of heating temperature for the incineration of biomass to ash using samples of coke particles, harvested biofilm (biomass) and bioparticles in a muffle furnace

Table 3.3 Data obtained from heating samples of coke, bioparticles and harvested biofilms at temperatures between 400 and 600 ^{0}C using a muffle furnace

		Heating Temperature ^{0}C						
Sample		400	420	450	500	550	575	600
Glassy coke	I	1.82	2.02	5.61	18.96	36.01	49.88	62.27
	II	3.79	4.65	8.83	18.31	36.29	48.13	61.00
	III	2.16	5.97	7.43	17.02	41.32	48.18	61.66
Mean		2.59	4.21	7.29	18.10	37.87	48.73	61.64
SD		0.86	1.64	1.32	0.81	2.44	0.81	0.52
Bioparticle	I	26.59	27.48	31.82	42	51.67	67.63	67.63
	II	26.63	26.98	32.01	37.50	52.01	66.68	68.59
	III	25.69	27.42	31.82	39.75	51.67	60.85	66.61
Mean		26.30	27.42	31.82	39.75	51.67	60.85	67.61
SD		0.43	0.34	0.16	1.84	0.28	4.00	0.81
Harvested biomass	I	78.71	87.42	90.17	89.08	84.94	87.12	91.01
	II	75.79	89.21	89.51	90.02	91.40	92.58	93. 74
	III	77.20	85.51	89.79	91.30	88.11	89.73	92.37
Mean		77.23	87.38	89.82	90.13	88.15	89.81	92.37
SD		1.19	1.51	0.27	0.91	2.64	2.23	1.11

There was no statistical significant difference in the percentage biomass of harvested biofilm samples heated at 420 ^{0}C, 500 ^{0}C or 575 ^{0}C (p – value 0.302, ANOVA.).

This means that, when heated at 420 ^{0}C for 3 hours, all the biofilm removed from the bioparticles was burnt to ash. The similar pattern of increase in the mass loss upon heating above 420 ^{0}C for the bioparticle and coke samples indicates that when bioparticles are heated above 420 ^{0}C, most of the mass lost is the coke particle burning and not the biomass, because by 420 ^{0}C, all the biomass is burnt off. Therefore, it was determined that for bioparticles associated with glassy coke particles, 420 ^{0}C is an adequate temperature to obtain the ash weight. At 420 ^{0}C, less than 5 % of the coke particle was burnt, compared to 63 % mass lost at 575 ^{0}C.

The biomass concentration for the bioparticle was calculated as:

$$\text{Biomass concentration (kg m}^3\text{)} = \frac{\text{Weight of biomass burnt off (420 }^0\text{C) (kg)}}{\text{Volume of sample (static bed height) (m}^3\text{)}} \quad \ldots\ldots\ldots\ldots\ 4.2$$

Because coke starts to burn at temperatures as low as 400 ^{0}C, when the bioparticle is heated to 420 ^{0}C, there is a loss of coke alongside the volatilization of biomass, (Fig 3.11). The weight of the biomass burnt off is therefore first corrected for the coke content before used for calculating (equation 4.2).

Corrected weight of biomass burnt off at 420 ^{0}C

= weight of biomass burnt off (g) – weight coke lost from control (g)..... *4.3*

A method has therefore been developed a method of determining the biomass concentration for biofilms associated with glassy coke support media using a muffle

furnace for the determination of the ash content of the biofilms. This method was used to determine the biomass concentration of bioparticle samples in this work.

Composition of bioparticle

Bacteria are composed of approximately 80 % water and 20 % dry matter. The 20 % dry matter in the bacterial cells consists of 90 % organic matter while 10 % is ash (Gray, 1989). Using the method developed in this work, the calculated composition of the bioparticles obtained from the lab-scale EBBR when the interstitial water was drained is about 85 % water, 11 % coke support and 4 % biomass (Fig. 3.10) (although this composition may vary for different biofilm thickness). The composition of the biofilm when heated at 420 ^{0}C is ≈ 88 % biomass and 12 % ash, which is close to the value reported by Gray (1989) for bacterial cells.

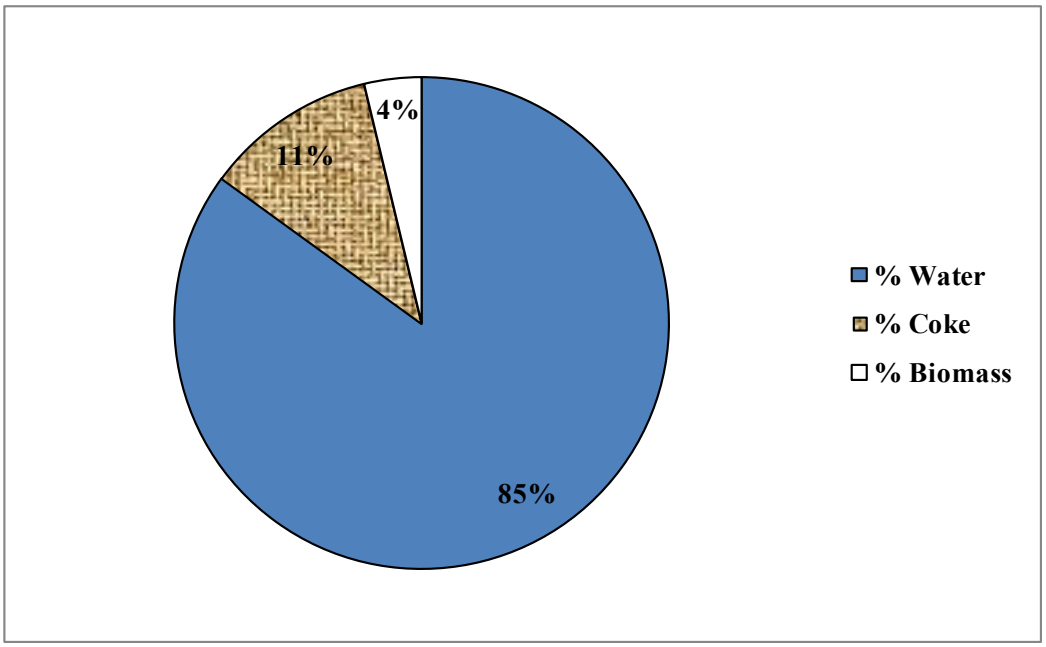

Fig. 3.10 The composition of bioparticles determined using the method developed for the determination of biomass concentration.

3.3.2. Maximum and specific volumetric nitrification rates of bioparticles.

Using biofilms of 100, 150, 490 and 600 µm average thickness, the maximum and specific volumetric nitrification rates of biofilms obtained from different points of the expanded bed were compared and the results are shown in Figure 3.13. Specific volumetric nitrification rates of 5.7, 3.4, 1.1 and 1.5 kg NH_3–N m^{-3} $_{EBBR}$ d^{-1}, and maximum volumetric nitrification rates of 5.7, 5.3, 4.6 and 2.7 kg NH_3–N m^{-3} $_{EBBR}$ d^{-1} were recorded for biofilms of 100, 150, 490 and 600 µm thickness respectively. The maximum volumetric nitrification rates and specific volumetric nitrification rates of biofilms of about 100 µm thickness were similar (Fig. 3.12). However, biofilms thicker than 100 µm had higher maximum volumetric nitrification rates than specific volumetric nitrification rates. The results also showed that above, 100 µm, the maximum and specific nitrification rates reduced with increase in biofilm thickness. After the 4 hour incubation time in both the specific and maximum nitrification rate experiments, the ammonia oxidized in the reactors was adjusted using the ammonia lost in the corresponding control reactors before determining the nitrification rates (Fig. 3.11). ATU was added to the reactors used as control for the thin and thick biofilms to inhibit nitrification

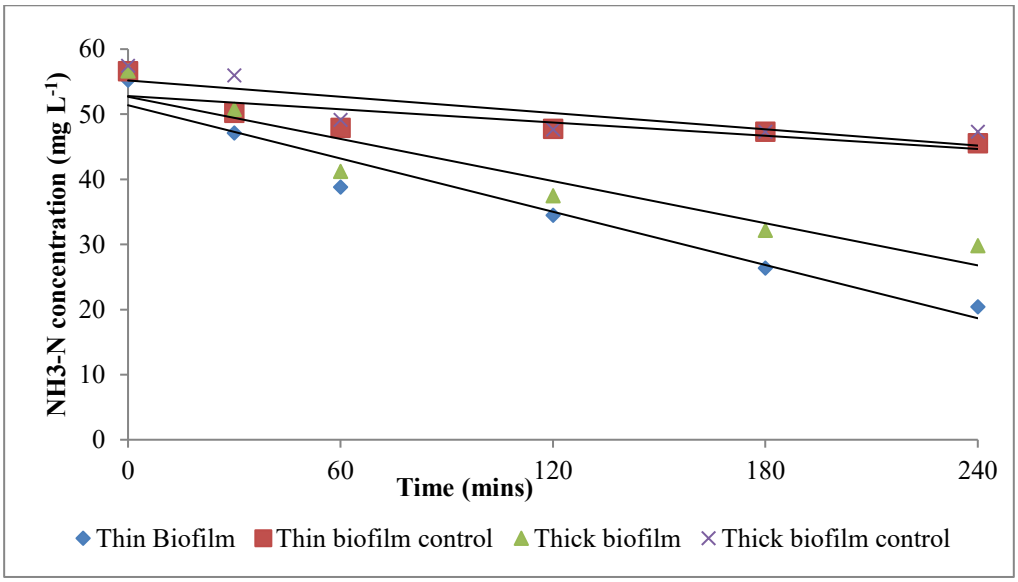

Fig.3.11 The residual ammonia concentration in the reactors for specific and maximum nitrification rate experiments.

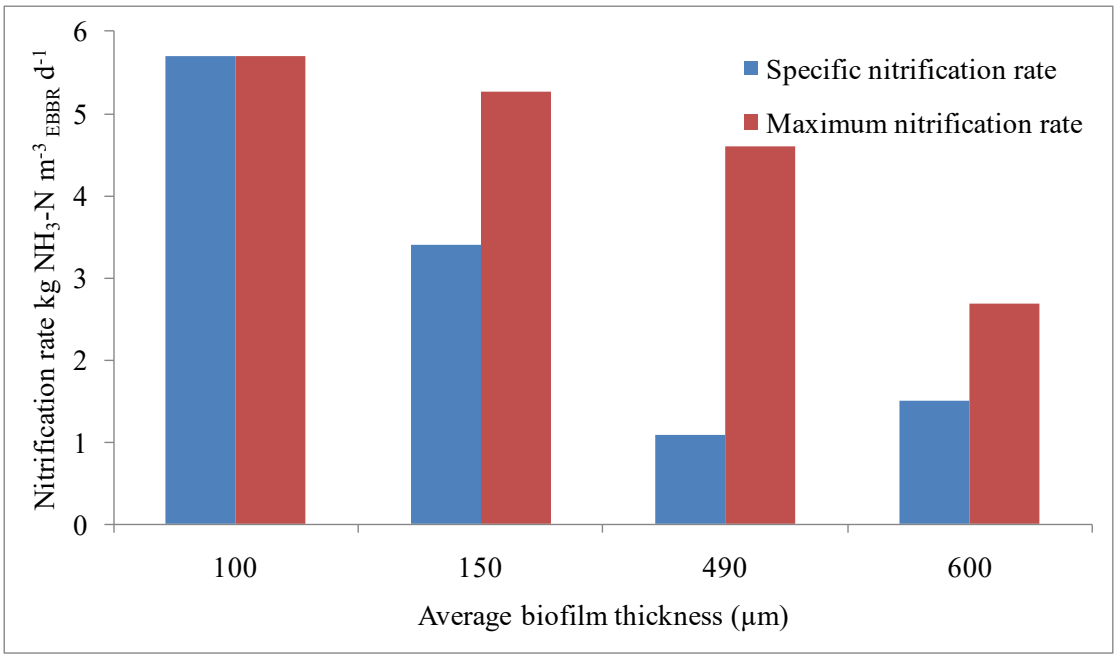

Fig. 3.12 Comparison of maximum (using disrupted biofilms) and specific (using intact biofilms) volumetric nitrification rates for biofilms of different thicknesses.

In both the specific and maximum volumetric nitrification experiment, at the end of the 4-hour experiment, the ammonia concentration was greater than 15 mg L^{-1} (Figures 3.14 to 3.17). This is important because oxidation of ammonia is the process limiting factor for nitrification and a final reactor concentration of 15 mg L^{-1} meant that the nitrification process was not ammonia limited (NH_3-N limiting concentration for EBBR is 1.0 mg L^{-1}, (Dempsey *et al.*, 2005)). While the residual ammonia concentrations in all the reactors were averagely the same at the end of the experiment, the nitrite produced during the experiment varied for the thin and thick biofilms.

The reactors for thick biofilm consistently had low nitrite concentrations (< 2mg L^{-1}) for the duration of the experiment (Fig. 3.14 and Fig. 3.16), while the nitrite concentrations in the thin biofilm reactors were unusually high (20 – 30 mg L^{-1}), (Fig. 3.13 and Fig. 3.15). The low nitrite concentration produced by the thick biofilms indicated that most of the nitrite produced in the biofilm was converted into nitrate by the nitrite oxidizing bacteria. The unusually high nitrite concentrations produced by the thin biofilms was probably due to a low nitrite oxidizing rate by the NOB population to match the ammonia oxidation rate of the ammonia oxidizing bacteria population as normally nitrite is readily oxidized to nitrate. This gives an indication to the diversity of the nitrifying population in thin and thick biofilms.

The results indicate that thin biofilms achieved higher volumetric nitrification rates than thicker biofilms, while the maximum nitrification rates were higher than the specific nitrification rates in the thin and thick biofilms. Complete nitrification of ammonia to nitrate was only evident in the thicker biofilms of 600 μm. Examples of raw data obtained in the determination of biofilm thickness, biomass concentration and bioparticle composition is shown in Appendix C, D, E and F respectively.

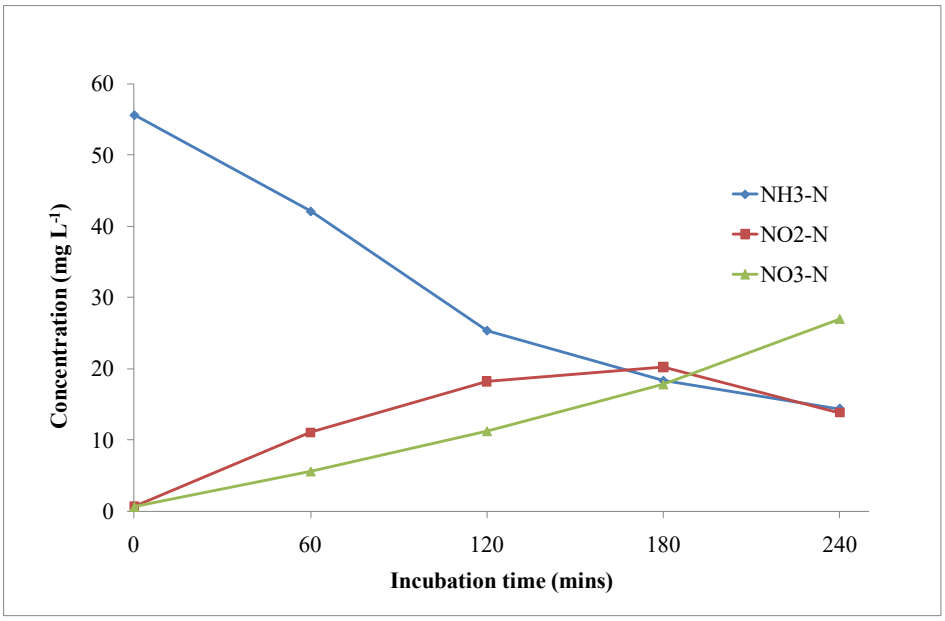

Fig. 3.13 Concentration of ammonia oxidation, nitrite and nitrate production biofilm by 150 µm intact biofilms (specific nitrification rate experiment).

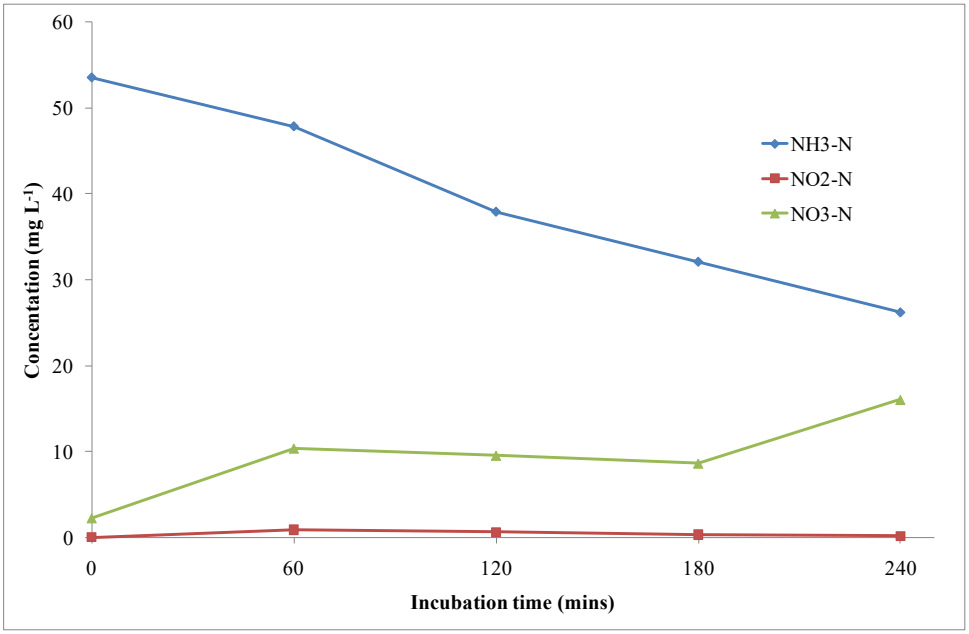

Fig. 3.14 Concentration of ammonia oxidation, nitrite and nitrate production biofilm by 600 µm intact biofilms (specific nitrification rate experiment).

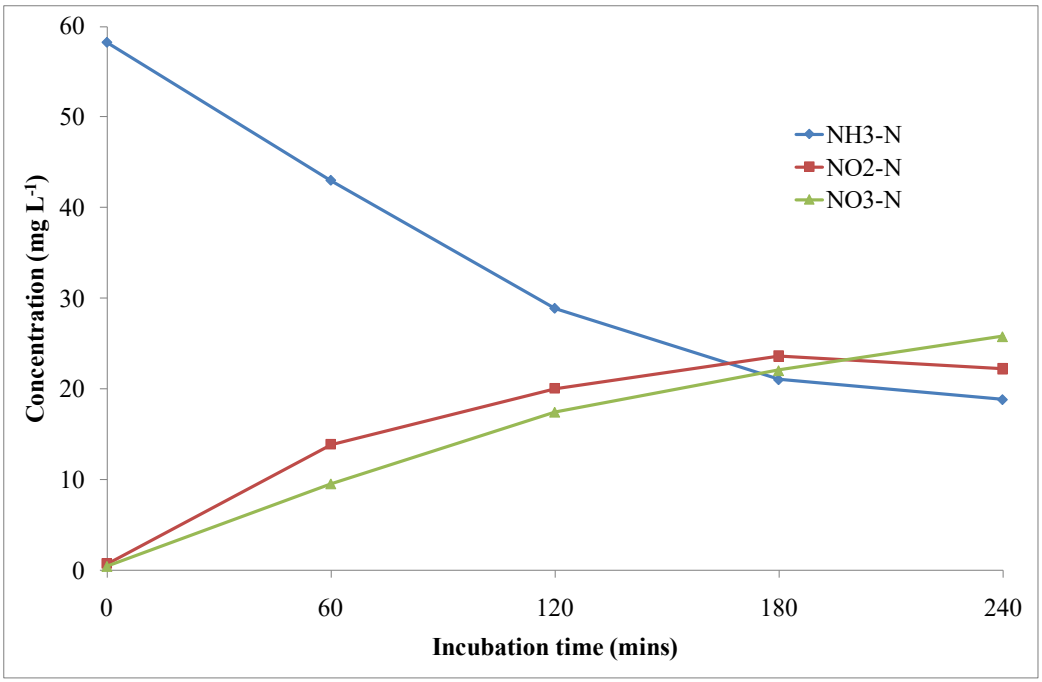

Fig. 3.15 The oxidation of ammonia, nitrite and nitrate production by 150 µm biofilms after removal from the coke support (maximum nitrification rate experiment).

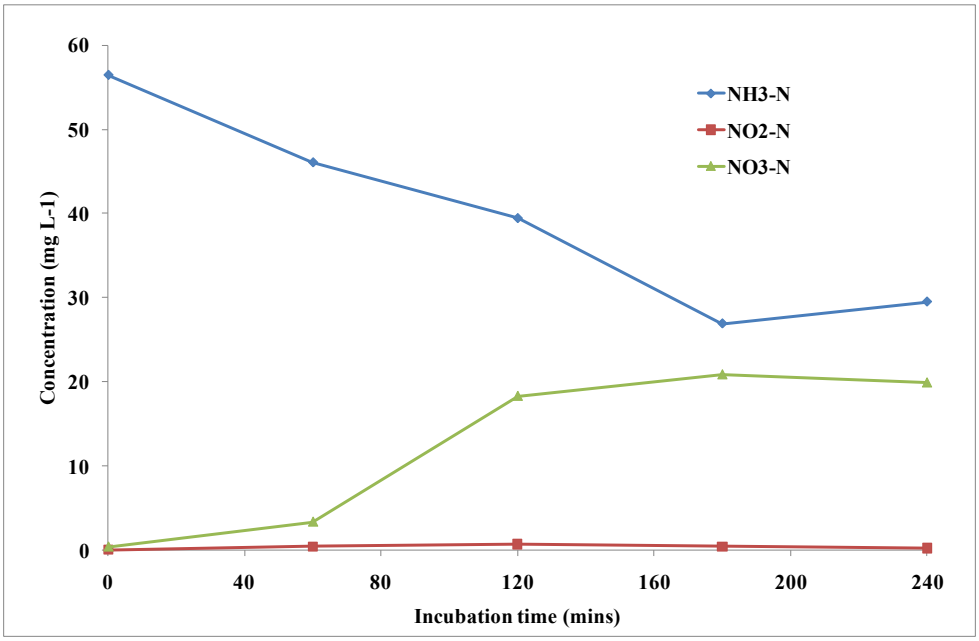

Fig. 3.16 The oxidation of ammonia, nitrite and nitrate production by 600 µm biofilms after removal from the coke support (maximum nitrification rate experiment).

The results of the preliminary investigation on the influence of biofilm thickness on specific volumetric nitrification rates using random samples of thin and thick biofilms from the top and bottom of the lab-scale expanded bed bioreactor are shown in Fig. 3.17.

The nitrification rates of biofilms from the bottom of the bed (70 – 90 µm thickness) was in the range of 2.8 - 4.5 kg NH_3-N m^{-3} $_{EBBR}$ d^{-1} while that for the biofilms from the top of the bed (295 – 385 µm) was 0.9 - 3.5 kg NH_3-N m^{-3} $_{EBBR}$ d^{-1}. The highest nitrification rate 4.5 kg NH_3-N m^{-3} $_{EBBR}$ d^{-1} was recorded for biofilms of 70 µm average biofilm thickness. The lowest nitrification rate, 0.9 kg NH_3-N m^{-3} $_{EBBR}$ d^{-1}, was recorded for the biofilms of 385 µm (Fig. 3.17).

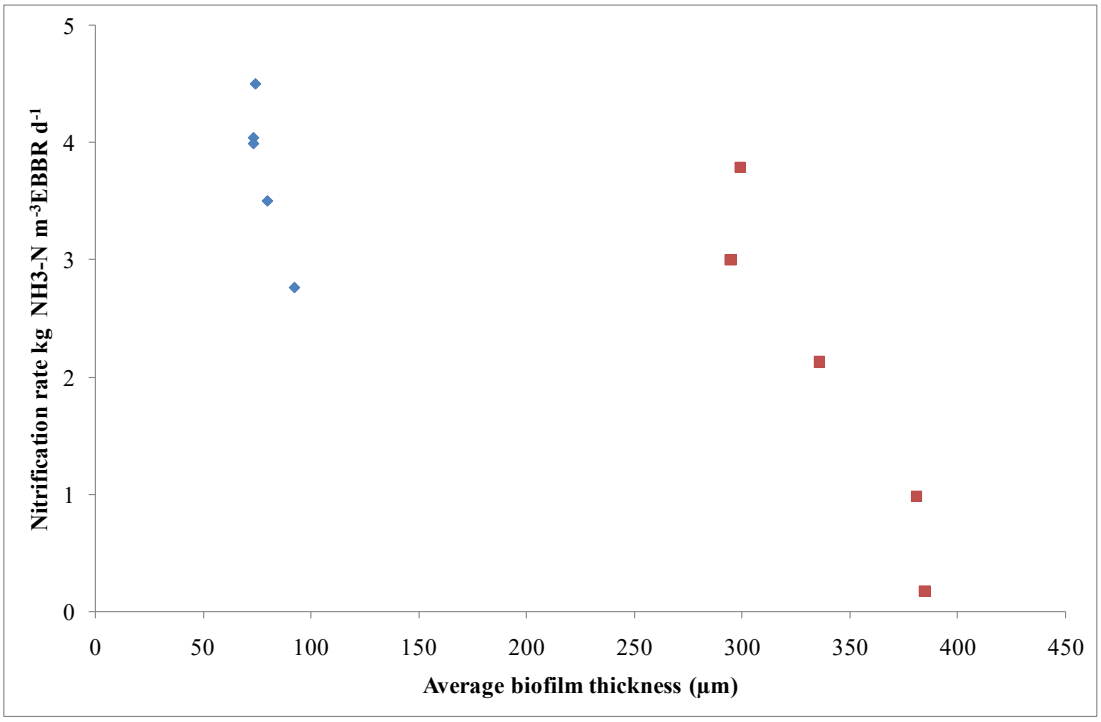

Fig. 3.17 Specific volumetric nitrification rates of random samples of bioparticles from the bottom (thin) and top (thicker) of the EBBR.

This work has demonstrated that thin biofilms have a higher nitrification rate than thicker biofilms (Fig 3.18). While both the thin and thin biofilms showed a reduction in nitrification rate with an increase in biofilm thickness, the nitrification rate for thin biofilms reduced from 4.5 to 2.76 kg NH_3-N m^{-3} $_{EBBR}$ d^{-1}, a change of 80 g NH_3-N per unit µm increase in biofilm while the thick biofilms demonstrated a reduction in nitrification rate of 30 g NH_3-N per unit µm increase in biofilm thickness (Fig. 3.17).

The thicker biofilms used in the initial investigation using random samples had a higher biomass concentrations (27 - 48 kg m^{-3}) than the thinner biofilms (21 - 29 kg m^{-3}) (Fig 3. 19).

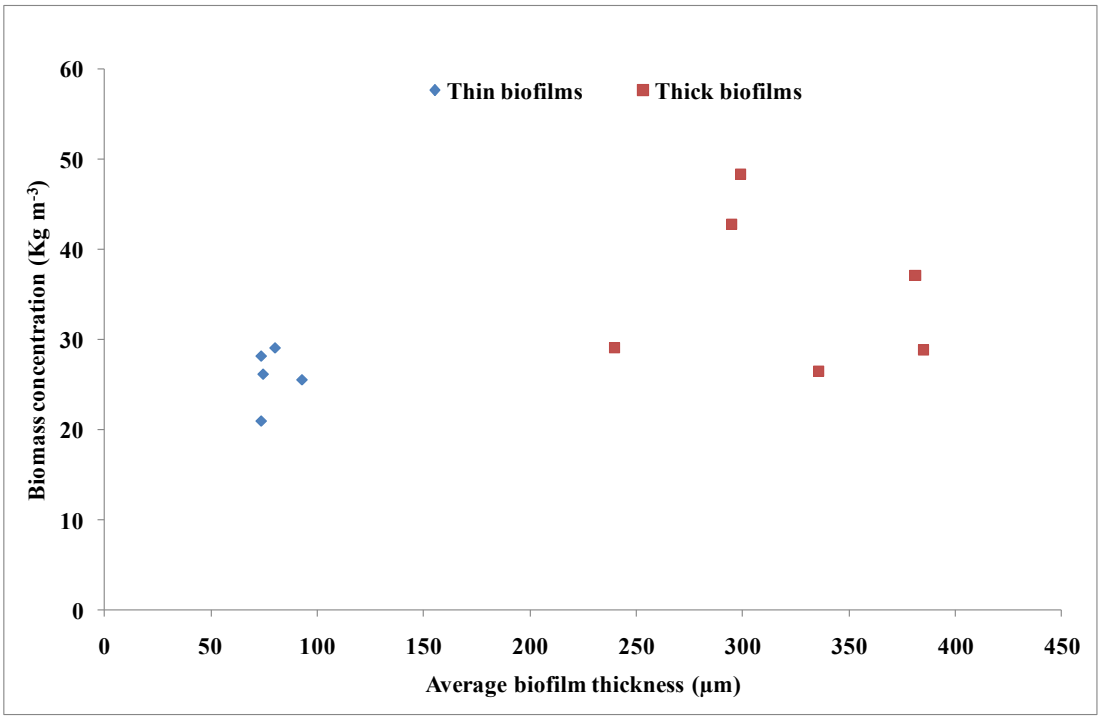

Fig. 3.18 The preliminary determination of the relationship between biofilm thickness and biomass concentration of the thin and thick bioparticles using random samples.

Although this initial investigation of the influence of biofilm thickness on nitrification rate indicated that thinner biofilms had a higher nitrification rate than thicker biofilms (Fig. 3.17), the relationship was investigated more thoroughly by selecting samples of 100 similar sized bioparticles for investigation. This method was a more accurate investigation into the influence of biofilm thickness on the nitrification rates as selection in this way minimized the variation in biofilm thickness of the samples.

The selected bioparticle samples used for the determination of specific volumetric nitrification rates also indicated that thin biofilms achieved higher nitrification rates than thick biofilms (Fig. 3.19). However, this relationship was only seen in biofilms greater than 100 μm thick. Although biofilms of 100 μm average thickness achieved the highest specific nitrification rates (5.4 kg NH_3-N m^{-3} $_{EBBR}$ d^{-1}), the thinnest biofilms (below 100 μm thickness) all achieved lower nitrification rates (Fig. 3.19). In biofilms of between 100 μm and 450 μm thickness, there was a steady decline in the specific nitrification rates (≈ 7 g NH_3-N m^{-3} $_{EBBR}$ d^{-1} per μm increase in biofilm thickness). Biofilms thicker than 450 μm showed no decrease in nitrification rates albeit a marginal increase was recorded (Fig. 3.19). This work has therefore produced a model for the relationship between biofilm development or growth signified by increase in biofilm thickness and nitrification rate. There was an increase in nitrification rate with a peak nitrification rate at about 100 μm.

The high nitrification rate achieved for thin biofilms (5.4 Kg NH_3-N m^{-3} $_{EBBR}$ d^{-1}) is an indication of the potential of this technology when operated under optimum

conditions (pH 7.5 and 22.5 °C). This rate is almost 40 % higher than that reported (3.6 kg NH_3-N m^{-3}_{EBBR} d^{-1}) by Dempsey and Minall (2009) for a technical-scale EBBR used for nitrification of sludge liquor and operated at the optimum pH for that process (7.8) but without temperature control (T ≈ 27 °C).

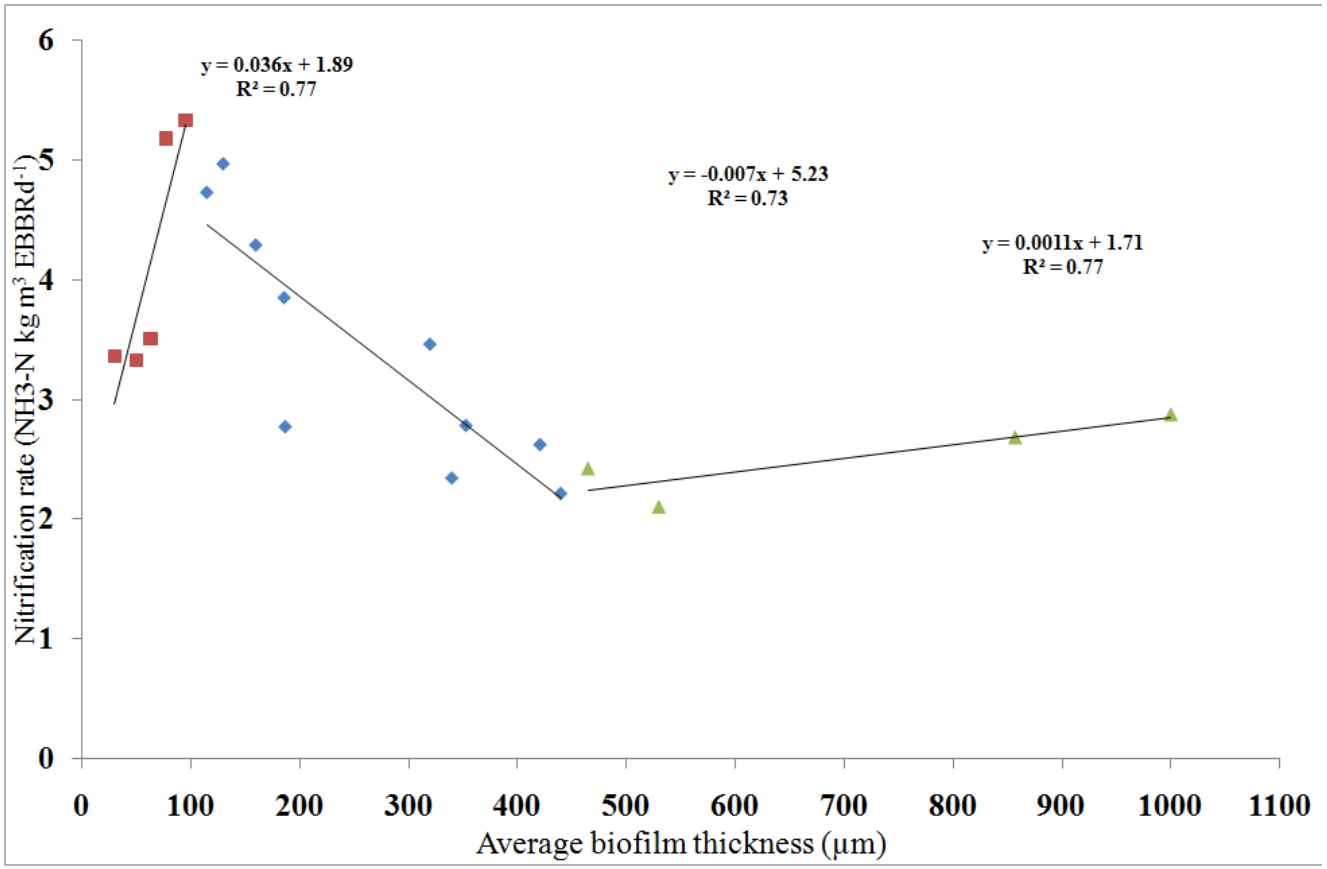

Fig. 3.19 The average nitrification rates of selected samples 100 similar-sized biofilms

The thicker biofilms from selected 100 bioparticles achieved higher biomass concentrations than the thinner biofilms (Fig. 3.20).

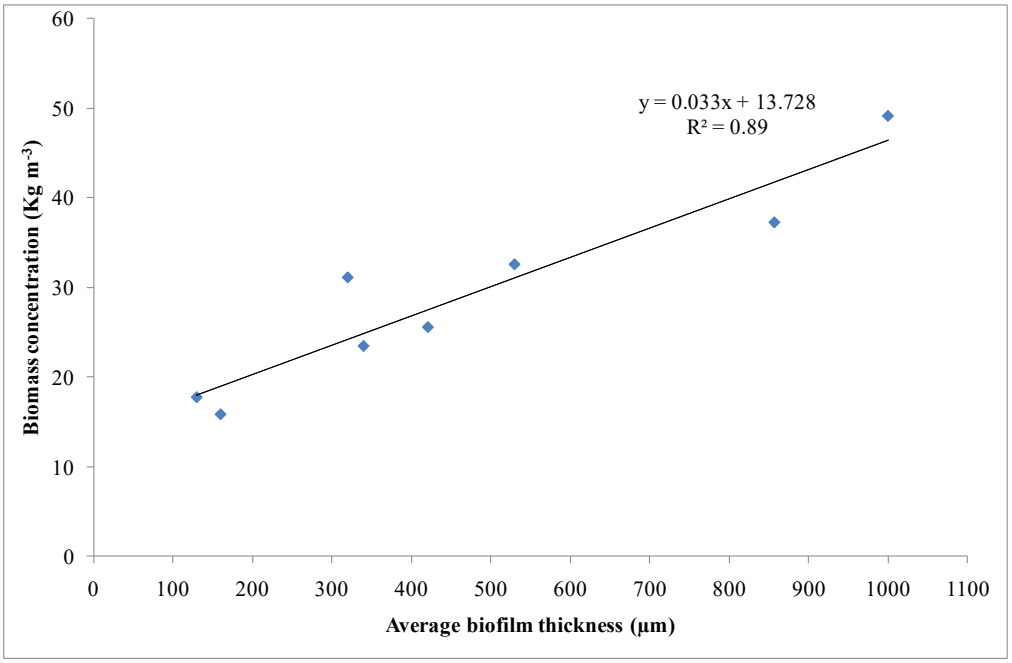

Fig. 3.20 The biomass concentration of samples of 100 bioparticles of different biofilm thickness.

Separation of the bioparticle samples into similar sized groups revealed a more accurate relationship between biofilm thickness and biomass concentration than when bioparticles were selected at random (Fig. 3.18). The biomass concentrations ranged from about 17 kg m^{-3} for thin biofilms to 50 kg m^{-3} for thick biofilms (Fig. 3.20). Clearly, the results show that an increase in biofilm thickness results in a corresponding increase in biomass concentration, and the average rate of increase

was 37 g per µm increase in biofilm thickness, for 1.0 m^3 of bioparticles in the expanded state (100 %).

One of the advantages of particulate biofilm bioreactors is the high surface area to volume ratio of small particles, which results in a high overall reaction rate. The thinner bioparticles had a higher specific surface to volume ratio than the thicker bioparticles (Fig. 3.21) and also achieved higher nitrification rates (Fig. 3.19).

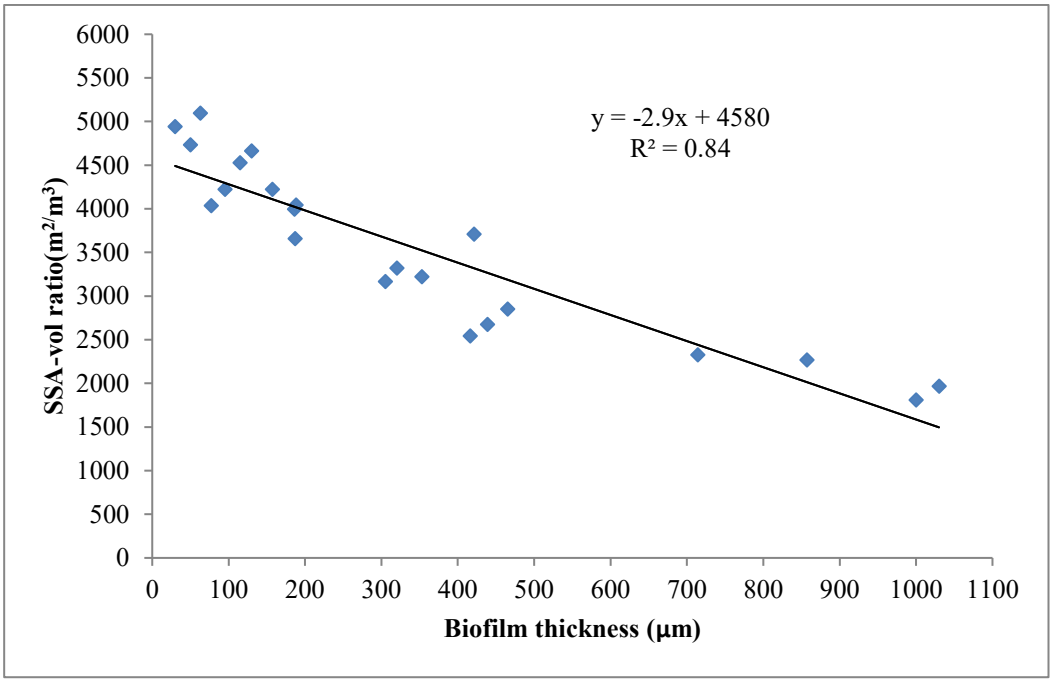

Fig. 3.21 The relationship between specific surface area to volume ratio of the bioparticles and biofilm thickness.

Biofilms less than 100 µm had a specific surface area to volume ratio of up to 5000 m^2 m^{-3}. The specific surface area to volume ratio reduced at a rate of about 3 m^2 m^{-3} per µm increase in biofilm thickness. Nicolella *et al*., (2000b) reported a biofilm surface area of 3 000 m^2 m^{-3} for particulate biofilm reactors, which would be attained by biofilms of about 500 µm in the EBBR using coke particles.

The investigation into the ability of coke particles stripped of their biofilm to carry out nitrification revealed that the coke particles stripped of their biofilms achieved about 40 % higher ammonia removal than the ammonia lost by the sterile coke particles in the miniature EBBR using the method for the determination of specific nitrification rate (chapter 3.2.3, pH 7.6, 20 – 22 ^{0}C) (Fig 3.23). Presumably the loss of ammonia from the control was mainly by the air stripping of ammonia

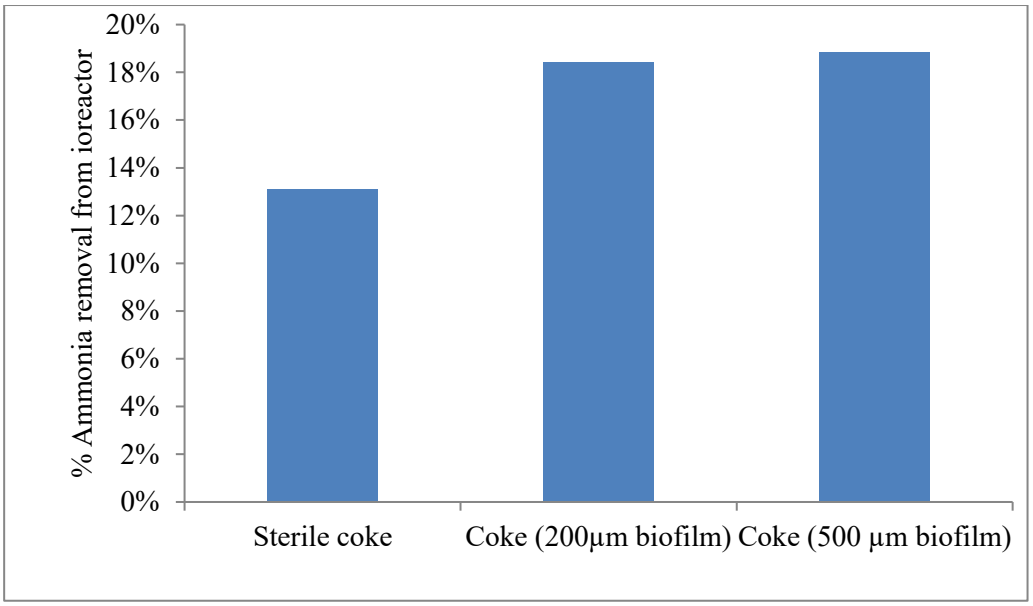

Fig. 3.22 The ammonia removal capacity of coke particles stripped of biofilm in the miniature fluidized bed reactor.

3.4 Discussion

The highest biomass concentration obtained in the lab-scale EBBR was 49 kg m^{-3}; this was higher than previously reported for particulate biofilm reactors and expanded bed (23.6 kg m^{-3} Dempsey *et al*., (2005); 30 kg m^{-3}, Nicolella *et al*., (2000a)). Because biofilms increase in thickness (size) by microbial growth and secretion of EPS, older, more mature biofilms would most likely be thicker as a result of cell growth and hence accumulate higher biomass concentrations.

Disrupted biofilms had a higher apparent volumetric nitrification rates than when left intact e.g. the disrupted biofilm of 490 μm average thickness, achieved nitrification rates 300 % higher than when intact biofilm (Fig. 3.12). This is because when the biofilms were removed from the support medium and the biofilm was completely mixed in the bulk liquid without mass transfer limitations. Although this result indicates higher volumetric nitrification rates for dispersed growth reactors e.g. activated sludge, due to better mass transport (no problem of substrate concentration and biomass distribution gradient), the advantages of attached growth (biofilm) reactors e.g. high biomass retention, high settling velocity are still highly significant.

The comparison between maximum and specific volumetric nitrification rates of the disrupted and intact biofilms indicated that the thin bioparticles had higher specific nitrification rates than the thick biofilms. Furthermore, when compared to the maximum volumetric nitrification rates of random samples of thin and thick biofilms, the higher maximum nitrification rates were obtained for thin biofilms than

thick biofilms (Fig. 3.17). Having already established that thin biofilms have a lower biomass concentration than thick biofilms (Fig. 3.20), it is expected that the thick biofilms with higher biomass concentrations should have higher maximum nitrification rates, as more biomass would release a higher microbial mass into the same reaction volume than would thinner biofilms. This higher biomass concentration, in addition to the lack of diffusional limitations, should lead to biomass from thicker biofilms having higher nitrification rates. The contrary result obtained (thin biofilms achieving higher nitrification rates than thick biofilms) (Fig. 3.12) leads to the conclusion that the greater surface area to volume ratio of thin bioparticles alone cannot be responsible for the higher nitrification of thinner biofilms compared to thicker biofilms.

One explanation for these results is that the not all of the biomass released from thick biofilms was active. The biofilm has two surfaces; one inner surface in contact with the support particle, and one outer surface in contact with the wastewater. Because the biofilm increases in thickness outwardly from the surface of the support material, and substrates penetrate inward from the external surface of the biofilm, the active part of the biofilm would be associated with its external surface. Also, because nutrients are utilized by the bacteria closest to the external surface of the biofilm as nutrients penetrate in, and mass transfer limitations with increase in biofilm thickness from the surface of the biofilm, the inner regions of the biofilm would experience lower substrate concentrations, reduced bacterial activity or even cell death.

The influence of biofilm thickness on specific volumetric nitrification rates was elucidated when samples of 100 bioparticles were selected and used for the experiment. Assuming uncolonized coke particles would have a nitrification rate of zero because they do not have a biofilm and would only cause air stripping (Fig. 3.19), the results show an increase in the nitrification rate of the developing biofilm with increase in biofilm thickness at a rate of 36 g NH_3-N m^{-3}_{EBBR} d^{-1} per unit µm increase in biofilm thickness until about 100 µm biofilm thickness (Fig. 3.19). There was therefore an initial increase in nitrification rate with increase in biofilm thickness due to the establishment, growth and development of the biofilms until 100 µm. The lowest average biofilm sample measurement made was 40 µm, (it achieved a high nitrification rate of 3.2 kg NH_3-N m^{-3}_{EBBR} d^{-1}), because there was a limitation in accurately measuring below 30 µm biofilms with the method. Although biofilms less than 40 µm could not be measured to determine their nitrification rates, it is known however that the porous nature of the glassy coke encourages the colonization and establishment of bacteria. Thus bioparticles in the early stage of bacterial colonization could have measureable nitrification rates but the biofilm thickness cannot be determined by the methods used here.

Above 100 µm biofilm thickness, the nitrification rate reduced at a rate of 7 g NH_3-N m^{-3}_{EBBR} d^{-1} per µm increase in biofilm thickness. The decrease in nitrification rate with increase in biofilm thickness levelled off at about 450 µm, above which there was no significant decrease in nitrification rate (Fig. 3.19). The reduction in nitrification rate may be due to the effect of diffusional limitations reducing the activity of the nitrifying biofilms above 100 µm biofilm thickness. Biofilms less than

100 µm would probably be limited by the biological properties of the biofilm as the optimum biofilm thickness for nitrification is 100 µm (Fig. 3.19).

Following the reduction in nitrification rates when using biofilms between 100 and 450 µm, there was no significant increase in nitrification rate upon further increase in biofilm thickness beyond 500 µm (Fig. 3.19). The biofilms above 450 µm maintained an average nitrification rate of 3.5 kg NH_3-N m^{-3}_{EBBR} d^{-1}, although there was approximately a 180 % reduction in bioparticle surface area to volume ratio (Fig. 3.19 and Fig. 3.21), the nitrification rate was maintained between 450 and 1000 µm biofilm thickness. This lack of change in nitrification rate indicates that there is an almost constant 450 µm region of biofilm activity from the surface of the biofilm in thick biofilms.

Seker *et al*. (1995) stated that diffusional limitations in particulate biofilms lead to the development of an inactive inner layer of organisms with increased biofilm thickness, whilst the outermost layer is responsible for the bulk of the reaction. Clearly, when substrates penetrate further, a larger fraction of the biofilm is active. The findings of Seker *et al*., (1995) identified a difference in the substrate consumption rates of biofilms approximately 90 µm and greater than 90 µm thickness; they noted that in biofilms of less than 90 µm thickness, substrate consumption rates for observed and active biofilm were similar but in biofilms greater than 90 µm thickness, substrate consumption rate was less rapid; implying a non active core layer of biofilm greater than 90 µm. The thick biofilms used in this study most likely had an outer active layer for nitrification that was about 450 µm

thick above which a substrate became limiting, therefore forming an inner layer of mostly inactive cells for biofilms thicker than 450 µm. Picioreanu *et al.,* (1999) reported that the biofilm top layer grows much faster than the bottom layer, due to the steep gradient of substrate concentration, it is therefore expected that the top 450 µm of the biofilms in this study would be the more active, growing portion. These findings indicate that there is a maximum biofilm thickness for high rate nitrification using the EBBR technology. The thinner the biofilm, the larger the fraction of the bed occupied by the inert support material (in this case, coke); whereas the thicker the biofilm, although the support particle fraction is less and the biomass fraction available for nitrification is higher, nitrification is more restricted because of mass transport limitations.

In the miniature EBBR used for the determination of specific volumetric nitrification rate, the most likely substrate limitation was dissolved oxygen, because the initial ammonia concentration was 56 mg L^{-1} and did not fall below 15 mg L^{-1} by the end of the 4 h batch incubation and therefore ammonia was not limiting the nitrification rate. The pH because of the buffering capacity of the medium was maintained close to 7.6, and the temperature of 20 - 22 ^{0}C were also not limiting the nitrification rates.. For the nitrifying particulate biofilm in which autotrophic nitrification is essentially aerobic, the depth of oxygen penetration would affect the nitrification rate. While Denac *et al.,* (1983) had earlier proposed that oxygen had a penetration depth of between 100 -150 µm, Hibiya *et al*., (2004), using nitrifying bioparticles with a cement ball fabrication made from coal ash for support reported that oxygen penetrates biofilms to depths of 300 µm. De Beer *et al,.* (1993), however, reported

that ammonium oxidation, which is the rate limiting step of nitrification by nitrifying bacteria, was restricted to a depth of 120 μm in nitrifying bacterial aggregates grown in a fluidized bed reactor. Hibiya *et al.,* (2004) reported the greatest depth of oxygen penetration in biofilms, 300 μm, in particulate biofilms. This depth of oxygen penetration would mean a cessation of activity for cells above 300 μm from the biofilm surface. This study however revealed nitrification activity in biofilms up to 450 μm thickness indicating a much deeper penetration depth of substrates in the fluidized bioparticles in the expanded bed operation.

This study also determined that the optimum biofilm thickness for ammonia oxidation using bioparticles was 100 μm (Fig. 3.19). The optimum biofilm thickness for complete nitrification of ammonia to nitrate, however, is determined by the biofilm thickness at which all the nitrite produced as a result of ammonia oxidation is converted to nitrate by the nitrite oxidizing bacteria. The high final nitrite concentrations when using thin biofilms (150 μm) measurements for either specific or maximum nitrification rate (Fig. 3.13 and Fig. 3.15) indicate that the nitrite oxidizing bacteria population was not large enough or active enough, as the excess nitrite could not be oxidized to match the nitrite production rates. Conversely, the thicker biofilms of 600 μm achieved complete nitrite oxidation; therefore nitrite oxidation matched the nitrite production by the ammonia oxidizing bacteria (Fig. 3.14 and Fig. 3.16).

The biofilm thickness range for microbial activity of 450 μm obtained in this study (Fig. 3.19) was much larger than previously reported in the literature e.g. 300 μm,

Hibiya *et al.*, (2004). But the bioparticles used in this study were found to contain 85 % water (Fig. 3.10).

Although the SEM observations did not show the activity or viability of the biofilm community (Chapter 2), it provided evidence of the bacterial presence (and sometimes arrangement) on the surface of the biofilm and the coke support supporting the possibility of a 450 μm 'active biofilm depth'. The ability of coke particles stripped of biofilms of 500 μm to undergo nitrification (Fig. 3.22), indicated that the presence of nitrifying activity at 500 μm. There was probably a thin layer of biofilm, still attached (probably even in patches) on the coke particles but not visible to the naked eye, after stripping of the biofilm. Furthermore, the 450 μm biofilm depth may be the range of an 'active biofilm depth' irrespective of biofilm thickness and biomass concentration of the bioparticle.

3.5 Conclusions

- The coke based bioparticles can attain biomass concentrations of up to 50 kg m^{-3} (using thick biofilms) and also 5 000 m^3 m^{-2} surface area for reaction (using thin biofilms).

- Although thick biofilms had higher biomass concentrations, thinner biofilms achieved higher volumetric nitrification rates than thick biofilms

- The optimum biofilm thickness for ammonia oxidation is was found to be 100 µm.

- There is evidence to infer that optimum biofilm thickness for nitrite oxidation is in the biofilms was greater than 100 µm.

- The biofilm depth for nitrification activity in the biofilms was about 450 µm. This indicates a penetration depth of 450 µm by substrates including oxygen.

CHAPTER FOUR

4.0 Quantification of nitrifying bacteria in biofilms

4.1 Introduction

Recent studies into the structure of biofilms involve microscopic, physicochemical (e.g. the use of microelectrodes), and molecular biological techniques (Wimpenny *et al.*, 2000). Understanding complex multispecies biofilm often involves mathematical modelling of the biofilm features. Various methods for modelling biofilm structures have been used; the main aim of modelling is to describe the structure and activity of the biofilms in a mathematical way (Picoreanu *et al.,* 2005). The models are simplified representations of biofilms but based on hypotheses and equations used to rationalize observations. However, methods have been developed to extract morphological features from images in order to quantify the characteristics of biofilm structure. Most of the methods developed are based on images obtained from 3D imaging techniques such as confocal microscopy. These methods involve the development of algorithms to quantify biofilm structure from digitalized computer images (Yang *et al.,* 2000). The algorithms are then integrated into computer software packages and the biofilm features e.g. cluster size and shape automatically derived.

The confocal scanning laser microscopic (CLSM) imaging of biofilms is an ideal source of data for the evaluation of 3D biofilm model predictions. Biofilm structures can be described by simple properties like thickness or density and spatial

distribution. The spatial distribution of EPS, bacterial cells of different species and even inorganic particles within the biofilm can be described (Picioreanu *et al.,* 2005).

The community structure, abundance and activity profiles of nitrifying bacterial species have been studied using different methods, including the use of molecular techniques and microelectrodes (De Beer *et al.,* 1993; Okabe *et al*., 1999; Kuehn *et al.,* 1998; Gieseke, *et al*., 2001; Nakamura *et al*., 2006). Using microelectrode sensors to monitor the oxygen, ammonia, nitrite and nitrate concentration with depth along the biofilm thickness, De Beer *et al.,* (1993) concluded that ammonium consumption and nitrate production were localized in the outer layer of approximately 100 to 120 μm thick, but that oxygen penetrated to a depth of 300 μm.

Schramm *et al.,* (1996) also measured the profiles of oxygen and nitrite concentration within trickling filter biofilms and reported that nitrification was restricted to the outer 50 μm of the biofilm, while Gieseke *et al*., (2001), reported that oxygen was restricted and limited to the first 200 μm depth of a phosphate removing biofilm. Furthermore, upon FISH analysis of the nitrifying bacteria population, the AOB were found to dominate the outer 100 μm. However, Gieseke *et al*., (2001) also reported the presence of AOB at biofilm depths of 400 μm.

In this chapter, a set of techniques to quantify the nitrifying bacteria on the biofilms from the lab scale EBBR are described. The techniques were based on the combination of Fluorescence *in situ* hybridization (FISH) and confocal image analysis (CLSM) to observe the 3D image of the internal structure of the biofilm.

The spatial arrangement of the ammonia oxidizing bacteria (AOB) and nitrite oxidizing bacteria (NOB) within the biofilm was investigated and the relative abundance of the two groups was determined.

4.2 Materials and methods

4.2.1 Fluorescence *in situ* Hybridization (FISH) technique

The quantification of AOB and NOB in intact biofilms was carried out using intact bioparticles obtained from the lab scale bioreactor. The bioparticles were stained using a Nitri-VIT kit (Vermicon AG, Munich) developed for wastewater nitrification bacteria which separately distinguished AOBs and NOBs. The Nitri-VIT kit utilizes fluorescently labelled 16S-rRNA-targeted oligonucleotide probes that detect the relevant bacterial rRNA sequences and thus allows visualization of both AOB and NOB nitrifying species within one sample. The FISH stained bioparticles were observed using a confocal scanning laser microscope (Leica TCS SPE DM2500, Germany) equipped with solid state lasers. Although the Nitri-VIT kit was provided with coded solutions, the FISH procedure used to stain the biofilm was similar to the reported protocol of previous work on the cultivation independent *in situ* identification and enumeration of multispecies bacterial communities (Amann *et al.*, 1995; Wagner *et al.*, 1995) which used fluorescently labelled rRNA targeted oligonucleotide probes for the quantification of complex bacterial communities.

FISH staining procedure: The bioparticles were stained using the protocol provided in the Nitri-VIT kit; freshly obtained samples of bioparticles were placed on a glass slide and incubated to dry in a hot air oven (46 ^{0}C) for 15 - 30 minutes. One drop of the AOB probe (coded Solution A) was added to the sample and incubated for 15 – 30 minutes (46 ^{0}C), and then a drop of the NOB probes (coded Solution B) was

added to the sample and incubated for 5 – 15 minutes (46 ^{0}C). The glass slide was then inserted horizontally into a sealed chamber into containing 25 ml of a solution C1 (probably hybridization buffer) in a tray beneath the glass slide and was incubated for at least 90 minutes (46 ^{0}C). The tray of solution was then removed from the sealed chamber and replaced with 30 cm^3 of a washing buffer (prepared by adding 3 cm^3 of a solution D1 to 27 cm^3 of distilled water) and incubated for a further 15 minutes. Finally the samples were dipped briefly into distilled water and then dried at 46 ^{0}C for 5 minutes and prepared for viewing. The fluorescent probes were excited at 512 nm and the ammonia oxidizing bacteria emitted red fluorescence (observed at 546 nm). When the fluorescent probes were excited at 450 nm, the nitrite oxidizing bacteria emitted green fluorescence (observed at 490 nm).

4.2.2 Confocal image analysis

The confocal laser scanning microscope was set up to sequentially scan sections of the FISH stained biofilms at the two different excitation wavelengths as the mounted biofilm moved along a z-plane, (i.e. each z-slice was scanned at 512 nm for AOB and then at 450 nm for NOB before the objective lens moved to scan the next z-slice); this gave a z-stack, time series or lambda series of the scanned specimen (Fig. 4.1) which when compiled produces a 3D image of the scanned biofilm section.

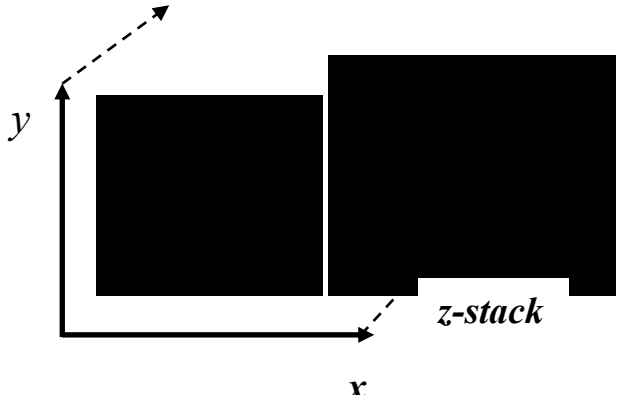

Fig. 4.1 The confocal scanning method for producing 3D images

Several challenges were encountered in the viewing of the FISH stained intact bioparticles for image analysis by the confocal scanning laser microscope. Most analysis of biofilms have been performed on biofilms that were grown on flat surfaces, which have a clearly defined base, but particulate biofilms from the EBBR grow outwardly from an irregular, but near-oval shaped coke support particle (Figs. 2.2 and 2.3, pages 66 - 67; Fig.3.6, page 106). Because coke is a dark material and cannot be penetrated by light, only the outer layer of the bioparticle, where the biofilm is separated from the coke, could be scanned. In addition, the whole bioparticle had to be mounted under the microscope and during scanning, movement along the z-axis was difficult as the specimen shifted across the field of view with each movement of the objective lens along the z-plane. The resulting images of the edges of the intact bioparticles were hard to interpret accurately, as the orientation of the image was hard to distinguish. Forcibly detaching the fragile biofilm from the coke support for FISH analysis was not ideal because, although a seemingly intact biofilm could be obtained, there was also loss of the integrity of the biofilm. Because

it was important to minimize damage to the biofilm, this method was abandoned. Another method attempted was to fix the bioparticle on a drop of superglue in a cavity slide, to prevent it shifting during observation. This method also proved to be ineffective, as bioparticles shifted once they came into contact with the objective lens. Another factor was that the biofilms from the EBBR were routinely above 600 μm in thickness, which was quite an extensive distance to observe; routine biofilm image analysis are performed with biofilms of less than a few 100 μm thickness.

Preparation of sample for viewing

A method to view the biofilm after staining with FISH probes was developed in order to overcome the difficulty in mounting and viewing the bioparticle. This method involved fixing the FISH stained intact bioparticles in molten 0.2 % agarose. A fixed bioparticle was then cut into thin sections using a sharp blade and the sectioned bioparticle was then placed on a glass slide and viewed under the microscope. This method allowed easy identification of the outside and inner regions of the biofilm (Fig. 4.2).

During the FISH staining process however, some biofilms routinely detached from their coke support and remained intact throughout the FISH staining process. Although the number of these were quite few, they were carefully broadened on a glass slide, immersed in oil and viewed as a flat structure. Thin biofilms of less than 100 μm, however, proved to be less amenable to the biofilm sectioning method, as

they collapsed easily upon slicing. Therefore, more data were obtained from thicker biofilms than from thinner ones.

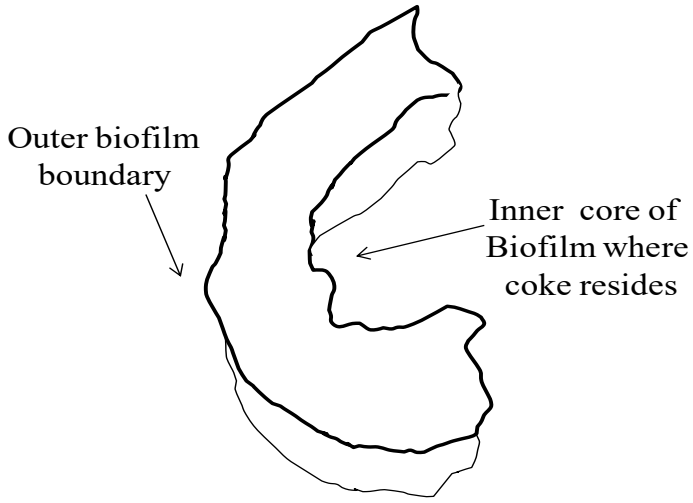

Fig. 4.2. A cross section of the biofilm embedded in agar and placed a glass slide for microscopic observation.

Image analysis

The abundance and spatial arrangement of the AOB and NOB of the images obtained from the CLSM were analysed using image processing software (Image J, free software available to the public from the National Institute of Health, USA). The CLSM-compiled 3D stacked images of each biofilm section were first imported into the Image J environment and then split into two different stacks according to the wavelength channels from which they were generated (for AOB and NOB). The separated images were then converted to binary form (8-bit gray scale), and then the images from each z-stack were then adjusted for minimising noise by thresholding.

Thresholding is a subjective operation where an attempt is made to find a value on a gray scale that best represents the distinction between the area of interest (e.g. stained biofilm or fluorescing aggregate) and the surrounding material (Yang *et al.*, 2000, Yang *et al.,* 2001)). The bacterial aggregates that fluoresced were identified as objects of interest and the software automatically made a distinction between the object and the surrounding. Although there may be some error in this method, as some aggregates may have been too transparent to be recognized as objects and maybe ignored and therefore not counted in the next step. Using the automatic thresholding tool therefore removed any factor of human error and made sure both channels were subjected to the same treatment and a common baseline for recognition and quantification of both AOB and NOB was applied.

The analysis tool in the Image J software was then used to analyze the separate z-stacks by first scanning the objects or aggregates until the edges are found, and recording the outline of the object. The number of objects, area and mean size of the objects were calculated in pixels. Because only objects of interest are counted in each z-stack, the total number of objects counted represented the number of fluorescing bacteria or aggregates of bacteria present in that stack. The compilation of all the stacks therefore gave information on e.g. number of fluorescing aggregates from the original 3D image obtained in colour from the confocal scanning.

Two methods were used to interpret the information obtained from the image J analysis;

1. When the image stacks obtained by confocal scanning were compiled along the biofilm thickness (in self-detached biofilms), the number of bacterial aggregates calculated per z-stack was plotted against the biofilm thickness, to produce a profile detailing the abundance of the AOB and NOB along the biofilm thickness.
2. The abundance AOB and NOB profiles along the biofilm thickness above could not be re-produced from the images of the cut sections of biofilms (Fig. 4.2) because the sections were scanned across the biofilm. The data of the quantification of the bacterial aggregates obtained by the Image J analysis was therefore manipulated to obtain the profile along the biofilm thickness.

   a. The quantification data of a transect of the biofilm section representing the total biofilm thickness scanned by the confocal microscope and obtained by Image J analysis was first extracted.

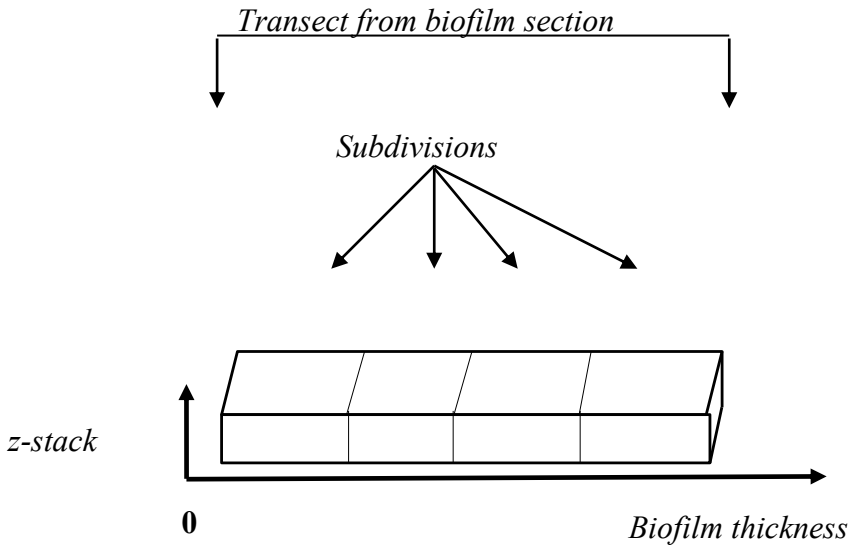

Fig. 4.3 The arrangement of data obtained from Image J analysis of the biofilm image in a transect along the biofilm thickness.

b. The transect data was then subdivided into four or five sectors and the total bacterial aggregates in each sector added (AOB and NOB separately) to obtain profile of the bacterial aggregates along the biofilm thickness (Fig 4.3).

An advantage of using cut sections of the biofilm was that a transect of a fixed volume of biofilm could easily be obtained using the software and the abundance of the bacterial populations deduced. Because the transect represented a volume of biofilm along the biofilm thickness, the abundance of the AOB and NOB species could be obtained along the biofilm thickness.

The nitrifying species quantified by these methods are described as 'bacterial aggregates' because the fluorescing objects could not be assumed to be made up of a single bacterial species.

Earlier results from the investigation into the influence of biofilm thickness on nitrification rate had indicated that the highest nitrification rates were obtained at biofilm thickness of about 100 μm (Fig. 3.19, page 124). Therefore, the outer 100 μm biofilm depth was used as an index in the biofilm analysis. The percentage abundance of the AOB and NOB in the initial 100 μm biofilm depth of the biofilms transects were calculated and compared as an AOB: NOB ratio.

A noticeable difference existed between the biofilm thickness of the intact, hydrated biofilm and the biofilms at the end of the FISH staining process; the FISH stained

biofilms were visibly thinner than the initial hydrated biofilm, due to several incubations at 46 ^{0}C during the staining procedure, which dried out the specimens. Although embedding in molten agarose helped to rehydrate the biofilm, the effect of the staining procedure on the biofilm thickness could not be accurately determined. Therefore, an investigation on of the effect of the staining process on the biofilm thickness was carried out, to identify the reduction in biofilm thickness post FISH staining.

Procedure: The biofilm thicknesses of different bioparticles were first measured using the light microscope method and the bioparticles were stained using the FISH staining procedure. The bioparticles were separated into two batches; one batch was immersed in oil and the other embedded in 0.2 % agarose and then the biofilm thickness were measured again. The change in biofilm thickness was then calculated.

Acridine orange staining - Bioparticles were stained with 0.03 % Acridine orange (AO) dye (prepared from 3 % AO in 2% glacial acetic acid) for 10 minutes. The excess dye was washed off with distilled water and the biofilm was physically detached from the coke support and observed using the confocal microscope (540 nm excitation and 620 nm emission wavelengths).

4.3 Results

4.3.1 Confocal imaging

Confocal microscope imaging of the detached, hydrated bioparticles stained with acridine orange revealed that the biofilm consisted of microcolonies of bacterial aggregates together in clusters and the clusters were suspended in the biofilm liquid (Fig 4.4).

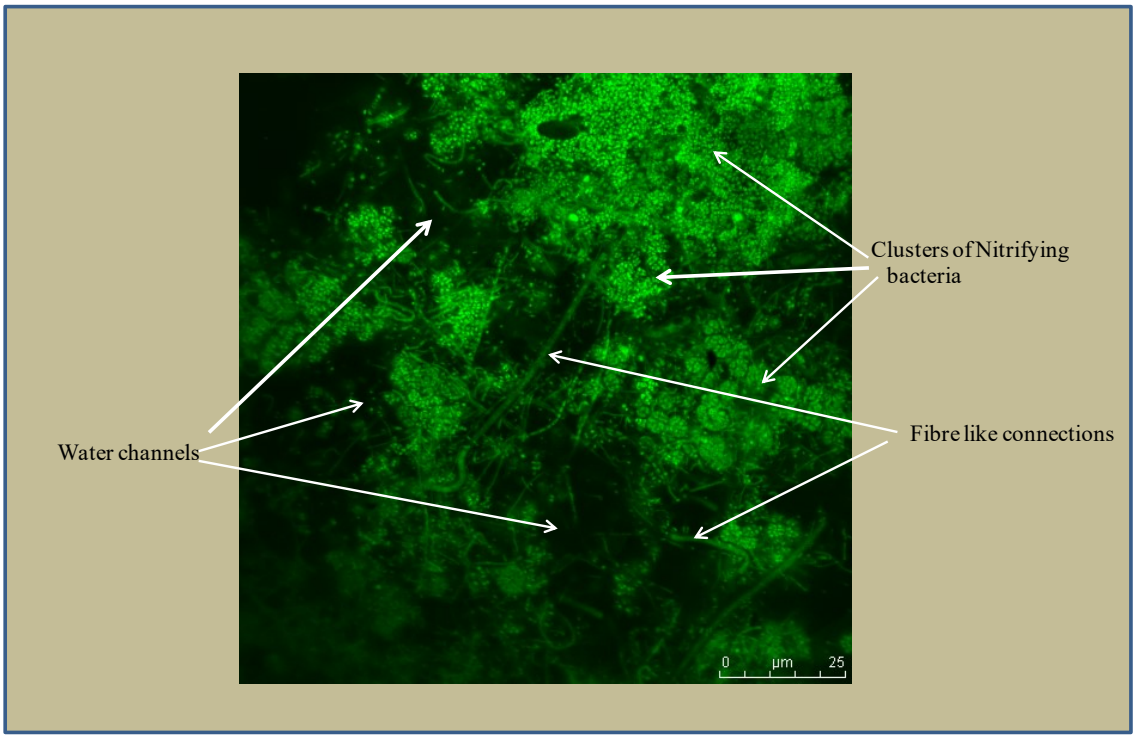

Fig. 4.4 Confocal microscope image of acridine orange stained hydrated biofilm, showing clusters of bacteria separated by water channels.

Confocal observation of the biofilm at the edge of the intact bioparticles (Fig. 4.5a - c) resulted in the movement of the edge of the biofilm across the field of view with increase in the laser scanning depth (z- stack - 45.6 µm to - 58.3 µm; c1 – c3). The resulting 3D images obtained were not an accurate representation of the biofilm therefore was not adequate for further analysis.

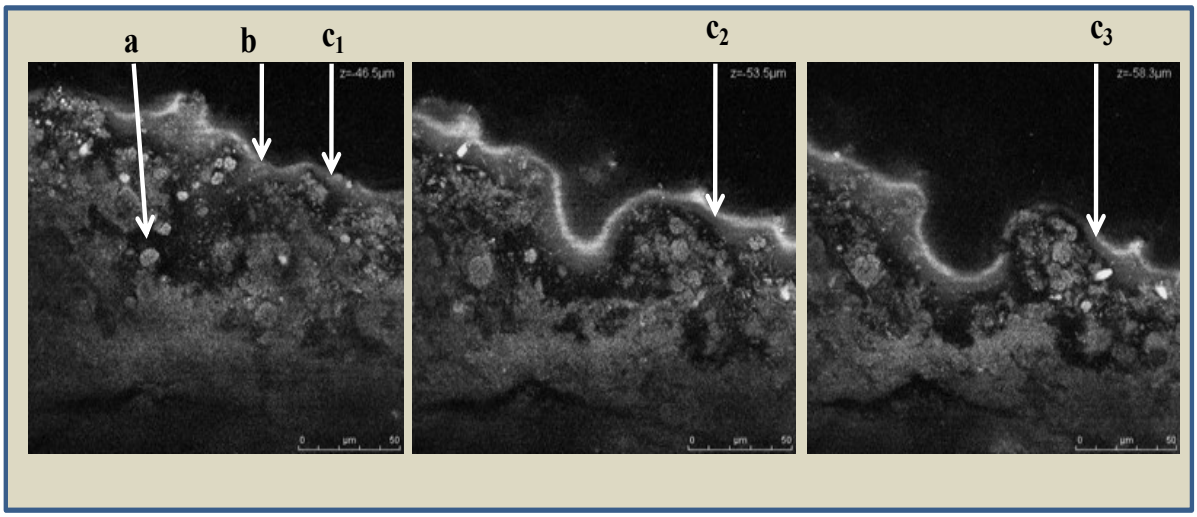

Fig. 4.5a – c. Confocal images of the biofilm at the edge of a FISH stained intact bioparticle showing the edge of the biofilm moving down the field of view during scanning. (a= water channels between microcolonies; b= biofilm surface; C_1-C_3 = distance moved by biofilm edge during scanning).

The investigation into the shrinkage of biofilms after FISH staining revealed that the biofilms immersed in oil reduced in thickness by about 87 % while those embedded in agar reduced by only 57 % (Table 4.1). The biofilms embedded in agarose probably absorbed water from the agarose and were able to regain about half of their original biofilm thickness. The biofilm thickness measured from the observations by

confocal microscopy were therefore adjusted for the degree of reduction during the staining process to estimate the original biofilm thickness.

Table 4.1. Average reduction in biofilm thickness for biofilms when immersed in oil and embedded in agarose after FISH staining.

Biofilms immersed in oil			Biofilms embedded in agarose		
Average thickness before FISH (μm)	Average thickness after FISH (μm)	% biofilm shrinkage	Average thickness before FISH (μm)	Average thickness after FISH (μm)	% biofilm shrinkage
564	84	85	633	303	52
475	45	91	477	174	64
266	42	84	309	137	56
229	32	86	227	98	57
Average % shrinkage		86.5			57

Confocal microscopy of the FISH stained biofilms revealed that the nitrifying biofilm community was made up of densely packed clusters or aggregates of AOB and NOB, closely arranged and often overlapping, both deep within the biofilm and at the outer edge (Fig. 4.6 a – d). In the detached biofilms immersed in oil (Fig. 4.6a)

and the biofilms embedded in agarose (Fig. 4.6b – d), dark regions in between the bacterial clusters were seen and probably represented water channels in the biofilm. The fibre-like interconnections observed in the hydrated acridine orange stained image (Fig. 4.4) were not visible in the FISH images but the difference in biofilm thickness as a result of the irregular shape of the coke support was clearly revealed in the biofilm sections embedded in agar. The 3D image of the section of biofilm gave a clear understanding of the orientation of the biofilm (Fig. 4.7), which was important for the analysis of the spatial configuration of the nitrifying species using Image J software. Examples of the data obtained in the determination of the abundance of AOB and NOB aggregates in the transects and the adjustments made for biofilm shrinkage and data obtained in the determination the percentage shrinkage of the biofilms embedded in 0.2 % Agarose after FISH staining is shown in Appendix G and H respectively.

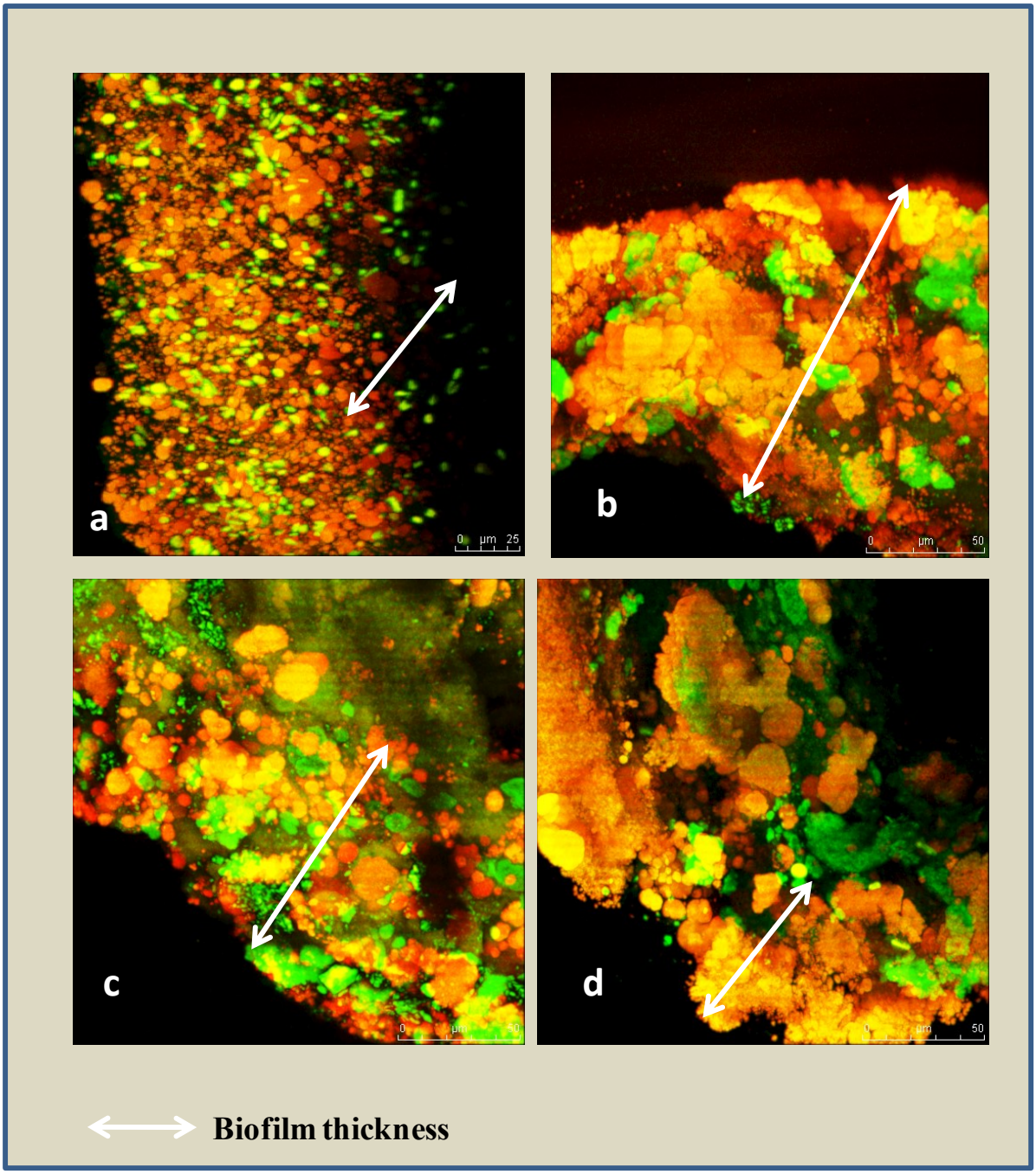

Fig. 4.6 3D images of biofilms obtained by confocal laser scanning microscopy. The biofilms were stained with the Nitri-VIT kit and the red clusters represent ammonia oxidizers while the green clusters represent the nitrite oxidizers. (a = side view of 3-D image of intact detached biofilm immersed in oil; b-d = images obtained from agar embedded biofilm sections).

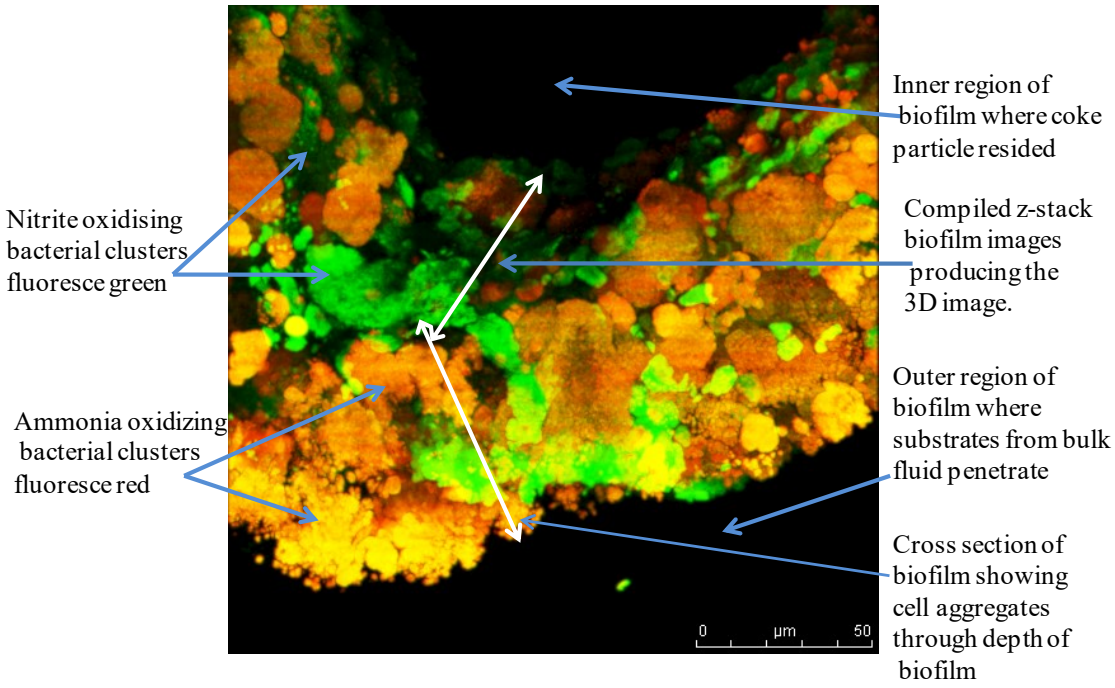

Fig 4.7. A 3D image of cross section of a FISH stained thick biofilm.

In the Image J environment, the aggregates of AOB and NOB in each z-stack were split up into the two separate images according to the channels they were obtained from (Fig. 4.8) and adjusted for noise by automatic thresholding and the aggregates were counted separately as individual objects (Fig. 4.9). The profiles of the AOB and NOB in random samples of the detached biofilms and biofilm sections fixed in agarose biofilms was then plotted using the data obtain form the using Image J analysis after adjusting the values to obtain the original biofilm thickness.

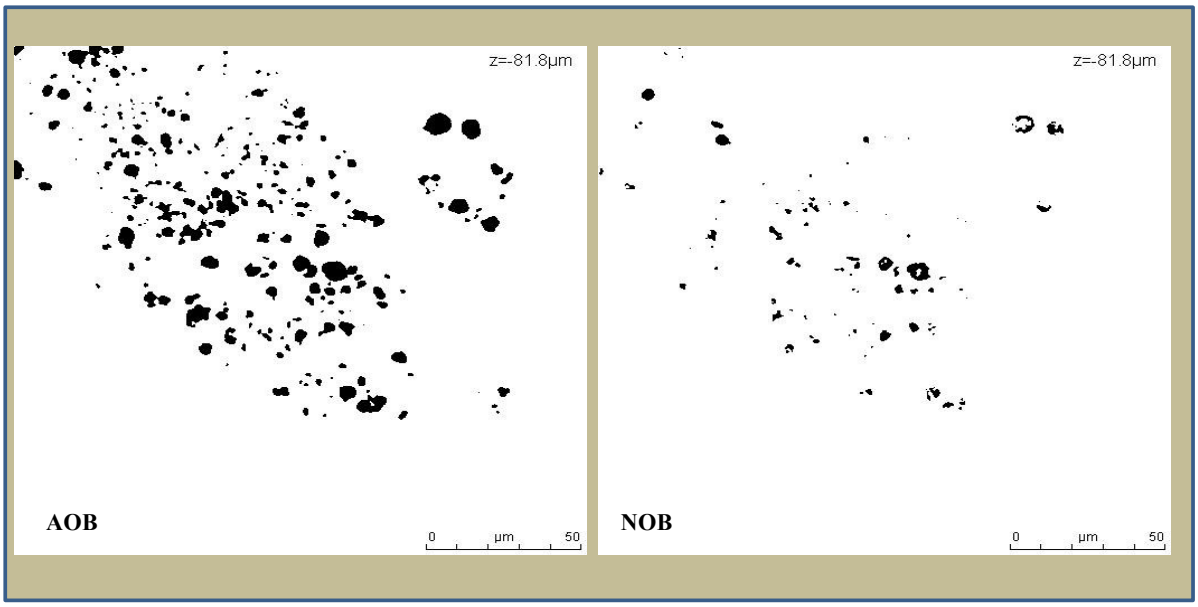

Fig. 4.8 Images of the threshold adjusted fluorescence producing objects, split into channels, showing AOB and NOB clusters or aggregates of the same z-stack.

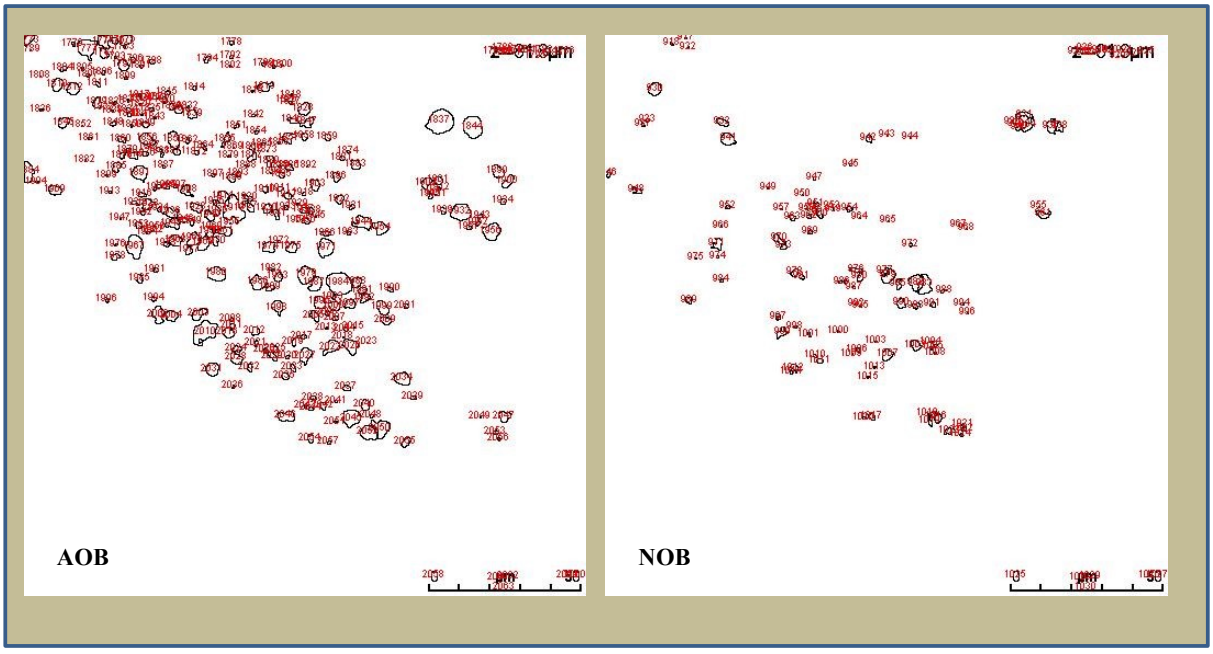

Fig. 4.9 The counted fluorescence producing objects after adjusting for noise by thresholding.

Following image analysis of the spatial distribution of the AOB and NOB species along the biofilm thickness of detached biofilm, regions up to 600 µm thick were observed (Fig. 4.10a - c). The AOB had a 2 to 4 times the abundance of NOB (Fig. 4.10a, Fig. 4.10b). In biofilms less than 350 µm thick, there was some evidence that the highest aggregate bacterial counts were found at about 100 µm biofilm thickness (Fig. 4.10b).

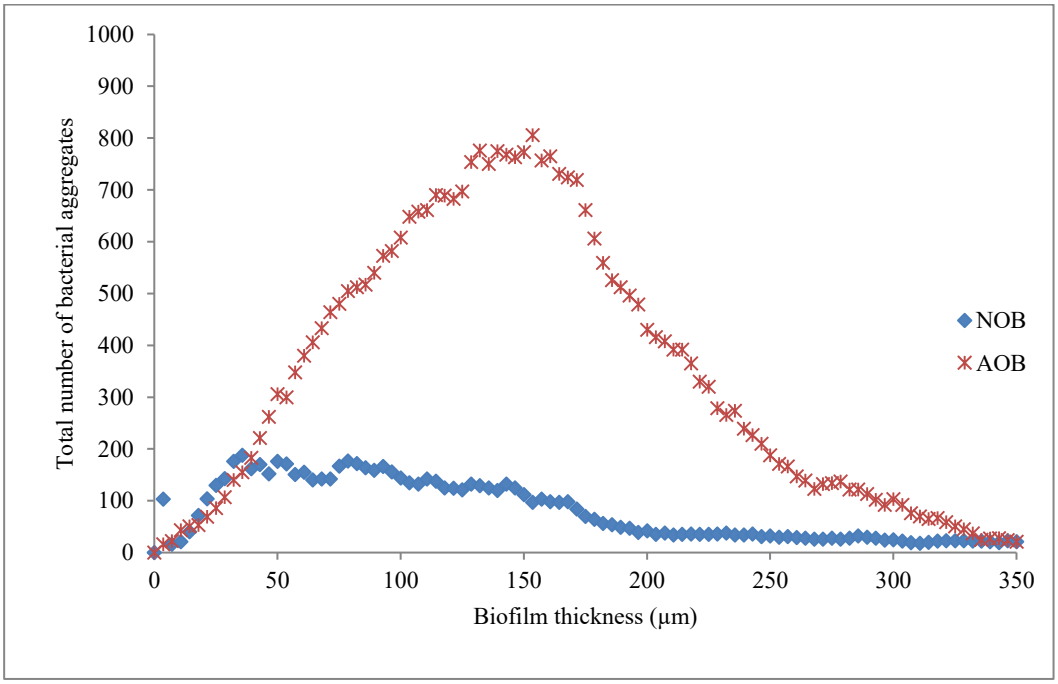

Fig. 4.10a Profile of AOB and NOB across the biofilm thickness of a detached biofilm of about 350 µm initial thickness (the biofilm thickness from the outer biofilm surface inward to the coke surface).

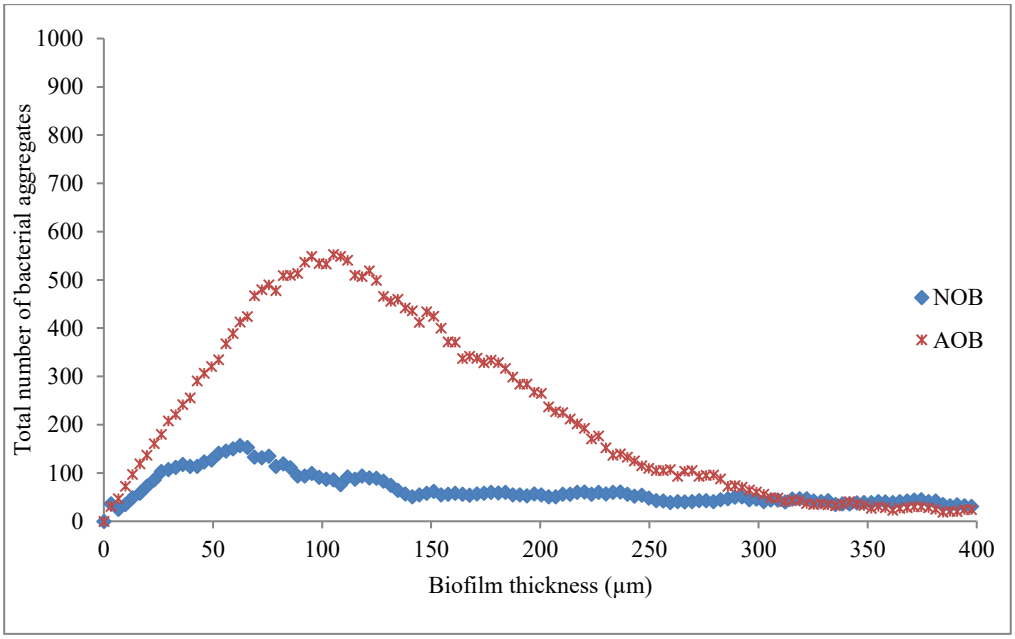

Fig. 4.10b Profile of AOB and NOB across the biofilm thickness of a detached biofilm of about 300 µm initial thickness (the biofilm thickness from the outer biofilm surface inward to the coke surface).

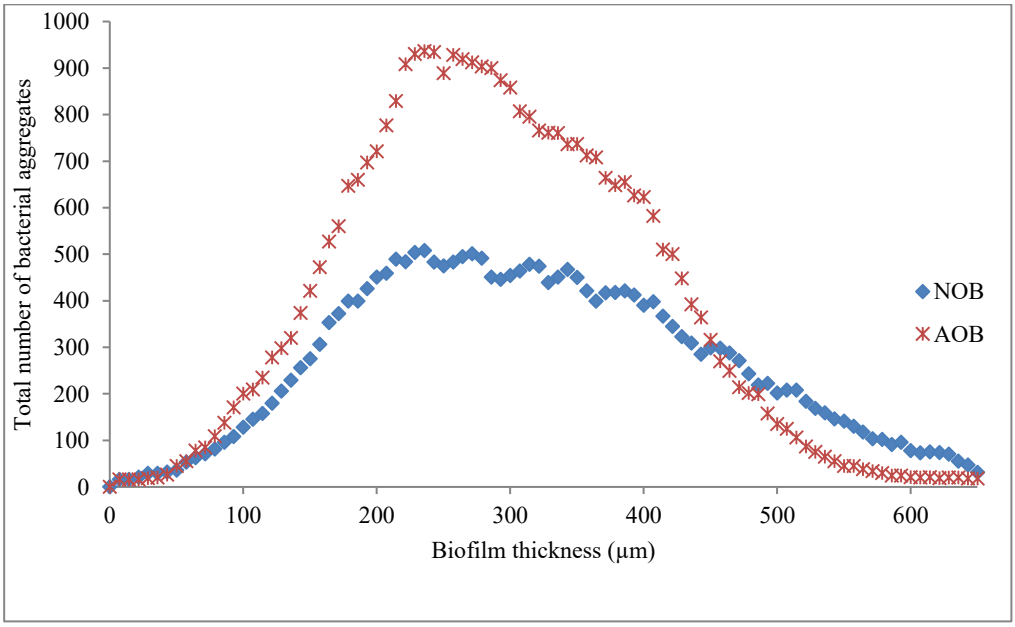

Fig. 4.10c Profile of AOB and NOB across the biofilm thickness of a detached biofilm of about 600 µm initial thickness (the biofilm thickness from the outer biofilm surface inward to the coke surface).

Image analysis of the spatial configuration of the transections from the agar-embedded biofilm sections also revealed that the AOB were more abundant than the NOB. The highest aggregate counts of the AOB in biofilms of about 150 µm (thinner biofilms) were about 2 to 3 times greater than that of the NOB (Fig. 4.11 – Fig. 4.13) while the biofilms greater than 150 µm the AOB aggregates were up to 5 times greater (Fig. 4.14 – 4.18). Both the images from the detached biofilms and shows clearly the spatial distribution of the AOBs and NOBs both across the biofilm thickness and the distribution in the innermost regions of the biofilm closest to the coke support.

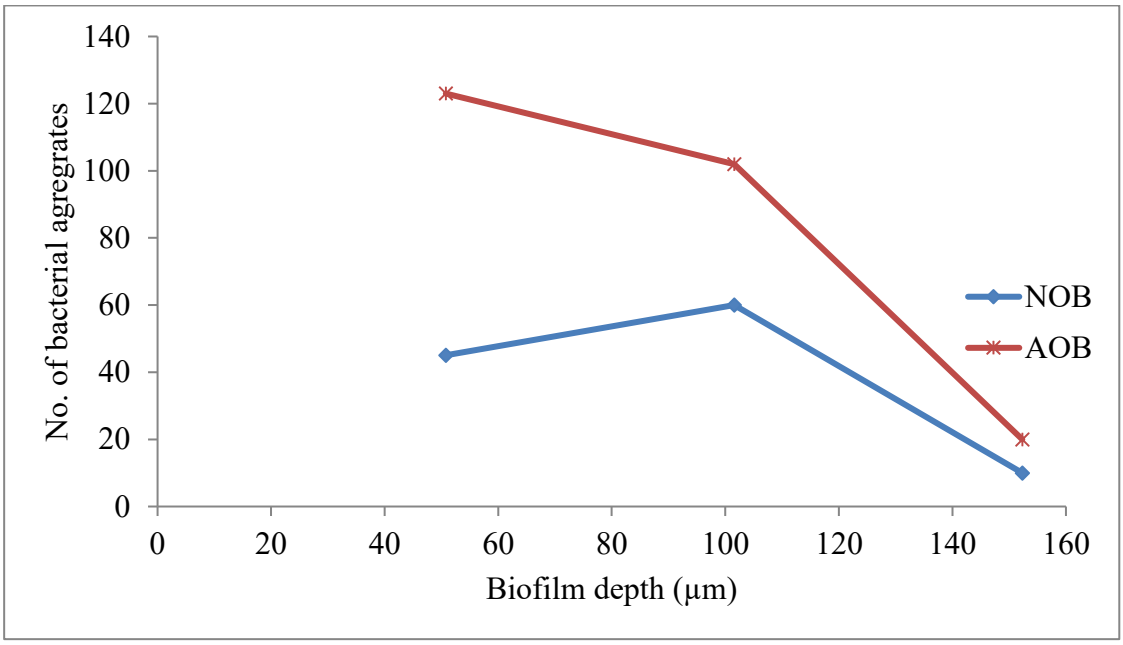

Fig. 4.11. Total AOB and NOB count in a biofilm transect of 150 µm (from the outer surface of the biofilm inward to the coke particle surface).

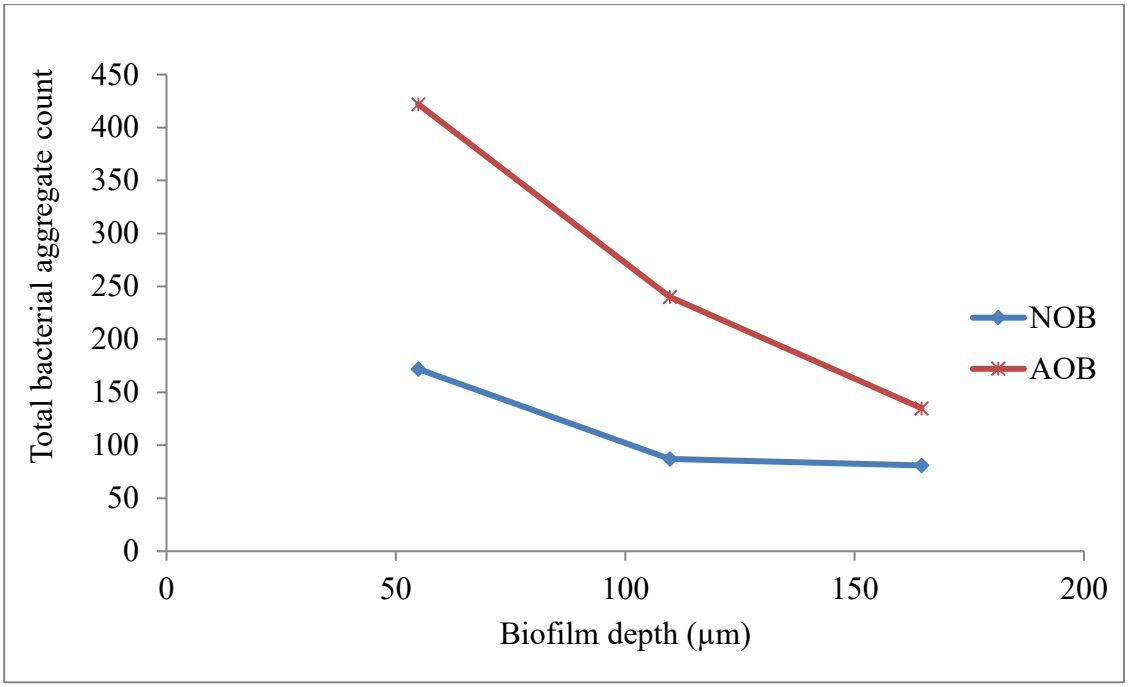

Fig 4.12 Total AOB and NOB count in a biofilm transect of 160 µm (from the outer surface of the biofilm inward to the coke particle surface).

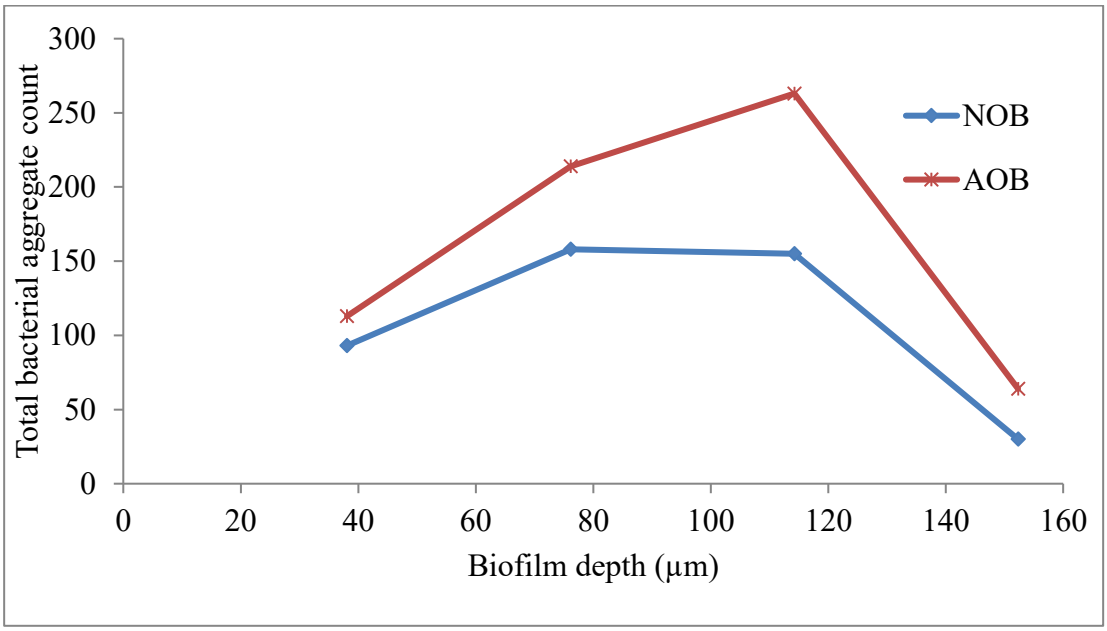

Fig 4.13 Total AOB and NOB count in a biofilm transect of 150 µm (from the outer surface of the biofilm inward to the coke particle surface).

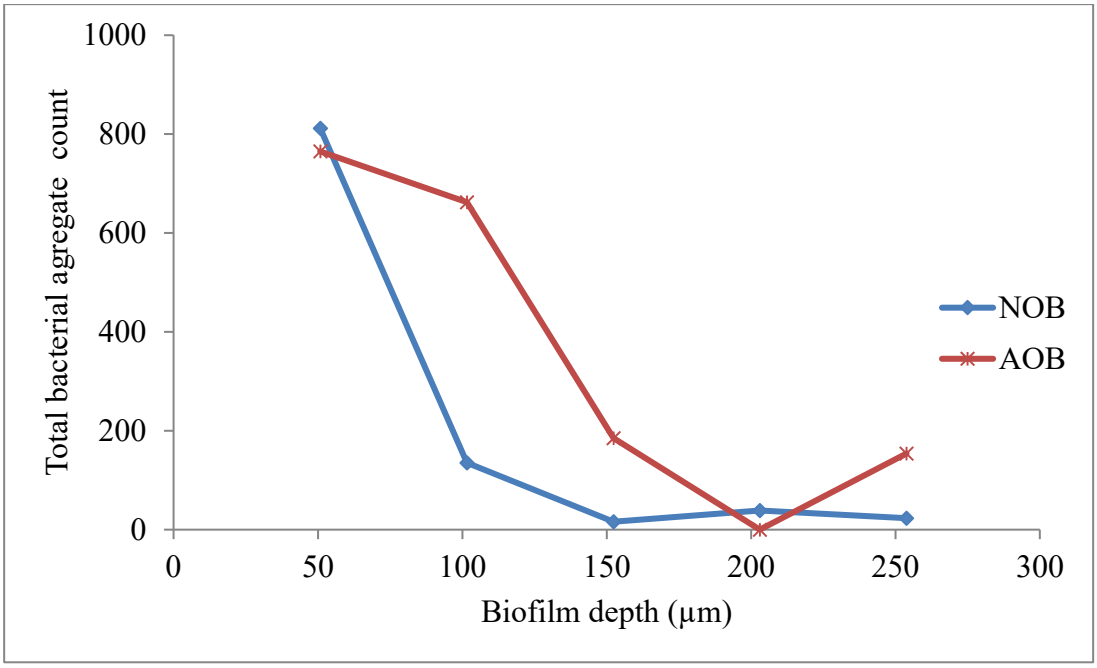

Fig 4.14 Total AOB and NOB count in a biofilm transect of 250 µm (from the outer surface of the inward biofilm to the coke particle surface).

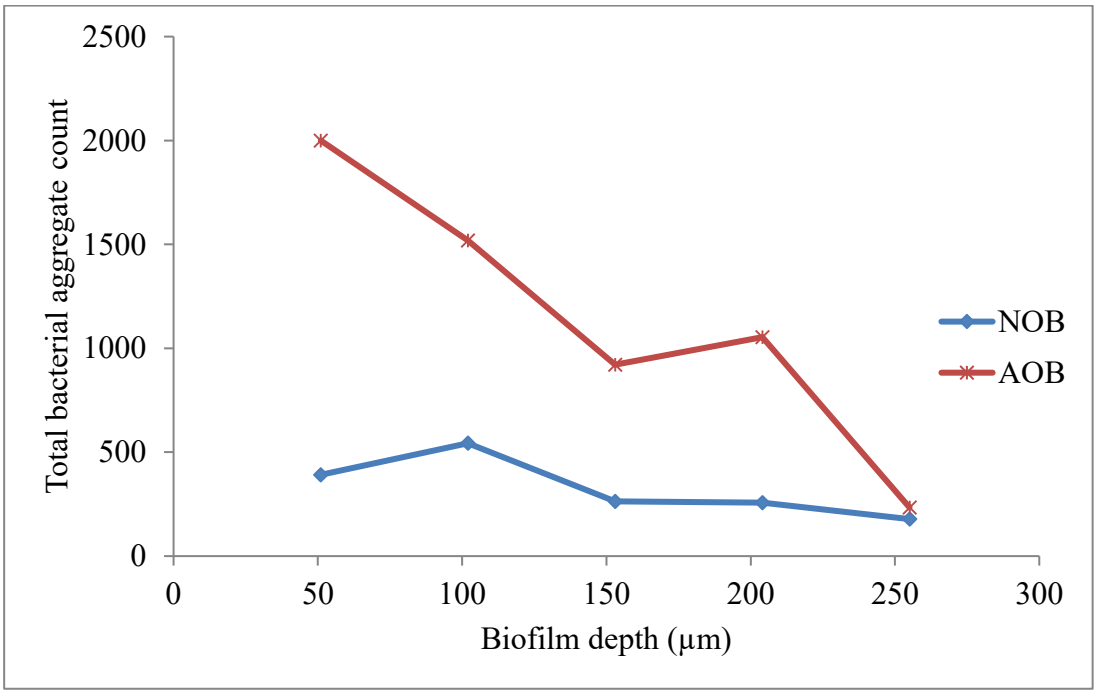

Fig. 4.15 Total AOB and NOB count in a biofilm transect of 250 µm (from the outer surface of the biofilm inward to the coke particle surface).

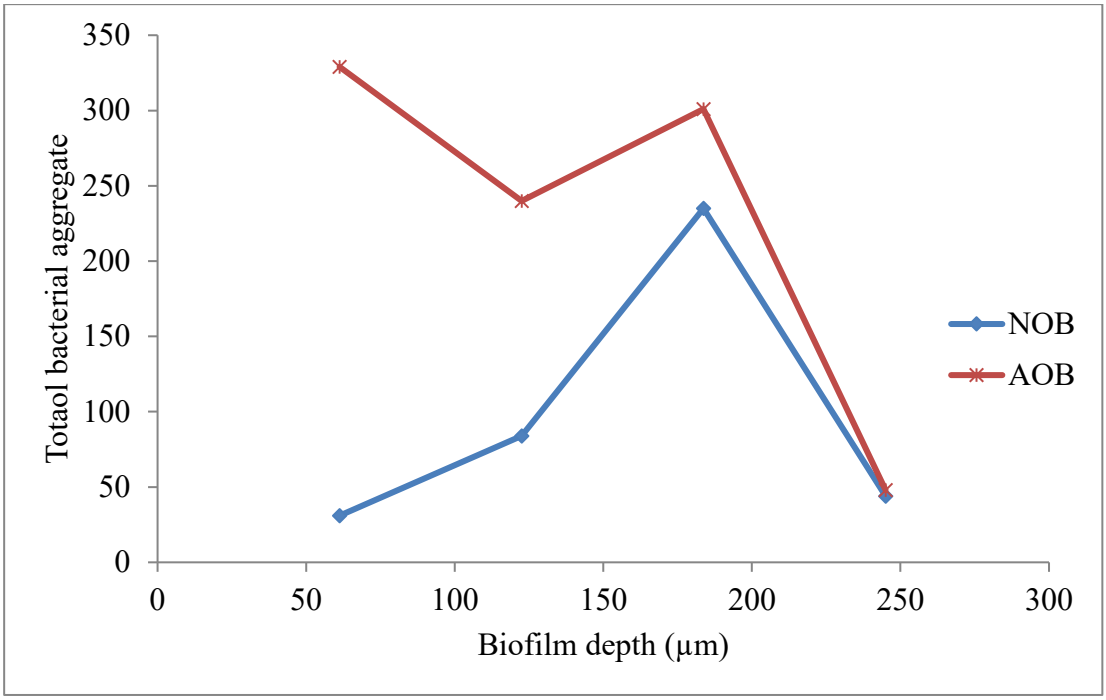

Fig. 4.16 Total AOB and NOB count in a biofilm transect of 240 µm (from the outer surface of the biofilm inward to the coke particle surface).

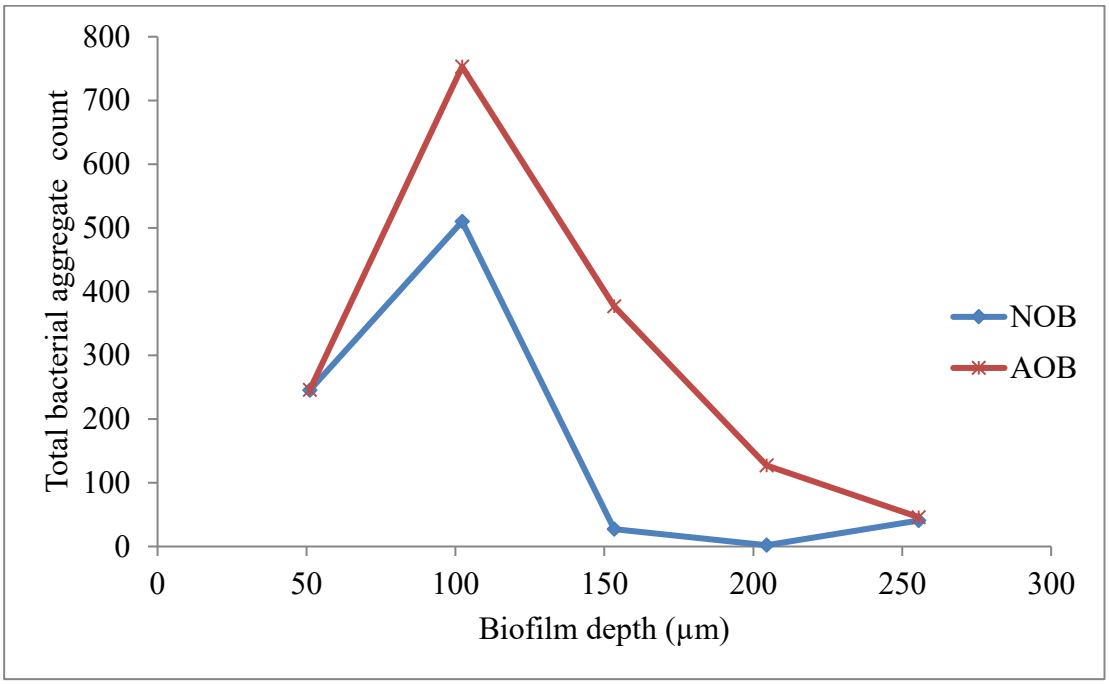

Fig. 4.17 Total AOB and NOB count in a biofilm transect of 255 µm (from the outer surface of the biofilm inward to the coke particle surface).

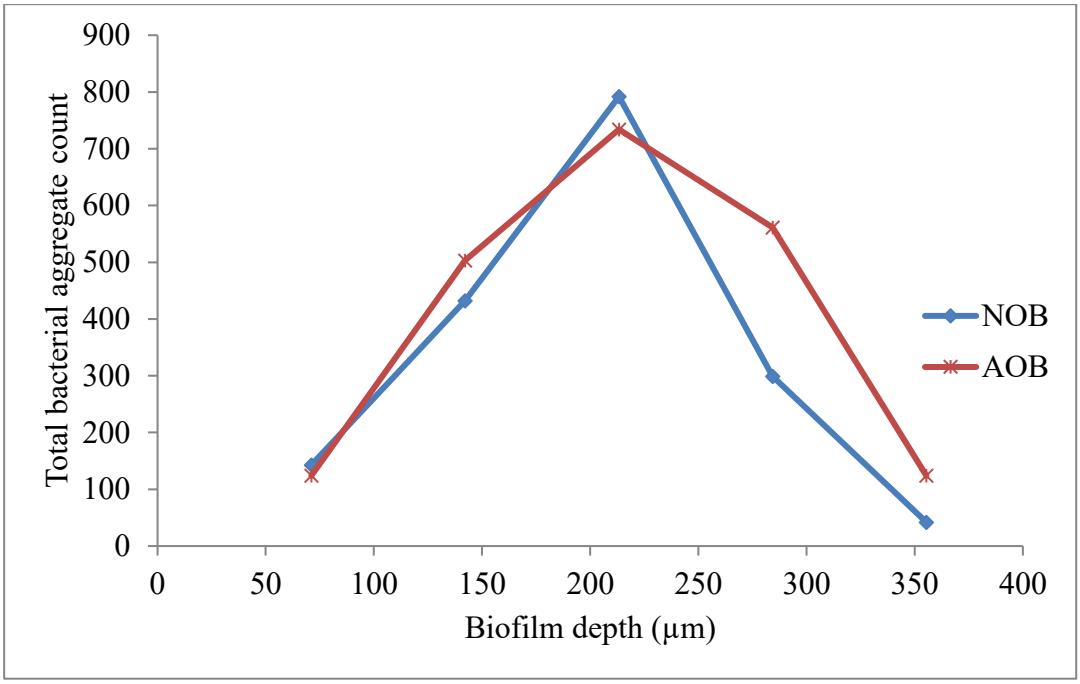

Fig. 4.18 Total AOB and NOB count in a biofilm transect of 350 µm (from the outer surface of the biofilm inward to the coke particle surface).

The transects of the cross section of the of the thinner biofilms (133 - 152 µm) revealed that most of the nitrifying species (AOB 76 – 90 %; NOB 78 – 95 %) were located in the outer 100 µm region and the AOB were about twice as dense as the NOB in that region (Table 4.2). In the thicker biofilms, (>250 um), a much lower percentage of the nitrifying species (AOB, 22 – 81 %; NOB, 24 - 92 %) were located in the outer 100 µm region and the AOB: NOB abundance ratio was about 1.0 (Table 4.2). There was also evidence of the presence of nitrifying bacteria at depths greater than 350 µm (Fig 4.18).

Table 4.2 The abundance of AOB and NOB in the initial 100 μm biofilm thickness derived from the analysis of the biofilm transect data.

Biofilm thickness (μm)	Ammonia oxidizers		Nitrite oxidizers		
	Abundance (%)	Cell aggregate volume (cm^{-3})	Abundance (%)	Cell aggregate volume (cm^{-3})	AOB : NOB ratio
133	91	8.3 x 10^{9}	95	4.2 x 10^{9}	2.0
145	72	2.8 x 10^{9}	81	0.72 x 10^{9}	3.9
152	76	6.5 x 10^{9}	78	4.4 x 10^{9}	1.5
203	87	0.76 x1 0^{9}	84	0.35 x 10^{9}	2.2
220	81	0.78 x 10^{9}	72	0.35 x 10^{9}	2.2
245	59	18.8 x 10^{9}	54	8.8 x10^{9}	2.3
254	81	800 x 10^{9}	92	920 x 10^{9}	0.9
256*	64	3.2 x 10^{9}	92	2.4 x 10^{9}	1.3
256*	48	480 x 10^{9}	38	380 x 10^{9}	1.3
255	61	620 x 10^{9}	57	570 x 10^{9}	1.1
355	22	2.2 x 10^{9}	24	2.0 x 10^{9}	1.1
**Measurements from the same biofilm*					

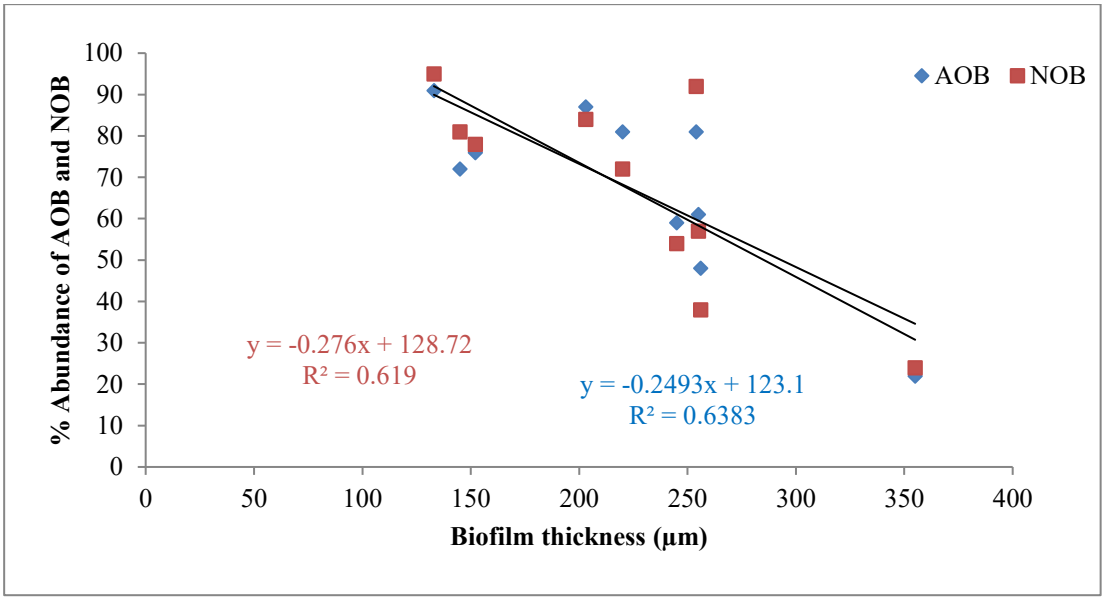

Fig. 4.19 The relationship between the percentage abundance of AOB and NOB and biofilm thickness in the outer 100 µm of a sample of bioparticles.

The percentage abundance of AOB and NOB both reduce with increase in biofilm thickness but also indicate the presence of a higher abundance of AOB and NOB in the outer 100 µm of thinner biofilms. .

4.4 Discussion

The confocal observations revealed an ‘active nitrifying region’, which taken as the biofilm thickness as no boundary layers (e.g. reported by De Beer *et al.*, (1993)) could be observed. The confocal microscope observations confirmed that, due to the irregular topography of the coke particle, the biofilm thickness varied from one point to another in the bioparticle surface (Fig. 4.6b and Fig. 4.6c). Observations of the biofilms stained with acridine orange with the confocal microscope established the biofilm internal structure to be of a heterogeneous nature (Fig. 4.4). The confocal observation of the FISH stained biofilm revealed the biofilm internal structure was a complex, heterogeneous community in which different sizes of AOB and NOB aggregates were observed (Fig. 4.6a - f). Although, the commonly described “mushroom” biofilm structure could not be identified, observations of the images show that, although the biofilm grew from the coke support and apparently was still attached to it, the biofilm microbial population seemed to form stacks of cell aggregates with no particular order and branching in all directions. Furthermore, they were connected, and maybe even held together by a network of fibre-like structures (Fig. 4.4). The fibre-like structures were not nitrifying bacteria as they were clearly absent in the FISH stained biofilms and therefore were not nitrifying bacteria and upon closer examination were found to be filamentous cells similar in structure to those found in the SEM observations of the biofilms (Fig 2.6e, page 69). The biofilms were well hydrated and the microcolonies completely immersed in the biofilm liquid with sometimes large voids between the microcolonies (Fig. 4.4).

The AOB and NOB profiles through the biofilm thickness revealed that the AOB were dominant in the biofilms, and this was in both the outer and inner regions of the biofilms (Fig. 4.10a, Fig. 4.10c). The higher abundance of AOB may be as a result of the concentration of the NH_3-N (125 ± 10 mg L^{-1}) in the reactor coupled with the higher specific growth rate of the AOB identified by Prosser (1989). The profile of the abundance of AOB and NOB through the biofilm thickness indicated that the AOB were 2 to 8 times more abundant than the NOB (Fig. 4.10a-c; Fig. 4.11 – Fig. 4.18). Although there were strong indications that the thinner biofilms had lower abundance of AOB and NOB than the thicker biofilms e.g. comparing Fig. 4.11 and 4.12 with and Fig. 4.17 and Fig. 4.18, AOB and NOB counts were 4 to 6 times higher in thicker biofilms. Because different transect sizes were used for the determination of the total aggregate counts, the best method of comparison was to determine the densities of the different nitrifying species in the transects.

The abundance ratio of the AOB: NOB in the outer 100 μm of the biofilms were similar in thicker biofilms while thinner biofilms (less than 150 μm) had a ratio of about 2:1 at the biofilm depth. NOB therefore have half the population of AOB in thinner biofilms (Table 4.2). However, the thicker biofilms achieved higher densities than the thinner biofilms in the same 100 μm region (Table 4.2). The inner regions of the thicker biofilms also showed presence of nitrifying bacteria (Fig. 4.18). Although the 3D confocal images of compacted biofilms embedded in agarose appear to show that the inner regions of the biofilm were just as dense as the outer regions (Fig 4.6d - e), the 3D images of the detached biofilms (Fig 4.6a - b) and the profiles of the nitrifying bacteria along the biofilm thickness reveal a gradual

reduction in the aggregate count with increase in biofilm thickness. The profile AOB and NOB in the detached biofilms shows the presence of nitrifying bacteria beyond 500 μm biofilm depth (Fig. 4.10c).

The image analysis of the biofilm data in transects revealed that the abundance of the nitrifying species present in the 100 μm depth decreased with increase in biofilm thickness. For example, biofilms of about 130 μm had greater than 90 % of nitrifying bacteria present in the outer 100 μm region, while biofilms about 360 μm had less than 25 %; a difference of about 70 % in the presence of nitrifying bacteria in the initial 100 μm for about a threefold increase in biofilm thickness (Table 4.2). The thicker biofilms therefore had a much broader distribution of the nitrifying species through the biofilm thickness. The presence of the AOB and NOB in the inner core of the bioparticle would only be actively nitrifying if there was available substrate (NH_3 or NO_2^-) and oxygen for metabolic activity. The 450 μm maximum biofilm depth of nitrifying activity determined in chapter 3 (Fig. 3.19, page 124) would support the presence of active nitrification by the inner core nitrifying bacteria but the 300 μm maximum depth of oxygen penetration reported by Hibiya *et al.* (2004), (using a completely mixed three-phase fluidized bed with particle based nitrifying biofilms) seems to preclude this possibility. However, there is evidence that AOB can exist and adapt to conditions of low ammonia and oxygen concentrations; Geets *et al.,* (2005) reported that AOB possess several traits that are advantageous for survival under conditions of variable oxygen and nutrient supply including enzymatic and molecular mechanisms that allow them to maintain the state of their cells during period of starvation.

4.5 Conclusion

- Using the method developed to quantifying the nitrifying bacterial species in the bioparticles from the EBBR, the spatial configuration of the AOB and NOB has been studied and the abundance of the AOB and NOB species through the biofilm thickness have been determined.
- The AOB were more abundant than the NOB in the biofilms. The conclusion that the highest population of AOB and NOB exists mainly in the outer 100 μm biofilm thickness could only be applied to the thinner biofilms of about 150 μm.
- About 90 % of the nitrifying species of thin biofilms (about 150 μm thick) exist in the outer 100 μm region, accounting for the high ammonia oxidation rates of the thinner biofilms. The thicker biofilms achieved a much higher densities of both AOB and NOB cell aggregates in the outer 100 μm.
- In the outer 100 μm of thin biofilms, the AOB had twice the abundance compared to NOB population. There is strong evidence to show that the optimum NOB activity occurred in biofilms greater than 100 μm in the bioparticles from the EBBR.

CHAPTER FIVE

5.0 The effect of oil refinery wastewaters on nitrifying biofilm

5.1 Introduction

Crude oil is best described as a mixture of hydrocarbons with some impurities (Cheresminoff and Haddadin, 2006). The hydrocarbons vary from straight chain hydrocarbons to cyclic hydrocarbons, aromatic hydrocarbons to high molecular resins and asphaltenes, and can be toxic to microorganisms (Green and Trent 1989; Sponza and Pala, 1994). Oil refining processes are used to distil the hydrocarbon fractions into different useful products, such fuel oil and gasoline with the associated production of large volumes of oily wastewater stream. Tatem, *et al.*, (1978) reported that oil refinery effluents often contain fewer of the lighter hydrocarbons, but more of the polycyclic aromatics than crude oil. The polycyclic hydrocarbons are more toxic than the other hydrocarbon components and tend to be persistent in the environment.

Some organisms have been applied in the treatment of oil refinery wastewaters e.g. *Pseudomonas aeruginosa,* and the plant *Coprinus cinerus* has been used to treat oil refinery wastewaters containing phenols (Agarry *et al.*, 2008; Ikehata *et al.*, 2003). Phenols and phenolic compounds are commonly found in oil refinery wastewaters (ORWW) and are relatively toxic causing the destruction of cellular membranes and are carcinogenic.

Although it has been reported that some aromatic compounds inhibit the nitrification process in activated sludge systems (Tomlinson *et al.*, 1966), nitrifying bacteria have been found to degrade complex hydrocarbons. *Nitrosomonas europaea* has been found to oxidize straight chain hydrocarbons (alkanes, alkenes, alkynes), the cyclic hydrocarbons (benzene and even the very toxic phenols), as well as halogenated and *n*-chlorinated hydrocarbons (Hyman and Wood (1985); Hyman *et al.,* (1988); Arciero *et al*., (1989); Rasche *et al.,* (1990); Keener and Arp, (1994)). Rasche *et al*., (1990) also used nitrifying bacteria (*Nitrosomonas europaea, Nitrosococcus multiformis* and *Nitrosococcus oceanus* to degrade the halogenated hydrocarbon fumigants methyl bromide, 1, 2-dichlorpropane and 1, 2-dichromo-3-chloropane. Oxidation of these fumigants was mediated by the enzyme ammonia monooxygenase. Oil refinery wastewaters also contain organic sulphur compounds, e.g. carbon disulfide and alkyl thiols have been reported to inhibit nitrification (Veenstra *et al.,* 1998; Juliette *et al.,* 1993).

Deni and Penninckx (1999) reported that ammonia oxidizing bacteria are capable of oxidizing hydrocarbons in soils contaminated with oil refinery wastewaters. Deni and Penninckx (1999) found that although hydrocarbons inhibited nitrification in hydrocarbon uncontaminated soils, soils with a long history of hydrocarbon pollution achieved 90 % ammonia removal and concluded that ammonia oxidizing bacteria acquired resistance to inhibition by hydrocarbons. They also attributed any inhibition of ammonia oxidizing bacteria to the inhibition of ammonia monooxygenase enzyme.

Although most of the experimental work described above mainly used pure cultures of nitrifying bacteria, the use of nitrifying biofilms in treatment of oil refinery wastewaters is not common. The main reason is that oil refinery wastewaters are traditionally treated on site or transported to public wastewater treatment plants for treatment as industrial wastewater, where the treatment is mainly by traditional activated sludge system. Little evidence in literature exists for the treatment of oil refinery wastewaters (ORWW) with biofilm reactors; Jou *et al*., (2003) used a fixed film bioreactor in a pilot plant packed bed of polyurethane foam for COD removal and phenol degradation of oil refinery wastewaters, achieving up to 85 % COD removal and 100 % phenol removal. Xianling *et al*., (2005) achieved effluent NH_3-N concentrations of 15 mg L^{-1} (73 – 88 % ammonia removal) in a pilot scale gas-liquid-solid three phase flow airlift loop bioreactor. More recently, Flournoy, *et al.,* (2008) reported the first oil company (Frontier Oil Refining and Marketing, Cheyenne, WY, USA) to upgrade their existing treatment system to a combination of Integrated fixed film activated sludge (IFAS) and activated sludge systems to achieve improved nitrification. The upgrade was necessary to meet new legislative guidelines for NH_3-N effluent of 5.45 mg L^{-1} monthly average (much steeper than the previous 20 mg L^{-1} monthly average). The newly installed biofilm system quickly achieved 73 % NH_3-N removal.

Oil refinery wastewaters contain a wide variety of compounds and the composition depends on the facility, the refining conditions and source of the crude oil. The bioparticles from the EBBR were exposed wastewaters from a local oil refinery to investigate the ability of the biofilm nitrifying population to maintain nitrifying

activity. The application of this novel technology to the oil refinery nutrient removal system depends on the ability of the biofilm to sustain nitrification irrespective of the composition of the ORWW. The emphasis in this chapter was therefore on the ability of the nitrifying population to retain ammonia oxidizing activity in the ORWW environment and not necessarily to degrade the ORWW components.

5.2 Materials and methods

Oil refinery wastewater samples

Sample source: Oil refinery wastewater was obtained from a wastewater treatment works near Manchester, UK that received domestic and industrial wastewater, including oil refinery effluent. Two batches of ORWW samples were obtained over 18 months apart for analysis. The ORWW samples were obtained from the holding tank which stores the oil refinery wastewaters upon arrival at the wastewater treatment works. The ORRW sample was collected in polyethene containers and transported to the laboratory in Manchester.

5.2.1 Determination of effect of oil refinery wastewaters on nitrifying biofilm

Preparation of oil refinery wastewater samples for use as reactor medium.

The oil refinery wastewater was a dark, viscous liquid (Fig 5.1). The top, oily layer of the ORWW sample was first skimmed off and a portion of the ORWW was filtered using 0.2 μm filters discs (Cronus, UK) to obtained clear ORWW samples. Using the miniature expanded bed reactor designed for specific nitrification rate experiments of bioparticles from the EBBR, filtered (free from suspended matter) and raw samples of ORWW and full medium (ISO 9509: 2006) were used as reactor wastewater for the investigation of the effect of ORWW on the activity of the nitrifying biofilm, using the method developed for the determination of specific nitrification rates of bioparticles described (Chapter 3.2.3, page 99). Biofilms of

average thickness of 300 µm were selected to be used in the experiment. The 300 µm biofilm thickness was chosen because the results from Chapter 3 show that biofilms of this thickness would undergo complete nitrification (Fig. 3.19). The experimental conditions are shown in Tables 5.1. Due to the low concentration of ammonia found the ORWW samples upon analysis by ion chromatography (Table 5.3), the ORWW was augmented with NH_4SO_4 to meet the NH_3-N concentration of 56 mg L^{-1} required by the protocol.

Fig 5.1 Samples of raw (left) and filtered (right) oil refinery wastewater in Erlenmeyer flasks.

Table 5.1 The experimental design for investigation of the effect of oil refinery wastewater on nitrifying biofilm

	Reactor 1 (Control)	Reactor 2	Reactor 3	Reactor 4	Reactor 5
Bioparticles (cm^3)	0	0.5	0.5	0.5	0.5
Full medium (cm^3)	25	24.5	0	12.25	0
Filtered ORWW (cm^3)	0	0	24.5	12.25	0
Unfiltered ORWW (cm^3)	0	0	0	0	24.5
Total volume (cm^3)	25	25	25	25	25

Long term effect of ORWW on nitrifying biofilm.

To determine the long term effect of oil refinery wastewater on the nitrifying biofilm, a 14-day experiment was also set up using 3 cm^3 samples of bioparticles of similar 300 µm average biofilm thickness from the lab scale EBBR. Because the miniature EBBR could not be operated for extended periods (the pump tubing melted when left to operate overnight), the bioparticles were incubated in a series of 4 Erlenmeyer flasks each containing 200 cm^3 of synthetic wastewater (SWW), (simulating the SWW media of the EBBR (Van Neil *et al.,* 1993), a 50:50 mixture of SWW and filtered ORWW, filtered ORRW and unfiltered ORWW in 250 cm^3 Erlenmeyer flasks. A flask containing only SWW was used as a control to determine the ammonia lost by air stripping. The NH_3-N concentrations of all the media were

adjusted to 125 mg L^{-1} with NH_4HCO_3 to match the NH_3-N concentration in the EBBR. Oxygen was supplied to the system by bubbling compressed air through each flask by tubes fitted with a plastic pipette tip at the ends and placed in the medium away from the bioparticles to avoid disruption of bioparticle and biofilm and held in place by tape. The medium was changed at approximately 48 hour intervals to ensure that the NH_3-N concentration in the flasks did not become rate limiting and affect the nitrifying population for the duration of the experiment.

The specific nitrification rates of the incubated bioparticle samples were determined before and after the 14-day incubation period, using the method described above. The results were then compared to determine the long term effect of oil refinery wastewaters on the activity of the nitrifying bacteria.

Table 5.2 The experimental design of 14-day incubation experiment.

	Reactor 1 (Control)	Reactor 2	Reactor 3	Reactor 4
Bioparticles (cm^3)	0	3	3	3
SWW (cm^3)	200	200	0	0
Filtered ORWW (cm^3)	0	0	200	0
Unfiltered ORWW (cm^3)	0	0	0	200

5.3 RESULTS

The ammonia concentration of the ORWW was determined by spectrophotometric method (ISO 7150-1:1984) and revealed a low NH_3-N concentration of 1.2 mg L^{-1}. The ion chromatography analysis of the anions and cations in the second batch of ORWW sample also revealed that the ORWW contained very little NH_3-N (1.5 mg L^{-1}) but had appreciable sodium and chloride concentrations of 42 and 56 mg L^{-1} respectively (Table 5.3).

Table 5.3 The Ion chromatography analysis of oil refinery wastewaters.

Cations (mg L^{-1})		Anions (mg L^{-1})	
NH_3-N	1.5	Cl^-	56.4
Ca^{2+}	15.8	NO_2^-	0
Mg^{2+}	2.3	CO_3^-	7.7
K^+	0.7	SO_4^{2-}	0.88
Na^+	42.3	NO_3^-	0
		PO_4^-	4.8

The bioparticles incubated to determine the long term effect of oil refinery wastewater on the nitrifying biofilm, all showed nitrifying activity during the incubation period (Figs. 5.2 - 5.4).There was evidence of a reduction in ammonia below the concentration of the ammonia lost form air stripping in control vessel (Fig. 5.2) as well as the production of nitrite and nitrate in the reactors (Fig. 5.3 and Fig. 5.3). There were some problems during the incubation, for example between days 4 and 7 the control flasks developed problems with the oxygen aerators, as the aerators became blocked overnight on each of the days. Therefore the media between days 5 and 7 and also between days 11 and 14 were not changed. The concentration of nitrite and nitrate produced in flasks during 14- day incubation are shown in Figures 5.3 and 5.4 respectively.

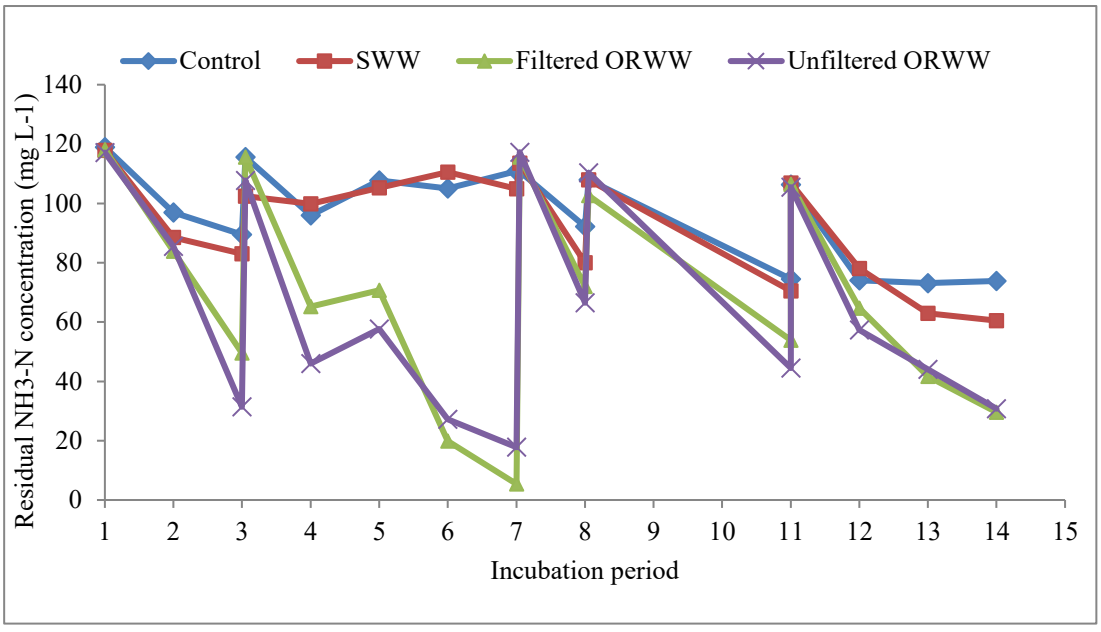

Fig. 5.2 The residual ammonia concentration in the incubation vessels during the 14-day incubation. The different reactor media were changed at 48 hours intervals.

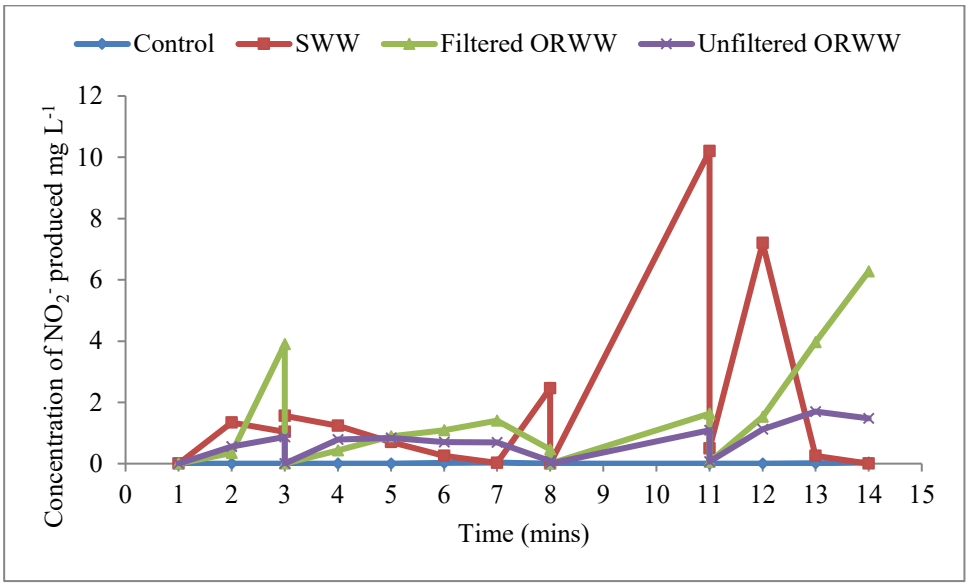

Fig. 5.3. The production of NO_2^- in the reactor flasks during the 14-day incubation while changing the reactor media at 48 hours intervals.

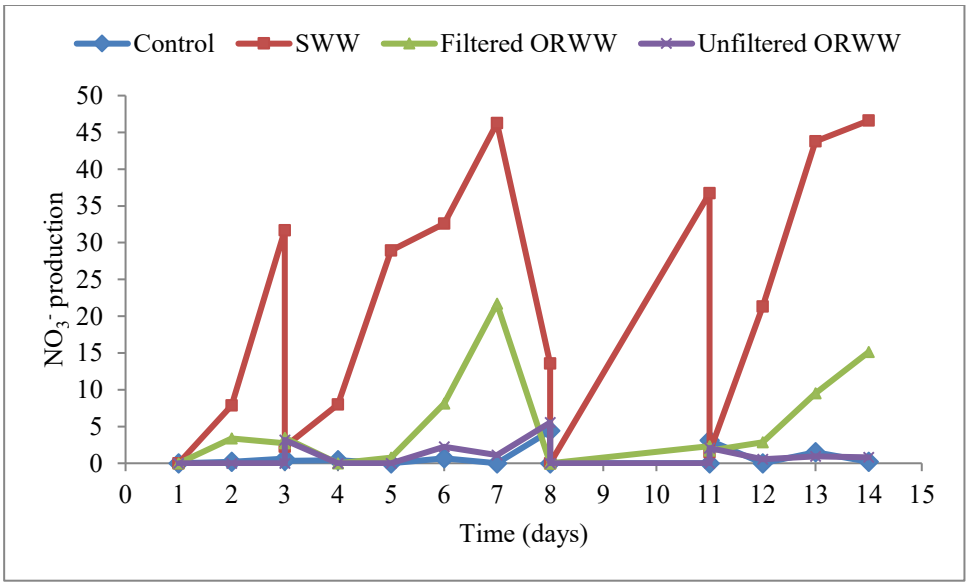

Fig. 5.4 The production of NO_3^- in the reactor flasks during the 14-day incubation while changing the reactor media at 48 hours intervals.

The nitrifying activity of the bioparticles was taken as the difference in the residual ammonia concentration between flasks containing the bioparticles and the control flasks without bioparticles (which only had a reduction of ammonia concentration due to volatilization). The results indicate that bioparticles incubated in the filtered and unfiltered ORWW showed a higher NH_3-N removal rate than those incubated in SWW (Fig 5.2) as they had much lower residual ammonia concentrations e.g. on day 3, 8, 11, 12, 13 and 14 (Fig 5.2). The bioparticles incubated in SWW showed little activity during the period of incubation e.g. on day 14, they achieved only 8 mg L^{-1} NH_3-N removal when compared to over 40 mg L^{-1} NH_3-N for bioparticles incubated in the reactors containing both filtered and unfiltered ORWW (Fig. 5.2).

The specific nitrification rates of the bioparticles obtained from using different reactor media decreased in the following order; full medium > full medium and ORWW (50:50mixture) > filtered ORWW > unfiltered ORWW (Fig 5.5). The bioparticles in the raw (unfiltered) ORWW achieved the lowest nitrification rates. After the 14-day incubation, the bioparticles all achieved higher specific nitrification rates after the incubation period than before (Fig. 5.5). Increase in nitrification rates of 12 %, 6 %, 7 % and 19 % were observed for bioparticles in full medium, mixture of full medium and ORWW, filtered and unfiltered ORWW respectively (Fig 5.5).

Also, after the 14-day incubation period, the bioparticles incubated in filtered and unfiltered ORWW medium achieved the same nitrification rates (2.7 NH_3-N m^{-3}_{EBBR} d^{-1}), although the nitrification rate was still lower than that achieved by the

bioparticles incubated in full medium (3.8 kg NH_3-N m^{-3} $_{EBBR}$ d^{-1}) and those in the 50:50 mixture of full medium and ORRW (3.4 kg NH_3-N m^{-3} $_{EBBR}$ d^{-1}) (Fig. 5.5).

During the 4-hour nitrification experiment also, there was a difference in the residual concentrations of NO_2^--N in the reactors containing ORRW before and after the 14-day incubation of the bioparticles (Fig. 5.6 – Fig. 5.9). The difference in final NO_2^--N concentrations of the reactor containing full medium before and after the 14-day incubation was about 1mg L^{-1} after the incubation (Fig. 5.7 and Fig. 5.8).While there was a difference of about 6 mg L^{-1}, for the reactors containing a mixture of full medium and ORRW and filtered ORWW, the reactor with unfiltered ORWW had a difference of about 20 mg L^{-1} NO_2^- -N concentration (Fig. 5.11 – Fig. 5.14).

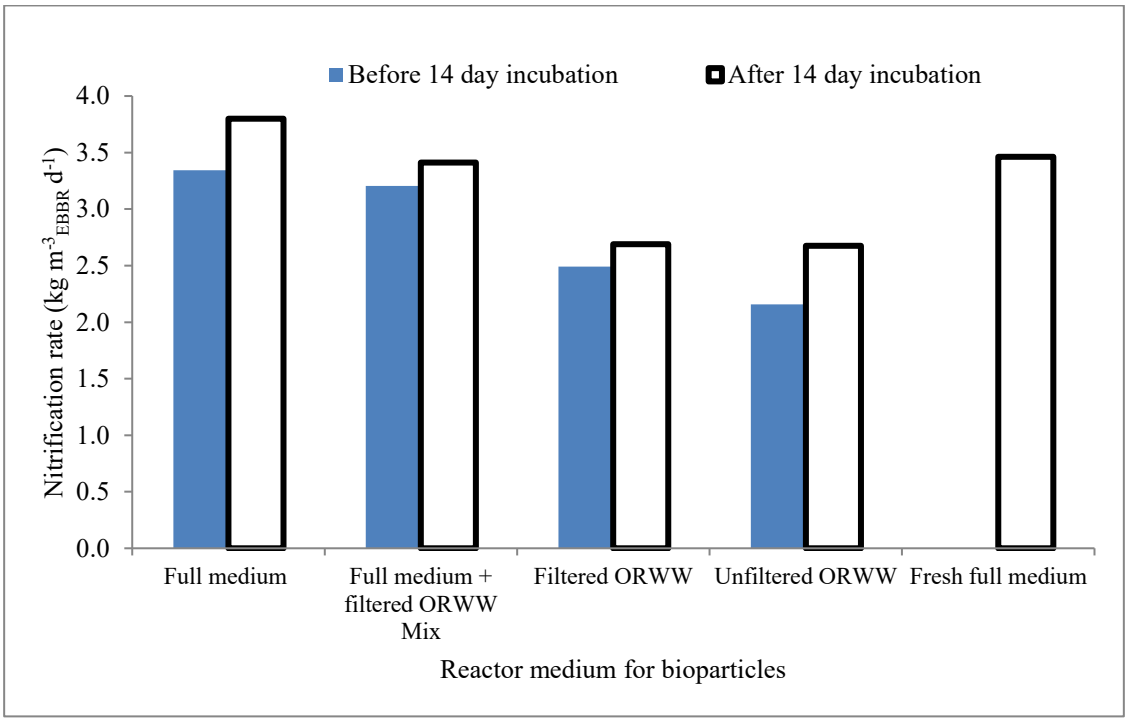

Fig 5 5. Specific volumetric nitrification rates of bioparticles placed in reactors with different media before and after 14-day incubation.

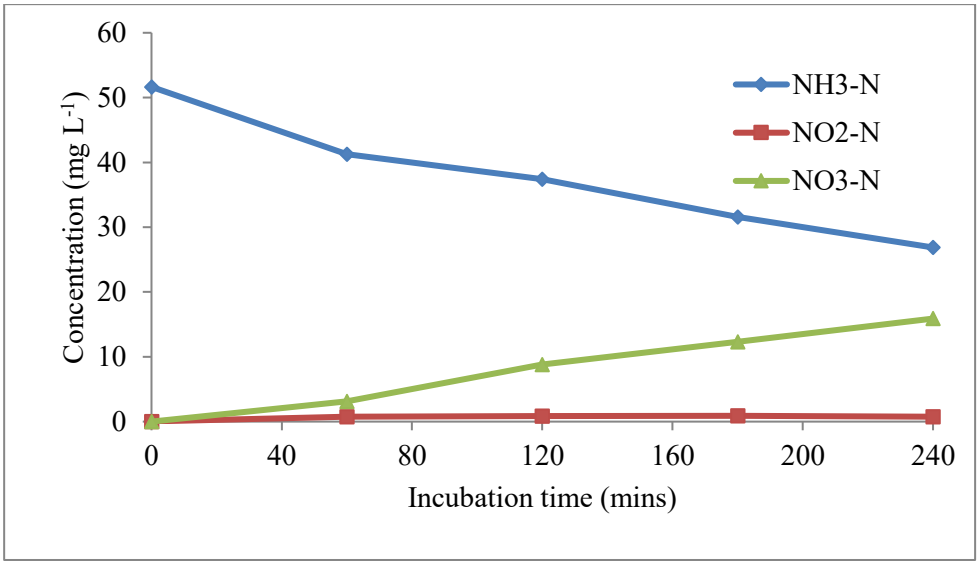

Fig 5.6 The concentration of ammonium, nitrite and nitrate during the specific nitrification rate experiment using bioparticles before the 14 day incubation using full medium in reactor vessel before incubation.

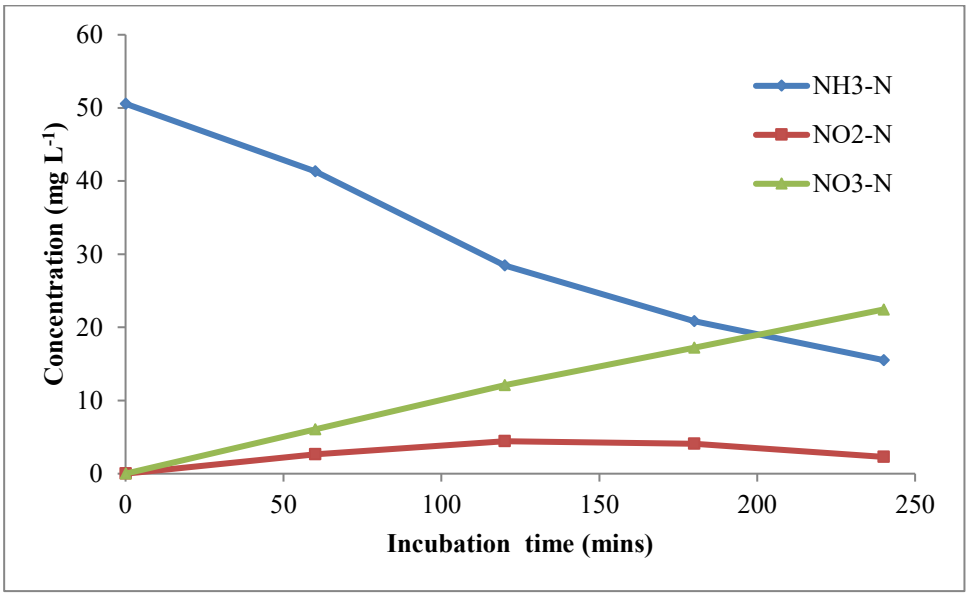

Fig 5.7 The concentration of ammonium, nitrite and nitrate during the specific nitrification rate experiment using bioparticles after the 14 day incubation, with full medium in reactor vessel.

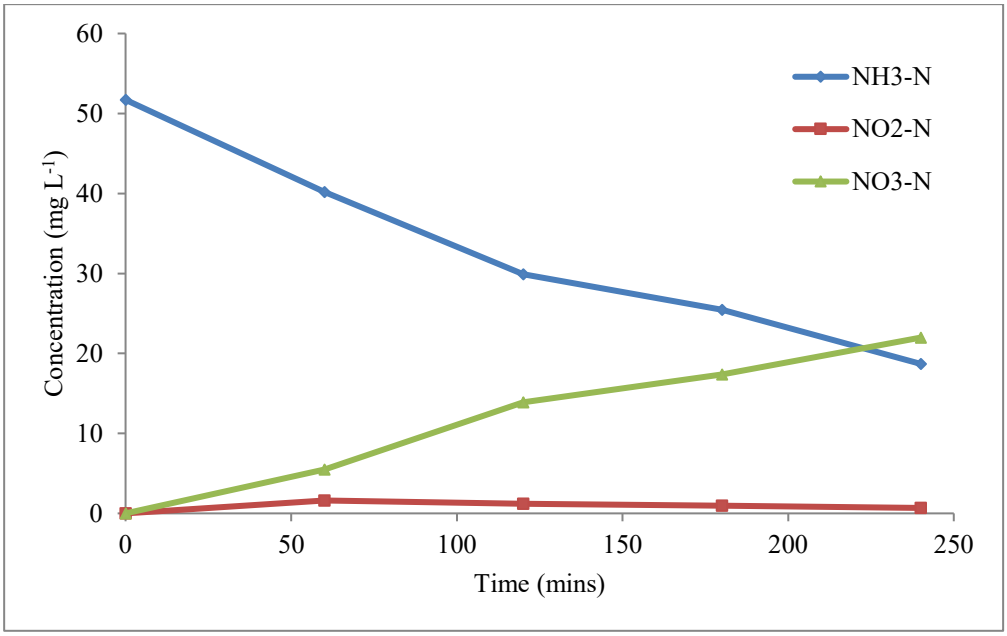

Fig. 5.8 The concentration of ammonium, nitrite and nitrate during the specific nitrification rate experiment using fresh bioparticles from lab scale EBBR on the day 14 of incubation, with full medium in reactor vessel.

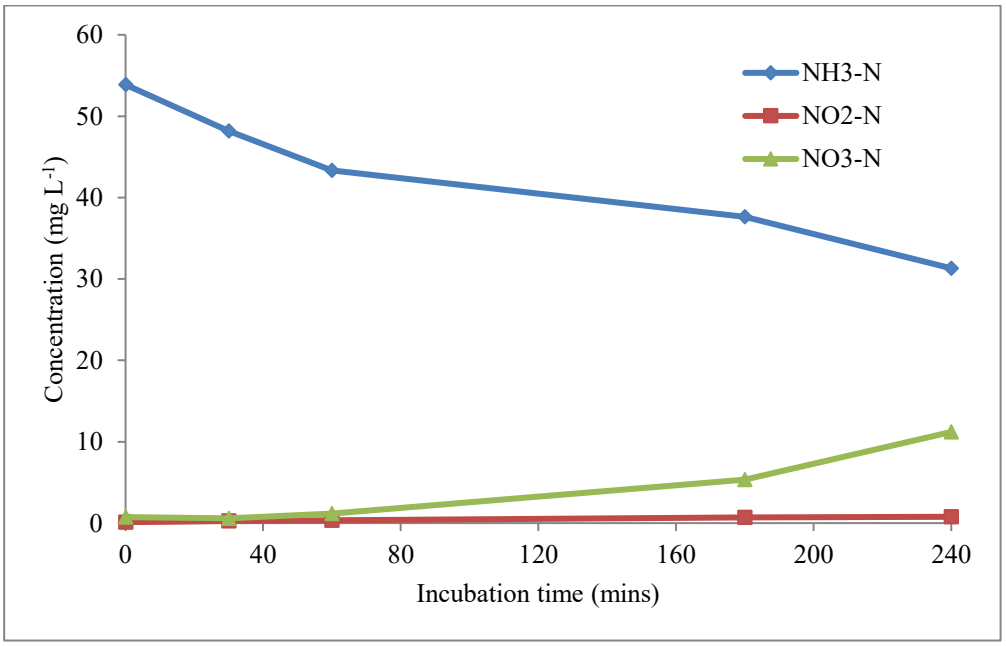

Fig. 5.9 The concentration of ammonium, nitrite and nitrate during the specific nitrification rate experiment using bioparticles before the 14 day incubation with a 50:50 mixture of full medium and filtered ORWW in reactor vessel incubation.

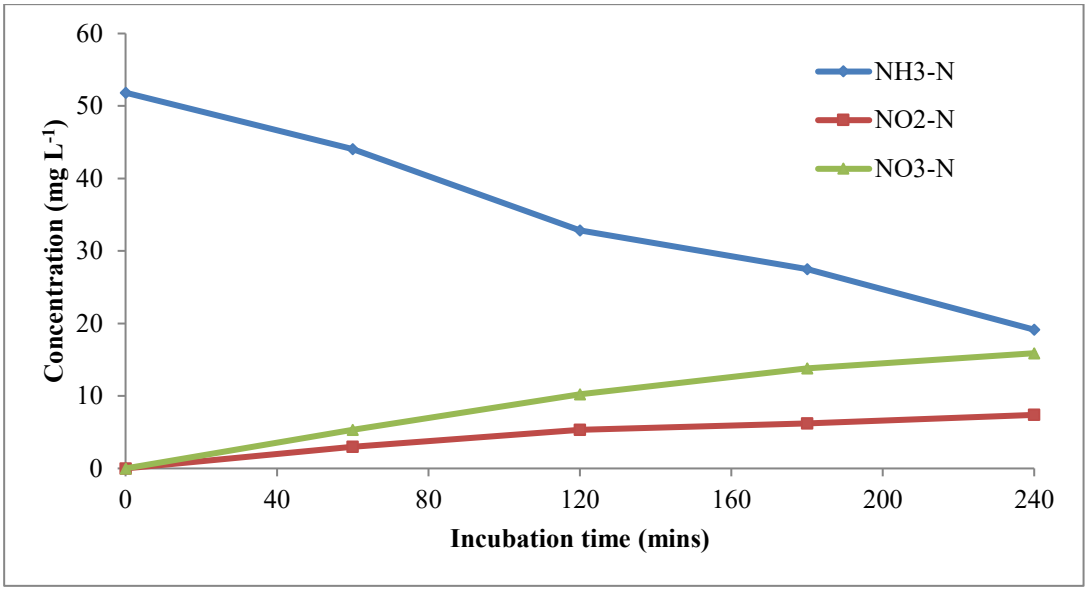

Fig. 5.10 The concentration of ammonium, nitrite and nitrate during the specific nitrification rate experiment using bioparticles after the 14 day incubation with a 50:50 mixture of full medium and filtered ORWW in reactor vessel.

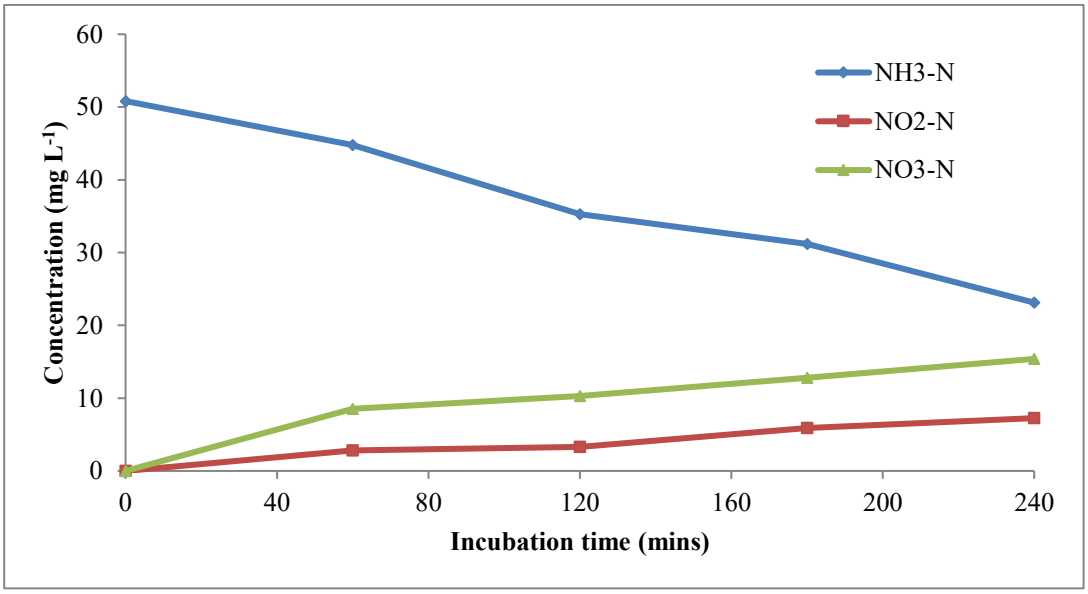

Fig. 5.11 The concentration of ammonium, nitrite and nitrate during the specific nitrification rate of bioparticles before the 14 day incubation using filtered ORWW in reactor vessel before incubation.

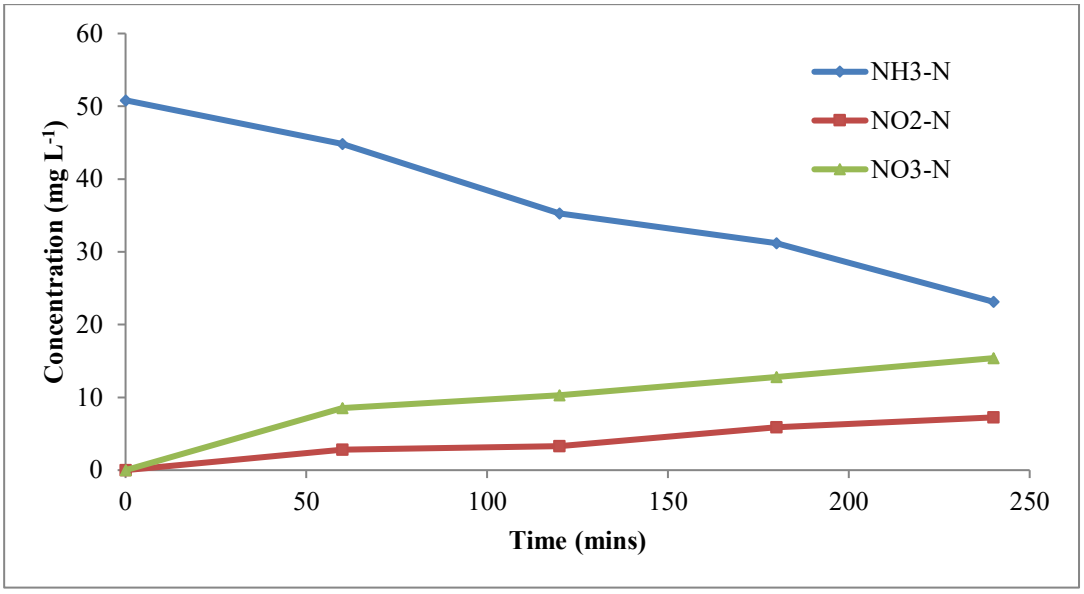

Fig. 5.12 The concentration of ammonium, nitrite and nitrate during the specific nitrification rate experiment using bioparticles after the 14 day incubation with filtered ORWW in reactor vessel.

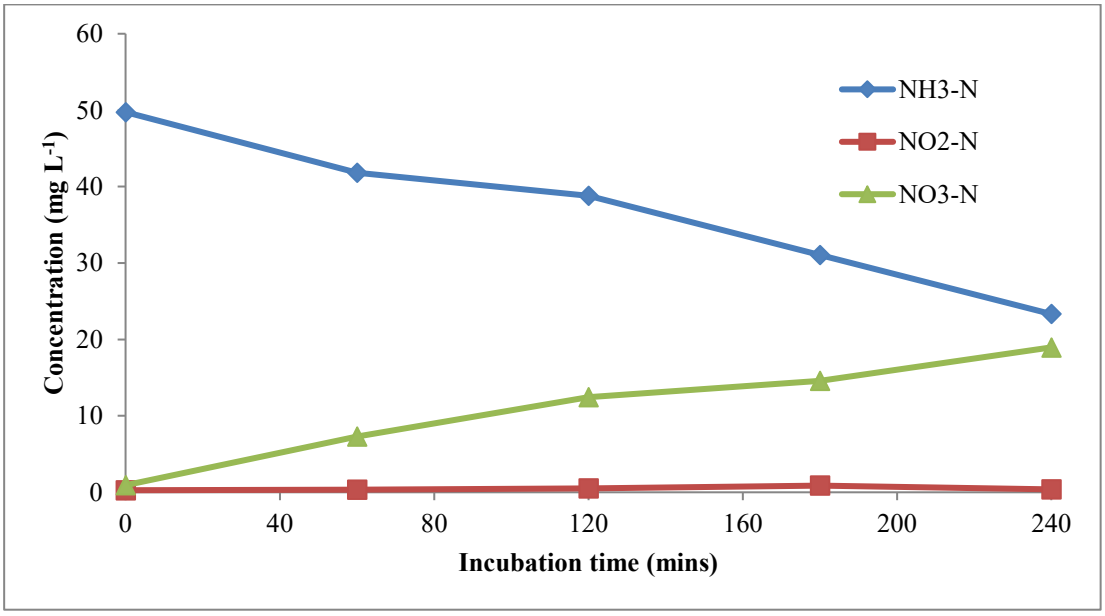

Fig. 5.13 The concentration of ammonium, nitrite and nitrate during the specific nitrification rate experiment using bioparticles before incubation the 14 day incubation with unfiltered ORWW in reactor vessel

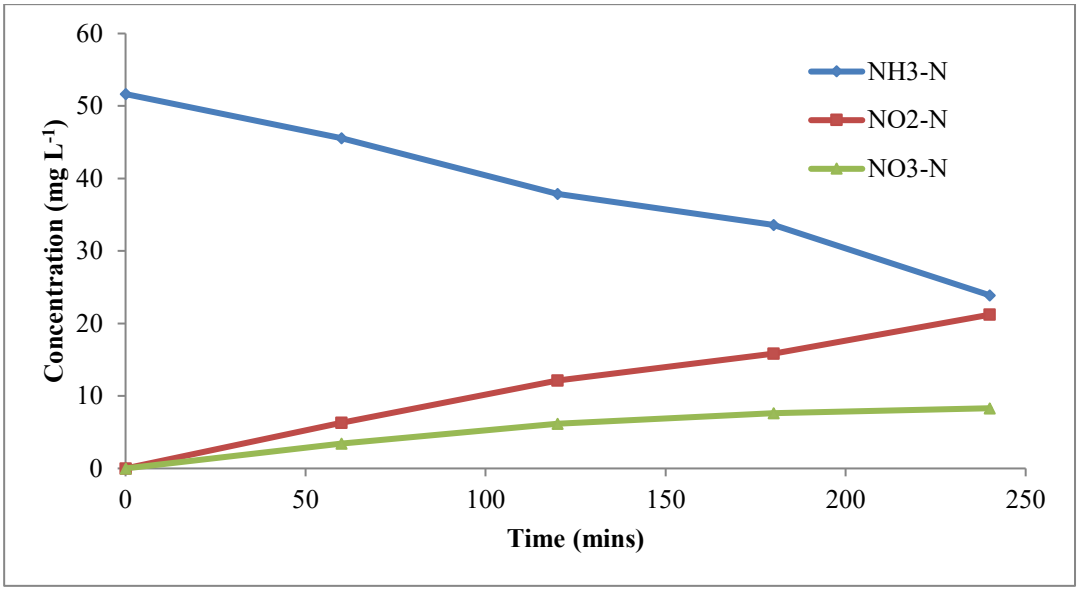

Fig. 5.14 The concentration of ammonium, nitrite and nitrate during the specific nitrification rate experiment using bioparticles after the 14 day incubation with unfiltered ORWW in reactor vessel.

5.4 Discussion

The complete nitrification of ammonia in wastewaters systems produces nitrate in the effluent. Therefore the detection of nitrate in both the 14-day incubation flasks and the miniature expanded bed reactors which only had NH_3-N as the only nitrogen species at the beginning of the incubation, is an indication of the activity of both ammonia oxidizers and nitrite oxidizers of the nitrifying biofilm in the presence of ORWW.

From the earlier determination in the investigation of the influence of biofilm thickness on nitrification rates, bioparticles of 300 μm biofilm thickness gave an average specific volumetric nitrification rate of about 3.0 NH_3-N kg m^{-3}_{EBBR} d^{-1} (Fig. 3.19, page 124). The bioparticles from the lab-scale expanded bed bioreactor achieved a specific nitrification rate of 3.3 NH_3-N kg m^{-3}_{EBBR} d^{-1} before the 14-day incubation using full medium (Fig. 5.2). The bioparticles in the reactor with a 50:50 mixture of full medium and filtered ORRW achieved a similar nitrification rate of 3.2 NH_3-N kg m^{-3}_{EBBR} d^{-1} while the bioparticles in the reactors containing filtered and unfiltered ORWW achieved 25 % and 35 % less than the bioparticles in the full medium reactor (2.5 and 2.2 NH_3-N kg m^{-3}_{EBBR} d^{-1} respectively), (Fig. 5.5).

Notwithstanding the problems encountered during the period of incubation, there was a statistical difference in the nitrification rates achieved by the nitrifying biofilm after the 14-day incubation period (p-value 0.024, paired t-test). Although the higher nitrification rates was achieved in all the incubated particles the biofilms incubated in

ORWW were of particular interest as they were able to achieve nitrification rates of over 2.0 NH_3-N kg m^{-3}_{EBBR} d^{-1}, both before and after the 14-day incubation in ORWW medium indicating that the nitrifying biofilms can survive in the ORWW environment. The 19 % increase in nitrification rate for the bioparticles incubated in unfiltered ORRW is a strong indication that the nitrifying bacteria adjusted to the ORWW medium after prolonged exposure the ORWW. The effect of the ORRW on the bioparticles upon initial exposure to ORRW was absent after the long incubation period as they achieved the same nitrification rates as the bioparticles in the ORRW diluted with full medium. Prior to incubation the bioparticles incubated in ORWW had achieved a lower nitrification rate than those in the mixture of full medium and ORWW (Fig. 5.5).

The bioparticles used in the reactor containing a 50:50 mixture of full medium and ORWW were from the lab scale expanded bed reactor before incubation and the flask containing filtered ORWW after the incubation but still achieved 6 % higher nitrification rate. The highest increase in nitrification rate achieved by the bioparticles incubated in the unfiltered ORWW (19 %) was probably due to the bioparticles adapting to the ORWW during incubation. The presence of minerals in the ORRW (Table 5.3) also would have aided the development of the biofilm microbial population. There was however no difference in nitrification rate between bioparticles in the filtered and unfiltered ORWW reactors as they both achieved 2.7 NH_3-N kg m^{-3}_{EBBR} d^{-1} (Fig 5.5).

There is evidence that the ORWW had an inhibitory effect on nitrifying biofilms and the greater effect was on the NOB than on the AOB. This reason is that after prolonged exposure to ORWW, the biofilm ammonia oxidation rates increased while the nitrite oxidation rates reduced (Fig. 5.5; Figs. 5.9 – 5.14). The reactor with biofilms incubated in unfiltered ORWW showed largest difference in residual NO_2^--N concentration of about 20 mg L^{-1} (Fig. 5.14). The over 150 % difference in the final residual reactor NO_2^--N concentration of biofilms incubated in ORWW over the other biofilm reactors is an indication that undiluted ORWW has an effect on the NOB.

5.5 Conclusion

Although the samples of oil refinery wastewater samples used in this study had very small quantities of ammonia in them, augmenting the ammonia concentrations using $(NH_4)_2 SO_4$), enabled the following conclusions:

- The nitrifying biofilm established in the EBBR could be used in the nitrification of oil refinery wastewaters as the biofilms can survive and adapt to ORWW environment and show significant specific nitrification rates.
- The ORWW had greater effect on the NOB than on the AOB

CHAPTER SIX

6.0 Concluding discussion

The investigation reported in this thesis were all based on the investigations on the nitrifying bioparticles established in the lab-scale expanded bed biofilm reactor. The optimization of the nitrification process established that pH had twice the effect on the nitrification process than temperature. The nitrifying bioparticles although slow growing proved to be quite resilient as they were able to overcome shocks like low pH environments (> 5.0) and overnight deprivation of oxygen due to compressed air supply failure and quickly regain nitrifying activity.

Because of the nature of the coke support material used in this novel technology, methods had to develop to investigate the nitrifying biofilms used in this study. The methods include; a method to determine the biomass concentration of bioparticles, the development of a miniature bed reactor similar to the lab-scale EBBR in order to determine the specific nitrification rate of bioparticles of a definite biofilm thickness and the development of methods to visualize and quantify the biofilms after staining with probes.

The scanning electron microscopic (SEM) and confocal scanning microscopic (CLSM) observations of the biofilm (Fig 2.6a-d., and Fig 4.6) established that the biofilms initially had mushroom shaped microcolonies but grew into complex structures with stacks of cell aggregates developing in all directions. The study also revealed that nitrite can accumulate in the EBBRs when receiving NH_3-N

concentrations of about 125 mg L^{-1} NH_3-N concentration and where this occurs, the ammonia oxidation rate may not be ideal to be regarded as an index for the complete nitrification rate.

The thinner biofilms (40 - 100 µm) achieved biomass concentrations of 20 to 28 kg m^{-3} while the thicker biofilms (250 - 400 µm) achieved biomass concentrations of 30 to 50 kg m^{-3} (Fig 3.19). However biofilms thicker than 300 µm were less efficient nitrifying biofilms, although there is evidence that an active ammonia oxidation region of a depth of about 450 µm exists in thicker biofilms (Fig. 3.19).

An important feature revealed by the FISH analysis of the outer 100 µm of the biofilm using data obtained from stained biofilm images by CLSM, was that the AOB had twice the abundance of NOB in the thinner biofilms. Meanwhile, the abundance of AOB and NOB was often equal in the same region for thicker biofilms. The lower abundance of the NOB compared to AOB in thin biofilms less than 200 µm, helps to explain the results obtained in the investigation of the influence of biofilm thickness on nitrification rates (Fig 3.20).

Measurements of nitrification rates revealed that in re-growing bioparticles; that had their biofilms stripped off and replaced into the EBBR and were therefore thinner, the biofilms achieved incomplete nitrification, resulting in high NO_2^--N concentrations after 4-hour incubation in the miniature EBBR. The thicker biofilms of about 300 µm on the other hand, achieved complete nitrification when subjected to the same conditions (Figs. 3.14 to 3.17).The study also revealed that thicker

biofilms achieved higher cell aggregate concentrations than the thin biofilms in the outer 100 μm region (sometimes up to 400 times that of thinner biofilms) (Table 4.2) and this supports the finding that thicker biofilms achieve higher biomass concentrations than thinner biofilms (Fig. 3.18 and Fig. 3.20.). Because the high cell aggregate concentrations of the thicker biofilms represents a larger population of nitrifying bacteria available for nitrification, coupled with the often equal densities of the AOB and NOB (Table 4.2), the rate of nitrite oxidation was higher in the thicker biofilms and therefore complete nitrite oxidation was achieved.

While the AOB population achieved optimum ammonia oxidation rates at about 100 μm biofilm thickness, the NOB population could only achieve optimum nitrite oxidation rates in thicker biofilms in the EBBR reactors at the concentration of the influent NH_3-N used in this work (56 mg L^{-1} or 125 mg L^{-1} for both the miniature and expanded bed bioreactors), which was much higher than the normal influent concentration of wastewater treatment plants. The re-growing bioparticles were therefore NOB biomass limited and therefore did not achieve nitrite oxidation rates to match the nitrite producing rates of the AOB. This finding is valuable as it presents an opening for research into the use of EBBR technology for nitritation.

There was evidence of active nitrifying bacterial activity at depths of 500 μm in the biofilms from the EBBR (Fig. 4.10c). Two possible reasons can be put forward for this; the diffusion of oxygen and substrates to depths of 500 μm or the ability of the nitrifying bacteria to survive in environments of low oxygen and ammonia

concentrations and retain the ability to quickly regain nitrifying activity upon exposure to oxygen and substrates.

A reasonable conclusion can be reached when two factors are considered.

1. Although the thicker biofilms were easily detached than thinner biofilms upon stripping in enclosed vessels, the absence of detached biofilms in the bioreactor indicates that the biofilms were still attached to the coke support during normal bed operation. This observation implies that the innermost core of the biofilm was not made up of dead bacterial cells; otherwise the biofilms would detach and be seen floating at the top of the expanded bed column.

2. Fluidization of the bioparticles causes them to become separated from each other (in the expanded state) but they also are able to collide gently thereby possibly enhancing the deeper penetration of oxygen and substrates into the biofilms.

The considerations above strengthens the conclusion that an active nitrifying bacteria at 450 μm as deduced from the calculations (Fig. 3.19, Table 4.2) and image analysis (Fig 4.10c.) is attainable in the nitrifying biofilms from the EBBR.

In the nitrifying biofilms from the EBBR, this work has confirmed that the optimum thickness for ammonia oxidation is 100 μm but the optimum thickness for nitrite oxidation is beyond 100 μm but can be achieved by 300 μm biofilm depth. The work on the influence of biofilm thickness on ammonia oxidation rates and the

quantification of the biofilm nitrifying bacteria reported in chapters 3 and 4 are the major contributions to knowledge from this work.

The investigation into the application of the expanded bed technology for oil refinery wastewater (ORRW) treatment revealed that the nitrifying biofilms could survive and adapt quickly to the ORWW. Although there was evidence of some inhibition of the activities of the nitrite oxidizing bacterial activity by the ORWW, the ammonia oxidizing bacteria achieved high volumetric ammonia oxidizing rates of over 2.0 NH_3-N m^{-3}_{EBBR} L^{-1} d^{-1} (Fig 5.5). There was also evidence that when not fluidized, the biofilms incubated in ORWW achieved higher ammonia removal than those incubated in the synthetic wastewater (SWW) found in literature. The most probable reason for the higher removal would be that the ORWW contained more micro and macro nutrients than the SWW. The expanded bed technology can be applied to the treatment of oil refinery wastewaters successfully.

REFERENCES

Agarry, S. E., Durojaiye, A. O., Yusuf, R.O., Aremu, Solomon, B. O. and Mojeed, O. (2008). Biodegradation of phenol in refinery wastewater by pure cultures of *Pseudomonas aeruginosa* NCIB 950 and *Pseudomonas fluorescence* NCIB 3756. *International Journal of Environment and Pollution* **32** (1): 3 -11.

Ahnell, A. and O'Leary, H. (2008). General introduction to environmental technology. In: Orszulik , S., Environmental technology in the oil industry (2nd Ed). Springer, UK. 1-16pp.

Amann, R. I, Wolfgang, L and Schleifer, K. (1995). Phylogentic identification and in-situ detection of individual microbial cells without cultivation. *Microbiological Reviews* **59**: 143-169.

American Public Health Association and American Water Works Association (APHA) (1995). Standard methods for examination of water and wastewater (4500-NO_3 – B)

American Society for Testing and Materials. (2001). Standard test method for ash in biomass (ASTM E1755-01).

American Society for Testing and Materials. (2001). Standard test method for determination of total solids in biomass (ASTM E1756-01)).

Amnesty International (2009). Nigeria: petroleum, pollution and poverty in the

Niger Delta. Amnesty International Publication , London 143P.

Anderson, M. J. and Whitcomb, P. J. (2005). RSM simplified – optimizing processes using response surface methods for design of experiment. Productivity press. New York 292P

Anderson, M. J. and Whitcomb, P. J. (2007a). Response surface methods (RSM) for peak process performance at the most robust operating conditions www.statease.com/pubs/RSM_for_peak_performance.pdf.

Antoniou, P., Hamilton, J., Koopman, B., Jain, R., Holloway, B., Lyberatos, G. and Svoronos, S. A. (1990). Effect of temperature and pH on the effective maximum specific growth rate of nitrifying bacteria. *Water Research.* **24**: 97 – 100

Arciero, D., Vannelli, T., Logan, M. and Hooper, A. B. (1989). Degradation of trichloroethylene by ammonia oxidizing bacterium *Nitrosomonas europaea*. *Biochem. Biophys. Resources. Commun*. **159**: 640-643

Atkinson, B. (1981). Immobilised biomass - a basis for the process development in wastewater treatment. In: Biological fluidised bed treatment of water and wastewater treatment. Cooper, P. F. and Atkinson B. Chichester, Ellis Horwood Ltd 22-34 pp.

Atkinson, B., Black, G. M. and Pinches, A. (1981). The characteristics of solid

supports and biomass support particles when used in fluidised beds. In: Biological fluidised bed treatment of water and wastewater treatment. Cooper, P. F. and Atkinson B. .Chichester, Ellis Horwood Ltd pp78-109.

Beun, J. J., van Loosdrecht, M. C. M. and Heijnen, J. J. (2002). Aerobic granulation in a batch airlift reactor. *Water Research* **36**: 702-712.

Beyenal, H. and Lewandowski, Z. (2002) Internal and external mass transfer in biofilms grown at various flow velocities. *Biotechnol. Prog*. **18** (1), 55 – 61.

Bishop, P. L. (2003). Modeling and simulation; conclusions. In: Biofilms in wastewater treatment, an interdisciplinary approach, Wuertz, S, Bishop, P. and Wilderer, (Eds) IWA Publishing Cornwall, 117 – 119pp.

Bitton, G. (2005). Wastewater Microbiology. (3rd Ed). John Wiley & Sons Inc. New Jersey. 746P

Bock, E. (1978). Lithographic and chemoorganothrophic growth of nitrifying bacteria. In: Microbiology. Schlessinger, D. (1978). American Society of Microbiology, Washington DC 310 - 314pp

Bock, E., Koops, H. and Harms, H. (1986). Cell biology of nitrifying bacteria. In : Nitrification. Prosser, J. I (Ed).Oxford IRL Press 17-38 pp.

Brading , M.G., Jass, J. and Lappin-Scott, H. M. (1995). Dynamics of bacterial biofilm formation. In: Microbial biofilms, Lappin-Scott and Costerton

(EDs) Cambridge University Press. Cambridge ,46 – 63pp

Cattaneo, S., Marciano, F., Masotti, L., Vecchiato, G, Verlicci, P., Zaffaroni, C. (2009). Nutrients removal upgrading at a petrochemical industrial wastewater treatment plant: the case of Porto Marghera, Venice. Conference proceedings of the 2nd IWA Specialized Conference. Nutrient management in wastewater treatment processes. Krakow, Poland. 6-9 September 2009, 855 – 865pp

Cheremisinoff, N. P. and Haddadin, M. B. (2006). Beyond compliance – The refinery managers guide to ISO 14001 implementation. Gulf Publishing 207P. ISBN 978-0-9765113-9-7

Concawe (1979). The environmental impact of refinery effluents. Concawe (The oil companies' European association for environment, health and safety in refining and distribution). Report no.5/79, 250pp

Concawe (2004). Trends in oil discharged with aqueous effluents from oil refineries in Europe: 2000 survey. (The oil companies European association for environment, health and safety in refining and distribution). Report no.4/04, 9pp (available at www.concawe.org)

Cooper, P. F. (2001). Historical aspects of wastewater treatment. In: Decentralised sanitation and reuse: concepts, systems and

implementation. Lens, P., Zeeman, G. and Lettinga, G. (Eds). IWA Publishing. London UK 11- 38pp

Cooper, P.F and Atkinson, B. (1981). Biological fluidized bed treatment of water and wastewater. Ellis Horwood Ltd Chichester. 411P

Costa, E., Perez, J. and Kreft, J. (2006). Why is metabolic labour divided in nitrification? *Trends in Microbiology.* **14** (5): 213-219

Costerton, J.W, Lewandowski, Z., de Beer, D., Caldwell, D., Korber, D. and James, G. (1994). Biofilm, the customized microniche. *Journal of Bacteriology*. **176** (8): 2137 – 2142.

Cote, R. P. (1976). The effects of petroleum wastes on aquatic life with special emphasis on the Canadian environment. National Research Council of Canada. NRC Associate Committee on Scientific Criteria for Environmental Quality, Ontario Canada K1A 0R6, publication no. 15021, 77pp

Council of European Communities (1991). Directive concerning urban wastewater treatment (91/271/EEC). *Official Journal* L135/40, 30TH MAY 1991.

Davis, M. L. and Masten, S. J. (2003). Principles of Environmental Engineering and Science. McGraw Hill Publishers New York 704P

de Beer, D., van den Heuvel, J. C. and Ottengraf, S. P. P. (1993). Microelectrode measurements of the activity distribution in nitrifying bacterial aggregates. *Applied and Environmental Microbiology*. **59** (2): 573 - 579.

De Roos, A. J., Ward, H. H., Lynche, C. F. and Cantor, K. P (2003). Nitrate in public water supplies and the risk of colon and rectum cancers. *Epidemiology.* **14**: 640 - 649

de Wilde, F. G. N. (1977). Treatment of effluents from ammonium plants. *Water Research* **7**:1137 - 1153

Dempsey, M. J. (2003). Nitrification process. **US6572773**.

Dempsey, M. J., Lannigan, K. C. and Minnal, R. J. (2005). Particulate-biofilm, expanded-bed technology for high rate-low cost wastewater treatment nitrification. *Water Research* **39**: 965-974.

Dempsey, M. J., Porto, I., Mustafa, M., Rowan, A.K. and Head, I. M. (2006). The expanded bed biofilter: combined nitrification, solids destruction and removal of bacteria. *Water Science Technology* **54** (8): 37 - 46

Dempsey, M. J . and Minall, R. J. (2009). Sludge liquor nitrification using expanded bed technology, Conference proceedings of the 2nd IWA Specialized Conference. Nutrient management in wastewater treatment processes. Krakow, Poland. 6 - 9 September 2009. 775 – 782pp

Denac, M., Uzman, S., Tanaka, H. and Dunn, I. J. (1983). Modelling and experiments on biofilm penetration effects in a fluidized bed nitrification reactor. *Biotechnology and Bioengineering*. **25**: 1841 – 1861.

Deni, J. and Penninckx, M. J. (1999). Nitrification and autotrophic nitrifying bacteria in a hydrocarbon-pollution soil. *Applied and Environmental Microbiology* **65** (9): 4008 - 4013

Di Felice. R. (1995). Hydrodynamics of liquid fluidisation. *Chem. Eng. Sci*. **50**: 1213 – 1245.

Dogsa, I., Kreichbaum, M., Stoper, D. and Laggner, P. (2005). Structures of Bacterial extracellular polymeric substances at different pH values as determined by SAXS. *Biophysical Journal* **89**: 2711 - 2720.

Eberl, H. J., Picioreanu, C., Heijnen, J. J. and van Loosdrecht, M. C. M. (2000). A three-dimensional numerical study on the correlation of spatial structure, hydrodynamic conditions, and mass transfer and conversion in biofilms. *Chemical Engineering Science* **55**: 6209 - 6222

Eberl, H. J. (2003). What do biofilm models, mechanical ducks, and artificial life have in common? *Mathematical modelling in biofilm research*. In: Biofilms in wastewater treatment, an interdisciplinary approach.

Wuertz, S, Bishop, P and Wilderer, (Eds) IWA Publishing. Cornwall, 8 – 31 pp

Ekema, G. A. and Wentzel, M. C (2008). Nitrogen removal. In: Biological wastewater treatment, principles, modelling and design. Henze, M., van Loosdrecht, M. C. M, Ekema, G. A and Brdjanovic, D. (Eds). IWA publishing. Cambridge University Press 85- 137pp

Energy Information Administration (2008). Ranking of US refineries. Official energy statistics for the US government. www.eia.doe.gov/neic/rankings/refineries.htm. accessed 21/09/09

EPA (1995). Profile of the petroleum refining industry. EPA office of compliance sector notebook project. EPA/310-R95-013

EPA (1998). Final standard promulgated for petroleum refining waste. Environmental Fact Sheet EPA 530-F-98-014

EPA (2002). Exemption of oil and gas exploration production and production of wastes from federal hazardous waste regulations. EPA530-K-01-004

EPA. (2004). Aerated, partial mix lagoons. Wastewater Technology Fact Sheet. EPA 832 – F - 02 – 008

Fabah, K. J. and Dahab, M. F. (2004). Biomass concentration and biofilm characteristics in high performance fluidized bed biofilm reactors. *Water Research* **38**: 4262 - 4270

Fernandez, I., Vazquez-Padin, J. R., Mosquera-Corral, A., Campos, J. L. and Mendez, R. (2008). Biofilm and granular systems to improve anammox biomass retention. *Biochemical Engineering Journal* **42**: 308-313

Flemming , H. and Wingender, J. (2003). The crucial role of extracellular polymeric substances in biofilms. In: Biofilms in wastewater treatment – an interdisciplinary approach. Wuertz, S, Bishop, P and Wilderer, P (Eds). IWA Publishing. Cornwall, 178 – 210 pp

Fletcher, M. (1996). Bacterial attachment in aquatic environments: a diversity of surfaces and adhesion strategies. In: Bacterial Adhesion: Molecular and Ecological diversity. Fletcher, M(Ed) New York. Wiley & Sons 1-24 pp

Flournoy,W. J., Grillo, R., Hubbell, S.B., Kalluri, R. and Mueller, C. (2008). Enhancing nitrification in oil refinery WWTP with IFAS*WEFTEC*©.09 142 – 150.

Francis, C. A., Roberts, K. J. Beman, J. M, Santaro, A. E. and Oakley, B. B. (2005). Ubiquity and diversity of ammonia-oxidizing archaea in water columns and sediments of the oceans. *Proceedings of the National Academy of the United States of America* **102** (41): 14683-14688.

Gary, J. H. and Handwerk, G.E. (2001). Petroleum refining: technologies and economics. Marcel & Dekker Inc. New York . 441P. ISBN 0-8247-0482-7

Geets, J., Boon, N. and Verstraete, W. (2005). Strategies of aerobic ammonia-oxidizing bacteria for coping with nutrient and oxygen fluctuations. *FEMS Microbiol. Ecol*. **58**:1 - 13

Gieseke, A., Purkhold, U, Wagner, M., Amman, R. and Schramm, A. (2001). Community structure and activity dynamics of nitrifying bacteria in a phosphate-removing biofilm. *Applied and Environmental Microbiology* **67**(3): 1351 - 1362

Grady, L., Daigger, G.T., Lim, H.C. (1999). Biological wastewater treatment. Marcel Dekker, New York. 1092P

Gray, N.F. (1989). Biology of wastewater treatment. Oxford University Press 828P

Gray, N.F. (2005).Wastewater technology. An introduction for environmental scientists and engineers. Butterworth-Heinemann. Oxford. 645P

Green, J. and Trent, M. W. (1989). The fate and effects of oil in fresh wastewater. Elsevier Science publishers. London 338P

Gulevich, V., Renn, C. E. and Liebman, J. C. (1968). Role of diffusion in biological waste treatment. *Environ. Sci. Tech*. **2:** 113 - 119

Gulyas, H. and Reich, M. (1995). Organic compounds at different stages of a refinery wastewater treatment plant. *Water Science and Technology.* **32**

(7): 119 - 126.

Guo, J., Wang, S, Huang, H., Peng, Y. Ge, S. Wu, C. and Sun, Z. (2009). Efficient and integrated start up strategy for partial nitrification to nitrite treating low C/N domestic wasteswater. Conference proceedings of the 2nd IWA Specialized Conference. Nutrient management in wastewater treatment processes. Krakow, Poland. 6-9 September 2009, 655 – 666pp.

Hagopian, D. S. and Riley, J. G. (1998). A closer look at the bacteriology of nitrification. *Aquacultural Engineering* **18**: 223 - 244

Hall, Jr., Buikema,, L.W., Cairns, A. L. (1978). The effects of a simulated refinery effluent on the grass shrimp *Palaemonetes pugio*. *Archives of Environmental Contamination and Toxicology* **7**: 23 - 35

Hayat, S., Ahmad, I., Azam, Z. M., Ahmad, A., Inam, A. and Samiullah (2002). Effect of long term application of oil refinery wastewater on soil health with special reference to microbiological characteristics. *Bioresource Technology* **84**: 159-163.

Heijnen, J. J. (1984). Biological industrial wastewater treatment minimizing biomass production and maximizing biomass concentration. PhD Thesis, Delft University of technology, Delft.

Hermanowicz, S. W. (2003). Biofilm architecture: interplay of models and

Experiments. In: Biofilms in wastewater treatment – an Interdisciplinary approach Wuertz, S, Bishop, P and Wilderer, P. (Eds). IWA publishing 32 - 45pp

Hibiya, K., Nagai, J., Tsuneda, S. and Hirata, A. (2004). Simple predictions of Oxygen penetration depth in biofilms for wastewater treatment. *Biochemical Engineering Journal* **19**: 61 - 68.

Horan, N. J. (1990). Biological wastewater treatment systems, theory and operation. John Wiley & Sons. Chichester, 310P

Hutton, W. C. and LaRocca, S. A. (1975). Influence of high pressure of carbon dioxide and/or oxygen on nitrification. *J. Chem. Technol. Biotechnol.* **32**: 213 - 223

Hyman, M. R. and Wood, P. M. (1985). Ethylene oxidations by *Nitrosomonas europaea. Arch Microbiol.* **137**: 155-158

Hyman, M. R., Murton, I. B. and Arp, D. J. (1988). Interaction of ammonia monooxygenase from *Nitrosomonas Europaea* with alkanes, alkenes and alkynes. *Applied and Environmental microbiology* **54** (12): 3187 – 3190.

Hyman, M. R., Kim, C. Y. and Arp, D. J. (1990). Inhibition of ammonia monooxygenase in *Nitrosomonas europaea* by carbon disulfide. *Applied and Environmental Microbiology* **172** (9): 4775 – 4775.

Ikehata, K., Buchana, I. D., Smith, D. W. (2003). Treatment of oil refinery Wastewater using *Corprinus cinereus* peroxidise and hydrogen peroxide. *Journal of Environmental Engineering* and Science **2** (6): 463 – 472

Image J. Image processing and analysis in java. http//rsb.info.nih.gov/ij/ index.html. Accessed on 30/10/09

Institute of Wastewater and Environmental Management IWEM (1994). Tertiary treatment. The hand books of UK wastewater practice. London. 98P

ISO-6777 (1984). Water quality - determination of nitrite – molecular absorption spectrometric method.

ISO-7150-1 (1984). Water quality – part 2: Physical, chemical and biochemical methods – ammonium section 2.11 Determination of ammonium: Manual spectrometric method.

ISO-9509 (2006). Water quality - toxicity test for assessing the inhibition of nitrification of activated sludge microorganisms

Jenkins, D., Richard, M. G. and Daigger, G. T. (2003) Manual on the causes and control of activated sludge bulking, foaming and other solids separation problems. IWA publishing London 224P

Jou, C. G. and Huang, G. (2003). A pilot study for oil refinery wastewater

treatment using a fixed bed biofilm bioreactor. *Advances in Environmental Research* **7**: 463 - 469

Juliette, L. Y., Hyman, M. R. and Arp, D. J. (1993). Inhibition of ammonia oxidation in *Nitrosomonas europaea* by sulphur compounds: thioethers are oxidized to sulfoxides by ammonia monooxygenase. *Applied and Environmental Microbiology* **59** (11): 3718 - 3727

Kampschreur, M. J., Temmink, H., Kleerebezem, R., Jetten, M. S. M, van Loosdrecht, M. C. M. (2009). Nitrous oxide emission during wastewater treatment. *Water Research* **43:** 4093 - 4104

Keener, W. K. and Arp, D. J. (1994). Transformation of aromatic compounds by *Nitrosomonas europaea*. *Applied and Environmental Microbiology* **60** (6): 1941 - 1920

Kelly, D. P. (1978). Bioenergetics of chemolithotrophic bacteria. In: Bill, A.T. and Meadow, P. M. Companion to Microbiology. Longman Publishing Group, London 363 - 368 pp

Kerksiek, K. (2008). A life of slime – biofilms rule the world. Infection research news and perspectives. www.infection-research.de

Keunen, J. G. (2008). Anammox bacteria: from discovery to application. *Perspectives*. **6**: 320 – 326.

Kim, D., Lee, D. and Keller, J. (2006). Effect of temperature and free ammonia on

nitrification and nitrite accumulation in landfill leachate and analysis of its nitrifying bacterial community by FISH. *Bioresource Technology* **97**: 459 – 468

Kim, H., Hubbell, S., Boltz, J.P., Flournoy, W., Gellner, J., Pitt, P., Dodson, R. and Schuler, A. J. (2007). Questions and answers about Integrated fixed film/activated sludge (IFAS) in a BNR pilot plant. *WEFTEC*©.07 143-154

Kissel, J. C., McCarthy, P.L. and Street R. L. (1984). Numerical simulations of mixed culture biofilms *J. Env Eng.* ASCE **110**:393 – 405

Konneke, M., Bernhard, A. E., de la Torre, J. R., Walker, C. B., Waterbury, J. B. and Stahl, D. A. (2005). Isolation of an autotrophic ammonia-oxidizing marine archaeon. *Nature* **437** (7058): 543 - 546.

Koops, H. and Pommerening-Roser, A. (2001). Distribution and ecophysiology of the nitrifying bacteria emphasizing cultured species. *FEMS Microbiology Ecology.* **37**: 1 - 9.

Kowalchuk, G. A. and Stephen, J. R. (2001). Ammonia-oxidizing bacteria: A model for Molecular Microbial ecology. *Annual Review of Microbiology* **55**: 485 - 529

Kuehn, M., Hausner, M., Bungart, H., Wagner, M., Wilderer, P. A. and Wuertz, S.

(1998). Automated confocal laser scanning microscopy and semi automated image processing for analysis of biofilms. *Applied and Environmental Microbiology* **64**(11): 4115 - 4127

Kuypers, M. M. M., Sliekers, A. O., Lavik, G., Schmid, M., Jorgensen, J. G., Sinninghe Damste, J. S., Strous, M and Jetten, M. S. M. (2003). Anaerobic ammonium oxidation by sea anammox bacteria in the Black sea . *Letters to Nature* **422**: 608 – 611

Leiknes, T. and Ødegaard, H. (2006). The development of a biofilm membrane reactor. *Desalination* **202**: 135-143

Lewandowski, Z. and Beyenal, H. (2003). Mass transport in heterogenous biofilms. In: Biofilms in wastewater treatment – an interdisciplinary approach. Wuertz, S, Bishop, P and Wilderer, P (Eds). IWA Publishing. Cornwall 147 – 177 pp

Lewis, W. M. and Morris, D. P. (1986). Toxicity of nitrite to fish; a review. *Transactions of the American Fisheries Society* **115**:183 - 195

Li, H., Zhang, C. G. and Chen, G. X. (2005). effect of petroleum containing wastewater irrigation on bacterial diversities and enzymatic activities in a paddy soil irrigation area. *J. Environm. Qual*. **34**: 1073 - 1080

Macdonald, R. (1986). Nitrification in soil: an introductory history. In: Nitrification. Prosser, J. I (Ed).Oxford IRL Press 1 - 16 pp.

Matsuba, D., Takazaki, H., Sato, Y. and Takahashi, R. (2002). Susceptibility of ammonia-oxidizing bacteria to nitrification inhibitors. *Verlag der Zeitschrift für Naturforschung, Tübingen* 282 -287

McQuarrie, J., Dempsey, M. J., Boltz, J. P. and Johnson, B. (2007). The expanded bed biofilm reactor (EBBR) – An innovative biofilm approach for tertiary nitrification. Proceedings of the Water Environment Federation, WEFTEC 2007. 184 - 200 pp

Merod, R.T., Warren, J.E., McCaslin, H. and Wuertz, S. (2007). Towards automated analysis of biofilm architecture: Bias caused by extraneous CLSM images. *American Society for Microbiology* **75** (15): 4922 – 4930.

Nakumara, Y., Satoh, H., Kindaichi, T and Okabe, S. (2006). Community structure and *in situ* activity of nitrifying bacteria in river sediments as determined by the combined use of molecular techniques and microelectrodes. *Environ. Sci. Technol.* **40**: 1532 - 1539

Nicol, G.W. and Schleper, C. (2006). Ammonia-oxidizing Crenarchaeota: important players in the Nitrogen cycle? *Trends in Microbiology* **14** (5):

207 - 212.

Nicolella, C., van Loosdrecht, M. C. M and Heijnen, S. J. (2000a). Particle-based biofilm reactor technology. *Trends in Biotechnology*. **18** (7): 312 - 320.

Nicolella, C., van Loosdrecht, M. C. M and Heijnen, S. J. (2000b). Wastewater treatment with particle biofilm reactors. *Journal of Biotechnology* **80**: 1 – 33.

Nielsen, H., Diams, H. and Lemmer, H. (2009) FISH handbook for biological wastewater treatment: identification and quantification of microorganisms in activated sludge and biofilms by FISH. IWA Publishing London. 123P

Nogeuira, R., Lazarova, V., Manem, J. and Melo, L. F. (1998). Influence of dissolved oxygen on the kinetics in a circulating bed biofilm reactor. *Bioprocess Engineering*, **19**: 441

Noguera, D. R., Pizarro, G. E and Regan, J. M. (2004). Modelling biofilms. In: Microbial biofilms, Ghannoum, M. A. and O'Toole, G. *American Society for Microbiology*. 222 – 249.

NSFC (2004). The attached growth process – an old technology takes on new forms. *Pipeline* **15 (**1): 1 - 6

Okabe, S., Satoh, H. and Wantanabe, Y. (1999). In situ analysis of nitrifying biofilms as determined by *in situ* hybridization and the use of microelctrodes. *Applied and Environmental Microbiology* **65** (7): 3182 –

3191

Oldham, W. K. and Rabinowitz, B. (2002). Development of biological nutrient removal technology in western Canada. *Journal of Environmental Engineering Science* **1**: 33 - 43

Oliviera, R., Azeredo, J. and Teixeira, P. (2003). The importance of physicochemical properties in biofilm formation and activity. In: Biofilms in wastewater treatment – an interdisciplinary approach. Wuertz, S, Bishop, P and Wilderer, P (Eds). IWA Publishing. Cornwall 211 – 231 pp

Olofsson, A., Zita, A. and Hermansson, M. (1998). Floc stability and adhesion of green-flourescent-protein-marked bacteria to flocs in activated sludge. *Microbiology* **114**: 519 - 528

211 – 231 pp

O'Toole, G., Kapplan, H. B. and Kolter, R. (2000). Biofilm formation as microbial development. *Annual Review of Microbiology* **54**: 49 - 79.

Painter, H. A. (1986). Nitrification in the treatment of sewage and wastewaters. In: Nitrification. Prosser, J.I (Ed) IRL Press Oxford 185 – 210 pp

Picioreanu, C., van Loosdrecht, M.C.M. and Heijnan, J. J. (1999). Discrete – differential modelling of biofilm structure. *Water Science Technology*,

39 (7): 115 – 122.

Picioreanu, C., Xavier, J. B. and van Loosdrecht, M.C.M. (2005). Advances in mathematical modelling of biofilm structures. *Biofilms* **1**: 337 – 349.

Pocrenich, M. and Litke, D. W. (1995). Nutrient concentrations in wastewater treatment plant effluents, South Platte river basin. *Journal of the American Water Association* **33**: 205 - 214

Powell, J. R. (1986). Laboratory studies of inhibition of nitrification. In: Nitrification. Prosser J.R. (Ed). IRL Press, Oxford. 79 – 97 pp.

Prosser, J.I. (1986). Experimental and theoretical models of nitrification. In: Nitrification, Prosser, J.I (Ed) IRL Press Oxford. 63 -78 pp.

Prosser, J. I. (1989). Autotrophic nitrification. In: Rose, A.H, Advances in microbial physiology. Academic Press Ltd, London 125-182 pp

Rajesh, D., Sunil, C., Lalita, R. and Sushila, S. (2009). *European Journal of Soil Biology*, doi:10.1016/j.ejsobi.2009.06.002

Rasche, M. E., Hyman, M. R. and Arp, D. J. (1990). Biodegradation of halogenated hydrocarbons fumigants by nitrifying bacteria. *Applied and Environmental Microbiology*. **56** (8): 2568 – 2571.

Raszka, A., Chorvatova, M and Wanner, J. (2006). The role and significance of extracellular polymers in activated sludge. *Acta hydrochim.hydrobiol.*

34:411-424.

Rice, G. (2005). The Nitrogen cycle serc.carleton.edu/.../northinlet/diaz.html). Accessed 14/04/2009

Richardson, J. (1997). Acute ammonia toxicity for eight New Zealand indigenous freshwater species. *New Zealand Journal of Marine and Freshwater Research* **31**: 185 - 190.

Rodgers, M, Zhan, X. M. and Pendergast, J. (2005). Wastewater treatment using a vertically moving biofilm system followed by a sand filter. *Process Biochemistry* **40**: 3132 – 3136

Rogalla, F. (2009). To BNR or Not to BNR : sustainability suggests sensible selection. Conference proceedings of the 2nd IWA Specialized Conference. Nutrient management in wastewater treatment processes. Krakow, Poland. 6-9 September 2009 947 – 954 pp.

Russell, D. (2006). Practical wastewater treatment. John Wiley & Sons Inc. New Jersey 288P

Schobert, H.H. (1978). Coal, the energy of the past and future. American Chemical Society Washington DC 289P.

Schramm, A., Larsen, L. H., Revsbech, N. P., Ramsing, N.B., Amann, R. and Schleifer, K. (1996). Structure and function of a nitrifying biofilm as

determined by in situ hybridization and the use of microelectrodes. *Applied and Environmental Microbiology* **62** (12): 4641 – 4647

Schultz, T. (2005). Water management in the petroleum industry. *Pollution Engineering*.

Seker, S, Beyenal, H. and Tanyyolac, A. (1995). The effect of biofilm thickness on biofilm Density and substrate consumption rate in a differential fluidized bed biofilm reactor (DFBBR). *Journal of Biotechnology* **41**(1): 39 - 47

Sotirakou, E., Kladitis, G., Diamantis, N. and Grigorpopoulou, H. (1999). Ammonia and phosphorus removal in municipal wastewater treatment plant with extended aeration. *Global nest: The International Journal* **1** (1): 47 - 53

Sponza, D.T. and Pala, A. I. (1994). The increase in biological treatment efficiency in petroleum refinery and petrochemical wastewaters by acclimated microorganisms In: Biotechnology for waste management and site restoration. Ronneau, C. and Bitchaeva, O. Kluwer Academic Publishers Dordrecht 181 – 186 pp.

Stewart, P. S. (2003). Diffusion in Biofilms. *Journal of Bacteriology.* **185** (5): 1485 - 1495.

Stoodley, P., Sauer, K., Davies, D. G. and Costerton, J. W. (2002).

Biofilms as complex differentiated communities. *Annual Review of Microbiology* **56:** 187 - 209

Suzuki, I., Dular, U. and Kwok, S. C. (1974). Ammonia or ammonium ion substrate for oxidation by *Nitrosomonas europaea* cells and extracts. *Journal of Bacteriology* **120** (1)556-558

Tanaka, H. and Dunn, I. J. (1982). Kinetics of biofilm nitrification. *Biotechnology Bioengineering* **24:** 669 – 689

Tatem, H. E., Cox, B. A. and Anderson, J. W. (1978). The toxicity of oils and petroleum hydrocarbons to estuarine crustaceans. *Estuarine, coastal and shelf Science*. **6**: 365 - 373

Tomasso, J. R., Wright, M. I., Simco, B. A. and Davis, K. B. (1980). Inhibition of nitrite induced toxicity in channel catfish by calcium chloride and sodium chloride. *The Progressive Fish-Culturist*: **42** (3): 144 - 146.

Tomlinson, T. G., Boon, A. G., and Trotman, N.A. (1966). Inhibition of nitrification in the activated sludge process of sewage disposal. *J. Appl. Bacteriol.* **29**: 266 - 291

Van Neil, E.W. J., Arts, P. A. M., Wesselink, B. J., Robertson, L. A. and Kuenen, J. G.(1993). Competition between heterotrophic and autotrophic nitrifiers for ammonia in chemostat cultures. *FEMS Microbiology letters* **2**: 521 - 525

van Loosdrecht, M. C. M. and Picioreanu, C. and Heinjnen, J. J. (1997). A more unifying hypothesis for biofilm structures. *FEMS Microbiol. Ecol.* **24**: 181 – 183

van Ravenswaay, E. (1998). EEP 255: Pollution prevention case study on petroleum refining. Adapted from US EPA, Profile of thre pertoluem refining industry, Washington, D.C.: U.S. government printing office, EPA 310-R-95-013, September 1995. Retrieved 15.07.2007 from www.msu.edu/course/eep/225/petroleumP2Casestudy. htm

Veenstra, N., J., Mohr, K.S., and Sanders, D.A. (1998). Refinery wastewater management using multiple-angle oil water separators. A paper presented at the International petroleum Environment Conference Albuquerque, New Mexico, October, 1998.

Veil, J., A., Puder, M. G., Elcock, D. and Redweik, R. J. (2004). A white paper describing produced water from production of crude oil, natural gas and coal bed methane. Prepared for US Department of Energy National Energy Technology Laboratory.

Villaverde, S., Garcia-Encina and Fdz-Polanco, F. (1997). Influence of pH over nitrifying biofilm activity in submerged biofilter. *Water Research.* **31**(5): 1180 – 1186

von Sperling .M. (2007a). Basic principles of wastewater treatment (Vol. 2). IWA publishing. 200P

von Sperling , M. (2007b). Activated sludge and aerobic biofilm reactors. IWA publishing. Biological wastewater treatment series (Vol 5) 328P.

– 204pp

Wagner, M., Rath, G., Amann, R.I., Koops, H, P. and Schleifer, K. H. (1995). *In situ* identification of ammonia-oxidizing bacteria. *System. Appl. Microbiol*. **18**: 251 -264

Wagner, M, Loy, A., Nogueira, R., Purkhold, U., Lee, N., and Daims, H. (2002). Microbial community composition and function in wastewater treatment plants. *Antonie van Leeuwenhoek* **81**: 665 - 680.

Wang, T., Zhang, h., Yang F., Liu, S., Fu, Z. and Chen, H. (2009). Start-up of the Anammox process from the conventional activated sludge in a membrane Bioreactor. *Bioresource Technology* **100** (9):2501- 2506

Wake, H. (2005). Oil refineries: a review of their ecological impacts on the aquatic environment. *Estuarine Coastal and Shelf Sciences*. **62**:131 - 140

Walker, J. T., Dowsette, A.B. and Rogers, J. (1995). Heterogeneous mosaic – a haven for water borne pathogens. In: Microbial biofilms. Lapin-Scott H.M. and Costerton, J.W. (Eds). Cambridge University Press UK. 196

Wanner, O. and Gujer, W. (1985). Competition in biofilms. *Water Science*

Technology. **17**(2/3), 27 – 44.

Wantanabe, Y., Masuda, S., Nishidome, K. and Wantawin, C. (1985). Mathematical model of simultaneous organic oxidation, nitrification and denitrification in rotating biological contactors. *Water Science Technology*. **17** (2/3): 385 – 397

Water Environment Federation WEF. (1998). Biological and chemical systems for nutrient removal. Alexandria, VA. 424P

Webb, C., Black, G.M. and Atkinson, B. (1986). Process engineering aspects of immobilised cell systems. Pergamon Press Ltd. Oxford. 320P

Wimpenny, J. W. T. and Colasanti, R. (1997). A unifying hypothesis for the structure of microbial biofilms. *Chem. Eng.Sci* **53**, 397- 425

Wimpenny, J., Manz, W. and Szewzyk, U. (2000). Heterogeneity in biofilms. *FEMS Microbiology Reviews* **24**: 661 - 671

Wong, J. M. and Hung, Y. (2006). The treatment of oil refinery wastes. In: wastewater treatment in the process industries. Wang L. K, Hung, Y, Lo, H. H. and Yapijakis, C. (Eds). CRC press 235 -306 pp

Wood, P. M. (1986). Nitrification as a bacterial energy source. In: Nitrification. Prosser, J.I (Ed). Oxford IRL Press 39 - 62 pp.

World Health Organisation (2003a). Ammonia in drinking water. Background

document for preparation of WHO guidelines for drinking water quality. Geneva. (WHO/SDE/WSH/03.04.01).

World Health Organisation (2003b). Nitrite and Nitrate in drinking water. Background document for preparation of WHO guidelines for drinking water quality. Geneva. (WHO/SDE/WSH/03.04.56).

Wuertz, S., Bishop, P. and Wilderer, P. (2003). Biofilms in wastewater treatment – an interdisciplinary approach. IWA publishing 401P

Wuertz, S. (2003). Architecture, population structure and function: introduction. In: Biofilms in wastewater treatment – an interdisciplinary approach. Wuertz, S, Bishop, P and Wilderer, P (Eds). IWA Publishing. Cornwall 124 – 146 pp

Xianling, L., Jianping, W., Quing, Y. and Xueming, Z. (2005). The pilot study for oil refinery wastewater treatment using a gas-liquid-solid three-phase flow airlift loop bioreactor. *Biochemical Engineering Journal* **27** (1): 40 - 44.

Yang, X., Beyenal, H., Harkin, G. and Lewandowski, Z. (2000). Quantifying biofilm structure using image analysis. *Journal of Microbiological Methods*. **39**: 109 - 119

Yang, X., Beyenal, H., Harkin, G. and Lewandowski, Z. (2001) Evaluation of biofilm image thresholding methods. *Water Research* **35** (5) :1149 - 1158

Zhang, T. and Fang, H. H. P. (2001). Quantification of extracellular polymeric substances in biofilms by confocal scanning microscopy. *Biotechnology letters* **23**: 405 - 409.

APPENDIX

A. The Lab scale expanded bed bioreactor

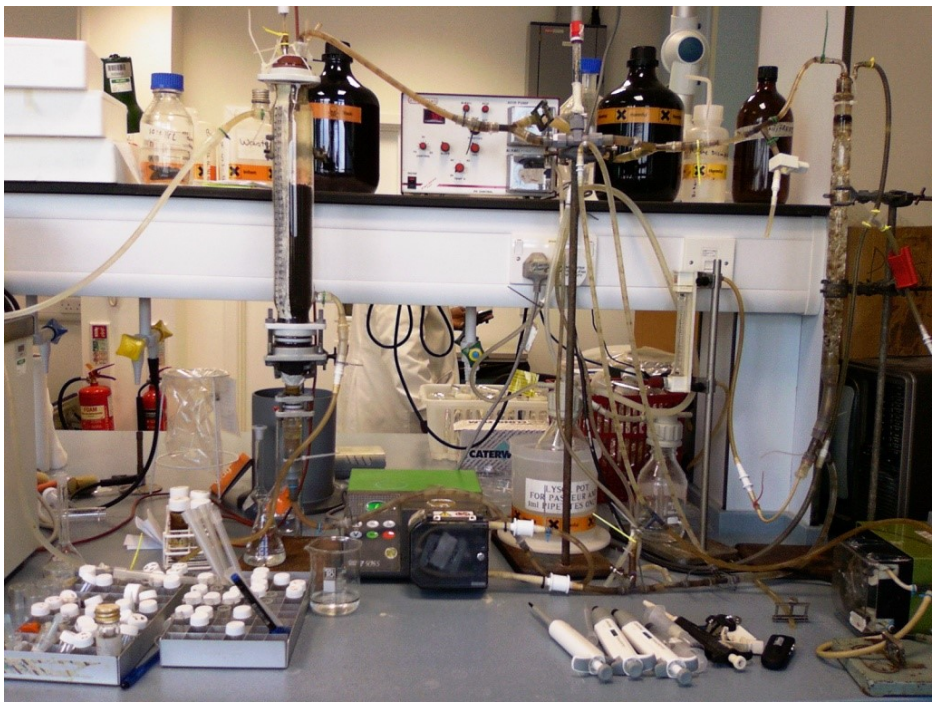

B. Bioparticles obtained from the lab scale EBBR placed in static bed

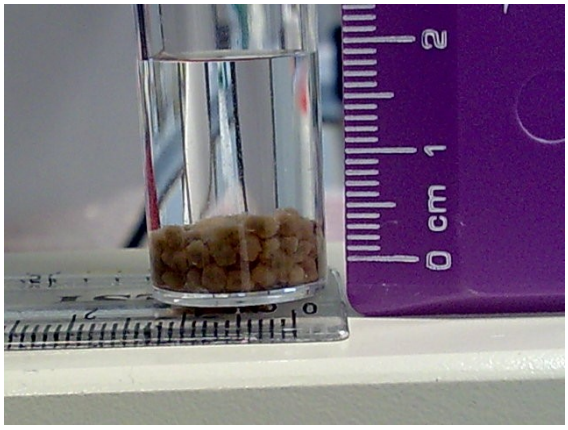

C. An example of Data from the determination of bioparticle diameter, bioparticle surface are and surface area to volume ratio using 100 bioparticles

No.	I(measured)	I(mm)	II(measured)	II(mm)	Average(mm)
1	63	1.993671	55	1.740506	1.86708861
2	62	1.962025	65	2.056962	2.00949367
3	54	1.708861	51	1.613924	1.66139241
4	60	1.898734	51	1.613924	1.75632911
5	56	1.772152	75	2.373418	2.07278481
6	60	1.898734	53	1.677215	1.78797468
7	66	2.088608	50	1.582278	1.83544304
8	60	1.898734	56	1.772152	1.83544304
9	64	2.025316	57	1.803797	1.91455696
10	70	2.21519	44	1.392405	1.80379747
11	66	2.088608	51	1.613924	1.85126582
12	56	1.772152	53	1.677215	1.72468354
13	62	1.962025	46	1.455696	1.70886076
14	65	2.056962	50	1.582278	1.81962025
15	64	2.025316	51	1.613924	1.81962025
16	60	1.898734	67	2.120253	2.00949367
17	55	1.740506	62	1.962025	1.85126582
18	69	2.183544	51	1.613924	1.89873418
19	52	1.64557	60	1.898734	1.7721519
20	54	1.708861	54	1.708861	1.70886076
21	70	2.21519	50	1.582278	1.89873418
22	51	1.613924	60	1.898734	1.75632911
23	60	1.898734	55	1.740506	1.81962025
24	70	2.21519	55	1.740506	1.9778481
25	64	2.025316	53	1.677215	1.85126582
26	52	1.64557	56	1.772152	1.70886076
27	50	1.582278	70	2.21519	1.89873418
28	47	1.487342	65	2.056962	1.7721519
29	61	1.93038	48	1.518987	1.72468354
30	60	1.898734	50	1.582278	1.74050633
31	48	1.518987	59	1.867089	1.69303797
32	41	1.297468	52	1.64557	1.47151899
33	58	1.835443	50	1.582278	1.70886076
34	60	1.898734	54	1.708861	1.80379747
35	58	1.835443	56	1.772152	1.80379747
36	55	1.740506	59	1.867089	1.80379747

37	60	1.898734	51	1.613924	1.75632911
38	50	1.582278	70	2.21519	1.89873418
39	45	1.424051	55	1.740506	1.58227848
40	57	1.803797	60	1.898734	1.85126582
41	52	1.64557	59	1.867089	1.75632911
42	55	1.740506	55	1.740506	1.74050633
43	55	1.740506	48	1.518987	1.62974684
44	56	1.772152	69	2.183544	1.9778481
45	55	1.740506	45	1.424051	1.58227848
46	55	1.740506	69	2.183544	1.96202532
47	52	1.64557	65	2.056962	1.85126582
48	75	2.373418	51	1.613924	1.99367089
49	61	1.93038	50	1.582278	1.75632911
50	55	1.740506	53	1.677215	1.70886076
51	62	1.962025	57	1.803797	1.88291139
52	55	1.740506	56	1.772152	1.75632911
53	53	1.677215	61	1.93038	1.80379747
54	56	1.772152	55	1.740506	1.75632911
55	50	1.582278	60	1.898734	1.74050633
56	77	2.436709	54	1.708861	2.07278481
57	60	1.898734	50	1.582278	1.74050633
58	66	2.088608	45	1.424051	1.75632911
59	55	1.740506	56	1.772152	1.75632911
60	44	1.392405	66	2.088608	1.74050633
61	70	2.21519	49	1.550633	1.88291139
62	66	2.088608	46	1.455696	1.7721519
63	62	1.962025	47	1.487342	1.72468354
64	56	1.772152	55	1.740506	1.75632911
65	57	1.803797	53	1.677215	1.74050633
66	56	1.772152	70	2.21519	1.99367089
67	42	1.329114	46	1.455696	1.39240506
68	51	1.613924	63	1.993671	1.80379747
69	70	2.21519	50	1.582278	1.89873418
70	60	1.898734	51	1.613924	1.75632911
71	70	2.21519	60	1.898734	2.05696203
72	60	1.898734	60	1.898734	1.89873418
73	58	1.835443	65	2.056962	1.94620253
74	76	2.405063	50	1.582278	1.99367089
75	48	1.518987	63	1.993671	1.75632911
76	66	2.088608	40	1.265823	1.67721519
77	60	1.898734	43	1.360759	1.62974684
78	49	1.550633	55	1.740506	1.64556962
79	67	2.120253	50	1.582278	1.85126582

80	55	1.740506	51	1.613924	1.67721519
81	50	1.582278	62	1.962025	1.7721519
82	61	1.93038	53	1.677215	1.80379747
83	60	1.898734	60	1.898734	1.89873418
84	57	1.803797	45	1.424051	1.61392405
85	48	1.518987	55	1.740506	1.62974684
86	50	1.582278	72	2.278481	1.93037975
87	64	2.025316	50	1.582278	1.80379747
88	73	2.310127	50	1.582278	1.94620253
89	60	1.898734	50	1.582278	1.74050633
90	60	1.898734	50	1.582278	1.74050633
91	56	1.772152	60	1.898734	1.83544304
92	60	1.898734	50	1.582278	1.74050633
93	47	1.487342	70	2.21519	1.85126582
94	55	1.740506	72	2.278481	2.00949367
95	55	1.740506	62	1.962025	1.85126582
96	56	1.772152	60	1.898734	1.83544304
97	60	1.898734	60	1.898734	1.89873418
98	72	2.278481	60	1.898734	2.08860759
99	50	1.582278	53	1.677215	1.62974684
100	65	2.056962	55	1.740506	1.89873418
Av	58.42	1.848734	55.7	1.762658	1.8056962
Total	5842	184.8734	5570	176.2658	180.56962
SD	7.486257	0.236907	7.332645	0.232046	0.12534316
Vol of Bp mm3					3.08
SurArea mm2					10.24
SSA-V ratio					3322.82

D. Data from the determination of biofilm thickness (μm)of the same 100 bioparticles

	I(measured)	W(mm)	II(measured)	L(mm)	Av(mm)	Av(μm)
1	10	0.316456	11	0.348101	0.332278	332.2785
2	10	0.316456	11	0.348101	0.332278	332.2785
3	10	0.316456	9	0.28481	0.300633	300.6329
4	10	0.316456	11	0.348101	0.332278	332.2785
5	10	0.316456	9	0.28481	0.300633	300.6329
6	8	0.253165	9	0.28481	0.268987	268.9873
7	11	0.348101	10	0.316456	0.332278	332.2785
8	10	0.316456	10	0.316456	0.316456	316.4557
9	11	0.348101	7	0.221519	0.28481	284.8101
10	14	0.443038	7	0.221519	0.332278	332.2785
11	8	0.253165	11	0.348101	0.300633	300.6329
12	8	0.253165	10	0.316456	0.28481	284.8101
13	10	0.316456	12	0.379747	0.348101	348.1013
14	12	0.379747	10	0.316456	0.348101	348.1013
15	14	0.443038	11	0.348101	0.39557	395.5696
16	10	0.316456	10	0.316456	0.316456	316.4557
17	13	0.411392	10	0.316456	0.363924	363.9241
18	11	0.348101	10	0.316456	0.332278	332.2785
19	7	0.221519	10	0.316456	0.268987	268.9873
20	9	0.28481	8	0.253165	0.268987	268.9873
21	10	0.316456	15	0.474684	0.39557	395.5696
22	7	0.221519	7	0.221519	0.221519	221.519
23	9	0.28481	11	0.348101	0.316456	316.4557
24	8	0.253165	15	0.474684	0.363924	363.9241
25	9	0.28481	10	0.316456	0.300633	300.6329
26	12	0.379747	11	0.348101	0.363924	363.9241
27	12	0.379747	10	0.316456	0.348101	348.1013
28	11	0.348101	7	0.221519	0.28481	284.8101
29	10	0.316456	6	0.189873	0.253165	253.1646
30	11	0.348101	8	0.253165	0.300633	300.6329
31	9	0.28481	9	0.28481	0.28481	284.8101
32	10	0.316456	10	0.316456	0.316456	316.4557
33	10	0.316456	10	0.316456	0.316456	316.4557
34	10	0.316456	10	0.316456	0.316456	316.4557
35	9	0.28481	8	0.253165	0.268987	268.9873
36	10	0.316456	9	0.28481	0.300633	300.6329
37	8	0.253165	16	0.506329	0.379747	379.7468
38	10	0.316456	11	0.348101	0.332278	332.2785

39	10	0.316456	14	0.443038	0.379747	379.7468
40	10	0.316456	10	0.316456	0.316456	316.4557
41	8	0.253165	10	0.316456	0.28481	284.8101
42	10	0.316456	12	0.379747	0.348101	348.1013
43	8	0.253165	8	0.253165	0.253165	253.1646
44	15	0.474684	10	0.316456	0.39557	395.5696
45	8	0.253165	10	0.316456	0.28481	284.8101
46	15	0.474684	10	0.316456	0.39557	395.5696
47	9	0.28481	12	0.379747	0.332278	332.2785
48	12	0.379747	10	0.316456	0.348101	348.1013
49	8	0.253165	9	0.28481	0.268987	268.9873
50	7	0.221519	10	0.316456	0.268987	268.9873
51	9	0.28481	10	0.316456	0.300633	300.6329
52	10	0.316456	9	0.28481	0.300633	300.6329
53	6	0.189873	13	0.411392	0.300633	300.6329
54	6	0.189873	11	0.348101	0.268987	268.9873
55	8	0.253165	12	0.379747	0.316456	316.4557
56	11	0.348101	9	0.28481	0.316456	316.4557
57	13	0.411392	9	0.28481	0.348101	348.1013
58	11	0.348101	8	0.253165	0.300633	300.6329
59	12	0.379747	11	0.348101	0.363924	363.9241
60	11	0.348101	10	0.316456	0.332278	332.2785
61	10	0.316456	9	0.28481	0.300633	300.6329
62	6	0.189873	10	0.316456	0.253165	253.1646
63	7	0.221519	10	0.316456	0.268987	268.9873
64	10	0.316456	10	0.316456	0.316456	316.4557
65	7	0.221519	9	0.28481	0.253165	253.1646
66	8	0.253165	10	0.316456	0.28481	284.8101
67	11	0.348101	12	0.379747	0.363924	363.9241
68	11	0.348101	10	0.316456	0.332278	332.2785
69	15	0.474684	13	0.411392	0.443038	443.038
70	10	0.316456	14	0.443038	0.379747	379.7468
71	10	0.316456	11	0.348101	0.332278	332.2785
72	12	0.379747	11	0.348101	0.363924	363.9241
73	8	0.253165	12	0.379747	0.316456	316.4557
74	11	0.348101	10	0.316456	0.332278	332.2785
75	11	0.348101	12	0.379747	0.363924	363.9241
76	15	0.474684	11	0.348101	0.411392	411.3924
77	7	0.221519	7	0.221519	0.221519	221.519
78	11	0.348101	12	0.379747	0.363924	363.9241
79	10	0.316456	10	0.316456	0.316456	316.4557
80	10	0.316456	11	0.348101	0.332278	332.2785
81	7	0.221519	8	0.253165	0.237342	237.3418

82	15	0.474684	14	0.443038	0.458861	458.8608
83	11	0.348101	13	0.411392	0.379747	379.7468
84	8	0.253165	13	0.411392	0.332278	332.2785
85	9	0.28481	11	0.348101	0.316456	316.4557
86	10	0.316456	13	0.411392	0.363924	363.9241
87	10	0.316456	13	0.411392	0.363924	363.9241
88	9	0.28481	10	0.316456	0.300633	300.6329
89	15	0.474684	15	0.474684	0.474684	474.6835
90	11	0.348101	8	0.253165	0.300633	300.6329
91	10	0.316456	10	0.316456	0.316456	316.4557
92	8	0.253165	9	0.28481	0.268987	268.9873
93	7	0.221519	7	0.221519	0.221519	221.519
94	8	0.253165	11	0.348101	0.300633	300.6329
95	10	0.316456	15	0.474684	0.39557	395.5696
96	7	0.221519	9	0.28481	0.253165	253.1646
97	11	0.348101	10	0.316456	0.332278	332.2785
98	10	0.316456	15	0.474684	0.39557	395.5696
99	7	0.221519	9	0.28481	0.253165	253.1646
100	9	0.28481	11	0.348101	0.316456	316.4557
Av	9.9	0.313291	10.44	0.33038	0.321835	321.6738
Total	990	31.32911	1044	33.03797	32.18354	32183.54
SD	2.124889	0.067243	2.0217	0.063978	0.049386	49.3859

E. An example of data from the determination of biomass concentration using 3cm^3 of bioparticles at 420 ^{0}C

	When using static bed volume		When using bioparticles drained of interstitial water to determine the % water in bioparticle	
	Coke control	Bioparticles	Coke control	Bioparticles
Wt Crucible (g)	11.93	8.65	27.2875	28.276
Wet Wt Crucible + Sample (g)	11.99	8.738	30.536	30. 233
Dry wt + Crucible (g)	11.96	8.68	29.172	28.575
Wet wt sample (g)	0.06	0.008	3.25	1.96
Dry wt sample (g)	0.032	0.03	1.88	0.30
% Water	-	-	41.99	84.72
Residue wt (g) (after heating)	0.03	0.026		
Ash wt (g)	0.002	0.004		
% Burnt off	6.667			
Coke in biomass		0.000267		
Adjusted biomass		0.0037		
% Biomass		12.44		
Original static bed volume of bioparticles (cm^3)		0.21		
Biomass concentration (kgm^{-3})		17.78		

F. Determination of water content of bioparticles (at 420 ^{0}C)

Samples	i	ii	iii	iv	v	vi	vii	Mean	SD
% water	86.49	84.71	85.42	85.72	84.76	83.59	82.07	84.70	1.5

G. Data of aggregate of AOB and NOB obtained in transects using Image J software from CLSM image of cross section of biofilm fixed in agarose, showing the aggregates along the biofilm thickness and adjusting for shrinking

	Transects				
	I	II	III	IV	V
Distance from outer biofilm surface (μm)	30.2	60.4	90.7	120.9	151.1
Adjusted distance (μm)	51.1	102.2	153.3	204.4	255.5
Total Aggregate AOB	246	753	377	2	46
Total Aggregate NOB	245	510	27	127	41

H. Determination of percentage shrinkage of biofilms embedded in agarose after FISH staining with Nitri-VIT kit..

Biofilm thickness of biofilms embedded in 0.2 % agarose before and after FISH staining procedure (μm)

No.	Before	After	Before	After	Before	After	Before	After
1	589	111	477	57	298	37	297	53
2	590	51	398	89	289	54	279	2
3	543	57	487	46	234	37	224	38
4	578	68	478	23	267	7	197	23
5	575	89	456	79	278	13	168	50
6	575	61	438	36	257	84	268	11
7	572	83	471	79	300	23	209	55
8	546	53	466	12	220	50	237	18
9	565	66	497	16	296	44	286	27
10	596	74	478	48	275	19	257	38
11	549	90	488	41	256	60	159	44
12	568	120	439	27	245	35	179	25
13	596	115	459	20	210	27	145	5
14	564	85	477	59	249	14	248	16
15	534	79	488	38	244	24	273	22
16	584	109	493	59	268	58	206	26
17	533	78	478	45	285	46	295	37
18	543	95	568	37	299	51	289	41
19	545	101	497	69	277	68	212	61
20	525	85	474	25	274	90	150	52
Mean	563.50	83.50	475.35	45.25	266.05	42.05	228.90	32.20
SD	21.72	20.16	31.44	21.61	25.64	22.38	49.84	16.84
% Reduction		85%		90%		84%		86%
Average % Reduction		86.5%						